Derivative-free Equilibrium Seeking in Multi-Agent Systems

Krilašević, S.

DOI
10.4233/uuid:998441fb-72b3-4a4b-b2bb-f3a5ba06042e

Publication date
2023

Document Version
Final published version

Citation (APA)
Krilašević, S. (2023). *Derivative-free Equilibrium Seeking in Multi-Agent Systems*. [Dissertation (TU Delft), Delft University of Technology]. https://doi.org/10.4233/uuid:998441fb-72b3-4a4b-b2bb-f3a5ba06042e

Derivative-free Equilibrium Seeking in Multi-Agent Systems

Derivative-free Equilibrium Seeking in Multi-Agent Systems

Proefschrift

ter verkrijging van de graad van doctor
aan de Technische Universiteit Delft,
op gezag van de Rector Magnificus Prof. dr. ir. T.H.J.J. van der Hagen,
voorzitter van het College voor Promoties,
in het openbaar te verdedigen
op dinsdag 3 oktober 2023 om 10.00 uur

door

Suad KRILAŠEVIĆ

Master of Electrical Engineering,
University of Sarajevo, Faculty of Electrical Engineering, Bosnië-Herzegovina,
geboren te Sarajevo, Bosnië-Herzegovina.

Dit proefschrift is goedgekeurd door de promotoren.

Samenstelling promotiecommissie:

Rector Magnificus,	voorzitter
Dr. ing. S. Grammatico,	Technische Universiteit Delft, promotor
Prof. dr. ir. B. De Schutter,	Technische Universiteit Delft, promotor
Onafhankelijke leden:	
Dr. J. Poveda,	UC San Diego
Prof. dr. D. Nešić,	University of Melbourne
Prof. dr. ir. M. Wisse,	Technische Universiteit Delft
Prof. dr. T. Keviczky,	Technische Universiteit Delft

The work in the thesis has been partially supported by the ERC under research project COSMOS (802348).

Style: TU Delft House Style, with modifications by Moritz Beller
https://github.com/Inventitech/phd-thesis-template

The author set this thesis in LaTeX using the Libertinus and Inconsolata fonts.

ISBN

An electronic version of this dissertation is available at
http://repository.tudelft.nl/.

بِسْمِ ٱللَّهِ ٱلرَّحْمَـٰنِ ٱلرَّحِيمِ

Contents

Summary

Both societal and engineering systems are growing in complexity and interconnectivity, making it increasingly challenging, and sometimes impossible, to model their dynamics and behaviors. Moreover, individuals or entities within these systems, often referred to as agents, have their own objectives that may conflict with one another. Examples include various economic systems where agents compete for profit, wind farms where upwind turbines reduce the energy extraction of downwind turbines, unwanted perturbation minimization in extremum seeking control, and cooperative source-seeking robotic vehicles. Despite having access to only limited observable information, it is crucial to ensure that all participants are content with the outcomes of these interactions. In this thesis, we choose to examine these problems within the framework of *games*, where each agent has their own cost function and constraints, and all costs and constraints are interconnected. Since the notion of optimum in multi-agent problems is difficult to define, we often seek to find a Nash equilibrium, i.e., a set of decisions from which no agent has an incentive to deviate.

This thesis primarily explores the development of Nash equilibrium seeking algorithms for scenarios where agents' cost functions are unknown and can only be assessed through measurements of a dynamical system's output, referred to as the zeroth-order (derivative-free) information case. We specifically concentrate on scenarios where partial derivatives can be estimated from these measurements and subsequently integrated into a full-information algorithm. Existing approaches exhibit significant drawbacks, such as the inability to handle shared constraints, stringent assumptions on the cost functions, and applicability limited to agents with continuous dynamics.

The thesis is divided into three parts: equilibrium seeking via output derivative estimators, equilibrium seeking without projections, and hybrid output feedback for equilibrium seeking. In Part 1, we explore the development of zeroth-order (generalized) Nash equilibrium-seeking methods for dynamical systems using output derivative-based estimators. We identify an issue with an existing extremum seeking method and leverage the gained insights to design several algorithms. The first is a single-timescale NE seeking algorithm for a restricted class of linear systems, while the second is a multi-time scale algorithm for a broader range of nonlinear systems, which can solve GNEPs in the zeroth-order information case for the first time.

Part 2 aims to relax the strong monotonicity assumption on the pseudogradient mapping required in the zeroth-order GNE seeking. The main challenge arises from the fact that full-information continuous-time GNE seeking algorithms, which require only the monotonicity of the pseudogradient, also necessitate multiple pseudogradient evaluations that cannot be provided by estimation schemes. We propose a new projectionless algorithm to address these challenges and demonstrate its effectiveness in various practical scenarios, such as distortion reduction in photovoltaic current.

Part 3 focuses on extending existing averaging theory for discrete systems and singular perturbation theory for hybrid systems. By demonstrating practical stability of a multi-

timescale discrete-time system with a practically stable averaged system, we can establish new results in discrete-time NE seeking. Moreover, by incorporating jumps from the boundary layer system of the restricted system into the singular perturbation theory, we can demonstrate stability for various systems where this was previously not the case. This allows us to show that discrete-time NE seeking algorithms can be applied in cases where agents have hybrid dynamics, significantly improving the real-life applicability of such algorithms.

To conclude, this thesis has established the stability of several zeroth-order game-theoretic control algorithms. In our final chapter, we evaluate how effectively we addressed our initial research questions. We also lay out potential directions for future research and acknowledge areas of interest or potential weaknesses that our research did not fully explore. This self-reflection allows us to set a clear path for further inquiries and improvements.

Samenvatting

Zowel maatschappelijke als technische systemen groeien in complexiteit en onderlinge verbondenheid, waardoor het steeds uitdagender, en soms onmogelijk, wordt om hun dynamiek en gedrag te modelleren. Bovendien hebben individuen of entiteiten binnen deze systemen, vaak aangeduid als agents, hun eigen doelstellingen die met elkaar kunnen botsen. Voorbeelden zijn economische systemen waar deelnemers concurreren om winst, windparken waar windturbines bovenwinds de energie-extractie van windturbines benedenwinds verminderen, ongewenste verstoring minimalisatie in extremum seeking control, en robotvoertuigen die samenwerken om een doelwit te zoeken. Ondanks dat ze slechts toegang hebben tot beperkte waarneembare informatie, is het cruciaal dat alle deelnemers tevreden zijn met de uitkomsten van deze interacties. In dit proefschrift onderzoeken we deze problemen binnen het kader van *spellen*, waarbij elke agent zijn eigen kostenfunctie en beperkingen heeft, en alle kostenfuncties en beperkingen onderling verbonden zijn. Aangezien het optimum in multi-agent problemen moeilijk te definiëren is, zoeken we vaak naar een Nash-evenwicht (NE), dat wil zeggen, een set beslissingen waarvan geen enkele agent de neiging heeft om ervan af te wijken.

In dit proefschrift focussen we voornamelijk op het ontwikkelen van Nash-evenwicht zoekende algoritmes voor scenario's waarin de kostenfuncties van de deelnemers onbekend zijn en alleen geschat kunnen worden aan de hand van de gemeten output van een dynamisch systeem, aangeduid als het nulde-order (afgeleide-vrije) informatie scenario. We concentreren ons specifiek op scenario's waarin partiële afgeleiden kunnen worden geschat op basis van deze metingen en vervolgens kunnen worden geïntegreerd in algoritmen voor scenario's met volledige informatie. Bestaande methodes vertonen aanzienlijke nadelen, zo zijn ze slechts toepasbaar voor deelnemers met continue dynamiek, accepteren ze geen gedeelde beperkingen, en maken ze sterke aannames over de kostenfuncties.

Het proefschrift is verdeeld in drie delen: het zoeken van evenwicht via output-afgeleide schatters, het zoeken van evenwicht zonder projecties, en hybride output feedback voor het zoeken van evenwicht. In Deel 1 verkennen we de ontwikkeling van nulde-orde (gegeneraliseerde) Nash-evenwicht zoekende methoden voor dynamische systemen met behulp van output-afgeleide gebaseerde schatters. We identificeren een probleem met een bestaande extremum zoekende methode en gebruiken de opgedane inzichten om verschillende algoritmen te ontwerpen. De eerste is een enkel-tijdschaal NE zoekend algoritme voor een beperkte klasse van lineaire systemen, terwijl de tweede een multi-tijdsschaal algoritme is voor een breder scala aan niet-lineaire systemen, dat voor het eerst GNEP's kan oplossen in het scenario van nulde-orde informatie.

Deel 2 is gericht op het versoepelen van de sterke monotonie-aanname op de pseudogradient-mapping die vereist is voor het zoeken van nulde-orde GNE. De belangrijkste uitdaging ontstaat uit het feit dat volledige-informatie continue-tijd GNE zoekende algoritmen, die alleen de monotonie van de pseudogradient vereisen, ook meerdere pseudogradient evaluaties vereisen die niet kunnen worden geleverd door schattingsmethode. Wij stellen een

nieuw algoritme zonder projecties voor om deze uitdagingen aan te pakken en tonen de effectiviteit ervan aan in verschillende praktische scenario's, zoals vervormingsreductie in fotovoltaïsche stroom.

Deel 3 richt zich op het uitbreiden van de bestaande ''theorie van middelen" voor discrete systemen en singuliere verstoringstheorie voor hybride systemen. Door de praktische stabiliteit van een multi-tijdsschaal discreet-tijd systeem met een praktisch stabiel gemiddeld systeem aan te tonen, kunnen we nieuwe resultaten vaststellen in discreet-tijd NE zoeken. Bovendien kunnen we, door sprongen vanuit de grenslaag van het beperkte systeem op te nemen in de theorie van singuliere verstoringen, de stabiliteit aantonen van verschillende systemen waarbij dit voorheen niet mogelijk was. Dit stelt ons in staat om aan te tonen dat discreet-tijd NE zoekende algoritmen kunnen worden toegepast in gevallen waar de deelnemers hybride dynamiek hebben, wat de toepasbaarheid van dergelijke algoritmen in de praktijk aanzienlijk verbetert.

Samengevat heeft dit proefschrift de stabiliteit van verschillende nulde-orde spelttheoretische controle-algoritmen vastgesteld. In ons laatste hoofdstuk evalueren we hoe effectief we onze oorspronkelijke onderzoeksvragen hebben aangepakt. We bespreken tevens mogelijke richtingen voor toekomstig onderzoek en erkennen aspecten, potentieel zwakke punten, die we niet volledig hebben onderzocht. Door middel van deze zelfreflectie stippelen we duidelijk pad uit voor verdere onderzoeksvragen en verbeteringen.

Symbols

Basic relations

$:=$	equal to by definition
$\mid$	such that
$\in$	belongs to
$\exists$	there exists
$\forall$	for all
$\Rightarrow$	implies
$\Leftrightarrow$	if and only if
$\to$	maps to an element
$\rightrightarrows$	maps to a set

Sets, spaces and set operators

$\mathbb{N}$	set of whole numbers
$\mathbb{Z}$	set of integers
$\mathbb{R}$	set of real numbers
$\mathbb{R}_+$	set of nonnegative real numbers
$\mathbb{R}^n$	set of real n-dimensional vectors
$\mathbb{R}^{n\times m}$	set of real n by m matrices
$\mathbb{B}$	$:= \{x \in \mathbb{R}^N \mid \|x\| \leq 1\}$, i.e. the unit ball set
$\mathbb{S}$	$:= \{z \in \mathbb{R}^2 : z_1^2 + z_2^2 = 1\}$, i.e. the unit circle set
$A \cup B$	union of sets A and B
$A \cap B$	intersection of sets A and B
$A \subset B$	A is a subset of B
$A \supset B$	A is a superset of B
$A \setminus B$	set of elements that are in A, but not in$B$
$A + B$	Minkowski sum of sets A and B
$A \times B$	Cartesian product of the sets A and B
$\prod_{i=1}^N A_i$	$:= A_1 \times A_2 \times \cdots \times A_N$
$\cup_{i=1}^N A_i$	$:= A_1 \cup A_2 \cup \cdots \cup A_N$
A^n	$:= \prod_{i=1}^N A$
$[a,b]$	closed set of real numbers
(a,b)	open set of real numbers

OPERATIONS ON VECTORS AND MATRICES, NORMS

I_n	identity matrix of dimensions n
$\mathbf{0}$	zero vector of appropriate dimension
$(\cdot)^\top$	transpose operator used on either a vector or a matrix
$\mathrm{col}(v_1,\dots v_N)$	$:= \left[v_1^\top,\dots,v_N^\top\right]^\top$
$\mathrm{diag}(v)$	a diagonal matrix with elements of the vector v on its diagonal
$\mathrm{blkdiag}(A_1,\dots,A_N)$	a block diagonal matrix with A_i matrices on its diagonal
$(v_k)_{k\in\mathcal{I}}$	sequence of vectors indexed via elements of set $\mathcal{I}$
M^{-1}	inverse of matrix M
$M \succ 0$	symmetric matrix M is positive definite
$M \succcurlyeq 0$	symmetric matrix M is positive semidefinite
$\langle v \mid u\rangle$	Euclidian vector product, i.e. $v^\top u$
$\|v\|$	Euclidian norm, i.e. $\sqrt{v^\top v}$
$\|v\|_M$	Euclidian weighted norm, i.e. $\sqrt{v^\top M v}$
$\|v\|_{\mathcal{A}}$	Euclidian distance to set $\mathcal{A}$

OPERATOR THEORY

$\circ$	composition of operators, i.e. $F\circ G(x) = F(G(x))$
Id	identitiy operator, i.e. $\mathrm{Id}(x) = x$
$\mathrm{dom}(f)$	domain of the function f
$\mathrm{zer}(F)$	zero set of an operator F
F^{-1}	inverse operator of F, i.e. $F^{-1}\circ F = F\circ F^{-1} = \mathrm{Id}$
$\nabla f(x)$	$:= \mathrm{col}\left(\frac{\partial f(x)}{\partial x_1},\dots,\frac{\partial f(x)}{\partial x_N}\right)$, i.e. the gradient of f
$\nabla_x f(x,y)$	$:= \mathrm{col}\left(\frac{\partial f(x,y)}{\partial x_1},\dots,\frac{\partial f(x,y)}{\partial x_N}\right)$, i.e. the partial gradient of f
$J_F(x)$	$:= (\mathrm{Id}+F)^{-1}(x)$, i.e. the resolvent operator of F
$\mathrm{N}_S(x)$	equal to $\emptyset$ if $x\notin S$, $\left\{v\in\mathbb{R}^n \mid \sup_{z\in S} v^\top(z-x)\le 0\right\}$ otherwise
$\mathrm{proj}_S(x)$	$:= \mathrm{argmin}_{y\in S}\|y-x\|$, i.e. projection of x onto a closed convex set S

GAME THEORY AND SYSTEMS THEORY

N	number of agents
$\mathcal{I}$	$:= \{1,2,\dots,N\}$ is the set of indices of agents
u_i	decision variable of agent i
$\boldsymbol{u}$	$:= \mathrm{col}(u_1,\dots,u_N)$, i.e. collective vector of N agents
$\boldsymbol{u}_{-i}$	$:= \mathrm{col}(u_1,\dots,u_{i-1},u_{i+1},\dots,u_N)$
$J_i(u_i,\boldsymbol{u}_{-i})$	cost function of agent i
Ω_i	feasible set of agent i
$F(u)$	$:= \mathrm{col}\left(\nabla_{u_1}J_1(u),\dots,\nabla_{u_N}J_N(u)\right)$
$D^+f(t)$	$:= \limsup_{h\to 0^+}\frac{f(t+h)-f(t)}{h}$, i.e. upper Dini derivative of f at t
class $\mathcal{K}$ function	$\mathbb{R}_+\to\mathbb{R}_+$ function that is zero at zero and strictly increasing
class $\mathcal{L}$ function	$\mathbb{R}_+\to\mathbb{R}_+$ function that is non-increasing and converges to zero as its arguments grows unbounded
class $\mathcal{KL}$ function	$\mathbb{R}_+\times\mathbb{R}_+\to\mathbb{R}_+$ function that is of class $\mathcal{K}$ in the first argument, and of class $\mathcal{L}$ in the second argument

1

Introduction

It is impossible for a man to learn what he thinks he already knows.

Epictetus

It is important to draw wisdom from different places. If you take it from only one place, it becomes rigid and stale.

Uncle Iroh, Avatar the Last Airbender

In the following chapter, we will explore the fundamental concepts utilized in this thesis by highlighting the key distinctions between optimization problems and games using an economic example. Moreover, we will demonstrate the necessity of zeroth-order equilibrium-seeking algorithms and illustrate their application and effectiveness. Lastly, we will address the research questions that guided the development of this thesis and offer an overview of its organizational structure.

1

1.1 Game theory versus optimization

Consider that you are a manager of a factory producing a unique product and selling it in the market as the sole producer. Your goal is to maximize profit, which is the number of sold units multiplied by the difference between the selling price and production cost. You strive for efficiency to lower production costs by minimizing waste, reducing resource use, improving resource allocation, and decreasing labor costs. Additionally, you carefully select the number of units produced to prevent market oversaturation and maintain a favorable selling price, as the product's price is determined by its demand and your supply.

Now imagine a competing factory starts producing and selling the same product in the same market. This new competition *fundamentally* changes your approach to the problem, as the competitors' decisions influence your profits. You may allocate additional resources to make your product more appealing to customers, which could come from your earnings, reallocating resources from quality maintenance, or even cutting labor expenses. Moreover, pricing becomes more complex since the price difference between your product and your competitor's impacts customer preference. If the competitor lowers their prices, you might also need to do so to maintain your market share. On the other hand, if the competitor decides to produce more units of the product, you might choose to do the same to maintain your comparative profits, but in doing so, you risk oversaturating the market. Therefore, you must carefully select your pricing and production strategy.

The previous example highlights the distinction between optimization problems and games. In optimization problems, there is a single decision-maker (or multiple in the case of distributed problems) whose *single* goal is to minimize its cost while adhering to constraints, ultimately achieving an optimal equilibrium. On the other hand, games involve multiple decision-makers, each with their own cost, which they wish to minimize subject to their constraints, as well as shared constraints, such as a fixed product demand in our example. In these situations, an optimal equilibrium is often elusive, as one agent's optimum may impose a significant price on another agent. Consequently, the usual solution concept in games is the Nash equilibrium, a set of strategies from which no agent has a reason to unilaterally deviate. In simpler terms, if an individual agent were to deviate from the equilibrium strategy, its cost would actually increase.

It is important to note that a problem can be formulated as a game, even though it has only one decision-maker. For various reasons, a game-theoretic representation and solution can exhibit better behavior than an optimization one, which is why the decision maker chooses to do so by *emulating* multiple decision makers. In an engineering example, it has been noted that treating the problem of power allocation in telecommunication networks as a game can result in a desirable allocation, even though, in reality, there is only one decision-maker in charge of the allocation [1]. Understandably, this approach does not always yield favorable outcomes. In an economic example, the American retailer Sears experienced a collapse due, in large part, to management's decision to separate various departments into individual entities competing for the company's resources. Consequently, these departments often made decisions that benefited them but were detrimental to the company as a whole [2], [3].

Various problems can be postulated as both optimization problems and game problems, with different pros and cons for each. Arguably, the most famous example is the organization of an entire economy. Communist countries experimented with planned

economies, in which the production inputs and outputs for every sector were centrally planned and attempted to be optimized. In some cases, this approach resulted in the absence of periodic recessions or depressions, a more egalitarian distribution of income, and more effective climate change policies [4], [5]. On the other hand, market-based economies leave production decisions to individual producers based on market demand and price signals. This approach often leads to more efficient resource distribution, innovative products, and better adaptability to changing conditions [6].

Considering our previous discussion, how might we, as the factory manager, devise a strategy to maximize our factory's profit? The task is further complicated by the difficulty in accurately modeling product desirability and the number of products sold based on their prices. Nevertheless, the solution is surprisingly simple. Although we may not know the precise analytical relationship governing the number of products sold, we do know *our profit*. By slightly perturbing the product price, we can observe whether our profits increase or decrease. If these perturbations are done strategically, we should gradually enhance our profit and eventually reach an equilibrium with our competitor [7].

Not only markets but numerous engineering systems also exhibit game-like behaviors. These systems aim to optimize various processes, such as enhancing productivity, extending lifespan, or decreasing energy use, among others. They are influenced by other systems, which are treated as opponents either because of limited control or because it is advantageous to do so. Furthermore, as in the factory example, accurately modeling these optimization processes, systems, and their interactions can be challenging or impossible, while observations of the end results are easily accessible, such as production quantities, signal strength, generated waste, oscillation amplitudes, etc. This motivates us to develop algorithms and strategies that utilize these quantities to achieve the objectives *without* exact knowledge of the underlying objective functions. Some prominent examples include:

- **Robot swarm connectivity control**
  A group of robots is assigned to locate a specific number of signal sources. In addition, each robot aims to maintain relative proximity to the other swarm members to ensure effective communication and rapid response in case assistance is required. The straightforward solution would be to allow for inter-agent communication and global coordinate tracking. However, this might require expensive equipment and comprehensive computing power. On the other hand, the robots have access to the measurements of the source signal strength and the signals emitted by their fellow robots, which could facilitate a different cost-effective algorithm design [8].

- **Wind farm wake minimization**
  To maximize energy production for a given area, wind farms usually have rows of turbines located behind each other. This, unfortunately, hurts energy production as the wake of the turbines in front reduces the energy production of the wind turbines in the back. A common approach is to have each turbine greedily maximize its power output, which does not guarantee maximal energy production. The wake effect can be somewhat alleviated by controlling the axial induction of the turbines, but these processes are notoriously hard to model and predict, thus making model-free payoff-based optimizing strategies a practical choice [9], [10].

1

- **Perturbation minimization in extremum seeking control**
  Some zeroth-order optimization methods incorporate perturbation signals into their control strategies. When transmitted to the system output, these perturbations can produce undesired behavior. To mitigate these issues, it can be advantageous to intelligently select the amplitudes and frequencies of these signals based on the measured output signal [11].

Taking into account the previous discussions and recognizing that optimization problems can be considered as a special case of game problems with a single agent, exploring game theory has the potential to offer innovative solutions for a wide range of engineering challenges.

1.2 Zeroth-order algorithms

In equilibrium-seeking algorithms, the knowledge of the cost function's various partial derivatives, known as first-order (derivative) information, is a common assumption. However, finding an equilibrium or its neighborhood is also possible using only cost function evaluations, referred to as zeroth-order (derivative) information. These algorithms either estimate the derivatives and apply them in a first-order-information-like algorithm [12], [13], [14], or utilize this information in a different manner that does not involve derivative estimation [15], [16]. Consequently, the first class of algorithms requires derivative estimators. The forward Euler method is arguably the most well-known derivative estimator in discrete time. For a real function f, the estimation is given by

$$\frac{\partial f(x)}{\partial x} \approx \frac{f(x+\delta x)-f(x)}{\delta x},$$

for very small δx. In continuous time, a sinusoidal perturbation scheme has received a lot of attention [12], [7], [17], [18]. Consider the Taylor expansion at x for small a of the following time-varying function:

$$\begin{aligned} f(x+a\sin(\omega t))\frac{2\sin(\omega t)}{a} &= f(x)\frac{2\sin(\omega t)}{a} + \frac{\partial f(x)}{\partial x} 2\sin^2(\omega t) + \mathcal{O}(a) \\ &= \frac{\partial f(x)}{\partial x} + \left(\frac{2f(x)}{a}\sin(\omega t) + \frac{\partial f(x)}{\partial x}\cos(2\omega t)\right) + \mathcal{O}(a). \end{aligned}$$

This perturbation scheme gives an estimate that oscillates and is biased. Arguably the most famous continuous-time zeroth-order optimization algorithm that uses this sort of estimators is extremum seeking control (ESC) proposed in [12]. The block diagram of ESC is depicted in Figure 1.1. In essence, the scheme is a simple gradient descent dynamic $\dot{x} = -k\xi$, which uses the filtered state ξ of the previously mentioned continuous-time estimator. Figure 1.2 illustrates the efficiency of the estimator and how the scheme steers the state toward the minimizer.

In this thesis, our focus is on zeroth-order Nash equilibrium-seeking algorithms. Unlike the previous example, which involves minimizing a single cost function, Nash equilibrium problems involve multiple interdependent cost functions, each associated with one agent in

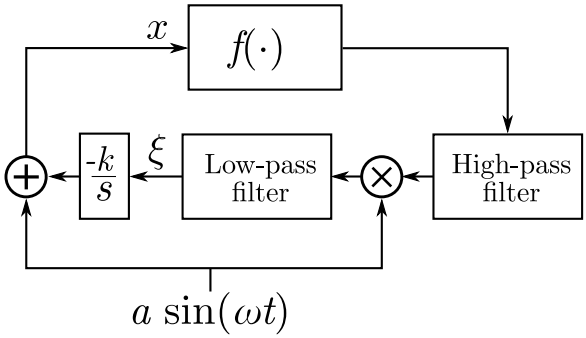

Figure 1.1: ESC scheme proposed in [12]. The highpass and lowpass filters are not necessary, but they drastically improve the algorithm's performance by reducing the variance and bias in the estimate.

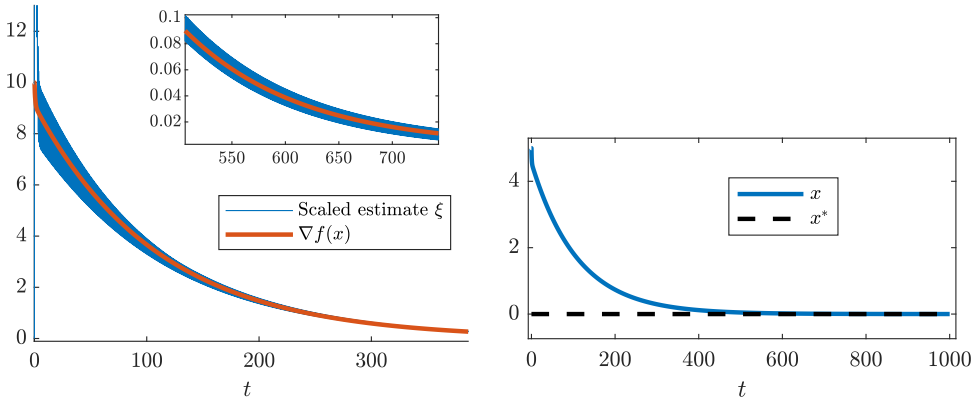

(a) Comparison of the real value of the gradient and its scaled-up estimate.

(b) Convergence of the state to the minimizer.

Figure 1.2: Results of using the extremum seeking scheme in Figure 1.1 to minimize the quadratic cost function $f(x) = \frac{1}{2}x^2$.

the game. Moreover, we aim to estimate the pseudogradient, a game-theoretic equivalent the gradient. This scenario has been studied numerous times in the literature for both continuous [7], [17] and discrete-time games [8], [19]. However, the current state-of-the-art algorithms do exhibit certain limitations.

- In generalized problems, the agents have shared constraints besides their local ones. Continuous-time zeroth-order algorithms have been used to solve only regular, non-generalized Nash equilibrium problems (GNEPs).
- Slow convergence times with dynamical agents are necessary in order to assure a time-layer separation between the agent's dynamics and their Nash equilibrium seeking algorithm.
- Strong monotonicity assumption on the pseudogradient can be restrictive in practical applications, e.g. whenever multiple equilibria might exist.
- Most results are given for dynamical agents with continuous-time dynamics only.

To the best of our ability, in this thesis, we try to tackle these problems, and our approach is summarized in the next section.

1.3 Research questions

The research objectives of this thesis follow from the following questions:

(Q_1) How to design derivative-free equilibrium seeking for GNEPs?

(Q_2) Is time-scale separation necessary for equilibrium seeking in systems with dynamical agents?

(Q_3) Is monotonicity of the pseudo-gradient sufficient to ensure convergence of derivative-free continuous-time equilibrium seeking?

(Q_4) Is discrete-time equilibrium seeking applicable to systems with hybrid dynamical agents?

The following chapters of the thesis are devoted to answering these questions.

1.4 Thesis organization

Figure 1.3 shows the structure of the thesis. We provide a summary of each chapter.

Part 1: Equilibrium seeking via output derivative estimators

To develop a zeroth-order GNE seeking method for dynamical systems, we focus on output derivative-based estimators, as, in principle, they do not require a time-scale separation between the equilibrium seeking algorithm and the system dynamics. We discover certain issues with the theory and propose two algorithms. The first is a single-timescale algorithm that converges for a restricted class of systems, while the second is a and multi-time scale algorithm that is applicable to a broader range of systems. In which real-life scenarios is it necessary to "blindly" optimize your cost?

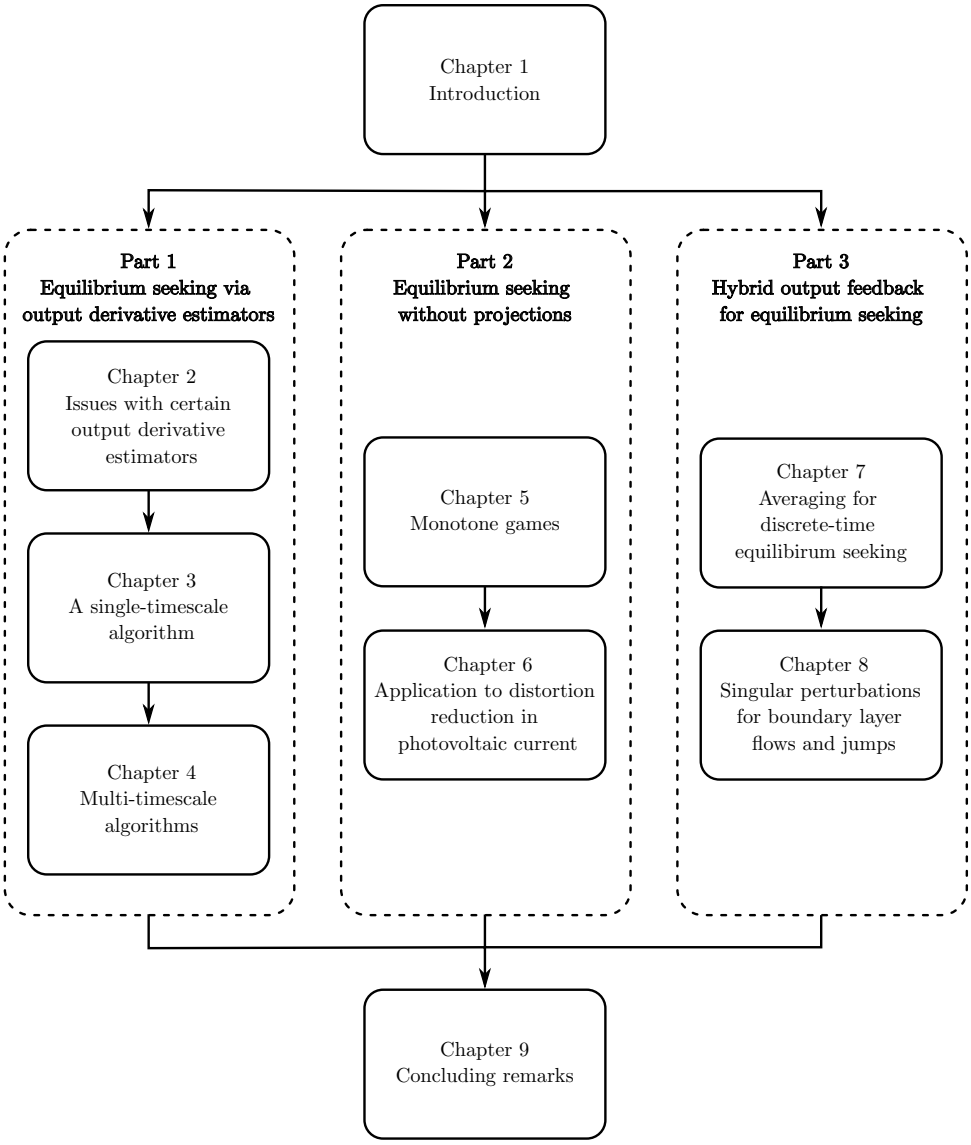

Figure 1.3: Structure of the thesis. Arrows indicate read-before relations.

1

- **Chapter 2: Issues with certain output derivative estimators**
  In this chapter, we present an error in one of the equations included in the proof of [20]. Furthermore, we derive a necessary Lyapunov stability condition for a certain class of problems and show how the condition predicts instability in numerical simulation. Lastly, we show inconsistencies in one of the underlying assumptions.
  This chapter is partially based on the following publication:

  [21] S. Krilašević and S. Grammatico. "Comments on "A proportional-integral extremum-seeking controller design technique"[Automatica 77 (2017) 61–67]". In: *Automatica* 135 (Jan. 2022), p. 109932. ISSN: 0005-1098. DOI: 10.1016/j.automatica.2021.109932.

- **Chapter 3: A single-timescale algorithm**
  Building on the findings of the previous chapter, we develop a zeroth-order algorithm for seeking Nash equilibrium for a specific class of linear systems that satisfy a condition similar to Equation 6 in [20]. Our simulations demonstrate that the proposed algorithm requires lower perturbation amplitudes and frequencies compared to other relevant algorithms.
  This chapter is partially based on the following publication:

  [22] S. Krilašević and S. Grammatico. "An integral Nash equilibrium control scheme for a class of multi-agent linear systems". In: *IFAC WC* 53 (2020), pp. 5375–5380. ISSN: 2405-8963. DOI: 10.1016/j.ifacol.2020.12.1521.

- **Chapter 4: Multi-timescale algorithms**
  Our application of output derivative estimators on equilibrium seeking concludes with the development of an algorithm that can find generalized Nash equilibrium using only zeroth-order information. We make dual dynamics commutable by preconditioning the forward-backward algorithm and use singular perturbation theory to handle a wider range of dynamical systems. While our main problem setup assumes the presence of a central coordinator responsible for dual variable computation, we also present a decentralized algorithm for computing the dual variables.
  This chapter is partially based on the following publication:

  [23] S. Krilašević and S. Grammatico. "Learning generalized Nash equilibria in multi-agent dynamical systems via extremum seeking control". In: *Automatica* 133 (Nov. 2021), p. 109846. ISSN: 0005-1098. DOI: 10.1016/j.automatica.2021.109846.

Part 2: Equilibrium seeking without projections

Some important obstacles must be tackled to relax the strong monotonicity assumption on the pseudogradient mapping in zeroth-order equilibrium seeking. One challenge is to devise an equilibrium seeking algorithm that requires only one pseudogradient "computation" during flows, as the pseudogradient estimation method solely provides an instant estimate. Furthermore, the present algorithms that meet these requirements do not involve projections, making them unsuitable for problems with local or shared constraints. In this

part of the thesis, we propose a new algorithm that meets the challenges and demonstrate its effectiveness in several practical scenarios.

- **Chapter 5: Monotone games**
  The continuous-time variant of the golden-ratio algorithm is able to find Nash equilibria in monotone games without constraints. Our approach involves using a projectionless dualization scheme with the golden-ratio algorithm to incorporate constraints in the problem and solve generalized Nash equilibrium problems (GNEPs) with only monotone pseudogradient mapping. Additionally, we improve the algorithm's numerical performance by implementing a hybrid gain adaptation scheme and showcase its effectiveness in two numerical simulations.
  This chapter is partially based on the following publication:

  [24] S. Krilašević and S. Grammatico. "Learning generalized Nash equilibria in monotone games: A hybrid adaptive extremum seeking control approach". en. In: *Automatica* 151 (May 2023), p. 110931. ISSN: 0005-1098. DOI: 10.1016/j.automatica.2023.110931.

- **Chapter 6: Application to distortion reduction in photovoltaic current**
  The use of extremum seeking methods in photovoltaic systems necessarily introduces perturbations into the output current of the system. To optimize the power output and minimize the distortions we formulate the so-called bilevel optimization problem by using a similar approach as in the numerical example of Chapter 5. Through a numerical simulation, we demonstrate that our approach diminishes total harmonic distortion, thus elevating the quality of the output current.
  This chapter is partially based on the following manuscript:

  [25] S. Krilašević and S. Grammatico. "Distortion reduction in photovoltaic output current via optimized extremum seeking control". In: *2023 21st European Control Conference (ECC)* (June 2023).

Part 3 - Hybrid output feedback for equilibrium seeking

Continuous time equilibrium seeking algorithms have the potential to solve a wide range of problems. However, one of their drawbacks is that they must be discretized for real-world implementation, which can reduce convergence speed and even result in instability. Conversely, although discrete-time algorithms can be implemented on a controller, zeroth-order GNE seeking algorithms generally do not produce results as strong as their continuous counterparts. To address these challenges and develop discrete-time algorithms for NE seeking with local constraints and asynchronous sampling, as well as to enable the application of hybrid equilibrium seeking algorithms on hybrid plants, we expand on existing averaging theory for discrete systems and singular perturbation theory for hybrid systems.

- **Chapter 7: Averaging for discrete-time equilibrium seeking**
  The estimation of the (pseudo)gradient in zeroth-order algorithms with sinusoidal perturbations relies on averaging, but incorporating local constraints is challenging due to the problems caused by projections. To address this, a three-layer algorithm is necessary, with the first layer performing (pseudo)gradient estimation without

projections, the second layer performs the filtering of the estimate, and the third layer with projections contains the equilibrium seeking algorithm with the filtered values of the estimate that steers the system towards the equilibrium. To design a multi-layer algorithm, we improve the existing discrete-time averaging theory by relaxing stability requirements for the averaged system and enabling its use on multi-timescale layer systems. Our theory also allows us to develop an asynchronous NE seeking algorithm with weak sampling period requirements for the agents. This chapter is partially based on the following manuscript:

[26] S. Krilašević and S. Grammatico. "A discrete-time averaging theorem and its application to zeroth-order Nash equilibrium seeking". In: arXiv:2302.04854 (Feb. 2023). arXiv:2302.04854 [cs, eess, math]. DOI: 10.48550/arXiv.2302.04854.

- **Chapter 8: Singular perturbations for hybrid reduced and boundary layer systems**
  The existing theory assumes that the reduced system can jump from anywhere in the jump set. Our theory restricts the jumps of the reduced system only to the boundary layer manifold. This new approach allows the convergence of the reduced system to be "jump-driven" rather than "flow-driven" as was previously the case. Additionally, we demonstrate that the fast states converge to the boundary layer manifold under a certain jump mapping condition rather than being only bounded as previously shown. We apply our theory to a connectivity control problem where the agents are hybrid unicycle systems, and the control algorithm used is the asynchronous NE seeking algorithm from the previous chapter.
  This chapter is partially based on the following publication:

  [27] S. Krilašević and S. Grammatico. "Stability of singularly perturbed hybrid systems with restricted systems evolving on boundary layer manifolds". In: arXiv:2303.18238 (Mar. 2023). arXiv:2303.18238 [cs, eess, math]. DOI: 10.48550/arXiv.2303.18238.

I

Equilibrium seeking via output derivative estimators

2

Issues with certain output derivative estimators

To err is human, to forgive is divine.

Alexander Pope

We don't make mistakes, we have happy accidents.

Bob Ross

In the proof of [20, Th.1], Equation 6 is incorrect. Additionally, Assumption 2 is infeasible.

This chapter is partly based on S. Krilašević and S. Grammatico. "Comments on "A proportional-integral extremum-seeking controller design technique"[Automatica 77 (2017) 61–67]". In: *Automatica* 135 (Jan. 2022), p. 109932. ISSN: 0005-1098. DOI: 10.1016/j.automatica.2021.109932.

2.1 Introduction

The extremum seeking control algorithm proposed in [20] claims convergence of the state trajectories to a neighborhood of the minimizer of the measured cost function. Unlike most of the previous extremum seeking algorithms, this is done by estimating the time derivative along the closed-loop trajectory, instead of the gradient, of the cost function. In this chapter, we show by counterexample that Equation 6 in [20],

$$\nabla h(\pi(\hat{u}))^\top g(\pi(\hat{u})) = \nabla h(\pi(\hat{u}))^\top \nabla \pi(\hat{u}) \tag{2.1}$$

which is used in the proof of Theorem 1 (page 65, left column, line 16) to obtain a negative Lyapunov derivative, is incorrect, as confirmed by the Authors [28].

2.2 Problem statement and Equation 6 in [20]

Let us use the same problem statement and notation as in [20], hence consider control affine systems:

$$\dot{x} = f(x) + g(x)u, \tag{2.2}$$
$$y = h(x), \tag{2.3}$$

where $x \in \mathbb{R}^n$ is the state vector, $u \in \mathcal{U} \subseteq \mathbb{R}^m$ is the control input and $y \in \mathbb{R}$ is the output which evaluates the cost function $h : \mathbb{R}^n \to \mathbb{R}$. The following state-feedback control is studied in [20], before Equation 3:

$$u(x) = \hat{u} - k^* g(x)^\top \nabla h(x), \tag{2.4}$$

where $\hat{u}$ is a constant vector and k^* is a nonnegative constant [20, p. 62, right coumn, line 16]. The extremum seeking literature often assumes convergence of the state vector towards an input-defined equilibrium vector, e.g., [12, Ass. 2.1], [17, Ass. 2]. The mapping that characterizes this convergence is the steady-state mapping, $\pi : \mathbb{R}^p \to \mathbb{R}^n$, which solves the equation

$$f(\pi(\hat{u})) + g(\pi(\hat{u}))\left[\hat{u} - k^* g(\pi(\hat{u}))^\top \nabla h(\pi(\hat{u}))\right] = \mathbf{0}.$$

Let us also consider the steady-state cost function [20, Equ. 3]:

$$l(\hat{u}) = h(\pi(\hat{u})). \tag{2.5}$$

Equation 6 in [20] claims that

$$\nabla h(\pi(\hat{u}))^\top g(\pi(\hat{u})) = \nabla h(\pi(\hat{u}))^\top \nabla \pi(\hat{u}) = \nabla l(\hat{u}). \tag{2.6}$$

2.3 Counterexample

We consider linear systems with strongly convex quadratic cost, i.e.,

$$f(x) = Ax, \quad g(x) = B,$$
$$h(x) = \tfrac{1}{2} x^\top Q x + x^\top p, \tag{2.7}$$

where $A \in \mathbb{R}^{n\times n}$ is Hurwitz, $B \in \mathbb{R}^{n\times m}$, $Q \in \mathbb{R}^{n\times n}$ is positive definite, $p \in \mathbb{R}^n$. Therefore, the steady-state mapping is given by

$$\pi(\hat{u}) = -\tilde{A}^{-1}B\hat{u} + V, \tag{2.8}$$

where $\tilde{A} \coloneqq A - k^* BB^\top Q$ and $V \coloneqq k^* \left(A - k^* BB^\top Q\right)^{-1} BB^\top p$. Since the gradient of the cost function is given by $\nabla h(x) = Qx + p$, it follows that $\nabla h(\pi(\hat{u})) = -Q\tilde{A}^{-1}B\hat{u} + QV + p$. In turn, the left-hand side of Equation (2.6) is calculated as:

$$\nabla h(\pi(\hat{u}))^\top g(\pi(\hat{u})) = \left(p^\top + V^\top Q - \hat{u}^\top B^\top \tilde{A}^{-\top} Q\right) B. \tag{2.9}$$

Seeing that $\nabla\pi(\hat{u}) = -\tilde{A}^{-1}B$, the right-hand side of Equation (2.6) is given by

$$\nabla h(\pi(\hat{u}))^\top \nabla\pi(\hat{u}) = -\left(p^\top + V^\top Q - \hat{u}^\top B^\top \tilde{A}^{-\top} Q\right) \tilde{A}^\top B. \tag{2.10}$$

Considering that the vectors in (2.9) and (2.10) are not equal in general (unless $A = -I, k^* = 0$ as in [22]), [20, Equ. 6] is incorrect.

2.4 A key Lyapunov stability condition

We note that Equation 6 in [20] is used in the proof of Theorem 1 on page 65, while applying Assumption 4, to prove that

$$\nabla h(\pi(\hat{u}))^\top g(\pi(\hat{u}))\tilde{u} = \nabla l(\hat{u})\tilde{u} \le -\alpha_u \|\tilde{u}\|^2, \tag{2.11}$$

for all $\hat{u}$. We now investigate how the incorrectness of [20, Equ. 6] affects the Lyapunov-based proof of [20, Thm. 1] for our counterexample in (2.7). Let u^* be the minimizer of $l(\hat{u})$ and $\tilde{u} \coloneqq u^* - \hat{u}$. From (2.9), it holds that

$$\begin{aligned}
&\nabla h(\pi(\hat{u}))^\top g(\pi(\hat{u}))\tilde{u} = \left(p^\top + V^\top Q - \hat{u}^\top B^\top \tilde{A}^{-\top} Q\right) B\tilde{u} \\
&+ \left(p^\top + V^\top Q - u^{*\top} B^\top \tilde{A}^{-\top} Q\right) B\tilde{u} - \left(p^\top + V^\top Q - u^{*\top} B^\top \tilde{A}^{-\top} Q\right) B\tilde{u} \\
&= -\tilde{u}^\top B^\top \tilde{A}^{-\top} QB\tilde{u} + \left(p^\top + V^\top Q - u^{*\top} B^\top \tilde{A}^{-\top} Q\right) B\tilde{u} \\
&= -\tfrac{1}{2}\tilde{u}^\top B^\top (\tilde{A}^{-\top} Q + Q\tilde{A}^{-1}) B\tilde{u} + \left(p^\top + V^\top Q - u^{*\top} B^\top \tilde{A}^{-\top} Q\right) B\tilde{u}
\end{aligned} \tag{2.12}$$

We note that the Lyapunov analysis in [20] relies on the strict negative-definiteness of the quadratic term in $\tilde{u}$, as it is used to majorize other positive terms (see for example, the last inequality of the left column on page 65). Therefore, for our case in (2.7), the matrix

$$M \coloneqq B^\top (\tilde{A}^{-\top} Q + Q\tilde{A}^{-1}) B \tag{2.13}$$

in (2.12) should be positive definite. It is possible for the matrix M to be negative definite, while the steady-state cost function, given by

$$l(\tilde{u}) = \frac{1}{2}\hat{u}^\top S\hat{u} - \hat{u}^\top B^\top \tilde{A}^\top (QV + p) + \frac{1}{2} V^\top QV + V^\top p \tag{2.14}$$

$$S \coloneqq B^\top \tilde{A}^\top Q\tilde{A}B, \tag{2.15}$$

to be strongly convex, i.e., $S \succ 0$.

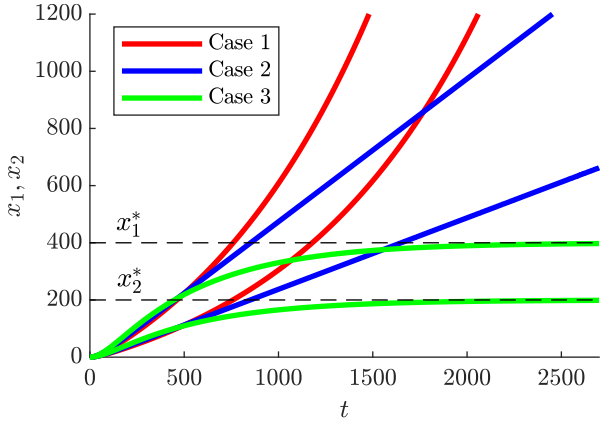

Figure 2.1: State evolution for all cases.

2.5 Numerical simulations

In view of (2.13), we simulate three different cases, $M \prec 0$, $M = 0$, and $M \succ 0$. To simplify the analysis, we use the perfect information variant of the algorithm in [20], i.e., $\hat{\theta}_1 = \theta_1$. The control law derived from [20, Equ. 20, 21], reads as

$$\begin{aligned} u &= -k_g g(x)^\top \nabla h(x) + \hat{u} \\ \dot{\hat{u}} &= -\tfrac{1}{\tau} g(x)^\top \nabla h(x). \end{aligned} \tag{2.16}$$

Specifically, for the system in (2.7) with the control law in (2.16), we have

$$\begin{aligned} u &= -k_g B^\top (Qx + p) + \hat{u} \\ \dot{\hat{u}} &= -\tfrac{1}{\tau} B^\top (Qx + p). \end{aligned} \tag{2.17}$$

Thus, the closed-loop dynamics read as

$$\begin{bmatrix} \dot{x} \\ \dot{u} \end{bmatrix} = \begin{bmatrix} A & B \\ B^\top Q\left(-\frac{1}{\tau} - k_g A\right) & -k_g B^\top Q B \end{bmatrix} \begin{bmatrix} x \\ u \end{bmatrix} + \begin{bmatrix} 0 \\ -\frac{1}{\tau} B^\top p \end{bmatrix}. \tag{2.18}$$

We use the same parameters for all three simulations except for the Q matrices:

$$A = \begin{bmatrix} -\frac{1}{2} & 1 \\ -\frac{1}{4} & 0 \end{bmatrix}, \quad B = \begin{bmatrix} 0 \\ -1 \end{bmatrix}, \quad p = \begin{bmatrix} 0 \\ -2 \end{bmatrix}, \quad k^* = \frac{1}{2}, \quad k_g = 10, \quad \tau_I = 20;$$

$$\text{Case 1:}\quad Q = Q_1 = \begin{bmatrix} 1 & -\frac{1}{2}+\epsilon \\ -\frac{1}{2}+\epsilon & 1 \end{bmatrix} \implies M = -0.04, \qquad S = S_1 = 12.2$$

$$\text{Case 2:}\quad Q = Q_2 = \begin{bmatrix} 1 & -\frac{1}{2} \\ -\frac{1}{2} & 1 \end{bmatrix} \implies M = 0, \qquad S = S_2 = 12$$

$$\text{Case 3:}\quad Q = Q_3 = \begin{bmatrix} 1 & -\frac{1}{2}-\epsilon \\ -\frac{1}{2}-\epsilon & 1 \end{bmatrix} \implies M = 0.04, \qquad S = S_3 = 11.8,$$

with $\epsilon = 0.01$. As expected, the control scheme proposed in [20] stabilizes the system only in Case 3, as seen in Figure 2.1.

2.6 Further issues

Under Assumption 2 in [20], there exists a diffeomorphism $\text{col}(\xi, y) = \Theta(x)$ that transforms the dynamics (2.2) and (2.3) into the Byrnes-Isidori normal form given by

$$\dot{\xi} = \phi(\xi, y), \tag{2.19}$$

$$\dot{y} = \nabla h(\Theta^{-1}(\xi, y))^\top f(\Theta^{-1}(\xi, y)) + \nabla h(\Theta^{-1}(\xi, y))^\top g(\Theta^{-1}(\xi, y))u. \tag{2.20}$$

Now, the first bullet point of Assumption 3 in [20] states that the zero dynamics in (2.19) are input to state stable (ISS) from y to ξ with some Lyapunov function W, i.e. by Theorem 4.19 in [29]:

$$\alpha_1(\|\xi - \xi_0\|) \leq W(\xi) \leq \alpha_2(\|\xi - \xi_0\|), \tag{2.21}$$

for some class $\mathcal{K}$ functions α_1 and α_2, and for ξ_0 that is the equilibrium of the zero dynamics. The second bullet-point of Assumption 3 in [20] states that the function $W(\xi) + h(x)$ satisfies

$$\beta_1 \|x - \pi(\hat{u})\|^2 \leq W(\xi) + h(x) \leq \beta_2 \|x - \pi(\hat{u})\|^2. \tag{2.22}$$

Now, by plugging in $x = \pi(\hat{u})$ it follows that

$$W(\xi) + h(\pi(\hat{u})) = 0, \tag{2.23}$$

which still, according to Assumption 3 in [20] must hold *for all* $\hat{u} \in \mathcal{U}$, not just for the optimizer u^*. Since the cost function h is assumed strictly convex by Assumption 1 in [20] and $W(\xi)$ is greater or equal than zero from Equation (2.21), it follows that Equation (2.23) cannot hold for all $\hat{u} \in \mathcal{U}$.

Remark 2.1. *To overcome the issue due to Assumption 3, one may consider the Lyapunov function candidate* $W(\xi) + h(x) - h(\pi(\hat{u}))$. *However, since* $\hat{u}$ *is not constant in the ESC algorithm [1, Equ. 21], the proofs of Theorems 1 and 2 in [20] would need substantial modification.*

2.7 Conclusion

Equation 6 in [20] is incorrect. Consequently, the PI-ESC in [20] may not work in general, not even for linear systems with convex quadratic cost functions, except for certain special cases like for $A = -I$, $k^* = 0$ [22].

3

A single-timescale algorithm

Why do we fall Bruce?

Thomas Wayne, Batman Begins

Those who do not move, do not notice their chains.

Rosa Luxemburg

We propose an integral Nash equilibrium seeking control (I-NESC) law which steers the multi-agent system composed of a special class of linear agents to the neighborhood of the Nash equilibrium in noncooperative strongly monotone games. First, we prove that there exist parameters of the integral controller such that the system converges to the Nash equilibrium in the full-information case, in other words, without the parameter estimation scheme used in extremum seeking algorithms. Then we prove that there exist parameters of the I-NESC such that the system converges to the neighborhood of the Nash equilibrium in the limited information case where parameter estimation is used. We provide a simulation example that demonstrates that smaller perturbation frequencies and amplitudes are needed to attain a similar convergence speed as the existing state-of-the-art algorithm.

This chapter is partly based on S. Krilašević and S. Grammatico. "An integral Nash equilibrium control scheme for a class of multi-agent linear systems". In: *IFAC WC* 53 (2020), pp. 5375–5380. ISSN: 2405-8963. DOI: 10.1016/j.ifacol.2020.12.1521.

3.1 Introduction

Extremum seeking control (ESC) is a class of data-driven, adaptive control techniques used in optimization problems where the cost is a function of the states of a dynamical system. The method is a *zero-order* method which means it only uses the value of the cost function for optimization, and no a priori knowledge of the cost function is needed, except for some basic assumptions. There was no analytical proof of stability of ESC for general nonlinear systems until the paper [12]. This sparked renewed interest in further development of this type of control. Most of the research was based on the original paper by Krstić and Wang, e.g. [30], [31] etc. There were also methods based on different ideas, such as [32], where the authors proposed an extremum seeking scheme based on Lie algebra, which turned out to be equivalent to the Krstić-Wang scheme. Based on a parameter estimation scheme, Guay and Dochain propose an extremum seeking scheme [20] which does not use singular perturbation and averaging theory. As a result, a faster convergence rate is obtained. This fact motivates further research on such a type of ESC.

Nash equilibrium problems (NEP) are different from (distributed) optimization problems, as they are characterized by a number of selfish agents whose goal is to optimize their individual cost functions, possibly dependent on the decision variables of other agents. In NEPs, the constraints of each agent are independent of other agents, while in generalized Nash equilibrium problems (GNEPs), they are coupled. Recent interest in GNEPs is motivated by many engineering problems, such as demand-side management in the smart grids [33], charging/discharging of electric vehicles [34] and formation control [35]. The literature on (G)NEPs mostly ignores the dynamics of individual agents, which may be a problem in multi-agent systems with non-negligible dynamics. The small portion of the literature on (G)NEPs with dynamical agents can be divided into two groups: passivity-based first-order algorithms and extremum seeking *zero-order* algorithms.

By using a passivity property, the authors in [36] design a control law that guarantees convergence to the Nash equilibrium (NE) of a multi-agent system with single-integrator dynamics over a network. In [37], the authors extend the result to the multi-integrator case. The network topology is time invariant in both cases. In [38], the authors extend the results of [36] by designing a network weight adaptation scheme. In [39], a controller is proposed that guarantees convergence to a GNE of a multi-agent system with integrator dynamics over a network. Most prominently, extremum seeking was used for NE seeking in [7] where it is proven that the extremum seeking control, under certain conditions on the individual cost functions, converges to a neighborhood of the NE for general nonlinear agents. In [40], it is proven that the use of stochastic perturbation signals also induces convergence to a neighborhood of the NE. The authors in [17] propose a framework for the synthesis of a hybrid controller which may be used for NEPs with nonlinear agents. All mentioned extremum seeking controllers are based on [12].

Contribution

Motivated by the recent research interest in NEPs, we adapt the ESC proposed in [41], [20]. Specifically, our contributions are the following:

- We extend a known proportional-integral extremum seeking control scheme to strongly monotone NEPs for multi-agent linear systems, and we prove a practical convergence to a Nash equilibrium;

- We numerically observe an improved performance with respect to [7], as smaller amplitudes and frequencies of the sinusoidal perturbations signals are needed for a comparable convergence rate.

3.2 Problem setup

We consider a multi-agent system with N agents indexed by $\mathcal{I} = \{1, 2, \dots, N\}$, each with the following dynamics:

$$\begin{aligned} \dot{x}_i &= -x_i + B_i u_i, \\ y_i &= h_i(x_i, \mathbf{x_{-i}}), \end{aligned} \tag{3.1}$$

where $x_i \in \mathbb{R}^{n_i}$ is the state vector, $u_i \in \mathbb{R}^{m_i}$ is the control input, $y_i \in \mathbb{R}$ is the output variable which evaluates the cost function $h_i : \mathbb{R}^{n_i} \times \mathbb{R}^{n_{-i}} \to \mathbb{R}$. Let us also define $n := \sum n_i$, $n_{-i} := \sum_{j \neq i} n_j$ and $m := \sum m_i$.

Standing Assumption 3.1 (Regularity). *For each $i \in \mathcal{I}$, the function h_i in (3.1) is continuous, differentiable in x_i and its partial gradient $\nabla_{x_i} h_i$ is Lipschitz continuous in x_i and $\mathbf{x_{-i}}$.* □

A common assumption amongst the extremum seeking literature (for example [20], [12], [17]) is the existence of the steady-state mapping, which tells us to which state(s) the system converges when a constant input is applied. For our subsystems (3.1), there exists a mapping

$$\pi(\mathbf{u}) := \operatorname{col}((\pi_\mathbf{i}(\mathbf{u_i}))_{\mathbf{i} \in \mathcal{I}}) = \operatorname{col}((\mathbf{B_i u_i})_{\mathbf{i} \in \mathcal{I}}) \tag{3.2}$$

such that for every $i \in \mathcal{I}$, $\pi_i(u_i) = B_i u_i$. Let us also define

$$\pi_{-i}(\mathbf{u_{-i}}) := \operatorname{col}\left(\left(\pi_\mathbf{j}(\mathbf{u_j}) \right)_{\mathbf{j} \neq \mathbf{i}} \right). \tag{3.3}$$

In this chapter, we assume that the goal of each agent is to minimize its steady-state cost function, i.e.,

$$\min_{u_i \in \mathbb{R}^{m_i}} h_i\left(\pi_i(u_i), \pi_{-i}(\mathbf{u_{-i}})\right), \tag{3.4}$$

which depends on the inputs of some other agents as well. From a game-theoretic perspective, we consider the problem to compute a Nash equilibrium (NE).

Definition 3.2 (Nash equilibrium). *A collective input $\mathbf{u}^*$ is a NE of the game (3.4) if for all $i \in \mathcal{I}$*

$$h_i\left(\pi_i(u_i^*), \pi_{-i}(\mathbf{u_{-i}^*})\right) \leq \inf_{u_i \in \mathbb{R}^{n_i}} h_i\left(\pi_i(u_i), \pi_{-i}(\mathbf{u_{-i}^*})\right). \qquad \blacksquare$$

In plain words, a set of inputs is a NE if no agent can improve its steady-state cost function by unilaterally changing its input. Since the steady-state cost functions are differentiable in u_i, it follows from Thm. 16.3 in [42] that a collective vector $\mathbf{u}^*$ is a NE if and only if

$$\nabla_{u_i} h_i\left(\pi_i(u_i^*), \pi_{-i}(\mathbf{u_{-i}^*})\right) = 0. \tag{3.5}$$

In view of (3.5), we can stack all of the partial gradients into a single vector and form the so-called pseudo-gradient mapping of the steady-state cost functions:

$$F(\mathbf{u}) \coloneqq \operatorname{col}\left(\left(\nabla_{\mathbf{u_i}} \mathbf{h_i}\left(\pi_{\mathbf{i}}(\mathbf{u_i}), \pi_{-\mathbf{i}}(\mathbf{u_{-i}})\right)\right)_{\mathbf{i}\in\boldsymbol{\mathcal{I}}}\right). \tag{3.6}$$

Therefore, by (3.5) and (3.6), we note that the problem of finding a Nash equilibrium of the game in (3.4) is equivalent to finding $\mathbf{u}^*$ such that $F(\mathbf{u}^*) = \mathbf{0}$, which is the problem of finding a zero of F in (3.6), $\mathbf{u}^* \in \operatorname{zer}(\mathbf{F})$. A relatively standard assumption in modern game theory literature [43], [44] is strong monotonicity of the pseudo-gradient mapping:

Standing Assumption 3.3 (Strong monotonicity)**.** *The mapping F in (3.6) is strongly monotone, i.e.,*

$$\langle F(\mathbf{u}) - \mathbf{F}(\mathbf{v}) \mid \mathbf{u} - \mathbf{v} \rangle \geq \mu \|\mathbf{u} - \mathbf{v}\|^2, \tag{3.7}$$

for all $(\mathbf{u}, \mathbf{v}) \in \mathbb{R}^{\mathbf{2m}}$, for some $\mu > 0$. □

Let us also define the pseudo-gradient of the cost functions

$$F_{\mathrm{x}}(\mathbf{x}) \coloneqq \operatorname{col}\left(\left(\nabla_{\mathbf{x_i}} \mathbf{h_i}\left(\mathbf{x_i}, \mathbf{x_{-i}}\right)\right)_{\mathbf{i}\in\boldsymbol{\mathcal{I}}}\right). \tag{3.8}$$

We note that, in general, monotonicity of $F_{\mathrm{x}}(\mathbf{x})$ does not imply monotonicity of $F(\mathbf{u})$.

3.3 Integral Nash equilibrium seeking control

3.3.1 Full-information case

We consider the case where every agent knows the analytic expression of its partial gradient and has access to the inputs of the other agents. Our proposed control law is inspired by the extremum seeking control in [20], [41]:

$$\forall i \in \boldsymbol{\mathcal{I}} \ : \ \dot{u}_i = -\tau_i^{-1} B_i^{\top} \nabla_{x_i} h_i(x_i, \mathbf{x}_{-\mathbf{i}}) \tag{3.9}$$

or in collective vector form

$$\dot{\mathbf{u}} = -\tau^{-\mathbf{1}} \mathbf{B}^{\top} \mathbf{F}_{\mathrm{x}}(\mathbf{x}), \tag{3.10}$$

where $\mathbf{B} \coloneqq \operatorname{blkdiag}(\mathbf{B_1}, \ldots, \mathbf{B_N})$ and $\tau \coloneqq \operatorname{blkdiag}(\tau_1, \ldots, \tau_{\mathbf{N}})$. Unlike [20], we do not use the proportional part, as it does not help with the convergence to the Nash equilibrium.

Theorem 3.4. *Let the Standing Assumptions hold and let $(\mathbf{x}(\mathbf{t}), \mathbf{u}(\mathbf{t}))$, $t \geq 0$, be the closed-loop solution to the dynamics in (3.1) with control law in (3.9)–(3.10). Then, there exists τ^*, such that if every agent chooses $\tau_i \in (\tau^*, \infty)$, the trajectories $(\mathbf{x}(\mathbf{t}), \mathbf{u}(\mathbf{t}))$ converge to $(\mathbf{x}^*, \mathbf{u}^*) = (\pi(\mathbf{u}^*), \mathbf{u}^*)$, where $\mathbf{u}^*$ is a Nash equilibrium of the game in (3.4).* □

Proof. See Appendix 3.A. ■

3.3.2 Limited information case

Next, we examine the scenario where agents can only access their individual cost output. We emphasize that they neither know the actions of other agents nor they know the analytic expressions of their partial gradients. This setup is a typical setting in extremum seeking methods such as those presented in [20], [12], and [17]. Our approach involves the use of pseudogradient estimates by agents in the control law of Equation (3.9) designed for perfect-information scenarios.

The extremum seeking control proposed by [20] assumes that the cost function of the system has a strong relative degree of value one. This means that the first derivative of the cost function directly influences the input to the system. In the case of multi-agent systems, where the cost functions do not depend only on the states of their agent but also of the others, we make an analogous assumption:

Assumption 3.5 (Degree of the output). *For every* $i \in \mathcal{I}$, $\nabla_{x_i} h_i(x_i, \mathbf{x}_{-\mathbf{i}})^\top \mathbf{B_i} \neq \mathbf{0}$ *for all* $(x_i, \mathbf{x}_{-\mathbf{i}}) \in \mathbb{R}^{\mathbf{n}} \setminus \{\mathbf{x}^*\}$. □

Let us first evaluate the derivative of the cost functions:

$$\begin{aligned}\dot{y}_i = &-\sum_{j=1}^{N} \nabla_{x_j} h_i(\mathbf{x})^\top \mathbf{x_i} + \sum_{\mathbf{j}\neq\mathbf{i}}^{\mathbf{N}} \nabla_{\mathbf{x_j}} \mathbf{h_i}(\mathbf{x})^\top \mathbf{B_j u_j} \\ &+ \nabla_{x_i} h_i(\mathbf{x})^\top \mathbf{B_i u_i},\end{aligned} \tag{3.11}$$

and introduce the following variables:

$$\begin{aligned}\theta_i^0 &:= -\sum_{j=1}^{N} \nabla_{x_j} h_i(\mathbf{x})^\top \mathbf{x_i} + \sum_{\mathbf{j}\neq\mathbf{i}}^{\mathbf{N}} \nabla_{\mathbf{x_j}} \mathbf{h_i}(\mathbf{x})^\top \mathbf{B_j u_j}, \\ \theta_i^1 &:= \nabla_{x_i} h_i(\mathbf{x})^\top \mathbf{B_i}.\end{aligned} \tag{3.12}$$

The variable θ_i^0 measures the effect of the autonomous dynamics of agent i on its cost function and the effects of inputs of the other agents. The variable θ_i^1 measures the effect of the input of agent i on the cost output y_i. By substituting θ_i^0 and θ_i^1 in (3.11), the derivative reads as

$$\dot{y}_i = \theta_i^0 + \theta_i^1 u_i = [1, u_i^\top]\theta_i, \tag{3.13}$$

Note that θ_i^1 is proportional to the right-hand side in (3.9). To estimate the local θ_i^0 and θ_i^1, we use a time-varying parameter estimation approach such as the one proposed in [20]. Let us provide a basic intuition. Let $\hat{y}_i$ and $\hat{\theta}_i$ be estimations of the output y_i and the variable θ_i respectively and let $e_i = y_i - \hat{y}_i$ be the estimation error. Then, the estimator model of (3.13) for agent i is given by

$$\dot{\hat{y}}_i = [1, u_i^\top]\hat{\theta}_i + K_i e_i + c_i^\top \dot{\hat{\theta}}_i, \tag{3.14}$$

where K_i is a free design parameter. Note that the first two terms on the right-hand side resemble high-gain observer schemes. As the structure of the problem does not allow the use of high-gain observers, it is necessary to introduce some other dynamics into the estimation. This is the primary role of the third term in (3.14). Therefore, the dynamics of $c_i(t)$ are chosen as

$$\dot{c}_i^\top = -K_i c_i^\top + [1, u_i^\top]. \tag{3.15}$$

Let us introduce an auxiliary variable η_i, with dynamics $\dot{\eta}_i = -K_i\eta_i - c_i^\top \dot{\theta}$, and its estimate $\hat{\eta}_i$, with dynamics

$$\dot{\hat{\eta}}_i = -K_i\hat{\eta}_i. \tag{3.16}$$

It is also necessary to define a symmetric, positive definite scaling matrix variable $\Sigma_i \in \mathbb{R}^{m_i+1\times m_i+1}$ with dynamics

$$\dot{\Sigma}_i = c_i c_i^\top - k_i^{\mathrm{T}}\Sigma_i + \sigma_i \tag{3.17}$$

$$\Sigma_i(0) = \alpha_i^1, \tag{3.18}$$

where $k_i^\top$, σ_i and α_1^i are free design parameters. The third term is added so that the matrix is always invertible. Equations (3.14)-(3.18) form the parameter update law presented in [45]:

$$\dot{\hat{\theta}}_i = \Pi_{\Theta_i}\left(\hat{\theta}_i, \Sigma_i^{-1}(c_i(e_i - \hat{\eta}_i) - \sigma_i\hat{\theta}_i)\right), \tag{3.19}$$

where $\Pi_{\Theta_i}(\hat{\theta}, v)$ denotes the projection of the vector v onto the tangent cone of the set Θ_i at $\hat{\theta}$, as defined by Equation 2.14 in [46]. This implies that if the starting value $\hat{\theta}_i(0)$ is in Θ_i, so will $\hat{\theta}_i(t)$ for all t. We are finally ready to propose an integral decentralized Nash equilibrium seeking control law of the form

$$\forall i \in \mathcal{I} : \begin{cases} u_i = \hat{u}_i + d_i(t) \\ \dot{\hat{u}}_i = -\tau_i^{-1}\hat{\theta}_i^1 \end{cases} \tag{3.20}$$

together with Equations (3.14)–(3.19). In the collective vector form, Equation (3.20) read as

$$\begin{cases} \mathbf{u} = \hat{\mathbf{u}} + \mathbf{d(t)} \\ \dot{\hat{\mathbf{u}}} = -\tau^{-1}\hat{\theta}^{\mathbf{1}} \end{cases} \tag{3.21}$$

As in [20], a persistency of excitation (PE) assumption for every agent is introduced for the parameter estimation scheme to converge.

Assumption 3.6 (Persistence of excitation)**.** *For every $i \in \mathcal{I}$, there exist constants α_i^2 and T_i such that*

$$\int_t^{t+T_i} c_i(\tau)c_i(\tau)^\top d\tau \geq \alpha_i^2 I, \quad \forall t > 0, \tag{3.22}$$

where $c_i(\tau)$ is the solution to (3.15). □

We conclude the section with the main theoretical result of the chapter, namely, the convergence of the closed-loop dynamics to a Nash equilibrium of the game.

Theorem 3.7. *Let the Standing Assumptions and Assumptions 3.5, 3.6 hold and let $(\mathbf{x(t)}, \mathbf{u(t)})$ be the closed-loop solution to the dynamics (3.1) with control law in (3.14) – (3.19), (3.20). Let π be the steady-state mapping in (3.2) and let D be the largest amplitude of the perturbation signals $\{d_i(t)\}_{i\in\mathcal{I}}$. Then, it is possible to tune gains $(\tau_i, \sigma_i, K_i, k_i^{\mathrm{T}},)_{i\in\mathcal{I}}$ in that order, so that the trajectories $(\mathbf{x(t)}, \mathbf{u(t)})$ converge towards the $\mathcal{O}(D^2)$ neighborhood of some $(\mathbf{x}^*, \mathbf{u}^*) = (\pi(\mathbf{u}^*), \mathbf{u}^*)$, where $\mathbf{u}^*$ is a Nash equilibrium of the game in (3.4).* □

Proof. See Appendix 3.B for both the proof and the details of the parameter tuning. ■

3.4 Simulation example

Consider a three agent system with dynamics:

$$\dot{x}_i = -x_i + u_i, \text{ for } i \in \{1,2,3\}. \tag{3.23}$$

The cost functions of agents are given by

$$\begin{aligned} y_1 &= 1.5(x_1-1)^2 + 1.5x_1x_2 + x_1x_3 \\ y_2 &= -2x_2x_1 + 1.5(x_2-2)^2 + x_2x_3 \\ y_3 &= -2.5x_3x_1 - x_3x_2 + 1.5(x_3-3)^2. \end{aligned} \tag{3.24}$$

Two types of controllers were simulated to have a comparison; the limited information controller proposed in this chapter and the controller from [7] with additional low-pass and high-pass filters as in [12] to improve the performance. The latter can be described by the following equations

$$\begin{aligned} \dot{\eta}_i &= -\omega_h^i \eta_i + \omega_h^i y_i, \\ \dot{\xi}_i &= -\omega_l^i \xi_i + \omega_l^i (y_i - \eta_i) A_i \sin(\omega_i t), \\ \dot{\hat{u}}_i &= -k_i A_i \xi_i, \; u_i = \hat{u}_i + A_i \sin(\omega_i t). \end{aligned} \tag{3.25}$$

For our controller, the following parameters were chosen: $\sigma_1 = \sigma_2 = \sigma_3 = 10^{-6}$, $K_1 = K_2 = K_3 = 50$, $k_T^1 = k_T^2 = k_T^3 = 50$, $\alpha_I^1 = \alpha_I^2 = \alpha_I^3 = 0.1$, $\tau_1 = 5$, $\tau_I^2 = 10$, $\tau_I^3 = 15$, $d_1(t) = \frac{1}{2}\sin(40t)$, $d_2(t) = \frac{1}{2}\sin(50t)$ and $d_3(t) = \frac{1}{2}\sin(60t)$. Initial states of $\mathbf{x}$, $\hat{\mathbf{u}}$, $\mathbf{c}$, θ and η were set to zero. The parameters K, k^{T}, and τ_I were initially chosen large enough to ensure stability. Then τ_I was decreased to speed up the convergence. Further decreases in τ_I made the states oscillate; further decreases of K and k^{T} did not improve the algorithm's performance. For the Frihauf et al., the following parameters were chosen: $\omega_h^1 = 180$, $\omega_h^2 = 200$, $\omega_h^3 = 220$, $\omega_l^1 = 45$, $\omega_l^2 = 50$, $\omega_l^3 = 55$, $\omega_1 = 90$, $\omega_2 = 100$, $\omega_3 = 110$, $k_1 = k_2 = k_3 = 0.5$ and $A_1 = A_2 = A_3 = 5$. Firstly, we chose ω_1, ω_2, and ω_3 such that the highest convergence rate for a fixed A_i was observed. Higher perturbation frequencies facilitate faster learning of the gradient, but also higher frequencies get damped out. At the chosen frequencies, the best trade-off was observed. Next, the amplitude was increased to speed up the convergence. After $A_i = 5$, a non-significant increase in performance was observed. The results of the numerical simulations can be seen in Figures 3.1 and 3.2. While the convergence speed of both algorithms is similar, the frequency and amplitude of the sinusoidal perturbation signals are much lower with our I-NESC law.

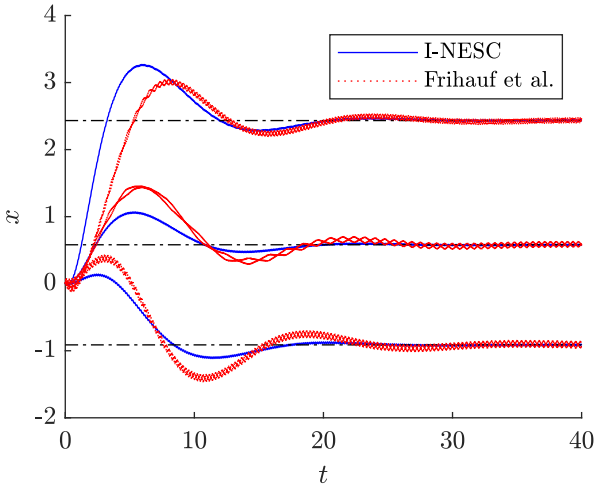

Figure 3.1: State trajectories of the three agents under I-NESC (solod blue) and [7] (doted red)

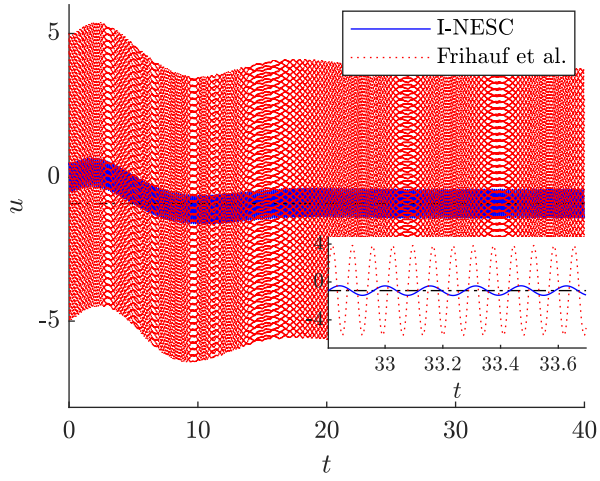

Figure 3.2: Input of the first agent under I-NESC (solid blue) and [7] (doted red)

3.5 Conclusion

Nash equilibrium problems can be solved efficiently via extremum seeking if the agents belong to a certain class of linear dynamics with strongly monotone and Lipschitz continuous game mapping.

Appendix

3.A Proof of Theorem 1

Stability of equilibrium points $\pi_i(u_i)$ for every agent $i \in \mathcal{I}$ can be characterised by the following Lyapunov function:

$$V_i(x_i, u_i) = \frac{\beta}{2} \|x_i - B_i u_i\|^2, \tag{3.26}$$

where $\beta > 0$. The derivative of (3.26) is equal to

$$\dot{V}_i(x_i, u_i) = -\beta \|x_i - \pi_i(u_i)\|^2 - \beta \langle x_i - \pi_i(u_i) \mid B\dot{u}_i \rangle. \tag{3.27}$$

For very slow changes of the input u_i, we expect the subsystems will converge to a small neighborhood of equilibrium points $\pi_i(u_i)$. We consider the controller in (3.10). Its goal is to estimate the Nash equilibrium input $\mathbf{u}^*$ and to preserve the stability of the subsystems. Therefore, we construct the following Lyapunov function candidate:

$$W(\mathbf{x}, \mathbf{u}) := \mathbf{T}(\mathbf{u}) + \mathbf{V}(\mathbf{x}, \mathbf{u}) = \frac{1}{2} \|\tilde{\mathbf{u}}\|^2_{\tau_{\min}^{-1}} + \sum_{\mathbf{i}=1}^{\mathbf{N}} \mathbf{V_i}(\mathbf{x_i}, \mathbf{u_i}), \tag{3.28}$$

where $\tilde{\mathbf{u}} = \mathbf{u} - \mathbf{u}^*$ and $\tau_{\min} = \min\{\tau_1, \ldots, \tau_N\}$. Now, we bound the derivative of T. By adding and subtracting $F(\mathbf{u})$ to (3.10), $\dot{\mathbf{u}}$ reads as

$$\dot{\mathbf{u}} = -\tau^{-1}\mathbf{F}(\mathbf{u}) - \tau^{-1}(\mathbf{B}^\top \mathbf{F}_{\mathrm{x}}(\mathbf{x}) - \mathbf{F}(\mathbf{u})). \tag{3.29}$$

From (3.28) and (3.29), we have

$$\dot{T}(\mathbf{x}, \mathbf{u}) = -\tau_{\min}^{-1} \langle \tilde{\mathbf{u}} \mid \mathbf{F}(\mathbf{u}) \rangle - \tau_{\min}^{-1} \left\langle \tilde{\mathbf{u}} \,\middle|\, \mathbf{B}^\top \mathbf{F}_{\mathrm{x}}(\mathbf{x}) - \mathbf{F}(\mathbf{u}) \right\rangle. \tag{3.30}$$

Considering $F(\mathbf{u})$ is strongly monotone and we have $F(\mathbf{u}^*) = \mathbf{0}$, since $\mathbf{u}^* \in \mathrm{zer}(\mathbf{F})$, (3.7) reads as

$$\langle F(\mathbf{u}) \mid \mathbf{u} - \mathbf{u}^* \rangle = \langle F(\mathbf{u}) \mid \tilde{\mathbf{u}} \rangle \geq \mu \|\mathbf{u} - \mathbf{u}^*\|^2. \tag{3.31}$$

To bound the second term in (3.30), we use the identity:

$$\nabla_{u_i} h_i(\pi_i(u_i), \pi_{-i}(\mathbf{u}_{-\mathbf{i}}))^\top = \nabla_{\mathbf{x_i}} \mathbf{h_i}(\pi_{\mathbf{i}}(\mathbf{u_i}), \pi_{-\mathbf{i}}(\mathbf{u}_{-\mathbf{i}}))^\top \mathbf{B_i}. \tag{3.32}$$

By using the relations (3.6), (3.8) and (3.32), it follows that:

$$\mathbf{B}^\top \mathbf{F}_{\mathrm{x}}(\pi(\mathbf{u})) = \mathbf{F}(\mathbf{u}). \tag{3.33}$$

By exploiting (3.31) and (3.33), from (3.30) we have

$$\dot{T} \leq -\frac{\mu}{\tau_{\min}}\|\mathbf{u}-\mathbf{u}^*\|^2 - \tau_{\min}^{-1}\left\langle \tilde{\mathbf{u}} \mid \mathbf{B}^\top \mathbf{F}_x(\mathbf{x}) - \mathbf{B}^\top \mathbf{F}_x(\pi(\mathbf{u}))\right\rangle. \tag{3.34}$$

Since all of the functions are Lipschitz continuous, the right-hand side in (3.34) can be upper bounded as follows:

$$\dot{T} \leq -\frac{\mu}{\tau_{\min}}\|\tilde{\mathbf{u}}\|^2 + \frac{L}{\tau_{\min}}\|\tilde{\mathbf{u}}\|\|\mathbf{x}-\pi(\mathbf{u})\|, \tag{3.35}$$

where $L>0$ is the Lipschitz constant of the mapping $\mathbf{B}^\top \circ \mathbf{F}_x$. Now, we turn our attention to the full Lyapunov function candidate W. The derivative is bounded as

$$\dot{W}(\mathbf{x},\mathbf{u}) \leq -\beta\|\mathbf{x}-\pi(\mathbf{u})\|^2 - \frac{\mu}{\tau_{\min}}\|\tilde{\mathbf{u}}\|^2 + \frac{\mathbf{L}}{\tau_{\min}}\|\tilde{\mathbf{u}}\|\|\mathbf{x}-\pi(\mathbf{u})\| - \beta\langle \mathbf{x}-\pi(\mathbf{u}) \mid \mathbf{B}\dot{\mathbf{u}}\rangle. \tag{3.36}$$

To complete the proof, we bound the derivative of V caused by the change of inputs:

$$-\beta\langle \mathbf{x}-\pi(\mathbf{u}) \mid \mathbf{B}\dot{\mathbf{u}}\rangle \leq \beta\|\mathbf{B}\|\|\dot{\mathbf{u}}\|\|\mathbf{x}-\pi(\mathbf{u})\|. \tag{3.37}$$

By using (3.29), the norm of the derivative is bounded:

$$\|\dot{\mathbf{u}}\| \leq \tau_{\min}^{-1}\|F(\mathbf{u})\| + \tau_{\min}^{-1}\|(\mathbf{B}^\top \mathbf{F}_x(\mathbf{x}) - \mathbf{F}(\mathbf{u}))\|. \tag{3.38}$$

Again, since all of the functions are Lipschitz continuous, the right-hand side of the previous equation can be bounded as follows

$$\|\dot{\mathbf{u}}\| \leq \frac{L_F}{\tau_{\min}}\|\tilde{\mathbf{u}}\| + \frac{L}{\tau_{\min}}\|\mathbf{x}-\pi(\mathbf{u})\|, \tag{3.39}$$

where $L_F>0$ is the Lipschitz constant of F. By using the bounds (3.37) and(3.39), $\dot{W}$ can be bounded as follows:

$$\dot{W}(\mathbf{x},\mathbf{u}) \leq -\begin{bmatrix} \|\tilde{\mathbf{u}}\| \\ \|\mathbf{x}-\pi(\mathbf{u})\| \end{bmatrix}^\top \mathbf{M} \begin{bmatrix} \|\tilde{\mathbf{u}}\| \\ \|\mathbf{x}-\pi(\mathbf{u})\| \end{bmatrix} \tag{3.40}$$

where

$$M = \begin{bmatrix} \beta - L\beta\|\mathbf{B}\|\tau_{\min}^{-1} & -\frac{1}{2}(L+\beta\|\mathbf{B}\|\mathbf{L}_F)\tau_{\min}^{-1} \\ -\frac{1}{2}(L+\beta\|\mathbf{B}\|\mathbf{L}_F)\tau_{\min}^{-1} & \frac{\mu}{\tau_{\min}} \end{bmatrix}. \tag{3.41}$$

Thus, if $\tau_{\min} > \frac{(L+\beta\|\mathbf{B}\|\mathbf{L}_F)^2+4\mathbf{L}\beta\|\mathbf{B}\|}{4\beta\mu}$, then the matrix M in (3.41) is positive definite, which in turn implies that $\dot{W}$ is negative definite, which concludes the proof. ∎

3.B Proof of Theorem 2

The proof is similar to the full-information case proof, but unlike the full-information case, our inputs use the estimation of the θ_i variables. Let us consider a Lyapunov function candidate of the form $L = W + V + T$, where

$$W(\tilde{\eta}, \tilde{\theta}) = \sum_{i=1}^{N} \left(\frac{1}{2} \|\tilde{\eta}_i\|^2 + \frac{1}{2} \left\|\tilde{\theta}_i\right\|_{\Sigma_i}^2 \right), \tag{3.42}$$

$$V(\mathbf{x}, \hat{\mathbf{u}}) = \sum_{\mathbf{i=1}}^{\mathbf{N}} \mathbf{V_i}(\mathbf{x_i}, \hat{\mathbf{u}}_\mathbf{i}), \tag{3.43}$$

$$T(\hat{\mathbf{u}}) = \frac{1}{2\tau_{\min}} \langle \hat{\mathbf{u}} - \mathbf{u}^* \mid \tau(\hat{\mathbf{u}} - \mathbf{u}^*) \rangle = \frac{1}{2\tau_{\min}} \|\tilde{\mathbf{u}}\|_\tau . \tag{3.44}$$

Therefore, our candidate consists of a parameter estimation term (W), a local state-input Lyapnuov term (V), and the Nash equilibrium estimation error term (T).

Parameter estimation term

We bound the time derivative of the W function similarly to [20] and [41] with the only difference that we let each agent choose their parameters $(\sigma_i, K_i, k_i^{\mathrm{T}})$. The Lyapunov derivative reads as follows:

$$\dot{W}(\tilde{\eta}, \tilde{\theta}) \leq -k_{\mathrm{a}} \|\tilde{\eta}\|^2 - k_{\mathrm{b}} \|\tilde{\theta}\|^2 + k_{\mathrm{c}} \|\dot{\theta}\|^2 + \frac{\sigma}{2} \|\theta\|^2, \tag{3.45}$$

where $k_{\mathrm{a}} := \min_i \left(K_i - \frac{1}{2} - \frac{k_1 \zeta_i}{2} \right)$, $k_{\mathrm{b}} := \min_i \left(\frac{k_i^{T\prime} \gamma_{1i}}{2} \right)$, $k_{\mathrm{c}} := \max_i \left(\frac{1}{2k_1} + \frac{\gamma_{2i}}{2k_2} \right)$ and $\sigma := \max_i \sigma_i$.

Local state-input Lyapunov term:

The derivative of the Lyapunov term $V_i(x_i, u_i)$ in (3.43) is

$$\dot{V}_i(x_i, u_i) = -\beta \|x_i - \pi_i(u_i)\|^2 - \beta \langle x_i - \pi_i(u_i) \mid B \dot{u}_i \rangle + \beta \langle x_i - \pi_i(\hat{u}_i)) \mid B_i d_i(t) \rangle . \tag{3.46}$$

The first addend is equal to the complete derivative of the Lyapunov function in the case of constant inputs, the amplitude of the second component is proportional to the amplitude of the perturbations, and the amplitude of the third component is equal to the amplitude of the derivative of the input u_i. To bound the third component, we need to bound $\dot{\hat{u}}_i$, hence $\dot{\hat{\mathbf{u}}}$, which reads as $\dot{\hat{\mathbf{u}}} = -\tau^{-1}(\mathbf{B}^\top \mathbf{F}_{\mathrm{x}}(\mathbf{x}) + \tilde{\theta}^{\mathbf{1}})$. By using the same argument as in (3.39), it follows

$$\dot{\hat{\mathbf{u}}} \leq \frac{L_{\mathrm{F}}}{\tau_{\min}} \|\tilde{\mathbf{u}}\| + \frac{L}{\tau_{\min}} \|\mathbf{x} - \pi(\hat{\mathbf{u}})\| + \tau_{\min}^{-1} \|\tilde{\theta}^{\mathbf{1}}\|. \tag{3.47}$$

By using the previous equation, it is possible to bound the second addend in (3.46):

$$\beta \left\langle \mathbf{x} - \pi(\mathbf{u}) \,\middle|\, \mathbf{B}\dot{\hat{\mathbf{u}}} \right\rangle \leq \frac{L_{\mathrm{F}} \beta}{\tau_{\min}} \|\mathbf{B}\| \|\tilde{\mathbf{u}}\| \|\mathbf{x} - \pi(\hat{\mathbf{u}})\| + \frac{\mathbf{L}\beta}{\tau_{\min}} \|\mathbf{B}\| \|\mathbf{x} - \pi(\hat{\mathbf{u}})\|^2 + \frac{\beta}{\tau_{\min}} \|\mathbf{B}\| \|\tilde{\theta}^{\mathbf{1}}\| \|\mathbf{x} - \pi(\hat{\mathbf{u}})\|.$$

Therefore, the derivative of V can be bounded as

$$\begin{aligned} \dot{V}(\mathbf{x}, \mathbf{u}) \leq & -\beta \|\mathbf{x} - \pi(\hat{\mathbf{u}})\|^2 + \frac{\mathbf{L}_{\mathrm{F}} \beta}{\tau_{\min}} \|\mathbf{B}\| \|\tilde{\mathbf{u}}\| \|\mathbf{x} - \pi(\hat{\mathbf{u}})\| + \frac{\mathbf{L}\beta}{\tau_{\min}} \|\mathbf{B}\| \|\mathbf{x} - \pi(\hat{\mathbf{u}})\|^2 \\ & + \frac{\beta}{\tau_{\min}} \|\mathbf{B}\| \|\tilde{\theta}^{\mathbf{1}}\| \|\mathbf{x} - \pi(\hat{\mathbf{u}})\| - \beta (\mathbf{x} - \pi(\hat{\mathbf{u}}))^\top \mathbf{B}\mathbf{d}(\mathbf{t}). \end{aligned} \tag{3.48}$$

The last term can be bounded by using the Cauchy—Bunyakovsky—Schwarz inequality and the inequality $\|x\|\|y\| \leq \frac{1}{2k}\|x\|^2 + \frac{k}{2}\|y\|^2$ to conclude the desired bound:

$$\dot{V} \leq -\left(\beta - \frac{L\beta\|\mathbf{B}\|}{\tau_{\min}} - \frac{\beta\|\mathbf{B}\|}{2\tau_{\min}k_3} - \frac{\beta\|\mathbf{B}\|}{2k_4}\right)\|\mathbf{x} - \pi(\hat{\mathbf{u}})\|^2 + \frac{\mathbf{L}_F\beta}{\tau_{\min}}\|\mathbf{B}\|\|\tilde{\mathbf{u}}\|\|\mathbf{x} - \pi(\hat{\mathbf{u}})\| + \frac{\beta k_3}{2\tau_{\min}}\|\mathbf{B}\|\|\tilde{\theta}^1\|^2 + \frac{1}{2}\beta\mathbf{k}_4\|\mathbf{B}\|\|\mathbf{d}(\mathbf{t})\|^2. \tag{3.49}$$

3

NASH EQUILIBRIUM ESTIMATION ERROR TERM

The parameter estimation also has an influence on the Nash equilibrium estimation error. The derivative of (3.44) is equal to

$$\dot{T}(\mathbf{x}, \hat{\mathbf{u}}) = -\tau^{-1}\tilde{\mathbf{u}}(\mathbf{B}^\top \mathbf{F}_x(\mathbf{x}) + \tilde{\theta}_i^1). \tag{3.50}$$

By the same method as in (3.35), (3.49), it follows that

$$\dot{T}(\hat{\mathbf{u}}) \leq -\frac{\mu}{\tau_{\min}}\|\tilde{\mathbf{u}}\|^2 + \frac{L}{\tau_{\min}}\|\tilde{\mathbf{u}}\|\|\mathbf{x} - \pi(\hat{\mathbf{u}})\| + \frac{1}{2\tau_{\min}\mathbf{k}_5}\|\tilde{\mathbf{u}}\|^2 + \frac{\mathbf{k}_5}{2\tau_{\min}}\|\tilde{\theta}^1\|^2. \tag{3.51}$$

THE FULL LYAPUNOV CANDIDATE

With the bounds (3.45), (3.49) and (3.51), the derivative of the full Lyapunov candidate function is bounded as follows:

$$\begin{aligned}\dot{L} \leq & -k_a\|\tilde{\eta}\|^2 - k_b\|\tilde{\theta}^0\|^2 - \left(\frac{\mu}{\tau_{\min}} - \frac{1}{2\tau_{\min}k_5}\right)\|\tilde{\mathbf{u}}\|^2 \\ & - \left(\beta - \frac{L\beta\|\mathbf{B}\|}{\tau_{\min}} - \frac{\beta\|\mathbf{B}\|}{2\tau_{\min}k_3} - \frac{\beta\|\mathbf{B}\|}{2k_4}\right)\|\mathbf{x} - \pi(\hat{\mathbf{u}})\|^2 - \left(\mathbf{k}_b - \frac{\mathbf{k}_5}{2\tau_{\min}} - \frac{\beta\|\mathbf{B}\|\mathbf{k}_3}{2\tau_{\min}}\right)\|\tilde{\theta}^1\|^2 \\ & + k_c\|\dot{\theta}\|^2 + \frac{\sigma}{2}\|\theta\|^2 + \frac{\mathbf{L}_F\beta\|\mathbf{B}\| + \mathbf{L}}{\tau_{\min}}\|\tilde{\mathbf{u}}\|\|\mathbf{x} - \pi(\hat{\mathbf{u}})\| + \frac{\beta\|\mathbf{B}\|\mathbf{k}_4}{2}\|\mathbf{d}(\mathbf{t})\|^2.\end{aligned} \tag{3.52}$$

We are left with determining bounds on $\|\theta\|$ and $\|\dot{\theta}\|$. Since all of the considered functions (and their composition) in (3.1), (3.12) and (3.21) are Lipschitz continuous, it follows

$$\|\theta\|^2 \leq L_1\|\mathbf{x} - \pi(\hat{\mathbf{u}})\|^2 + \mathbf{L}_2\|\tilde{\mathbf{u}}\|^2 \tag{3.53}$$

$$\|\dot{\theta}\|^2 \leq L_3\|\mathbf{x} - \pi(\hat{\mathbf{u}})\|^2 + \mathbf{L}_4\|\tilde{\mathbf{u}}\|^2, \tag{3.54}$$

for some $L_1, L_2, L_3, L_4 > 0$. Substituting (3.53) and (3.54) into (3.52), we obtain

$$\begin{aligned}\dot{L} \leq & -\left(\frac{\mu}{\tau_{\min}} - \frac{1}{2\tau_{\min}k_5} - \frac{L_2\sigma}{2} - k_cL_4\right)\|\tilde{\mathbf{u}}\|^2 - \left(\mathbf{k}_b - \frac{k_5}{2\tau_{\min}} - \frac{\beta\|\mathbf{B}\|\mathbf{k}_3}{2\tau_{\min}}\right)\|\tilde{\theta}^1\|^2 - k_a\|\tilde{\eta}\|^2 - k_b\|\tilde{\theta}^0\|^2 \\ & - \left(\beta - \frac{L_1\sigma}{2} - \frac{L\beta\|\mathbf{B}\|}{\tau_{\min}} - \frac{\beta\|\mathbf{B}\|}{2\tau_{\min}k_3} - \frac{\beta\|\mathbf{B}\|}{2k_4} - k_cL_3\right)\|\mathbf{x} - \pi(\hat{\mathbf{u}})\|^2 \\ & + \frac{L_F\beta\|\mathbf{B}\| + \mathbf{L}}{\tau_{\min}}\|\tilde{\mathbf{u}}\|\|\mathbf{x} - \pi(\hat{\mathbf{u}})\| + \frac{\beta\|\mathbf{B}\|\mathbf{k}_4}{2}\|\mathbf{d}(\mathbf{t})\|^2.\end{aligned} \tag{3.55}$$

Now we prove that there exist parameters K, k^{T} and $\tau_{\min}$ such that the RHS in (3.55), apart from the term with $\|\mathbf{d}(\mathbf{t})\|^2$, is negative definite. The proof goes by the same lines as in [20]. Consider the following reformulation of (3.55):

$$\begin{aligned}\dot{L} \leq & -k_{\mathrm{a}}\|\tilde{\eta}\|^2 - k_{\mathrm{b}}\|\tilde{\theta}^0\|^2 - \left(-\frac{L_2\sigma}{2} - k_{\mathrm{c}}L_4\right)\|\tilde{\mathbf{u}}\|^2 - \left(-\frac{\beta\|\mathbf{B}\|}{2k_4} - \frac{L_1\sigma}{2} - k_{\mathrm{c}}L_3\right)\|\mathbf{x}-\pi(\hat{\mathbf{u}})\|^2 \\ & - \left(k_{\mathrm{b}} - \frac{k_5}{2\tau_{\min}} - \frac{\beta\|\mathbf{B}\|\mathbf{k_3}}{2\tau_{\min}}\right)\|\tilde{\theta}^1\|^2 - \begin{bmatrix} \|\tilde{\mathbf{u}}\| \\ \|\mathbf{x}-\pi(\mathbf{u})\| \end{bmatrix}^{\top} \mathbf{M} \begin{bmatrix} \|\tilde{\mathbf{u}}\| \\ \|\mathbf{x}-\pi(\mathbf{u})\| \end{bmatrix} + \frac{\beta\|\mathbf{B}\|\mathbf{k_4}}{2}\|\mathbf{d}(\mathbf{t})\|^2,\end{aligned} \tag{3.56}$$

where

$$\mathbf{M} = \begin{bmatrix} \beta - \frac{L\beta\|\mathbf{B}\|}{\tau_{\min}} - \frac{\beta\|\mathbf{B}\|}{2\tau_{\min}k_3} & -\frac{L+\beta\|\mathbf{B}\|\mathbf{L_F}}{2\tau_{\min}} \\ -\frac{L+\beta\|\mathbf{B}\|\mathbf{L_F}}{2\tau_{\min}} & \frac{2\mu-1/k_5}{2\tau_{\min}} \end{bmatrix}. \tag{3.57}$$

Let $\lambda = \sigma_{\min}(\mathbf{M})$. The inequality (3.56) can be reformulated as

$$\begin{aligned}\dot{L} \leq & -k_{\mathrm{a}}\|\tilde{\eta}\|^2 - k_{\mathrm{b}}\|\tilde{\theta}^0\|^2 - \left(\lambda - \frac{L_2\sigma}{2} - k_{\mathrm{c}}L_4\right)\|\tilde{\mathbf{u}}\|^2 - \left(\lambda - \frac{\beta\|\mathbf{B}\|}{2k_4} - \frac{L_1\sigma}{2} - k_{\mathrm{c}}L_3\right)\|\mathbf{x}-\pi(\hat{\mathbf{u}})\|^2 \\ & - \left(k_{\mathrm{b}} - \frac{k_5}{2\tau_{\min}} - \frac{\beta\|\mathbf{B}\|\mathbf{k_3}}{2\tau_{\min}}\right)\|\tilde{\theta}^1\|^2 + \frac{\beta\|\mathbf{B}\|\mathbf{k_4}}{2}\|\mathbf{d}(\mathbf{t})\|^2.\end{aligned}$$

Note, parameters k_3, k_4 and k_5 are artifacts of the proof and are not "real" tuning parameters we can control. The parameter k_3 can be chosen arbitrarily, while k_5 has to be chosen such that lower diagonal element in $\mathbf{M}$ is positive, i.e. $2\mu - 1/k_5 > 0$. Also, for $\mathbf{M}$ to be positive definite and so that the coefficient next to $\|\tilde{\theta}^1\|^2$ is negative, τ_i have to be chosen so that

$$\begin{aligned}\tau_{\min} &> \frac{(L+\beta\|\mathbf{B}\|\mathbf{L_F})^2 + 2\mathbf{L}\beta\|\mathbf{B}\| + \beta\|\mathbf{B}\|/\mathbf{k_3}}{2\beta(2\mu - 1/k_5)} \\ \tau_{\min} &> \frac{Lk_3 + k_5}{k_{\mathrm{b}}}.\end{aligned}$$

The parameters σ, k_{c} must be chosen small enough, while k_4 must be large enough such that the following equations hold true:

$$\begin{aligned}\lambda - \frac{L_2\sigma}{2} - k_{\mathrm{c}}L_4 &> 0 \\ \lambda - \frac{\beta\|\mathbf{B}\|}{2k_4} - \frac{L_1\sigma}{2} - k_{\mathrm{c}}L_3 &> 0.\end{aligned}$$

The parameter σ is a free design parameter; the parameter k_{c} can be made arbitrarily small by increasing the gains K and k^{T} (or to be more precise K_i and k_i^{T}, see [20] for more details). Therefore, it is possible to choose the controller parameters τ_i, σ, k_i^{T} and K_i such that all of the constants that multiply the squares of the norms in (3.56) (except for $\mathbf{d}(\mathbf{t})$) are positive. Next, we consider the Lyapunov functions of the subsystems in (3.43), the bounds on matrices Σ_i, and the quadratic elements of the Lyapunov function candidate L. Let D be

the largest amplitude of all the perturbation signals $d_i(t)$. Then it can be concluded that there exists a positive constant α_L such that $\dot{L} \leq -\alpha_L L + \frac{\beta\|\mathbf{B}\|\mathbf{k_4}\mathbf{D}^2}{2}$. With $z = \left(\tilde{\eta}, \tilde{\theta}, \mathbf{x}, \tilde{\mathbf{u}}\right) \in \mathbb{R}^N \times \mathbb{R}^{m+N} \times \mathbb{R}^n \times \mathbb{R}^m$, let us define the set $\Omega_\gamma = \{z \mid L(z) \leq \gamma\}$. We choose γ such that $z \in \Omega_\gamma \Rightarrow \hat{\theta} \in \Theta_1 \times \Theta_2 \times \cdots \times \Theta_N$. It follows that the trajectories $\tilde{\eta}, \tilde{\theta}, \mathbf{x}, \tilde{\mathbf{u}}$ enter the set $\Omega_{\gamma_0} = \left\{ z \mid L(z) \leq \frac{\beta\|\mathbf{B}\|\mathbf{k_4}\mathbf{D}^2}{2\alpha_L} \right\}$. Thus, for D chosen such that $\Omega_{\gamma_0} \subset \Omega_\gamma$, the set Ω_{γ_0}, which is contained in a ball containing the point $(0, 0, \mathbf{x}^*, \mathbf{0})$ with radius of order $\mathcal{O}\left(D^2\right)$, is exponentially stable for the closed-loop system. ■

4

Multi-timescale algorithms

A man is like a fraction whose numerator is what he is and whose denominator is what he thinks of himself. The larger the denominator, the smaller the fraction.

Leo Tolstoy

The darker the night, the brighter the stars.

Fyodor Dostoevsky

In this chapter, we consider the problem of learning a generalized Nash equilibrium (GNE) in strongly monotone games. First, we propose semi-decentralized and distributed continuous-time solution algorithms that use regular projections and first-order information to compute a GNE with and without a central coordinator. As the second main contribution, we design a data-driven variant of the former semi-decentralized algorithm where each agent estimates their individual pseudogradient via zeroth-order information, namely, measurements of their individual cost function values, as typical of extremum seeking control. Third, we generalize our setup and results for multi-agent systems with nonlinear dynamics. Finally, we apply our methods to connectivity control in robotic sensor networks and almost-decentralized wind farm optimization.

This chapter is partly based on S. Krilašević and S. Grammatico. "Learning generalized Nash equilibria in multi-agent dynamical systems via extremum seeking control". In: *Automatica* 133 (Nov. 2021), p. 109846. ISSN: 0005-1098. DOI: 10.1016/j.automatica.2021.109846.

4.1 Introduction

Multi-agent optimization problems and games with self-interested decision-makers or agents appear in many engineering applications, such as demand-side management in smart grids [47], [33], charging/discharging coordination for plug-in electric vehicles [48], thermostatically controlled loads [49], [50] and robotic formation control [35]. Typically, in these games, the cost functions and the constraints of the agents are coupled together, e.g., due to common congestion penalties and shared resource capacity, respectively. Since the agents are self-interested, their interaction might be unstable. Thus, one main research area is that of finding (seeking) agent decisions that are self-enforceable, e.g., decisions such that no agent has an incentive to deviate from - the so-called Generalized Nash equilibrium (GNE) [1]. From a control-theoretic perspective, in the presence of dynamical agents, the main challenge is to design distributed, possibly almost decentralized, control laws that ensure both the convergence of the agent decisions to a GNE and the asymptotic stability of the equilibrium for the agent dynamics.

Literature review: The literature on generalized Nash equilibrium problems (GNEPs) is vast, see [1] for a survey. What differentiates GNEPs from Nash equilibrium problems (NEPs) is the presence of shared constraints. Although the difference seems minor, it introduces several technical challenges. The main one is that the primal-dual Lagrangian reformulation of the GNEP, which is necessary to decouple the coupling constraints, *does not preserve the strong monotonicity of the* (extended) *pseudogradient* [51, p. 13], the usual background assumption in the NEP literature, as this is a sufficient condition for the projected pseudogradient descent to converge [44, Lemma 5], [42, Thm. 26.14]. This issue can be avoided for a particular class of GNEPs in so-called aggregative games. In these games, each cost function depends on the local decision and on the aggregate (e.g. average) of the decisions of all (other) agents. Various semi-distributed [34] and decentralized [52], [53] algorithms have been developed for NE seeking in aggregative games. The aforementioned technical challenge has only been addressed recently in [44] by applying a preconditioning matrix on the operators. In turn, in [44] the authors propose a GNE-seeking algorithm in games with linear coupling constraints. In [54], the authors overcome the lack of strong monotonicity by adopting an algorithm (the forward-backward-forward) with weaker assumptions on the projected pseudogradient, at the expense of one additional computation of the pseudogradient at each iteration.

In most of the literature and all of the previously mentioned work, GNE-seeking algorithms are designed in discrete-time and for static agents, i.e., where the agent costs instantaneously reflect the chosen decisions. However, this is not the case when the cost functions depend on some internal states of the agents and not on their decisions (control inputs). Let us refer to this class of agents as dynamical agents. The two main approaches to reach a (G)NE for dynamical agents are passivity-based *first-order* algorithms and payoff-based *zeroth-order* algorithms. By using a passivity property, in [36], [37], Pavel and co-authors design a control law that guarantees convergence to a Nash equilibrium (NE) in a multi-agent system with single and multi-integrator dynamics over a time-invariant network. With the same goal, in [38], De Persis and Grammatico relax the network connectivity assumption in [36] by designing a network weight adaptation scheme. In [55], the authors extend the convergence results to GNEPs for the first time via a preconditioning approach as in [44] and the use of non-Lipschitz continuous projections onto tangents

cones.

In payoff-based algorithms, each agent can only measure the value of their cost function but does not know its analytic form. Many such algorithms are designed for NEPs with static agents with finite action spaces, e.g., [56], [10], [57]. In the case of continuous action spaces, the measurements of the cost functions are often used to estimate the pseudogradients. Perhaps the most popular class of control algorithms that exploits this principle is that of extremum seeking control (ESC). The main idea is to use perturbation signals to "excite" the cost function and estimate its gradient which is then used in a gradient-descent-like algorithm [12], [32], [58]. As ESC estimates only one value of the (pseudo)gradient in a time instant, it is not possible to adopt it in algorithms that require multiple (pseudo)gradient computations. ESC was used for non-generalized NE seeking in [7], where the proposed algorithm is proven to converge to a neighborhood of a NE for nonlinear dynamical agents. The results are extended in [40] to include stochastic perturbation signals. In [17], Poveda and Teel propose a framework for the synthesis of a hybrid controller, which could also be used for NEPs with nonlinear dynamical agents. For a class of NEPs called N-cluster games, the authors in [59] propose an ESC-based algorithm. The extension of these algorithms to GNEPs is nontrivial. Only for a special class of so-called population games, the authors in [60] propose an approach based on Shahshahani gradients. In fact, there is still no methodology on data-driven (zeroth-order) GNE learning in strongly monotone games for nonlinear dynamical agents. The reasons for that are technical: (i) the lack of strong monotonicity of the extended pseudogradient in the primal-dual framework; (ii) additional pseudogradient computations necessary in other dynamics; (iii) the incompatibility of projections with available extremum seeking techniques. In fact, in [7], Frihauf, Krstić, and Başar specifically mention: "*Several challenges remain in the development of convergence proofs for Nash seeking players with projection*".

Contribution: Motivated by the above literature and open research problem, to the best of our knowledge, we consider and solve for the first time the problem of learning a GNE in strongly monotone games with nonlinear dynamical agents. Specifically, our main technical contributions are summarized next:

- We design novel continuous-time GNE seeking algorithms (§4.3.1, §4.3.2), which use projections onto fixed convex sets instead of projections onto state-dependent tangent cones as in [55]. In this way, the state flow is Lipschitz continuous and admits solutions in the classical sense. We overcome the lack of strong monotonicity of the primal-dual pseudogradient thanks to suitable preconditioning of the operators defining the optimality conditions.

- We design an extremum seeking scheme that learns a GNE in strongly monotone games with static agents who perform local computations and receive broadcast information from a central coordinator (§4.3.3) Differently from [58], where an optimization problem is considered, we study a noncooperative game. Furthermore, we prove that, with a time-scale separation, our algorithm learns a GNE in (strongly) monotone games with nonlinear dynamical agents (§4.4).

We also apply for the first time semi-decentralized GNE learning to the robot connectivity problem and to wind farm optimization (§4.5).

4.2 Multi-agent dynamical systems

We consider an N agents multi-agent system indexed by $i \in \mathcal{I} = \{1, 2, \dots, N\}$, each with the following dynamics:

$$\dot{x}_i = f_i(x_i, u_i) \tag{4.1a}$$
$$y_i = h_i(x_i, \boldsymbol{x}_{-i}) \tag{4.1b}$$

where $x_i \in \mathcal{X}_i \subset \mathbb{R}^{n_i}$ is the state variable, $u_i \in \Omega_i \subset \mathbb{R}^{m_i}$ is the control input (decision variable), $y_i \in \mathbb{R}$ is the output variable which evaluates the cost function $h_i : \mathbb{R}^{n_i} \times \mathbb{R}^{n_{-i}} \to \mathbb{R}$, and $f_i : \mathcal{X}_i \times \Omega_i \to \mathbb{R}^{n_i}$ is the state flow mapping. Let us also define $n := \sum n_i$, $m := \sum m_i$ and $n_{-i} := \sum_{j \neq i} n_j$.

To ensure the existence and uniqueness of the solutions to (4.1a), we make a common assumption in the nonlinear system literature [29, Thm. 3.3]:

Assumption 4.1 (Local Lipschitz continuity)**.** *For each $i \in \mathcal{I}$, f_i is locally Lipschitz continuous.* □

Furthermore, we assume that the decision variables of the agents are subject to local constraints $u_i \in \Omega_i$ and coupling constraints $A\boldsymbol{u} \leq b$, where $A \in \mathbb{R}^{q \times m}$, $b \in \mathbb{R}^q$, and $\boldsymbol{u} := \operatorname{col}((u_i)_{i \in \mathcal{I}})$ collects all the control inputs. Let us denote the collection of local constraints as

$$\Omega := \Omega_1 \times \cdots \times \Omega_N. \tag{4.2}$$

As the decision variables are also coupled together, the overall feasible decision set $\boldsymbol{\mathcal{U}}$ is contained in Ω, i.e.

$$\boldsymbol{\mathcal{U}} := \Omega \cap \{\boldsymbol{u} \in \mathbb{R}^m \mid A\boldsymbol{u} \leq b\}, \tag{4.3}$$

Let us also denote the feasible set of each agent i as

$$\mathcal{U}_i(\boldsymbol{u}_{-i}) := \Omega_i \cap \{u_i \in \mathbb{R}^{m_i} \mid A\boldsymbol{u} \leq b\}. \tag{4.4}$$

In equilibrium seeking problems, we can consider only equilibrium points of the nonlinear systems as possible solutions. Here we consider the setting where agents have a continuum of possible equilibria. To characterize them, we assume they are input-dependent points, similar to reference tracking problems. In fact, this motivates a common assumption amongst the extremum seeking literature (e.g. [12, Ass. 2.1], [20, Equ. 3], [17, Ass. 2]), namely the existence of the steady-state mappings which characterizes the behavior of the systems for a constant input.

Standing Assumption 4.2 (Steady-state mapping)**.** *For each $i \in \mathcal{I}$, there is a differentiable mapping $\pi_i : \mathbb{R}^{m_i} \to \mathbb{R}^{n_i}$ (called the steady-state mapping) such that for every $\overline{u}_i \in \Omega_i$, it holds that $f_i(\pi_i(\overline{u}_i), \overline{u}_i) = 0$.* □

By using the previous definition, let us also define the collective steady-state mappings

$$\pi(\boldsymbol{u}) \coloneqq \operatorname{col}((\pi_i(u_i))_{i\in\mathcal{I}}),$$
$$\pi_{-i}(\boldsymbol{u}_{-i}) \coloneqq \operatorname{col}\Big(\big(\pi_j(u_j)\big)_{j\in\mathcal{I}\setminus\{i\}}\Big). \tag{4.5}$$

Another common assumption in ESC is the (local) exponential stability of the equilibrium points $\pi_i(u_i)$, under constant input ($\dot{u}_i = 0$) [12, Ass. 2.2], [7, Ass. 4.2]. Thus, with the change of coordinates $z_i \coloneqq x_i - \pi_i(u_i)$, we adopt the following assumption throughout the paper:

Standing Assumption 4.3 (Lyapunov stability). *For each $i \in \mathcal{I}$, there is a smooth Lyapunov function, $z_i \mapsto V_i(z_i, u_i)$, with Lipschitz continuous partial derivatives, i.e. for every constant $\overline{u}_i \in \mathcal{U}_i$, it holds that*

$$\underline{\alpha}_i\|z_i\|^2 \le V_i(z_i,\overline{u}_i) \le \overline{\alpha}_i\|z_i\|^2$$
$$\frac{\partial V_i}{\partial z_i}(z_i,\overline{u}_i)^\top f_i(z_i+\pi_i(\overline{u}_i),\overline{u}_i) \le -\kappa_i\|z_i\|^2$$
$$\frac{\partial V_i}{\partial z_i}(0,\overline{u}_i) = 0,$$

for some positive constants $\underline{\alpha}_i$, $\overline{\alpha}_i$ and κ_i. Moreover, for every constant $\overline{u}_i \in \mathcal{U}_i$, it holds that

$$\frac{\partial V_i}{\partial u_i}(0,\overline{u}_i) = 0. \qquad \square$$

Formally, let the goal of each agent be to minimize their steady-state cost function, i.e.,

$$\forall i \in \mathcal{I} : \min_{u_i\in\mathcal{U}_i(\boldsymbol{u}_{-i})} J_i(u_i,\boldsymbol{u}_{-i}), \tag{4.7}$$
$$\coloneqq \min_{u_i\in\mathcal{U}_i(\boldsymbol{u}_{-i})} h_i(\pi(u_i),\pi_{-i}(\boldsymbol{u}_{-i})), \tag{4.8}$$

which depends on the decision variables of other agents as well. From a game-theoretic perspective, we actually consider the problem to compute a generalized Nash equilibrium (GNE) as formalized next.

Definition 4.4 (Generalized Nash equilibrium). *A set of control actions $\boldsymbol{u}^* \coloneqq \operatorname{col}\left(u_i^*\right)_{i\in\mathcal{I}}$ is a generalized Nash equilibrium if, for all $i \in \mathcal{I}$,*

$$u_i^* \in \operatorname*{argmin}_{v_i} J_i\left(v_i,\boldsymbol{u}_{-i}^*\right) \text{ s.t. } \left(v_i,\boldsymbol{u}_{-i}^*\right) \in \boldsymbol{\mathcal{U}}, \tag{4.9}$$

with $\boldsymbol{\mathcal{U}}$ as in (4.3) and J_i as in (4.8). $\square$

In plain words, a set of inputs is a GNE if no agent can improve its steady-state cost function by unilaterally changing its input. To ensure the existence of the GNE, we postulate the following assumption [1, Thm. 3.3]:

Standing Assumption 4.5 (Regularity). *For each $i \in \mathcal{I}$, the function J_i in (4.8) is continuous; the function $J_i(\cdot,\boldsymbol{u}_{-i})$ is convex for every $\boldsymbol{u}_{-i}$. For each $i \in \mathcal{I}$, the set Ω_i is non-empty, closed, and convex; $\boldsymbol{\mathcal{U}}$ is non-empty and satisfies Slater's constraint qualification.* $\square$

More precisely, we focus on a subclass of GNE called variational GNE (v-GNE) [1, Def. 3.10]. A collective decision $\boldsymbol{u}^*$ is a v-GNE in (4.9) if and only if there exists a dual variable $\lambda^* \in \mathbb{R}^q$ such that the following KKT conditions are satisfied [1, Th. 4.8]:

$$\mathbf{0}_{m+q} \in \begin{bmatrix} F(\boldsymbol{u}^*) + A^\top \lambda^* \\ -(A\boldsymbol{u}^* - b) \end{bmatrix} + \begin{bmatrix} \mathrm{N}_\Omega(\boldsymbol{u}^*) \\ \mathrm{N}_{\mathbb{R}^q_+}(\lambda^*) \end{bmatrix}, \tag{4.10}$$

where by stacking the partial gradients $\nabla_{u_i} J_i(u_i, \boldsymbol{u}_{-i})$ into a vector, we have the pseudogradient mapping:

$$F(\boldsymbol{u}) := \mathrm{col}\left(\left(\nabla_{u_i} J_i(u_i, \boldsymbol{u}_{-i})\right)_{i \in \mathcal{I}}\right). \tag{4.11}$$

Let us postulate additional common assumptions ([61, Std. Ass. 2], [38, Ass. 1]) in order to assure the convergence of the algorithm we propose later on.

Standing Assumption 4.6 (Well-behavedness). *For each $i \in \mathcal{I}$, J_i in (4.8) is twice differentiable, and its gradient ∇J_i is ℓ-Lipschitz continuous, with $\ell > 0$. The pseudogradient mapping F in (4.11) is μ-strongly monotone, i.e., for any pair $\boldsymbol{u}, \boldsymbol{v} \in \mathbb{R}^n$, $(\boldsymbol{u}-\boldsymbol{v})^\top (F(\boldsymbol{u}) - F(\boldsymbol{v})) \geq \mu \|\boldsymbol{u}-\boldsymbol{v}\|^2$, with $\mu > 0$.* □

4.3 Generalized Nash Equilibrium seeking for static agents

Let us start with the case of static agents to highlight the proposed algorithm and its integration with the zeroth-order gradient scheme.

Assumption 4.7 (Static agents). *For each $i \in \mathcal{I}$, $x_i = u_i$ (in place of (4.1a)).* □

We propose three control schemes for GNE seeking with static agents. In the first two, the agents have perfect information about the decisions of other agents and know the analytic expression of their partial gradient. The third scheme is data-driven, i.e. the agents have access to the output of their cost function only. Additionally, the first scheme assumes the existence of the central coordinator for dual variable calculation, while in the second one, the computation of the dual variable is distributed.

4.3.1 Gradient-based case with central coordinator

Our GNE seeking algorithm is based on the forward-backward splitting [42, Thm. 26.14], [62, Thm. 12] applied to a variant of the KKT operator in (4.10). In fact, we emphasize that there is a fundamental issue in applying the forward-backward splitting directly to (4.10): the forward part of the monotone operator must be cocoercive [42, Def. 4.2]. Thus, the standard approach must move all the non-cocoercive elements in the backward step, but this would make the backward step impossible to compute (non-causal equations). Other splitting methods that only require monotonicity of the operator require multiple evaluations of the pseudogradient [42, Th. 26.17], which makes them incompatible with ESC as the latter can only estimate one pseudogradient. To overcome these issues, we apply a continuous-time variant of the approach introduced in [44], where a preconditioning matrix is used. However, differently from [55], we do not use projections onto tangent

cones to enable the use of extremum seeking techniques later on. We refer to Appendix A for technical details.

In our proposed algorithm, each agent updates their decision, u_i, based on: (i) decisions of all other agents; (ii) the dual variable, which is computed by a central coordinator, indexed by 0, who is in a bidirectional computation with all of the agents:

$$\begin{aligned}\forall i \in \mathcal{I} \,:\, \dot{u}_i &= -u_i + \operatorname{proj}_{\Omega_i}\left(u_i - \gamma_i(\nabla_{u_i} J_i(\boldsymbol{u}) + A_i^\top \lambda)\right)\\ \dot{\lambda} &= -\lambda + \operatorname{proj}_{\mathbb{R}^q_+}(\lambda + \gamma_0(A\boldsymbol{u} - b + 2A\dot{\boldsymbol{u}})),\end{aligned}$$

or in collective form

$$\begin{bmatrix}\dot{\boldsymbol{u}}\\ \dot{\lambda}\end{bmatrix} = \begin{bmatrix}-\boldsymbol{u} + \operatorname{proj}_{\Omega}\left(\boldsymbol{u} - \Gamma(F(\boldsymbol{u}) + A^\top\lambda)\right)\\ -\lambda + \operatorname{proj}_{\mathbb{R}^q_+}(\lambda + \gamma_0(A\boldsymbol{u} - b + 2A\dot{\boldsymbol{u}}))\end{bmatrix}, \tag{4.12}$$

where A_i are the m_i columns of A which correspond to coupling constraints on u_i, $\lambda \in \mathbb{R}^q_+$, $(\gamma_i)_{i\in\mathcal{I}_0}$ are the step sizes chosen by the agents and the central coordinator; $\mathcal{I}_0 := \mathcal{I} \cup \{0\}$; $\Gamma = \operatorname{blkdiag}\left((\gamma_i I_{m_i})_{i\in\mathcal{I}}\right)$. We note that the decision dynamics are primal-dual pseudogradient dynamics, while those of the dual variable resemble the dual ascent, here with the additional pricing term $2A\dot{\boldsymbol{u}}$. We are now ready to state our first convergence result:

Theorem 4.8 (v-GNE seeking)**.**
Let the Standing Assumptions and Assumption 4.7 hold and let $(\boldsymbol{u}(t), \lambda(t))_{t\geq 0}$ be the solution to (4.12). Then, there exist small enough $(\gamma_i)_{i\in\mathcal{I}_0}$ such that the pair $(\boldsymbol{u}(t), \lambda(t))_{t\geq 0}$ converges to some $(\boldsymbol{u}^*, \lambda^*) \in \boldsymbol{\mathcal{U}} \times \mathbb{R}^q_+$, where $\boldsymbol{u}^*$ is the v-GNE of the game in (4.7). □

Proof. See Appendix 4.A. ■

4.3.2 Gradient-based case without a central coordinator

Let us study the case where the agents communicate with each other in order to calculate the dual variable. The communication structure is described via a graph $\mathcal{G} := (\mathcal{I}, \mathcal{E})$, where the first member of the ordered pair is the set of nodes (agents) and the second member is the set of edges (communication links) $\mathcal{E} \in \mathcal{I} \times \mathcal{I}$. The weight of the communication link $w_{ij} \geq 0$ equals zero if there is no edge between nodes i and j. We make a common assumption for consensus algorithms [44], [55]:

Assumption 4.9. *The communication graph $\mathcal{G}$ is strongly connected, undirected, and its Laplacian satisfies $L = L^\top$.* □

Each agent updates his decision variable u_i, dual variable estimate λ_i and auxiliary variable z_i as follows:

$$\begin{aligned}\dot{u}_i &= -u_i + \operatorname{proj}_{\Omega_i}\left(u_i - \gamma_i\left(\nabla_{u_i} J_i(\boldsymbol{u}) + A_i^\top \lambda_i\right)\right)\\ \dot{z}_i &= \gamma_i \textstyle\sum_{j\in\mathcal{N}_i} w_{ij}(z_i - z_j)\\ \dot{\lambda}_i &= -\lambda_i + \operatorname{proj}_{\mathbb{R}^q_+}\left(\lambda_i + \gamma_i\left(A_i(u_i + 2\dot{u}_i) - \tfrac{b}{N} + \sum_{j\in\mathcal{N}_i} w_{ij}(2\dot{z}_i - 2\dot{z}_j - z_i + z_j - \lambda_i + \lambda_j)\right)\right),\end{aligned} \tag{4.13}$$

or, as in collective from:

$$\begin{bmatrix}\dot{\boldsymbol{u}}\\ \dot{\boldsymbol{z}}\\ \dot{\boldsymbol{\lambda}}\end{bmatrix} = \begin{bmatrix}-\boldsymbol{u}+\mathrm{proj}_{\Omega}\left(\boldsymbol{u}-\Gamma_m(F(\boldsymbol{u})+\Lambda^\top\boldsymbol{\lambda})\right)\\ \bar{\Gamma}\bar{L}\boldsymbol{\lambda}\\ \boldsymbol{\lambda}+\mathrm{proj}_{\mathbb{R}^{Nq}_+}(-\boldsymbol{\lambda}+\bar{\Gamma}(\Lambda(\boldsymbol{u}+2\dot{\boldsymbol{u}})-\frac{\boldsymbol{b}}{N}\\ +\bar{L}(2\dot{\boldsymbol{z}}-\boldsymbol{z}-\boldsymbol{\lambda})))\end{bmatrix}, \tag{4.14}$$

where $z_i \in \mathbb{R}^q$ is an auxiliary variable; $\bar{L} := L \otimes I_q$; $\hat{\mathcal{N}}_i$ is a set of agents with whom agent i has a communication link; $\bar{\Gamma} := \mathrm{blkdiag}\left((\gamma_i I_q)_{i\in\mathcal{I}}\right)$; $\Lambda := \mathrm{blkdiag}\left((A_i)_{i\in\mathcal{I}}\right)$; $\boldsymbol{b} = \mathrm{col}(b,\dots,b)$, where b repeats N times. We conclude the subsection with our convergence result:

Theorem 4.10 (Distributed v-GNE seeking)**.** *Let the Standing Assumptions, Assumptions 4.7 and 4.9 hold and let $(\boldsymbol{u}(t),\boldsymbol{z}(t),\boldsymbol{\lambda}(t))_{t\geq 0}$ be the solution to (4.14). Then, there exist small enough $(\gamma_i)_{i\in\mathcal{I}}$ such that $(\boldsymbol{u}(t),\boldsymbol{z}(t),\boldsymbol{\lambda}(t))_{t\geq 0}$ converges to some $(\boldsymbol{u}^*,\mathbf{1}_N\otimes z^*,\mathbf{1}_N\otimes\lambda^*) \in \boldsymbol{\mathcal{U}}\times\mathbb{R}^{Nq}_+\times\mathbb{R}^{Nq}_+$, where $\boldsymbol{u}^*$ is the v-GNE of the game in (4.7).* □

Proof. See Appendix 4.B. ■

4.3.3 Data-driven case

In this section, we consider that the agents only have access to the cost output. We emphasize that in this case, they neither know the other agents' actions nor the analytic expressions of their partial gradients. In fact, this is a standard setup used in extremum seeking ([12], [20], [17] among others). However, we assume that the agents can communicate with a central coordinator to whom they send their decision variable and its derivative. Let us first evaluate the time derivative of the cost output $l_i = J_i(u_i,\boldsymbol{u}_{-i})$ along the trajectories of $\boldsymbol{u}$:

$$\dot{l}_i = \theta_i^0(\boldsymbol{u}) + \theta_i^1(\boldsymbol{u})\dot{u}_i = [1,\dot{u}_i^\top]\theta_i(\boldsymbol{u}), \tag{4.15}$$

where we define

$$\theta_i^0 = \theta_i^0(\boldsymbol{u}) := \nabla_{\boldsymbol{u}_{-i}} J_i(u_i,\boldsymbol{u}_{-i})^\top \dot{\boldsymbol{u}}_{-i} \tag{4.16}$$

$$\theta_i^1 = \theta_i^1(\boldsymbol{u}) := \nabla_{u_i} J_i(u_i,\boldsymbol{u}_{-i})^\top \tag{4.17}$$

$$\theta_i = \theta_i(\boldsymbol{u}) := [\theta_i^0,\theta_i^{1\top}] \tag{4.18}$$

In (4.16), the variable θ_i^0 measures the influence of the decision variables of the other agents on the cost output of agent i. Instead, in (4.17), the variable θ_i^1 measures the effect of the decision variable of agent i on the cost output l_i, which is needed for (4.12). To estimate the local θ_i^0 and θ_i^1, we use a time-varying parameter estimation approach, as proposed in [20] for centralized optimization. Let us provide a basic intuition first. Let $\hat{l}_i$ and $\hat{\theta}_i$ be estimations of the output l_i and the variable θ_i respectively and let $e_i = l_i - \hat{l}_i$ be the estimation error and $\tilde{\theta}_i = \theta_i - \hat{\theta}_i$ the parameter estimation error. Then, the estimator model in (4.15) for agent i is given by

$$\dot{\hat{l}}_i = [1,\dot{u}_i^\top]\hat{\theta}_i + K_i e_i + c_i^\top \dot{\hat{\theta}}_i, \tag{4.19}$$

where K_i is a free design parameter. Note that the first two terms on the right-hand side resemble high gain observer schemes [63]. As the structure of the problem does not directly allow the use of high-gain observers, it is necessary to introduce some other dynamics into the estimation. This is the primary role of the third term in (4.19). Therefore, the dynamics of $c_i(t)$ are chosen as

$$\dot{c}_i^\top = -K_i c_i^\top + [1, \dot{u}_i^\top]. \tag{4.20}$$

Let us also introduce an auxiliary variables $\tilde{\eta}_i = \eta_i - \hat{\eta}_i$, $\eta_i = e_i - c_i^\top \tilde{\theta}_i$, with dynamics $D^+\eta_i = -K_i\eta_i - c_i^\top D^+\theta$, and its estimate $\hat{\eta}_i$, with dynamics

$$\dot{\hat{\eta}}_i = -K_i\hat{\eta}_i. \tag{4.21}$$

It is also necessary to define a positive definite matrix variable $\Sigma_i \in \mathbb{R}^{(m_i+1)\times(m_i+1)}$ with dynamics given by

$$\dot{\Sigma}_i = c_i c_i^\top - \rho_i\Sigma_i + \sigma_i I \tag{4.22}$$

$$\Sigma_i(0) = \Sigma_i^0, \tag{4.23}$$

where ρ_i, σ_i and Σ_i^0 are free design parameters. We note that in [45], $\dot{\Sigma}_i = c_i c_i^\top$, but this proved to be inconvenient in practical implementations, as the elements of Σ_i grow unbounded. Instead, as in (4.23), dynamics of Σ_i behave as a first-order system. The third term is added so that the matrix is always invertible. Equations (4.19)-(4.23) form the parameter update law in [45]:

$$\dot{\hat{\theta}}_i = \Sigma_i^{-1}(c_i(e_i - \hat{\eta}_i) - \sigma_i\hat{\theta}_i). \tag{4.24}$$

We are finally ready to propose our semi-decentralized v-GNE learning algorithm:

$$\forall i \in \mathcal{I} : \dot{u}_i = -u_i + \mathrm{proj}_{\Omega_i}\left(u_i - \gamma_i(\hat{\theta}_i^1 + A_i^\top\lambda) + d_i\right),$$
$$\dot{\lambda} = -\lambda + \mathrm{proj}_{\mathbb{R}^q_+}(\lambda + \gamma_0(A\boldsymbol{u} - b + 2A\dot{\boldsymbol{u}})),$$

where d_i represents the perturbation signal of agent i. In collective form, it can be written as

$$\begin{bmatrix}\dot{\boldsymbol{u}}\\ \dot{\lambda}\end{bmatrix} = \begin{bmatrix}-\boldsymbol{u} + \mathrm{proj}_{\Omega}\left(\boldsymbol{u} - \Gamma(\hat{\boldsymbol{\theta}}^1 + A^\top\lambda) + d\right)\\ -\lambda + \mathrm{proj}_{\mathbb{R}^q_+}(\lambda + \gamma_0(A\boldsymbol{u} - b + 2A\dot{\boldsymbol{u}}))\end{bmatrix}, \tag{4.25}$$

where $\hat{\boldsymbol{\theta}}^1 \operatorname{col}\left(\left(\hat{\theta}_i^1\right)_{i\in\mathcal{I}}\right)$. For $\hat{\boldsymbol{\theta}}^1$ to successfully estimate $F(\boldsymbol{u})$, it is necessary to assume that the input signals are "exciting" enough. As in [20, Ass. 5], we postulate a persistency of excitation (PE) assumption.

Assumption 4.11 (Persistence of excitation)**.**
For each $i \in \mathcal{I}$, there exist $\alpha_i, T_i > 0$, such that

$$\int_t^{t+T_i} c_i(\tau)c_i(\tau)^\top d\tau \geq \alpha_i I, \quad \text{for all } t > 0, \tag{4.26}$$

where c_i is the solution to (4.20). □

We conclude the section with the convergence result. For any initial condition of the decision variables, there exist gains such that the control variables converge to an arbitrarily small neighborhood of a v-GNE.

Theorem 4.12 (v-GNE static learning)**.**
Let the Standing Assumptions and Assumptions 4.7 and 4.11 hold and let $(s(t) := (\hat{\boldsymbol{\eta}}(t), \hat{\boldsymbol{\theta}}(t), \boldsymbol{u}(t), \lambda(t)))_{t\geq 0}$ *be the closed-loop solution to (4.19)–(4.25). Then, for any compact set* $\mathcal{K}$ *and any* $\varepsilon > 0$*, there exist small enough parameters* γ_0 *and* $(\gamma_i, \sigma_i, \frac{1}{K_i}, \frac{1}{\rho_i})_{i\in\mathcal{I}}$*, tuned in that order, such that for every solution with* $s(0) \in \mathcal{K}$*,* $\boldsymbol{u}(t)$ *converges to the set* $\{\boldsymbol{u}^*\} + \varepsilon\mathbb{B}$*, where* $\boldsymbol{u}^*$ *is a v-GNE of the game in (4.7).* □

Proof. See Appendix 4.C. ■

4

4.4 Generalized Nash equilibrium learning for dynamical agents

In this section, we propose a control scheme for generalized Nash equilibrium learning for dynamical agents. We consider a data-driven scenario only, i.e., the agents have access to the cost output measurements and the information that is given to them by a central coordinator. They are not aware of the analytic expression of their steady-state cost function, nor of their pseudogradient, nor can they observe the states and decisions of the other agents.

For the multi-agent dynamical system

$$\epsilon\dot{\boldsymbol{x}} = \operatorname{col}\left((f_i(x_i, u_i))_{i\in\mathcal{I}}\right) = f(\boldsymbol{x}, \boldsymbol{u}), \tag{4.27}$$

where $\epsilon > 0$ is a time scale separation constant with the objective of reaching a neighborhood of a v-GNE, we propose the same control law as in (4.25), with the distinction that $\hat{\boldsymbol{\theta}}^1$ is estimated by a parameter estimation scheme (4.19) – (4.24), where we collect the measurements of the output y_i in (4.1b) instead of $J_i(u_i, \boldsymbol{u}_{-i})$ directly. Thus, the estimation error is hereby redefined as

$$e_i = y_i - \hat{l}_i. \tag{4.28}$$

We conclude the section with the most general theoretical result of the paper, namely, the convergence of the closed-loop dynamics to a neighborhood of a v-GNE.

Theorem 4.13. *[v-GNE dynamic learning]*
Let the Standing Assumptions and Assumptions 4.1 and 4.11 hold and let $(s(t) := (\hat{\boldsymbol{\eta}}(t), \hat{\boldsymbol{\theta}}(t), \boldsymbol{x}(t), \boldsymbol{u}(t), \lambda(t)))_{t\geq 0}$ *be the closed-loop solution to (4.19)–(4.25), (4.27), (4.28). Then, for any compact set* $\mathcal{K}$ *and any* $\varepsilon > 0$*, there exist small enough parameters* γ_0*,* $(\gamma_i, \sigma_i)_{i\in\mathcal{I}}$*,* ϵ *and* $(\frac{1}{K_i}, \frac{1}{\rho_i})_{i\in\mathcal{I}}$*, tuned in that order, such that every solution with* $s(0) \in \mathcal{K}$*,* $(\boldsymbol{x}(t), \boldsymbol{u}(t))$ *converges to an* ε *neighborhood of some* $(\pi(\boldsymbol{u}(t)), \boldsymbol{u}^*)$*, where* $\boldsymbol{u}^*$ *is a v-GNE of the game in (4.7).* □

Proof. See Appendix 4.D. ■

4.5 Illustrative applications

4.5.1 Connectivity control in robotic swarms

The problem of connectivity control has been considered in [8] as a Nash equilibrium problem. In many practical scenarios, multi-agent systems, besides their primary objective, are designed to uphold certain connectivity as their secondary objective. In what follows, we consider a similar problem in which each agent is tasked with finding a source of an unknown signal while maintaining certain connectivity. Unlike [8], we require the existence of a central coordinator and allow for coupled restrictions on the decision variables. Moreover, we model the agents as unicycles with setpoint regulators, which do not require a constant angular velocity as in [8].

Consider a multi-agent system consisting of unicycle vehicles, indexed by $i \in \{1,\dots N\}$, where each one implements the feedback controller studied in [64] for target tracking, to have the following dynamics:

$$\begin{bmatrix} \dot{x}_i \\ \dot{y}_i \\ \dot{\phi}_i \end{bmatrix} = \begin{bmatrix} -K_i^1 \|r_i - u_i\| \cos(\phi_i) \cos\left(\phi_i - \arctan\frac{y_i}{x_i}\right) \\ -K_i^1 \|r_i - u_i\| \cos(\phi_i) \sin\left(\phi_i - \arctan\frac{y_i}{x_i}\right) \\ -K_i^2 \phi_i \end{bmatrix}, \tag{4.29}$$

where x_i, y_i are position variables, ϕ_i is the relative angle with respect to the setpoint, $K_i^1, K_i^2 > 0$ controller parameters, $r_i = \mathrm{col}(x_i, y_i)$ and $u_i = \mathrm{col}\left(u_i^x, u_i^y\right)$ is the input of the transformed system, which represents the coordinates of the setpoint input. Note that, in the new dynamics (4.29), we do not follow the global angle coordinate, but rather ϕ_i (local coordinate), as illustrated in Figure [64, Fig. 1]. For each i, the steady-state mapping is then given by $\pi_i(u_i) = \mathrm{col}(u_i, 0)$.

Each agent is tasked with locating a source of a unique unknown signal. The strength of all signals abides by the inverse-square law, i.e., proportional to $1/r^2$. Therefore, the inverse of the signal strength can be used in the cost function. Additionally, the agents must not drift apart from each other too much, as they should provide quick assistance to each other in case of critical failure. This is enforced in two ways: by incorporating the signal strength of fellow agents in the cost functions and by communicating with the central coordinator. Thus, we design the cost output and position constraints as

$$\forall i \in \mathcal{I} : \begin{cases} h_i(r_i) = \|r_i - r_i^s\|^2 + c \sum_{j \in \mathcal{I}_{-i}} \|r_i - r_j\|^2, \\ \left\| \mathrm{col}\left((u_i - u_j)_{j \in \mathcal{I}_{-i}}\right) \right\|_\infty \leq b \end{cases} \tag{4.30}$$

where $\mathcal{I}_{-i} := \mathcal{I} \setminus \{i\}$, $c, b > 0$ and r_i^s represents the position of the source assigned to agent i. The safe traversing area is described by a rectangle: $[x_{\min}, x_{\max}] \times [y_{\min}, y_{\max}]$.

For our numerical simulations, we choose the parameters: $N = 4$, $(x_{\min}, x_{\max}) = (-16, 16)$, $(y_{\min}, y_{\max}) = (-6, 6)$, $r_1^s = (-4, -8)$, $r_2^s = (-12, -3)$, $r_3^s = (1, 7)$, $r_4^s = (16, 8)$, $(c, b) = (0.04, 14)$, $K_i = 100$, $k_i^\sigma = 100$, $\sigma_i = 10^{-6}$, $\Sigma_i(0) = 0.1I$, $\gamma_i = 0.002$, $\gamma_0 = 0.002$, $\epsilon = 0.1$, $K_1^i = 3$, $K_2^i = 6$, $(\overline{\omega}_1^1, \overline{\omega}_1^2) = (5.11, 6.38)$, $(\overline{\omega}_2^1, \overline{\omega}_2^2) = (4.42, 5.16)$, $(\overline{\omega}_3^1, \overline{\omega}_3^2) = (10.59, 11.91)$, $(\overline{\omega}_4^1, \overline{\omega}_4^2) = (14.65, 16.12)$. We run simulations for different values of perturbation amplitudes in range $[0.1, 0.5]$ and

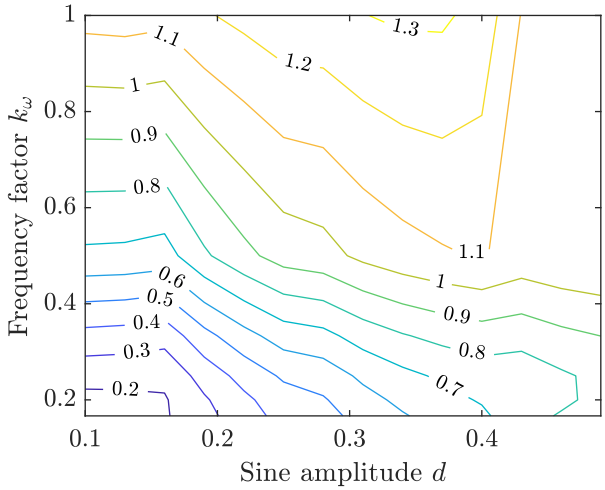

Figure 4.1: Distance of the final average steady-state trajectory from the v-GNE for agent 4.

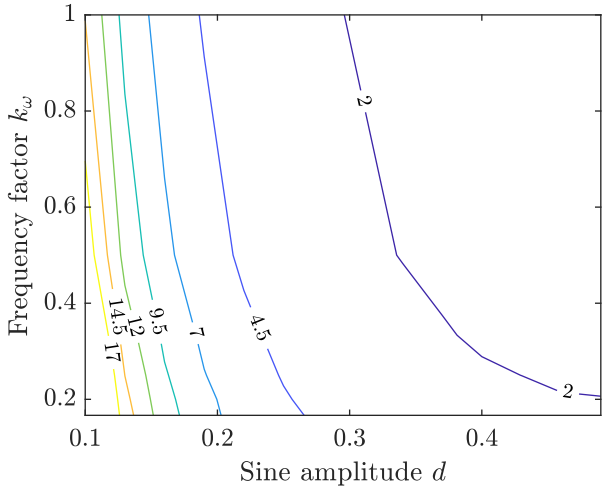

Figure 4.2: Hours required to enter a ball of size $\varepsilon = 1.5$ centered around the v-GNE for agent 4.

different values of the frequency factor k_ω in range $[0.17, 1]$. The numerical results are illustrated in Figures 4.1, 4.2 and 4.3. In Figure 4.1, we see that smaller perturbations and frequency factors bring the system closer to the v-GNE; however, in Figure 4.2, we see that the convergence rate slows down significantly. Thus, there is a trade-off between convergence speed and closeness to the solution. Moreover, we numerically test robustness to output noise on a representative example of agent trajectories. We simulate noise with zero mean and variance equal to 1 and 3. In Figure 4.3, the shaded regions represent

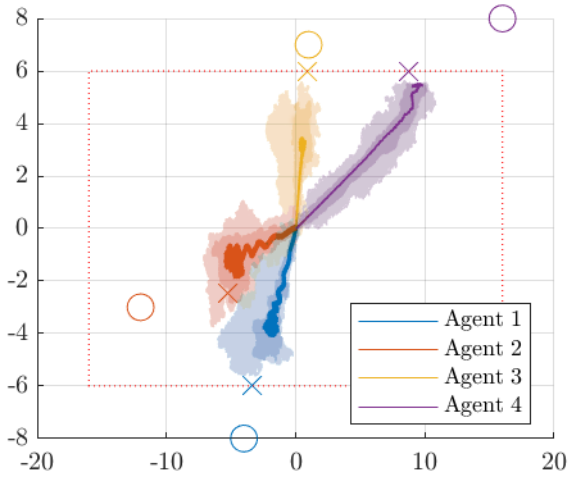

Figure 4.3: State trajectories in the $x-y$ plane for the case of $d_i = 0.49$ and various noise levels. Circle symbols represent locations of the sources, while the × symbols represent locations of the v-GNE.

envelopes of the trajectories (ten simulations per variance). The darkest shade represents the case without noise, while the lightest represents the case with the largest variance. We observe that the algorithm still converges to a neighborhood of the v-GNE.

4.5.2 Wind farm optimization

As one of the main sources of renewable energy, wind farms, and their optimization has been addressed extensively from different perspectives, such as power tracking of single turbines [65], [66], power tracking via extremum seeking [67], power tracking with load reduction [68], [69], distributed optimization of wind farms [70], [9] and distributed optimization via extremum seeking [71]. While in the power tracking case, often the torque or some other related variable is taken as the control input, in the distributed optimization case, the axial induction factor (AIL) is usually taken as the control input.

In what follows, we consider a similar problem in which a wind farm tries to maximize its power output with AIL as the control input. The control variables are subject to local constraints (feasible values of AIL). Also, we require that the turbines experience a similar amount of mechanical stress. To do that, we impose that the AILs of a row of wind turbines cannot differ too much from AILs of the succeeding row, which introduces coupling constraints to the optimization problem. Unlike the previously mentioned literature on distributed wind farm optimization, here we also allow for AIL dynamics to reflect the turbine time constant and its effect on the power output. One possible way of solving the problem would be via global optimization, where a central coordinator would minimize a global cost function and send AIL commands to the turbines. To avoid having a single

critical node for computation and communication, an alternative approach is to pose the problem as a potential game, where the cost function of the turbines are “aligned" to a global utility function. In our case, the potential function would be the sum of all power outputs. We choose that the individual cost functions are equal to the potential function, and each agent minimizes their cost function on their own, with limited information from the central coordinator. In this setup, a v-GNE corresponds to an optimal solution to the global power maximization problem.

Technically speaking, we consider N wind turbines, indexed by $i \in \{1, \dots, N\}$, each with the following AIL dynamics and power output:

$$\dot{a}_i = -\tfrac{1}{\tau}(a_i - u_i) \tag{4.31}$$

$$y_i = -\sum_{i \in \mathcal{I}} P_i(\boldsymbol{a}) = -\tfrac{1}{2}\rho A \sum_{i \in \mathcal{I}} C_P(a_i) V_i(\boldsymbol{a})^3, \tag{4.32}$$

where a_i represent the state variable, u_i represent the control input, namely the AIL reference, y_i is the measured power output of the wind farm, which is broadcasted by the central coordinator, ρ is the air density, A is the surface area encompassed by the blades of a single turbine, $C_P(a_i) := a_i(1-a_i)^2$ is the power efficiency coefficient and V_i is the average wind speed experienced by wind turbine i, as in [70, Equ. 5]:

$$V_i(a) = U_\infty \left(1 - 2\sqrt{\sum \left(a_j c_{ji}\right)^2}\right). \tag{4.33}$$

The wind turbines are placed in R rows and C columns with coordinates x_i and their indices can be written as $i = i_c + i_r C$, where $i_c \in \{1, \dots, C\}$ and $i_r \in \{0, \dots, R-1\}$. They are tasked to maximize the wind farm power output under local constraints $a_i \in [a_{\min}, a_{\max}]$ and coupling constraints $|a_i - a_j| \leq b$ for all i, j, where it holds that $j_r = i_r + 1$.

For our numerical simulation, we choose a similar setup as in [70]. The wind farm setup geometric setup is shown in Figure 4.4 and the following parameters are chosen: $\rho = 1.225$, $U_\infty = 8$, $\tau = 10$, $\gamma_i = \gamma_0 = 0.05$, $\epsilon = 0.005$, $b = 0.03$, $a_{\min} = 0.1$, $a_{\max} = \frac{1}{3}$. We take the same parameter estimation scheme as in previous numerical simulation, apart from the perturbation frequencies that we randomly choose in the interval $[3, 11]$ and perturbation amplitudes that we take as $\|d_i\| = 0.01$. All initial conditions, apart from a_i, were set to zero. The initial condition for a_i was set to $\frac{1}{3}$, which corresponds to the greedy strategy in [70]. In our simulations, we use three different wind directions. In the time interval $[0, 50000)$, the wind was blowing with speed direction vector $\vec{v}_1 = (2, -1)$; in the time interval $[50000, 100000)$, the wind was blowing with the speed direction vector $\vec{v}_2 = (0, -1)$; and finally, in the time interval $[100000, 150000]$, the wind was blowing with speed direction vector $\vec{v}_3 = (-1, -1)$. We assume that the wind turbines instantly adjust their orientation towards the wind direction as this process is relatively fast compared with the GNE learning process. The simulation results are shown in Figure 4.5. We can see that the wind turbines reach a neighborhood of the v-GNE, even with the delay introduced by AIL dynamics.

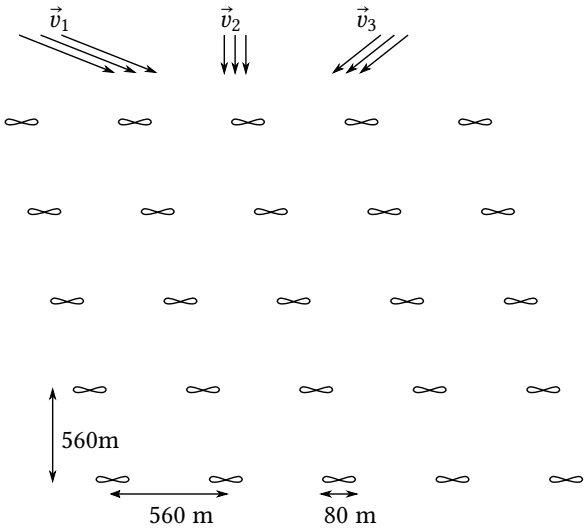

Figure 4.4: Layout of the wind turbines and the wind directions.

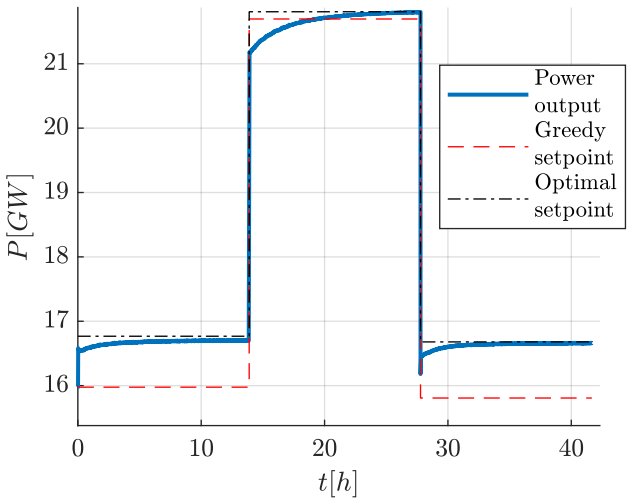

Figure 4.5: Power generation with the proposed algorithm (solid line) compared to the greedy power output setpoint (dashed red) and the global optimal power setpoint (dot-dashed black).

4.6 Conclusion

Generalized Nash equilibrium problems with nonlinear dynamical agents can be solved via a preconditioned forward-backward algorithm that uses estimates of the pseudogradient mapping if it is strongly monotone and Lipschitz continuous, and if the dynamical agents have a certain exponential stability property. Regular projections enable the use of a parameter estimation scheme. Numerical simulations show that there is a trade-off between closeness to the equilibrium solution and the speed of convergence.

Appendix

4.A Proof of Theorem 4.8

To prove the convergence of the algorithm, we show that equation in (4.12) is equivalent to a continuous-time preconditioned forward-backward algorithm, whose convergence is proven using well-known properties of monotone operators. First, we show the equivalence. Let us denote $\omega = \mathrm{col}(\boldsymbol{u}, \lambda)$. We write Equation (4.12) as:

$$\dot{\omega} = -\omega + \mathrm{proj}_{\Omega\times\mathbb{R}^q_+}\left(\omega + \boldsymbol{\Gamma}\begin{bmatrix} -F(\boldsymbol{u}) - A^\top\lambda \\ A\boldsymbol{u} - b + 2A\dot{\boldsymbol{u}}\end{bmatrix}\right), \tag{4.34}$$

where $\boldsymbol{\Gamma} = \mathrm{blkdiag}\left(\Gamma, \gamma_0 I_q\right)$. Next, by the property of projection operator in [42, Prep. 6.47], Equ. (4.34) reads as

$$\dot{\omega} + \omega + \boldsymbol{\Gamma}\mathrm{N}_{\Omega\times\mathbb{R}^q_+}(\dot{\omega} + \omega) \ni \omega + \boldsymbol{\Gamma}\begin{bmatrix} -F(\boldsymbol{u}) - A^\top\lambda \\ A\boldsymbol{u} - b + 2A\dot{\boldsymbol{u}}\end{bmatrix}. \tag{4.35}$$

When the elements of the last matrix product in (4.35) are rearranged and the equation is premultiplied by $\boldsymbol{\Gamma}^{-1}$, the equations read as follows:

$$\begin{aligned}\left(\boldsymbol{\Gamma}^{-1} + \mathrm{N}_{\Omega\times\mathbb{R}^q_+}\right)(\dot{\omega} + \omega) &\ni \hat{\Phi}\omega + \begin{bmatrix} -F(\boldsymbol{u}) \\ -b\end{bmatrix} + \begin{bmatrix} 0 \\ 2A\dot{\boldsymbol{u}}\end{bmatrix} \\ \left(\boldsymbol{\Gamma}^{-1} + \mathrm{N}_{\Omega\times\mathbb{R}^q_+}\right)(\dot{\omega} + \omega) &\ni \Phi\omega - \begin{bmatrix} F(\boldsymbol{u}) \\ b\end{bmatrix} + \hat{A}(\omega + \dot{\omega}).\end{aligned} \tag{4.36}$$

where we have used the notation

$$\hat{\Phi} = \begin{bmatrix} \Gamma^{-1} & -A^\top \\ A & \gamma_0^{-1} I_q\end{bmatrix}, \quad \Phi = \begin{bmatrix} \Gamma^{-1} & -A^\top \\ -A & \gamma_0^{-1} I_q\end{bmatrix}, \quad \hat{A} = \begin{bmatrix} 0 & 0 \\ 2A & 0\end{bmatrix}.$$

Next, the following expression is valid for the matrices:

$$\boldsymbol{\Gamma}^{-1} - \hat{A} = \Phi + \begin{bmatrix} 0 & A^\top \\ -A & 0\end{bmatrix} = \Phi + \Psi. \tag{4.37}$$

From Equations (4.36) and (4.37), it follows

$$\left(\mathrm{Id} + \Phi^{-1}\left(\mathrm{N}_{\Omega\times\mathbb{R}^q_+} + \Psi\right)\right)(\dot{\omega} + \omega) \ni \omega - \Phi^{-1}\begin{bmatrix} F(\boldsymbol{u}) \\ b\end{bmatrix}.$$

By inverting the operator on the left side of the previous expression, we finally arrive at the desired equation:

$$\begin{aligned}\dot{\omega} &= -\omega + \left(\mathrm{Id} + \Phi^{-1}\mathcal{A}\right)^{-1} \circ \left(\omega - \Phi^{-1}\mathcal{B}(\omega)\right) \Leftrightarrow \\ \dot{\omega} &= -\omega + J_{\Phi^{-1}\mathcal{A}}\left(\omega - \Phi^{-1}\mathcal{B}(\omega)\right),\end{aligned} \tag{4.38}$$

where $\mathcal{A} = \mathrm{N}_{\Omega\times\mathbb{R}^q_+} + \Psi$ and $\mathcal{B} = \mathrm{col}\,(F(\boldsymbol{u}), b)$. Equation (4.38) represents a forward-backward algorithm preconditioned by matrix Φ^{-1}. Fixed points of the operator on the right-hand side of (4.38) ([42, Prep. 26.1, (iv)(a)], [44, Lemma 1], (4.10)) represent GNE that are the solutions to the game in (4.7) and equilibrium points of dynamics in (4.25). Before proving convergence, we have to prove an additional result.

Lemma 4.14. *Let $T = (\mathrm{Id}+\mathcal{A})^{-1}\circ(\mathrm{Id}-\mathcal{B})$, where $\mathcal{A}$ is maximally monotone. Then it holds:*

$$\langle Tx - x^* \mid x - Tx\rangle \geq \langle Tx - x^* \mid \mathcal{B}x - \mathcal{B}x^*\rangle.$$

for all $(x, x^*) \in \mathrm{dom}(T)\times\mathrm{fix}(T)$. □

Proof. Let us denote $x^* = Tx^* = J_{\mathcal{A}}y^*$ as the fixed point of operator T. Then it holds:

$$\begin{aligned}
&\langle Tx - x^* \mid x - Tx - (\mathcal{B}x - \mathcal{B}x^*)\rangle\\
&= \langle Tx - x^* \mid x - \mathcal{B}x - Tx + x^* - (x^* - \mathcal{B}x^*)\rangle\\
&= \langle Tx - x^* \mid y - Tx + x^* - y^*\rangle\\
&= \langle J_{\mathcal{A}}y - J_{\mathcal{A}}y^* \mid (\mathrm{Id}-J_{\mathcal{A}})y - (\mathrm{Id}-J_{\mathcal{A}})y^*\rangle\\
&\geq 0,
\end{aligned} \tag{4.39}$$

where the last equation holds due to properties of firmly nonexpansive operators. ■

Now we denote $\tilde{\mathcal{A}} = \Phi^{-1}\mathcal{A}$, $\tilde{\mathcal{B}} = \Phi^{-1}\mathcal{B}$ and $T = (\mathrm{Id}+\tilde{\mathcal{A}})^{-1}\circ(\mathrm{Id}-\tilde{\mathcal{B}})$. Then, the dynamics in (4.38) read as $\dot{\omega} = -\omega + T\omega$. We propose the Lyapunov function candidate

$$V(\omega) = \tfrac{1}{2}\|\omega - \omega^*\|^2, \tag{4.40}$$

where ω^* is a fixed point of operator T. Its derivative along the trajectory in (4.38) is then

$$\begin{aligned}
\dot{V}(\omega) &= -\langle \omega - \omega^* \mid \omega - T\omega\rangle\\
&= -\|\dot{\omega}\|^2 - \langle T\omega - \omega^* \mid \omega - T\omega\rangle
\end{aligned} \tag{4.41}$$

From Lemma 4.14, it follows that

$$\begin{aligned}
\dot{V}(\omega) &\leq -\|\dot{\omega}\|^2 - \left\langle T\omega - \omega^* \,\middle|\, \tilde{\mathcal{B}}\omega - \tilde{\mathcal{B}}\omega^*\right\rangle\\
&\leqq -\|\dot{\omega}\|^2 - \left\langle T\omega - \omega \,\middle|\, \tilde{\mathcal{B}}\omega - \tilde{\mathcal{B}}\omega^*\right\rangle - \left\langle \omega - \omega^* \,\middle|\, \tilde{\mathcal{B}}\omega - \tilde{\mathcal{B}}\omega^*\right\rangle\\
&\leqq -\|\dot{\omega}\|^2 - \left\langle T\omega - \omega \,\middle|\, \Phi^{-1}(\mathcal{B}\omega - \mathcal{B}\omega^*\right\rangle - \left\langle \omega - \omega^* \,\middle|\, \Phi^{-1}(\mathcal{B}\omega - \mathcal{B}\omega^*\right\rangle.
\end{aligned} \tag{4.42}$$

Bounds on the eigenvalues of Φ can be estimated with Gershgorin's theorem. For small enough step sizes, we denote the lower and upper bound on the eigenvalues as $\sigma_{\min} = \frac{1}{\max_{i\in I_0}(\gamma_i^{-1}) + \|A\|}$ and $\sigma_{\max} = \frac{1}{\min_{i\in I_0}(\gamma_i^{-1}) - \|A\|}$, respectively. We bound (4.42) as

$$\dot{V}(\omega) \leq -\|\dot{\omega}\|^2 + \sigma_{\max}\|\dot{\omega}\|\|\mathcal{B}\omega - \mathcal{B}\omega^*\| - \sigma_{\min}\langle \omega - \omega^* \mid \mathcal{B}\omega - \mathcal{B}\omega^*\rangle. \tag{4.43}$$

Since $F(\boldsymbol{u})$ is strongly monotone and Lipschitz continuous, it is also cocoercive [44, Lemma 5]. Therefore, the operator $\mathcal{B}$ is $\frac{\mu}{L^2}$ cocoercive. Equ. (4.43) then becomes:

$$\begin{aligned}\dot{V}(\omega) &\leq -\|\dot{\omega}\|^2 + \sigma_{\max}\|\dot{\omega}\|\|\mathcal{B}\omega - \mathcal{B}\omega^*\| - \tfrac{\sigma_{\min}}{2}\beta\|\mathcal{B}\omega - \mathcal{B}\omega^*\|^2 - \tfrac{\sigma_{\min}}{2}\langle \omega - \omega^* \mid \mathcal{B}\omega - \mathcal{B}\omega^*\rangle \\ &\leq -\tfrac{1}{2}\|\dot{\omega}\|^2 - \tfrac{\sigma_{\min}}{2}\langle \omega - \omega^* \mid \mathcal{B}\omega - \mathcal{B}\omega^*\rangle - \tfrac{1}{2}\begin{bmatrix}\|\dot{\omega}\| & \|\mathcal{B}\omega - \mathcal{B}\omega^*\|\end{bmatrix}\begin{bmatrix}1 & \sigma_{\max} \\ \sigma_{\max} & \beta\sigma_{\min}\end{bmatrix}\begin{bmatrix}\|\dot{\omega}\| \\ \|\mathcal{B}\omega - \mathcal{B}\omega^*\|\end{bmatrix} \end{aligned} \tag{4.44}$$

Since, it is always possible to choose parameters γ_i and γ_0 small enough such that $\beta\sigma_{\min} \geq \sigma_{\max}^2$ and the matrix in (4.44) is negative definite, the last equation reads as

$$\begin{aligned}\dot{V}(\omega) &\leq -\tfrac{1}{2}\|\dot{\omega}\|^2 - \tfrac{\sigma_{\min}}{2}(\omega - \omega^*)^\top(\mathcal{B}\omega - \mathcal{B}\omega^*) \\ &\leq -\tfrac{1}{2}\|\dot{\omega}\|^2 - \tfrac{\mu\sigma_{\min}}{2}\|\tilde{\boldsymbol{u}}\|^2,\end{aligned} \tag{4.45}$$

where $\tilde{\boldsymbol{u}} = \boldsymbol{u} - \boldsymbol{u}^*$ and the last line follows from strong monotonicity of $F(\boldsymbol{u}^*)$. The rest of the proof represents a La Salle argument. As the right-hand side is a sum of negative squares, it follows that $\dot{V}(\omega) \leq 0$ for all ω. Let us denote the following sets

$$\begin{aligned}\zeta_c &:= \{\omega \in \Omega \times \mathbb{R}_+^q \mid V(\omega) \leq c\} \\ \zeta_o &:= \{\omega \in \zeta_c \mid \|\dot{\omega}\| = 0 \text{ and } \|\tilde{\boldsymbol{u}}\| = 0\} \\ \mathcal{Z} &:= \{\omega \in \zeta_c \mid \dot{V}(\omega) = 0\} \\ \mathcal{O} &:= \{\omega \in \zeta_c \mid \omega(0) \in \mathcal{Z} \implies \omega(t) \in \mathcal{Z}\ \forall t \in \mathbb{R}\}, \\ \mathcal{A} &:= \{\omega \in \zeta_c \mid \dot{\omega} = \mathbf{0}\},\end{aligned} \tag{4.46}$$

where ζ_c is a compact level set chosen such that it is nonempty, $\mathcal{Z}$ is the zero set of (4.41), ζ_o is the superset of $\mathcal{Z}$ which follows from (4.45), $\mathcal{O}$ is the maximum invariant set as explained in [29, Chp. 4.2] and $\mathcal{A}$ is the equilibrium set. It holds that $\zeta_c \supseteq \zeta_o \supseteq \mathcal{Z} \supseteq \mathcal{O} \supseteq \mathcal{A}$. As ζ_c is invariant and the right-hand side equations of (4.12) are (locally) Lipschitz, by [29, Thm. 3.3] we conclude that solutions to (4.12) exist and are unique. Next we note that $\dot{\omega} = 0 \Leftrightarrow \omega \in \mathrm{fix}(T)$. Therefore, the set $\mathcal{A}$ is the set of fixed points, and it holds $\zeta_o \equiv \mathcal{Z} \equiv \mathcal{O} \equiv \mathcal{A}$. Hence, by La Salle's invariance principle [29, Thm. 4.4], trajectories converge to the set $\mathcal{A}$. Additionally, as $\tilde{\boldsymbol{u}} = \mathbf{0}$ in $\mathcal{A}$, it follows that u^* is a singleton, which is not necessarily true for λ^*.

4.B Proof of Theorem 4.10

Similarly to Theorem 1, it can be shown that the dynamics in (4.14) can be written as

$$\dot{\bar{\omega}} = -\bar{\omega} + J_{\bar{\Phi}^{-1}\bar{\mathcal{A}}}\left(\bar{\omega} - \Phi^{-1}\bar{\mathcal{B}}(\omega)\right), \tag{4.47}$$

where $\bar{\omega} := \mathrm{col}(\boldsymbol{u}, \boldsymbol{z}, \boldsymbol{\lambda})$, $\bar{\mathcal{A}} := \mathrm{N}_{\Omega \times \mathbb{R}^{Nq} \times \mathbb{R}_+^{Nq}} + \bar{\Psi}$, $\bar{\mathcal{B}} := \mathrm{col}\left(F(\boldsymbol{u}), \mathbf{0}_{Nq}, \frac{\boldsymbol{b}}{N} + \bar{L}\lambda\right)$,

$$\bar{\Psi} := \begin{bmatrix} 0 & 0 & \Lambda^\top \\ 0 & 0 & -\bar{L} \\ -\Lambda^\top & \bar{L} & 0 \end{bmatrix}, \qquad \bar{\Phi} := \begin{bmatrix} \Gamma^{-1} & 0 & -\Lambda^\top \\ 0 & \bar{\Gamma}^{-1} & \bar{L} \\ -\Lambda & \bar{L} & \bar{\Gamma}^{-1} \end{bmatrix}.$$

Proof that an equilibrium point $\bar{\omega}^*$ of (4.47) exist and that $\boldsymbol{u}^*$ is the solution to the game in (4.7) is analogous to the proof of Theorem 2 in [44] and is omitted for brevity. Furthermore, as all of the operators and matrices hold the same properties as the ones in Theorem 1 of this paper, convergence is proven in the same manner.

4.C Proof of Theorem 4.12

Let us consider a Lyapunov function candidate $V = V_\theta + V_\omega$, where V_θ represents a parameter estimation error and V_ω represents a primal-dual convergence error:

$$V_\theta(\tilde{\boldsymbol{\eta}}, \tilde{\boldsymbol{\theta}}) = \sum_{i \in \mathcal{I}} \left(\tfrac{1}{2} \|\widetilde{\eta}_i\|^2 + \tfrac{1}{2} \left\|\widetilde{\theta}_i\right\|_{\Sigma_i} \right), \tag{4.48}$$

$$V_\omega(\omega) = \tfrac{1}{2} \|\omega - \omega^*\|^2. \tag{4.49}$$

Since we anticipate that the derivative of the projection function does not exist on some corner points, we use the Lyapunov theory for differential inclusions as in [72, Chp. 2], namely we use upper Dini derivatives (D^+) instead of regular time derivatives. For ease of notation, we use the regular derivatives whenever they are equal to Dini derivatives.

Outline of the proof: We first bound all of the positive terms in D^+V_θ with functions of variables $(\boldsymbol{\eta}, \hat{\boldsymbol{\theta}}, \omega)$, then we similarly bound all of the terms in D^+V_ω introduced by the parameter estimates. Finally, we use the quadratic terms of D^+V to show that the negative terms majorize the positive terms.

Parameter estimation term

We bound the Dini derivative of V_θ similarly to [20, Thm. 1] and [41, Eq. 31] with the only difference that we let each agent choose their parameters (σ_i, K_i, ρ_i). The Lyapunov derivative, similar to [20, p. 4, col. 1], reads as follows:

$$\begin{aligned} D^+V_\theta(\tilde{\boldsymbol{\eta}}, \tilde{\boldsymbol{\theta}}) \leq \sum_{i \in \mathcal{I}} \Bigg(& -\widetilde{\eta}_i^\top \left(K_i - \tfrac{1}{2} - \tfrac{k_1 \zeta_i}{2} \right) \widetilde{\eta}_i - \tfrac{1}{2} \|e_i - \eta_i\|^2 - \tfrac{\rho_i' \gamma_i^1}{2} \left\|\widetilde{\theta}_i\right\|^2 + \tfrac{\sigma_i}{2} \|\theta_i\|^2 \\ & + \tfrac{1}{2k_1} \left\|D^+\theta_i\right\|^2 + \tfrac{\gamma_i^2}{2k_2} \left\|D^+\theta_i\right\|^2 \Bigg) \\ \leq & -k_{\mathrm{a}} \|\tilde{\boldsymbol{\eta}}\|^2 - k_{\mathrm{b}} \|\tilde{\boldsymbol{\theta}}\|^2 - \tfrac{1}{2} \|\boldsymbol{e} - \boldsymbol{\eta}\|^2 + k_{\mathrm{c}} \|D^+\boldsymbol{\theta}\|^2 + \tfrac{\sigma}{2} \|\boldsymbol{\theta}\|^2, \end{aligned} \tag{4.50}$$

where $k_1, k_2 > 0$, $\zeta_i = c_i c_i^\top$, $0 < \gamma_i^1 \leq \gamma_i^2$ are bounds for matrices Σ_i, $\rho_i' = \rho_i - k_2$ for all $i \in \mathcal{I}$, $k_{\mathrm{a}} := \min_i \left(K_i - \tfrac{1}{2} - \tfrac{k_1 \zeta_i}{2} \right)$, $k_{\mathrm{b}} := \min_i \left(\tfrac{k_i^\Sigma \gamma_i^1}{2} \right)$, $k_{\mathrm{c}} := \max_i \left(\tfrac{1}{2k_1} + \tfrac{\gamma_i^2}{2k_2} \right)$ and $\sigma := \max_i \sigma_i$[1]. Assumption 4.11 is used to derive these expressions. We define the compact set $\zeta_c := \{(\omega, \hat{\boldsymbol{\eta}}, \hat{\boldsymbol{\theta}}) \in \mathcal{U} \times \mathbb{R}^q \times \mathbb{R}^N \times \mathbb{R}^m \mid V(\omega, \tilde{\boldsymbol{\eta}}, \tilde{\boldsymbol{\theta}}) \leq c\}$. Next, we bound the positive terms in (4.50). The analysis starts with $\boldsymbol{\theta} = \operatorname{col}\left(\boldsymbol{\theta}^0, \boldsymbol{\theta}^1\right)$, where

$$\boldsymbol{\theta}^0 := \operatorname{col}\left(\left(\nabla_{\boldsymbol{u}_{-i}} J_i(u_i, \boldsymbol{u}_{-i})^\top \dot{\boldsymbol{u}}_{-i} \right)_{i \in \mathcal{I}} \right) = J^0(\boldsymbol{u}) \dot{\boldsymbol{u}}, \tag{4.51}$$

$$\boldsymbol{\theta}^1 := F(\boldsymbol{u}). \tag{4.52}$$

We have that

$$\begin{aligned} &\|\boldsymbol{\theta}^0\| \leq \|J^0(\boldsymbol{u})\| \|\dot{\boldsymbol{u}}\| = L^0 \|\dot{\boldsymbol{u}}\|, \\ &\|\boldsymbol{\theta}^1\| = \|F(\boldsymbol{u})\| \leq \|F(\boldsymbol{u}) - F(\boldsymbol{u}^*)\| + \|F(\boldsymbol{u}^*)\| \leq \ell \|\tilde{\boldsymbol{u}}\| + \|F(\boldsymbol{u}^*)\|, \end{aligned}$$

[1] The term $\tfrac{1}{2}\|\boldsymbol{e} - \boldsymbol{\eta}\|^2$ was omitted in [20] (page 4, first column, second to last equation) and [41], as it is not required.

where $L^0 := \max_{\boldsymbol{u}\in\mathcal{U}} \left\|J^0(\boldsymbol{u})\right\| < \infty$, since $\mathcal{U}$ is bounded. Then, we bound $\|\theta\|$ as follows

$$\begin{aligned}\|\theta\|^2 &\leq {L^0}^2\|\dot{\boldsymbol{u}}\|^2 + (\ell\|\tilde{\boldsymbol{u}}\| + \|F(\boldsymbol{u}^*)\|)^2\\ &\leqq L_1\|\dot{\boldsymbol{u}}\|^2 + L_2\|\tilde{\boldsymbol{u}}\|^2 + L_3\|F(\boldsymbol{u}^*)\|^2,\end{aligned}$$

for $L_1 := {L^0}^2$, $L_2 := 2\ell^2$ and $L_3 = 2$. In order to bound $\|D^+\boldsymbol{\theta}\|$, we observe the dini derivatives of $\boldsymbol{\theta}^0$ and $\boldsymbol{\theta}^1$:

$$\|D^+\boldsymbol{\theta}^0\| \leq \|\dot{\boldsymbol{u}}^\top H_{J^0}\dot{\boldsymbol{u}}\| + \|J^0(\boldsymbol{u})D^+\dot{\boldsymbol{u}}\|, \tag{4.53}$$

$$\|D^+\boldsymbol{\theta}^1\| = \|\nabla F(\boldsymbol{u})\dot{\boldsymbol{u}}\| \leq L\|\dot{\boldsymbol{u}}\|, \tag{4.54}$$

$$\begin{aligned}\|D^+\dot{\boldsymbol{u}}\| &= \left\|\dot{\boldsymbol{u}} + D^+\operatorname{proj}_\Omega\left(\boldsymbol{u} - \Gamma(\boldsymbol{\theta}^1 + A^\top\lambda) + d(t)\right)\right\|\\ &\leq 2\|\dot{\boldsymbol{u}}\| + \sigma_{\max}(\Gamma)\|\dot{\hat{\boldsymbol{\theta}}}^1\| + \sigma_{\max}(\Gamma)\|A\|\|\dot{\lambda}\| + \|\dot{d}(t)\|\end{aligned}$$

Next, we bound $\|\dot{\hat{\boldsymbol{\theta}}}^1\|$ using the dynamics in (4.24):

$$\|\dot{\hat{\boldsymbol{\theta}}}\| \leq \sum_{i\in\boldsymbol{I}}(\|\Sigma_i^{-1}c_i(e_i - \eta_i)\| + \sigma_i\|\Sigma_i^{-1}\|\|\theta_i - \tilde{\theta}_i\|$$

On a compact set ζ_c, c_i and Σ_i are bounded. Therefore, the last equation reads as:

$$\|\dot{\hat{\boldsymbol{\theta}}}\| \leq L_3^*\|(\boldsymbol{e} - \boldsymbol{\eta})\| + L_4^*\|\boldsymbol{\theta}\| + L_5^*\|\tilde{\boldsymbol{\theta}}\|,\ L_3^*, L_4^*, L_5^* > 0$$

Now, bound on $\|D^+\dot{\boldsymbol{u}}\|$ equals to:

$$\begin{aligned}\|D^+\dot{\boldsymbol{u}}\| \leq{}& 2\|\dot{\boldsymbol{u}}\| + \sigma_{\max}(\Gamma)L_3^*\|(\boldsymbol{e} - \boldsymbol{\eta})\| + \sigma_{\max}(\Gamma)L_4^*\|\boldsymbol{\theta}\|\\ &+ \sigma_{\max}(\Gamma)L_5^*\|\tilde{\boldsymbol{\theta}}\| + \sigma_{\max}(\Gamma)\|A\|\|\dot{\lambda}\| + \|\dot{d}(t)\|\end{aligned} \tag{4.55}$$

On a compact set ζ_c, $\dot{\boldsymbol{u}}^\top H_{J^0}$ is bounded, therefore by combining (4.53), (4.54), (4.55) and the arithmetic mean - quadratic mean inequality, it follows:

$$\begin{aligned}\|D^+\boldsymbol{\theta}\|^2 \leq{}& L_4\|\dot{\boldsymbol{u}}\|^2 + L_5\|\dot{\lambda}\|^2 + L_6\|\boldsymbol{\theta}\|^2 + L_7\|\tilde{\boldsymbol{\theta}}\|^2\\ &+ L_8\|\boldsymbol{e} - \boldsymbol{\eta}\|^2 + L_9\|\dot{d}(t)\|^2,\end{aligned}$$

for some positive L_4 to L_9. By using the previously calculated bounds, D^+V_θ reads as:

$$\begin{aligned}D^+V_\theta \leq{}& -k_a\|\tilde{\eta}\|^2 - (k_b - k_c L_7)\|\tilde{\boldsymbol{\theta}}\|^2 - \left(\tfrac{1}{2} - k_c L_8\right)\|\boldsymbol{e} - \boldsymbol{\eta}\|^2 + (k_c L_4 + (\sigma + k_c L_6)L_1)\|\dot{\boldsymbol{u}}\|^2\\ &+ (\sigma + k_c L_6)L_2\|\tilde{\boldsymbol{u}}\|^2 + k_c L_5\|\dot{\lambda}\|^2 + k_c L_9\|\dot{d}(t)\|^2 + (\sigma + k_c L_6)L_3\|F(\boldsymbol{u}^*)\|.\end{aligned} \tag{4.56}$$

Primal-dual term

Unlike the full-information case, our agents use the estimate $\hat{\boldsymbol{\theta}}^1$ instead of $F(\boldsymbol{u})$. Therefore, by adding and subtracting the derivative of the full-information case in the Dini derivative

of (4.48), we have:

$$\begin{aligned}
D^+V_\omega(\omega) = \Big\langle \omega-\omega^* \Big| -\omega + J_{\Phi^{-1}\mathcal{A}}\left(\omega-\Phi^{-1}\mathcal{B}(\omega)\right) - \mathrm{proj}_{\Omega\times\mathbb{R}^q_+}\left(\omega+\Gamma\begin{bmatrix}-F(\boldsymbol{u})-A^\top\lambda\\ A\boldsymbol{u}-b+2A\dot{\boldsymbol{u}}\end{bmatrix}\right)\\
+\mathrm{proj}_{\Omega\times\mathbb{R}^q_+}\left(\omega+\Gamma\begin{bmatrix}-\boldsymbol{\theta}^1-A^\top\lambda\\ A\boldsymbol{u}-b+2A\dot{\boldsymbol{u}}\end{bmatrix}+\begin{bmatrix}d(t)\\0\end{bmatrix}\right)\Big\rangle\\
\leq -\tfrac{1}{2}\|\dot\omega\|^2 - \tfrac{\mu\sigma_{\min}}{2}\|\tilde{\boldsymbol{u}}\|^2 + \sigma_{\max}(\Gamma)\|\tilde{\boldsymbol{u}}\|\|\tilde{\boldsymbol{\theta}}\| + \|\tilde{\boldsymbol{u}}\|\|d(t)\|\\
\leq -\tfrac{1}{2}\|\dot\omega\|^2 - \left(\tfrac{\mu\sigma_{\min}}{2} - \tfrac{\sigma_{\max}(\Gamma)}{2k_3} - \tfrac{1}{2k_4}\right)\|\tilde{\boldsymbol{u}}\|^2 + \tfrac{\sigma_{\max}(\Gamma)k_3}{2}\|\tilde{\boldsymbol{\theta}}\|^2 + \tfrac{k_4}{2}\|d(t)\|^2,
\end{aligned}$$

where the last line follows from the inequality

$$ab \leq \tfrac{1}{2k}a^2 + \tfrac{k}{2}b^2, \quad \forall (a,b,k)\in(\mathbb{R}^2\times\mathbb{R}_{>0}). \tag{4.57}$$

Complete Lyapunov candidate

Finally, the Dini derivative of V is bounded as follows:

$$\begin{aligned}
D^+V_\omega + D^+V_\theta \leq& -\left(\tfrac{1}{2}-k_cL_4-(\sigma+k_cL_6)L_1\right)\|\dot{\boldsymbol{u}}\|^2 - \left(\tfrac{\mu\sigma_{\min}}{2} - \tfrac{\sigma_{\max}(\Gamma)}{2k_3} - \tfrac{1}{2k_4} - (\sigma-k_cL_6)L_2\right)\|\tilde{\boldsymbol{u}}\|^2\\
&-\left(\tfrac{1}{2}-k_cL_5\right)\|\dot\lambda\|^2 - k_a\|\tilde{\boldsymbol{\eta}}\|^2 - \left(\tfrac{1}{2}-k_cL_8\right)\|\boldsymbol{e}-\boldsymbol{\eta}\|^2\left(k_b - k_cL_7 - \tfrac{\sigma_{\max}(\Gamma)k_3}{2}\right)\|\tilde{\boldsymbol{\theta}}\|^2\\
&+k_cL_9\|\dot d(t)\|^2 + (\sigma+k_cL_6)L_3\|F(\boldsymbol{u}^*)\|^2 + \tfrac{k_4}{2}\|d(t)\|^2\\
\leqq& -b_1\|\dot{\boldsymbol{u}}\|^2 - b_2\|\dot\lambda\|^2 - k_a\|\tilde{\boldsymbol{\eta}}\|^2b_3 - b_3\|\boldsymbol{e}-\boldsymbol{\eta}\|^2 - b_4\|\tilde{\boldsymbol{u}}\|^2 - b_5\|\tilde{\boldsymbol{\theta}}\|^2\\
&+k_cL_9\|\dot d(t)\|^2 + (\sigma+k_cL_6)L_3\|F(\boldsymbol{u}^*)\|^2 + \tfrac{k_4}{2}\|d(t)\|^2.
\end{aligned} \tag{4.58}$$

Now, we can make the last three norms arbitrarily small and b_1, b_2, b_3 positive by choosing k_c, σ and k_4 small enough, we can make b_4 positive by choosing $(\sigma_i)_{i\in\mathcal{I}}$ small enough, we can make b_5 positive by making k_b large enough. Of the mentioned parameters, only k_b and k_c cannot be chosen arbitrarily. To make k_c small enough we have to chose parameters k_1 and k_2 small enough, to make k_b large enough, we chose $(K_i)_{i\in\mathcal{I}}$ and $(\rho_i)_{i\in\mathcal{I}}$ large enough. Since the positive terms can be made arbitrarily small, we conclude that the Lyapunov derivative can be made negative on the boundary of the set ζ_c, which implies that the set is invariant. As the right-hand side of equations (4.19)–(4.23), (4.25) is (locally) Lipschitz on their domain, by [29, Thm. 3.3], we conclude that their solutions exist and are unique. Furthermore, as ζ_c was chosen for arbitrary c, it follows that for any compact set K of initial conditions, it is possible to find such control parameters that for $(\boldsymbol{\eta}(0), \hat{\boldsymbol{\theta}}(0), \boldsymbol{u}(0)) \in K$, $(\tilde{\boldsymbol{\eta}}, \tilde{\boldsymbol{\theta}}, \boldsymbol{u})$ converge to an arbitrarily small neighborhood of $(0,0,\boldsymbol{u}^*)$, which concludes the proof. For λ, we can only claim that this is bounded.

4.D Proof of Theorem 4.13

We have to prove that there exists a timescale separation between the GNE learning scheme described in section 3 and the dynamics of the multi-agent system in (4.27) such that the interconnection is also stable. Let us consider a Lyapunov function candidate $V = V_\theta + V_\omega + V_z$, where V_θ and V_ω are the same as (4.48), (4.49) and V_z is formed using Standing Assumption 4.3 in the following way:

$$V_z(\boldsymbol{z},\boldsymbol{u}) = \textstyle\sum_{i\in\mathcal{I}} V_i(z_i,u_i). \tag{4.59}$$

Outline of the proof: We first bound all of the terms in D^+V_z introduced by nonconstant inputs with functions of the variables $(\boldsymbol{\eta}, \hat{\boldsymbol{\theta}}, \omega, \boldsymbol{z})$, then we bound all of the terms in D^+V_θ introduced by the redefinition of error e_i in (4.28) in the same manner. Ultimately, we use the quadratic terms of the complete D^+V to show that the negative terms majorize the additional terms.

Multi-agent term

Let us do a change of variables $\boldsymbol{z} = \boldsymbol{x} - \pi(\boldsymbol{u})$ in (4.27). New dynamics read as

$$\epsilon \dot{\boldsymbol{z}} = f(\boldsymbol{z} + \pi(\boldsymbol{u}), \boldsymbol{u}) - \epsilon \nabla \pi(u) \dot{\boldsymbol{u}}. \tag{4.60}$$

Dini derivative of (4.59), by plugging in (4.60), reads as

$$\begin{aligned} D^+V_z(\boldsymbol{z}, \boldsymbol{u}) &= \nabla_{\boldsymbol{z}} V_{\boldsymbol{z}}^\top \dot{\boldsymbol{z}} + \nabla_{\boldsymbol{u}} V_{\boldsymbol{z}}^\top \dot{\boldsymbol{u}} \\ &= \tfrac{1}{\epsilon} \nabla_{\boldsymbol{z}} V_z(\boldsymbol{z}, \boldsymbol{u})^\top f(\boldsymbol{z} + \pi(\boldsymbol{u}), \boldsymbol{u}) - \nabla_{\boldsymbol{z}} V_z(\boldsymbol{z}, \boldsymbol{u})^\top \nabla \pi(\boldsymbol{u}) \dot{\boldsymbol{u}} + \nabla_{\boldsymbol{u}} V_z(\boldsymbol{z}, \boldsymbol{u})^\top \dot{\boldsymbol{u}} \end{aligned}$$

By using Standing Assumption 4.3 and inequality (4.57), we can further improve the bound:

$$\begin{aligned} D^+V_z(\boldsymbol{z}, \boldsymbol{u}) &\leq -\tfrac{\kappa}{\epsilon} \|\boldsymbol{z}\|^2 + L_{10} \|\boldsymbol{z}\| \|\dot{\boldsymbol{u}}\| \\ &\leq -\left(\tfrac{\kappa}{\epsilon} - \tfrac{L_{10} k_5}{2} \right) \|\boldsymbol{z}\|^2 + \tfrac{L_{10}}{2k_5} \|\dot{\boldsymbol{u}}\|^2, \end{aligned}$$

where $L_{10} > 0$ is the Lipschitz constant of the function $\max_{\boldsymbol{u} \in \mathcal{U}} \nabla_{\boldsymbol{u}} V_z(\boldsymbol{z}, \boldsymbol{u}) - \nabla_{\boldsymbol{z}} V_z(\boldsymbol{z}, \boldsymbol{u})^\top \nabla \pi(\boldsymbol{u})$ and $k_5 > 0$.

Parameter estimation term

GNE learning is identical as in the static case, apart from the measurements of the cost function. Let us denote

$$\begin{aligned} \boldsymbol{l} &:= \operatorname{col}((l_i)_{i \in \mathcal{I}}), \\ \boldsymbol{y} &:= \operatorname{col}\left((y_i)_{i \in \mathcal{I}}\right), \\ h(\boldsymbol{x}) &:= \operatorname{col}((h_i(u_i, \boldsymbol{u}_{-i}))_{i \in \mathcal{I}}). \end{aligned}$$

The difference in the measurement introduces an additional component in the bound for the derivative of the Lyapunov function of the parameter estimation term:

$$\begin{aligned} \|\tilde{\boldsymbol{\eta}}\| \left\| \dot{\boldsymbol{y}} - \dot{\boldsymbol{l}} \right\| &= \left\| \tilde{\boldsymbol{\eta}} \right\| \tfrac{d}{dt} (h(\boldsymbol{x}) - h(\pi(\boldsymbol{u}))) \Big\| \\ &= \|\tilde{\boldsymbol{\eta}}\| \left\| \tfrac{1}{\epsilon} \nabla h(\boldsymbol{x}) f(\boldsymbol{x}, \boldsymbol{u}) - \nabla h(\pi(\boldsymbol{u})) \nabla \pi(\boldsymbol{u}) \dot{\boldsymbol{u}} \right\| \\ &\leq \tfrac{1}{\epsilon} \|\tilde{\boldsymbol{\eta}}\| \|\nabla h(\boldsymbol{x}) f(\boldsymbol{x}, \boldsymbol{u}) - \nabla h(\boldsymbol{x}) f(\pi(\boldsymbol{u}), \boldsymbol{u})\| + \|\tilde{\boldsymbol{\eta}}\| \|\nabla h(\pi(\boldsymbol{u})) \nabla \pi(\boldsymbol{u}) \dot{\boldsymbol{u}}\| \\ &\leq \tfrac{L_{11}}{\epsilon} \|\tilde{\boldsymbol{\eta}}\| \|\boldsymbol{z}\| + L_{12} \|\tilde{\boldsymbol{\eta}}\| \|\dot{\boldsymbol{u}}\| \\ &\leq \left(\tfrac{L_{11} k_6}{2\epsilon} + \tfrac{L_{12} k_7}{2} \right) \|\tilde{\boldsymbol{\eta}}\|^2 + \tfrac{L_{11}}{2\epsilon k_6} \|\boldsymbol{z}\|^2 + \tfrac{L_{12}}{2k_7} \|\dot{\boldsymbol{u}}\|^2, \end{aligned}$$

where $L_{11}, L_{12}, k_7, k_6 > 0$ and the second to last equation follows from the (local) Lipschitz continuity of the functions and the fact that the variables are bounded on a compact set $\zeta_c := \{(\boldsymbol{x}, \omega, \hat{\boldsymbol{\eta}}, \hat{\boldsymbol{\theta}}) \in \boldsymbol{\mathcal{X}} \times \boldsymbol{\mathcal{U}} \times \mathbb{R}^q \times \mathbb{R}^N \times \mathbb{R}^m \mid V(\boldsymbol{z}, \omega, \tilde{\boldsymbol{\eta}}, \tilde{\boldsymbol{\theta}}) \leq c\}$.

Complete Lyapunov candidate

Finally, the Dini derivative of the complete Lyapunov function candidate is:

$$
\begin{aligned}
&D^+V_\theta(\omega)+D^+V_\theta(\hat{\boldsymbol{\eta}},\hat{\boldsymbol{\theta}})+D^+V_z(\boldsymbol{z},\boldsymbol{u})\\
&\leq -\left(\tfrac{1}{2}-k_cL_4-(\sigma+k_cL_6)L_1-\tfrac{L_{10}}{2k_5}-\tfrac{L_{12}}{2k_7}\right)\|\dot{\boldsymbol{u}}\|^2-\left(\tfrac{1}{2}-k_cL_5\right)\|\dot{\lambda}\|^2-\left(k_a-\tfrac{L_{11}k_6}{2\epsilon}-\tfrac{L_{12}k_7}{2}\right)\|\tilde{\boldsymbol{\eta}}\|^2\\
&\quad-\left(k_b-k_cL_7-\tfrac{\sigma_{\max}(\Gamma)k_3}{2}\right)\|\tilde{\boldsymbol{\theta}}\|^2-\left(\tfrac{\mu\sigma_{\min}}{2}-\tfrac{\sigma_{\max}(\Gamma)}{2k_3}-\tfrac{1}{2k_4}-(\sigma-k_cL_6)L_2\right)\|\tilde{\boldsymbol{u}}\|^2\\
&-\left(\tfrac{\kappa}{\epsilon}-\tfrac{L_{10}k_5}{2}-\tfrac{L_{11}}{2\epsilon k_6}\right)\|\boldsymbol{z}\|^2-\left(\tfrac{1}{2}-k_cL_8\right)\|\boldsymbol{e}-\boldsymbol{\eta}\|^2+k_cL_9\|\dot{d}(t)\|^2+(\sigma+k_cL_6)L_3\|F(\boldsymbol{u}^*)\|+\tfrac{k_4}{2}\|d(t)\|^2\\
&\leqq -b_1\|\dot{\boldsymbol{u}}\|^2-b_2\|\dot{\lambda}\|^2-b_3\|\tilde{\boldsymbol{\eta}}\|^2-b_4\|\tilde{\boldsymbol{\theta}}\|^2-b_5\|\tilde{\boldsymbol{u}}\|^2-b_6\|\boldsymbol{z}\|^2-b_7\|\boldsymbol{e}-\boldsymbol{\eta}\|^2+b_8\|F(\boldsymbol{u}^*)\|^2+b_9\|\dot{d}(t)\|^2\\
&\quad+b_{10}\|d(t)\|^2. \qquad (4.61)
\end{aligned}
$$

The rest follows analogously to the proof of Theorem 3 with the addition of the parameter ϵ. We conclude that it is possible to find such control parameters that for $(\tilde{\boldsymbol{\eta}}(0),\tilde{\boldsymbol{\theta}}(0),\boldsymbol{u}(0),\boldsymbol{z}(0))\in K$, $(\tilde{\boldsymbol{\eta}},\tilde{\boldsymbol{\theta}},\boldsymbol{u},\boldsymbol{z})$ converge to an arbitrarily small neighborhood of $(0,0,\boldsymbol{u}^*,0)$, which concludes the proof. For λ, the dual variable, we can only claim boundedness.

II

Equilibrium seeking without projections

5

Monotone games

The heart is the strongest muscle.

Braum, League of Legends

The best revenge is not to be like your enemy.

Marcus Aurelius

This chapter addresses the problem of learning a generalized Nash equilibrium (GNE) in merely monotone games. First, we propose a novel continuous semi-decentralized solution algorithm without projections that uses first-order information to compute a GNE with a central coordinator. As the second main contribution, we design a gain adaptation scheme for the previous algorithm in order to alleviate the problem of improper scaling of the cost functions versus the constraints. Third, we propose a data-driven variant of the former algorithm, where each agent estimates their individual pseudogradient via zeroth-order information, namely, measurements of their individual cost function values. Finally, we apply our method to a perturbation amplitude optimization problem in oil extraction engineering.

This chapter is partly based on S. Krilašević and S. Grammatico. "Learning generalized Nash equilibria in monotone games: A hybrid adaptive extremum seeking control approach". en. In: *Automatica* 151 (May 2023), p. 110931. ISSN: 0005-1098. DOI: 10.1016/j.automatica.2023.110931.

5.1 Introduction

Decision problems where self-interested intelligent systems or agents wish to optimize their individual cost objective function arise in many engineering applications, such as charging/discharging coordination for plug-in electric vehicles [48], [73], demand-side management in smart grids [47], [33], robotic formation control [35], and thermostatically controlled loads [49]. The key feature that distinguishes these problems from multi-agent distributed optimization is the fact the cost functions and constraints are coupled together. Currently, one active research area is that of finding (seeking) actions that are self-enforceable, e.g., actions such that no agent has an incentive to unilaterally deviate from - the so-called generalized Nash equilibrium (GNE) [1, Eq. 1]. Due to the aforementioned coupling, information on other agents must be communicated, observed, or measured to compute a GNE algorithmically. The nature of this information can vary from knowing everything (full knowledge of the agent actions) [44], estimates based on distributed consensus between the agents [52], to payoff-based estimates [10], [7]. The latter is of special interest as it requires no dedicated inter-agent communication infrastructure.

Literature review: In payoff-based algorithms, each agent can only measure the value of their cost function but does not necessarily know its analytic form. Many of such algorithms are designed for Nash equilibrium problems (NEPs) with finite action spaces where each agent has a fixed policy that specifies what a player should do under any condition, e.g., [56], [10], [57]. On the other hand, the main component of continuous action space algorithms is the payoff-based (pseudo)gradient estimation scheme. A notable class of payoff-based algorithms called Extremum Seeking Control (ESC) is based on the seminal work by Krstić and Wang [12]. The main idea is to use perturbation signals to “excite” the cost function and estimate its gradient, which is then used in a gradient-descent-like algorithm. Since then, various different variants have been proposed [40], [32], [74], [75], [76], [77]. A full-information algorithm where the (pseudo)gradient is known can be “transformed" into an extremum seeking one if it satisfies some properties, like the continuity of the dynamics, use of only one (pseudo)gradient in the dynamics, appropriate stability of the optimizer/NE, etc. At first, (local) exponential stability of the optimizer/NE was assumed or implied with other assumptions [12, Assum. 2.2], [7, Assum. 3.1]. Thanks to results in averaging and singular perturbation theory [78],[79] in the hybrid dynamical systems framework [80], the assumption was relaxed to just (practical) asymptotic stability [17]. Subsequently, extremum seeking algorithms were developed for many different applications, such as event-triggered optimization [81], Nesterov-like accelerated optimization with resetting [82], optimization of hybrid plants [83], population games [60], N-cluster Nash games [59], fixed-time Nash equilibrium seeking for strongly monotone games [18], Nash equilibrium seeking for merely monotone games [84] and generalized Nash equilibrium seeking in strongly monotone games [23].

GNEPs can be solved efficiently by casting them into a variational inequality (VI) [85, Equ. 1.4.7], and in turn into the problem of finding a zero of an operator [85, Equ. 1.1.3], for which there exists a vast literature [42]. For GNEPs, this operator is the KKT operator, composed of the pseudogradient (whose monotonicity determines the type of the game), dual variables, constraints, and their gradients. In the case of merely monotone operators, the most widely used solution algorithms are the forward-backward-forward [42, Rem. 26.18], the extragradient [86] and the subgradient extragradient [87]. The main drawback of

all of these algorithms, with respect to an extremum seeking adaptation, is that they require two pseudogradient computations per iteration. Recently, the golden ratio algorithm has been proven to converge in the monotone case with only one pseudogradient computation [88]. There also exist continuous-time versions of the aforementioned algorithms, like the forward-backward-forward algorithm [89], and the golden ratio algorithm [90], albeit without projections in the latter case, rendering it unusable for GNEPs, as projections are essential for the dual dynamics. To the best of our knowledge, in the merely monotone case, no continuous-time GNEP algorithm currently exists that can be paired with extremum seeking.

Contribution: Motivated by the above literature and open research problem, to the best of our knowledge, we consider and solve the problem of learning (i.e., seeking via zeroth-order information) a GNE in merely monotone games. Specifically, our main technical contributions are summarized next:

- We propose a novel, projection-less continuous-time algorithm for solving GNEPs. Unlike [90], we consider the presence of shared constraints that are satisfied asymptotically.
- We propose a novel dual variable gain adaptation scheme using the framework of hybrid dynamical systems to alleviate the problem of improper scaling of the cost and constraint functions.
- We propose an extremum seeking scheme that exploits the aforementioned properties of the previous algorithms and, in turn, solves for the first time monotone GNEPs with zeroth-order information feedback.

Comparison with [84] and [23]: Since here we assume non-strong monotonicity of the pseudogradient mapping, the methodology in [23] based on the forward-backward splitting is not applicable - see [90, Equ. 4] for an example of non-convergence. Furthermore, by incorporating projection-less dual dynamics, here we allow for the presence of constraints, in contrast with the methodology in [84], which cannot be extended to the constrained case. Thus, in this chapter, we develop a novel splitting methodology that solves the issues of non-convergence and coupled feasible set and consequently addresses a much wider class of equilibrium problems. The hybrid gain adaptation is also novel and not considered in [84], [23].

The framework of hybrid dynamical systems (HDS) theory [80] like [78], [79], [17, Lemma 4] is especially attractive for extremum seeking, as it allows one to quickly and elegantly prove various stability theorems [17], [81], [18], [82]. Thus, we also use the framework of HDSs to model our algorithms. An HDS is defined as

$$\dot{x} \in F(x) \quad \text{if} \quad x \in C \tag{5.1a}$$
$$x^+ \in G(x) \quad \text{if} \quad x \in D, \tag{5.1b}$$

where $x \in \mathbb{R}^n$ is the state, $F : \mathbb{R}^n \to \mathbb{R}^n$ is the flow map, and $G : \mathbb{R}^n \to \mathbb{R}^n$ is the jump map, the sets C and D, are the flow set and the jump set, respectively, that characterize the points in space where the system evolves according to (5.1a), or (5.1b), respectively. The data of

the HDS is defined as $\mathcal{H} := \{C, D, F, G\}$. Solutions $x : \mathrm{dom}(x) \to \mathbb{R}^n$ to (5.1) are defined on hybrid time domains, and they are parameterized by a continuous-time index $t \in \mathbb{R}_+$ and a discrete-time index $j \in \mathbb{Z}_+$. Solutions with unbounded time or index domains are said to be complete [80, Chp. 2]. We now define the sufficient hybrid basic conditions that enable the use of various results from HDS theory. Unlike [80, Assum. 6.5], we require continuity of our mappings.

Definition 5.1 (Hybrid basic conditions)**.** *An HDS in (5.1) is said to satisfy the Hybrid basic conditions if C and D are closed, $C \subset \mathrm{dom}(F)$, $D \subset \mathrm{dom}(G)$, F and G are continuous on C and D respectively.* □

5.2 Generalized Nash equilibrium problem

We consider a multi-agent system with N agents indexed by $i \in \mathcal{I} := \{1, 2, \dots N\}$, each with cost function

$$J_i(u_i, \boldsymbol{u}_{-i}), \tag{5.2}$$

5

where $u_i \in \mathbb{R}^{m_i}$ is the decision variable, $J_i : \mathbb{R}^{m_i} \times \mathbb{R}^{m_{-i}} \to \mathbb{R}$. Let us also define $m := \sum_{j \in \mathcal{I}} m_j$ and $m_{-i} := \sum_{j \neq i} m_j$. Formally, we do not consider local constraints as in [84], [18], [59], but they could be approximated softly via penalty-barrier functions into the cost function. All agents are subject to convex coupling constraints $g_j(\boldsymbol{u})$ indexed by $j \in \mathcal{Q} := \{1, 2, \dots q\}$. Therefore, let us denote the overall feasible decision set as

$$\mathcal{U} := \{\boldsymbol{u} \in \mathbb{R}^m \mid g(\boldsymbol{u}) \leq \boldsymbol{0}\}, \tag{5.3}$$

and the feasible set of agent i as

$$\mathcal{U}_i(\boldsymbol{u}_{-i}) := \{u_i \in \mathbb{R}^{m_i} \mid g(\boldsymbol{u}) \leq \boldsymbol{0}\}, \tag{5.4}$$

where $g(\boldsymbol{u}) = \mathrm{col}\Big(\big(g_j(\boldsymbol{u})\big)_{j \in \mathcal{Q}}\Big)$.
The goal of each agent is to minimize its cost function, i.e.,

$$\forall i \in \mathcal{I} : \min_{u_i \in \mathcal{U}_i(\boldsymbol{u}_{-i})} J_i(u_i, \boldsymbol{u}_{-i}), \tag{5.5}$$

which depends on the decision variables of other agents as well. Thus, a game $\mathcal{G}$ is defined by the set of cost functions and the feasible set, i.e., $\mathcal{G} := \{(J_i(\boldsymbol{u}))_{i \in \mathcal{I}}, (g_j(\boldsymbol{u}))_{j \in \mathcal{Q}}\}$. From a game-theoretic perspective, this is the problem to compute a generalized Nash equilibrium (GNE), as formalized next.

Definition 5.2 (Generalized Nash equilibrium)**.** *A set of control actions $\boldsymbol{u}^* := \mathrm{col}\left(u_i^*\right)_{i \in \mathcal{I}}$ is a generalized Nash equilibrium if, for all $i \in \mathcal{I}$,*

$$u_i^* \in \operatorname*{argmin}_{v_i} J_i\left(v_i, \boldsymbol{u}_{-i}^*\right) \text{ s.t. } \left(v_i, \boldsymbol{u}_{-i}^*\right) \in \mathcal{U}. \tag{5.6}$$

with J_i as in (5.2) and $\mathcal{U}$ as in (5.3). □

In plain words, a set of inputs is a GNE if no agent can improve its cost function by unilaterally changing its input.

A common approach for solving a GNEP is to translate it into a quasi-variational inequality (QVI) [1, Thm. 3.3] that can be simplified to a variational inequality (VI) [1, Thm. 3.9] for a certain subset of solutions called variational-GNE (v-GNE), which in turn can be translated into a problem of finding zeros of a monotone operator [85, Equ. 1.1.3]. To ensure the equivalence of the GNEP and QVI, we postulate the following assumption [1, Thm. 3.3]:

Standing Assumption 5.3 (Regularity). *For each $i \in \mathcal{I}$, the function J_i in (5.2) is differentiable and its gradient is locally Lipschitz continuous; the function $J_i(\cdot, \boldsymbol{u}_{-i})$ is convex for every $\boldsymbol{u}_{-i}$; For each $j \in \mathcal{Q}$, convex constraint $g_j(\boldsymbol{u})$ is continuously differentiable, $\mathcal{U}$ is non-empty and satisfies Slater's constraint qualification.* □

We focus on a subclass of GNE called variational GNE [1, Def. 3.10]. A collective decision $\boldsymbol{u}^*$ is a v-GNE in (5.6) if and only if there exists a dual variable $\lambda^* \in \mathbb{R}^q$ such that the following KKT conditions are satisfied [1, Th. 4.8]:

$$\mathbf{0}_{m+q} \in F_{\text{ex}}(\boldsymbol{u}^*, \lambda^*) := \begin{bmatrix} F(\boldsymbol{u}^*) + \nabla g(\boldsymbol{u}^*)^\top \lambda^* \\ -g(\boldsymbol{u}^*) + \mathrm{N}_{\mathbb{R}^q_+}(\lambda^*) \end{bmatrix}, \tag{5.7}$$

where by stacking the partial gradients $\nabla_{u_i} J_i(u_i, \boldsymbol{u}_{-i})$ into a single vector, we have the so-called pseudogradient mapping:

$$F(\boldsymbol{u}) := \operatorname{col}\left(\left(\nabla_{u_i} J_i(u_i, \boldsymbol{u}_{-i}) \right)_{i \in \mathcal{I}} \right). \tag{5.8}$$

Let us also postulate the weakest working assumption in GNEPs with continuous actions, i.e. the monotonicity of the pseudogradient mapping [85, Def. 2.3.1, Thm. 2.3.4]:

Standing Assumption 5.4 (Monotonicity). *The pseudogradient mapping F in (5.8) is monotone, i.e., it holds that*

$$\inf_{\boldsymbol{u}, \boldsymbol{v} \in \operatorname{dom} F} \langle \boldsymbol{u} - \boldsymbol{v} \mid F(\boldsymbol{u}) - F(\boldsymbol{v}) \rangle \geq 0.$$ □

The regularity and monotonicity assumptions are not enough to ensure the existence of a v-GNE [85, Thm. 2.3.3, Corr. 2.2.5], [1, Thm. 6], hence let us postulate its existence:

Standing Assumption 5.5 (Existence). *There exists $\omega^* := \operatorname{col}(\boldsymbol{u}^*, \lambda^*) \in \mathbb{R}^m \times \mathbb{R}^q_+$ such that Equation (5.7) is satisfied.* □

In this chapter, we consider the problem of finding a v-GNE of the game in (5.5) via zeroth-order information, i.e., local measurements of the cost functions in (5.2).

5.3 Full-information generalized Nash equilibrium seeking

We present two novel full-information GNE seeking algorithms. In the first algorithm, the dual variables are calculated without the use of projections by a central coordinator. The

lack of projections onto tangent cones, along with the fact that the flow map of the algorithm contains only one pseudogradient computation and that the algorithm itself converges merely under the monotonicity assumption, enables us to use hybrid dynamical system theory for the zeroth-order extension of the algorithm later on. In the second algorithm, we propose a hybrid gain adaptation scheme to improve the algorithm's performance when we do not know a priori how to best tune the gains.

5.3.1 Projection-less GNE seeking algorithm

The algorithm in [90] proves convergence to a NE for a monotone pseudogradient by combining additional filtering dynamics and state z with the standard NE seeking one. Similarly, we propose a Lagrangian first-order primal dynamics with filtering for each agent:

$$\begin{bmatrix} \dot{u}_i \\ \dot{z}_i \end{bmatrix} = \begin{bmatrix} -u_i + z_i - \gamma_i \left(\nabla_{u_i} J_i(u_i, \boldsymbol{u}_{-i}) + \nabla_{u_i} g(\boldsymbol{u})^\top \lambda \right) \\ -z_i + u_i \end{bmatrix}.$$

The authors in [90] propose a passivity framework for the convergence of their golden-ratio inspired algorithm. Instead, we offer a different intuition for convergence. Via the invariance theorem, it follows that the stable equilibrium points must be in the Lyapunov invariant set. Without the additional dynamics and under the monotonicity assumption, the invariant set would cover the whole flow set. With the filtering dynamics, the invariant set is restricted to the points where the flow map equals zero. In the case of the dual dynamics, in order to avoid projections, we propose the following dynamics:

$$\begin{aligned} \forall j \in \mathcal{Q} : \dot{\lambda}_j &= \lambda_j \left(g_j(\boldsymbol{u}) - \lambda_j + w_j \right) \\ \dot{w} &= -w + \lambda. \end{aligned} \tag{5.9}$$

While the classic dual Lagrangian dynamics preserve the positivity of the dual variables by projecting onto the positive orthant, the same is accomplished in (5.9) by multiplying the "standard" dual dynamics of each individual variable with the dual variable. Consequentially, a positive dual variable cannot become negative over time as it cannot cross zero. Unlike [91], [92], where strict convexity of the cost and constraint functions is assumed to avoid having the invariant set be equivalent to the entire flow set, thanks to our newfound understanding of the filtering dynamics, we can incorporate them to relax the strict convexity assumption.

Thus, in collective form, we have

$$\dot{\omega} = \begin{bmatrix} \dot{\boldsymbol{u}} \\ \dot{\boldsymbol{z}} \\ \dot{\lambda} \\ \dot{w} \end{bmatrix} = \begin{bmatrix} -\boldsymbol{u} + \boldsymbol{z} - \Gamma(F(\boldsymbol{u}) + \nabla g(\boldsymbol{u})^\top \lambda) \\ -\boldsymbol{z} + \boldsymbol{u} \\ \operatorname{diag}(\lambda)(g(\boldsymbol{u}) - \lambda + w) \\ -w + \lambda \end{bmatrix}. \tag{5.10}$$

To properly understand the behavior of this system, we first need to define the key sets. Let us define the set of equilibrium points of the dynamics in (5.10) as

$$\mathcal{M} := \left\{ \omega \in \mathbb{R}^{2m} \times \mathbb{R}^{2q}_+ \mid \boldsymbol{u} = \boldsymbol{z}, w = \lambda, \mathbf{0}_m = F(\boldsymbol{u}) + \nabla g(\boldsymbol{u})^\top \lambda, \operatorname{diag}(\lambda) \operatorname{diag}(g(\boldsymbol{u})) = 0 \right\}, \tag{5.11}$$

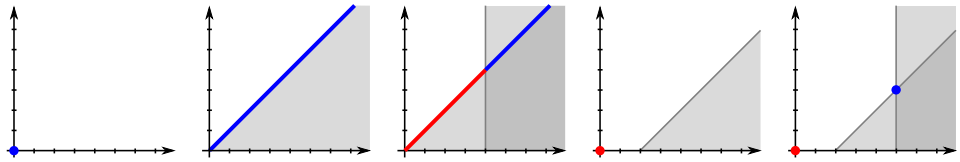

(a) $\mathcal{A}$ (blue dot) contains a single point.

(b) $\mathcal{A}$ (blue line) contains multiple points.

(c) $\mathcal{A}$ (blue line) and $\mathcal{M} \setminus \mathcal{A}$ (red line) are connected.

(d) $\mathcal{A}$ contains no points, set $\mathcal{M}$ (red dot) is a single point.

(e) $\mathcal{A}$ (blue dot) and $\mathcal{M} \setminus \mathcal{A}$ (red dot) disconnected.

Figure 5.1: The figures represent projections of the sets $\mathcal{M}$ and $\mathcal{A}$ onto the subspace of $\boldsymbol{u}$ coordinates with $F(\boldsymbol{u}) := \operatorname{col}(u_2, -u_1)$: $\mathcal{A}$ is shown in blue, while the other equilibrium points of (5.10) $\mathcal{M} \setminus \mathcal{A}$, are shown in red. Areas that satisfy the constraints are shown in gray. The set $\mathcal{M}$ is not necessarily connected, as shown in Figure 5.1e. Without constraints, $\mathcal{M}$ is equivalent to $\mathcal{A}$, and it contains only the zeros of the pseudogradient as shown in Figure 5.1a. By adding constraints, we can either create new equilibrium solutions (Figures 5.1b, 5.1e) or "remove" previous ones (Figure 5.1d). Either way, "all" the solutions are still included in the set $\mathcal{M}$, which is the union of all solutions to games $\{(J_i(\boldsymbol{u}))_{i\in\mathcal{I}}, (g_j(\boldsymbol{u}))_{j\in\tilde{\mathcal{Q}}}\}$, where $\tilde{\mathcal{Q}}$ is a subset of $\mathcal{Q}$.

its subset $\mathcal{A}$ which relates to the solutions of the game in (5.5) as

$$\mathcal{A} := \left\{ \omega \in \mathbb{R}^{2m} \times \mathbb{R}^{2q}_{+} \mid \boldsymbol{u} = \boldsymbol{z}, w = \lambda, \mathbf{0}_m \in F_{\text{ex}}(\boldsymbol{u}, \lambda) \right\} \subseteq \mathcal{M}, \tag{5.12}$$

and $\mathcal{L}$ as the set where at least one dual variable is equal to zero:

$$\mathcal{L} := \{\omega \in \mathbb{R}^{2m} \times \mathbb{R}^{2q}_{+} \mid \lambda_1 \cdot \lambda_2 \cdot \ldots \cdot \lambda_q = 0\}.$$

Let us make a few key observations. Firstly, not all equilibrium points in $\mathcal{M}$ are related to the solutions of the GNEP like the points in $\mathcal{A}$ (see Figures 5.1c, 5.1d, 5.1d). Secondly, if the dynamics are initiated in the set $\mathcal{L}$, then the dual variables initiated with zero will stay zero for the whole trajectory. Thus, such trajectories do not converge to the solution unless the dual variables are initialized correctly. To avoid this problem, it is sufficient to initialize the trajectories outside of $\mathcal{L}$. To further understand the properties of these sets, we show some examples in Figure 5.1.

We later show that $\mathcal{M}$ is attractive. Additionally, the following Lemma characterizes the stability of points in $\mathcal{M} \setminus \mathcal{A}$.

Lemma 5.6. *Let the Standing Assumptions hold. Then, the equilibrium points in $\mathcal{M} \setminus \mathcal{A}$ are unstable for dynamics in (5.10).* □

Proof. See Appendix 5.B. ■

Therefore, in order to prove the stability of $\mathcal{A}$, we need the sets $\mathcal{A}$ and $\mathcal{M} \setminus \mathcal{A}$ to be disjoint, as the latter is the set of undesired equilibria. In Figures 5.1b and 5.1c, we illustrate this

situation happens when the solution set contains multiple points, and some of them are "removed" by the introduction of the new constraints. Thus, we have to assume this is not the case:

Standing Assumption 5.7 (Isolation of solutions)**.** *By removing constraints that are not active in the solution set $\mathcal{A}$ (for which $\lambda_j^* = 0$) from the overall feasible decision set $\boldsymbol{\mathcal{U}}$ in (5.3), additional solutions that are connected to $\mathcal{A}$ are not created.* □

We note that this assumption fails only in very specific conditions. For example, let $F(\boldsymbol{u}) = \mathrm{col}(u_2, -u_1)$, $g_1(\boldsymbol{u}) = a_1u_1 + b_1u_2 + c_1$ and $g_2(\boldsymbol{u}) = a_2u_1 + b_2u_2 + c_2$. Standard Assumption 5.7 fails only if $c_1 = 0$ or $c_2 = 0$. Even if Standard Assumption 5.7 is not satisfied, by Lemma 5.6, the equilibrium points in $\mathcal{M} \setminus \mathcal{A}$ are unstable, hence there would be no problem in practice.

Since we cannot claim attractivity from all points in the domain, we should use the notion of local stability as formalized next.

5

Definition 5.8 (UL(p)AS and UG(p)AS)**.** [83]
A compact set $\mathcal{A} \subset \mathbb{R}^n$ is said to be Uniformly Locally pre-Asymptotically Stable (ULpAS) with basin of attraction $\mathcal{B}_\mathcal{A}$ if for every proper indicator $\omega(\cdot)$ of $\mathcal{A}$ on $\mathcal{B}_\mathcal{A}$ there exists $\beta \in \mathcal{KL}$ such that any solution x of $\mathcal{H}$ with $x(0,0) \in \mathcal{B}_\mathcal{A}$ satisfies $\omega(x(t,j)) \leq \beta(\omega(x(0,0)), t+j)$, for all $(t,j) \in \mathrm{dom}(x)$. If this bound holds with $\omega(\cdot)$ replaced by $\|\cdot\|_\mathcal{A}$, and for all $x(0,0) \in C \cup D$, the set $\mathcal{A}$ is said to be Uniformly Globally pre-Asymptotically Stable (UGpAS). If all solutions are complete, we use the acronyms ULAS and UGAS, respectively. □

Finally, we show that the dynamics in (5.10) converge to the solutions of the game in (5.5) if the initial value of the dual variables is different from zero, as formalized next:

Theorem 5.9. *Let the Standing Assumptions hold and consider the system dynamics in (5.10). The set $\mathcal{A}$ in (5.12) is ULAS with basin of attraction $(\mathbb{R}^{2m} \times \mathbb{R}^{2q}_+ \setminus \mathcal{L}) \cup \mathcal{A}$.* □

Proof. See Appendix 5.A. ■

Remark 5.10. *It is mathematically also possible to derive a distributed (center-free) implementation of our semi-decentralized algorithm, similarly to [23, Equ. 14], where each agent estimates the dual variables using the information exchanged with the neighbors. While technically possible, this approach is less in line with the almost-decentralized philosophy of extremum seeking since it would require a dedicated communication network.*

5.3.2 Hybrid adaptive gain

It is known that primal-dual dynamics satisfy the constraints only asymptotically, thus, they allow for constraint violation in the transient [44], [55]. Such behavior might happen for longer periods if the norm of the pseudogradient $F(\boldsymbol{u})$ is "dominant" over that of the gradient of the constraint vector, $\nabla g(\boldsymbol{u})$. Furthermore, as the zeroth-order variant from §4 introduces perturbations to the primal dynamics, it can happen that the perturbations "overpower" either the pseudogradient or the constraint part of the dynamics, thus hindering the convergence to the solution for a wide set of perturbation amplitude parameters. Therefore, to reduce the violation behavior during the transients and to enable a more applicable

zeroth-order adaptation, it is fundamental to scale the functions properly. When we do not know the cost functions a priori, it is difficult to scale the constraints. To address this potential numerical issue, we propose a gain adaptation scheme based on hybrid dynamical systems. In simple words, we design an outer-semicontinuous mapping which turns on the increase of the gain k_j when there is some level of constraint violation $g_j(\boldsymbol{u}) \geq 2\epsilon$, and turns it off when the constraint violation is minimal $g_j(\boldsymbol{u}) \leq \epsilon$, or when the gain reaches the maximum value $\overline{k}$. The collective flow set and flow map for $\xi := \operatorname{col}(\boldsymbol{u}, \boldsymbol{z}, \lambda, w, k, s)$ read as:

$$\xi \in C := \mathbb{R}^{2m} \times \mathbb{R}^{2q}_{+} \times \mathcal{K}^q \times \mathcal{S}^q \tag{5.13a}$$

$$\begin{bmatrix} \dot{\boldsymbol{u}} \\ \dot{\boldsymbol{z}} \\ \dot{\lambda} \\ \dot{w} \\ \dot{k} \\ \dot{s} \end{bmatrix} = F(\xi) := \begin{bmatrix} -\boldsymbol{u} + \boldsymbol{z} - \Gamma(F(\boldsymbol{u}) + \nabla g(\boldsymbol{u})^\top \lambda) \\ -\boldsymbol{z} + \boldsymbol{u} \\ \operatorname{diag}(k)\operatorname{diag}(\lambda)(g(\boldsymbol{u}) - \lambda + w) \\ -w + \lambda \\ \frac{1}{2} c S^2 (\mathbf{1} + s) \\ \mathbf{0} \end{bmatrix}, \tag{5.13b}$$

and the collective jump set and jump map

$$\xi \in D := \bigcup_{j=1}^{q} D_j, \quad D_j := \left(D_j^+ \cup D_j^- \cup D_j^0\right) \tag{5.14a}$$

$$\xi^+ \in G(\xi) := \left\{ \left(\bigcup^{j \in \mathcal{C}} G_j(\xi),\ \xi \in \bigcap^{j \in \mathcal{C}} D_j \right)_{\mathcal{C} \in \mathcal{P}(\mathcal{Q})}, \right. \tag{5.14b}$$

where k is a vector of gains for the dual dynamics; $\mathcal{K} := [\underline{k}, \overline{k}]$ is the set of possible values for these gains; s is a vector of discrete states which indicate if the gains in k are increasing or not; $\mathcal{S} := \{-1, 0, 1\}$ is the set of possible discrete states; $c > 0$ is positive constant which regulates the increase of k; $S := \operatorname{diag}(s)$, $\epsilon > 0$ is a positive number, $D_j^+ := \{\boldsymbol{u} \mid g_j(\boldsymbol{u}) \geq 2\epsilon\} \times \mathbb{R}^m \times \mathbb{R}^{2q}_{+} \times \mathcal{K}^q \times \mathcal{S}^{j-1} \times \{-1\} \times \mathcal{S}^{q-j}$ is the set which triggers the increasing k_j dynamics; $D_j^- := \{\boldsymbol{u} \mid g_j(\boldsymbol{u}) \leq \epsilon\} \times \mathbb{R}^m \times \mathbb{R}^{2q}_{+} \times \mathcal{K}^q \times \mathcal{S}^{j-1} \times \{1\} \times \mathcal{S}^{q-j}$ is the set which triggers the stopping of the k_j dynamics; $D_j^0 := \mathbb{R}^{2m} \times \mathbb{R}^{2q}_{+} \times \mathcal{K}^{j-1} \times \{\overline{k}\} \times \mathcal{K}^{q-j} \times \mathcal{S}^{j-1} \times \{-1, 1\} \times \mathcal{S}^{q-j}$ is the set which triggers the permanent stop of k_j dynamics; $\mathcal{P}(\mathcal{X})$ is the set of all subsets of $\mathcal{X}$; the jump maps $G_j(\xi)$ are defined as

$$G_j(\xi) := \begin{cases} \Delta_{-j}\xi - \Delta_j \xi, & \xi \in D_j^+ \cup D_j^- \\ \Delta_{-j}\xi, & \xi \in D_j^0 \\ \{\Delta_{-j}\xi - \Delta_j, \Delta_{-j}\xi\}, & \xi \in (D_j^+ \cup D_j^-) \cap D_j^0 \end{cases}$$

where Δ_j is a diagonal matrix with all zeros on the diagonal, except for the row corresponding to the s_j state, which is equal to one and $\Delta_{-j} := I - \Delta_j$.
The set-valued definitions are necessary for outer-semicontinuity, which in turn via hybrid systems theory, provides us with some robustness properties. An example trajectory can be seen in Figure 5.2. We note that due to the design of the jump sets, no jumps can occur in a sufficiently small neighborhood of a GNE, and no solution can have an infinite number of jumps, as formalized next:

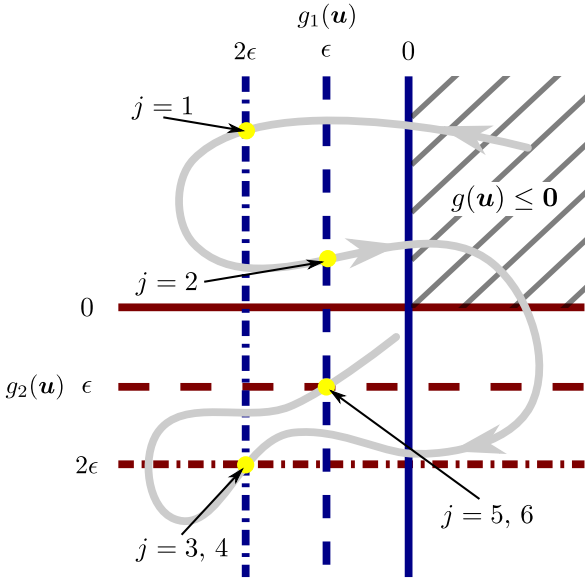

Figure 5.2: The trajectory is denoted with a gray line, events with yellow dots, first constraint with red and second with blue lines. The trajectory starts in the set where constraints are satisfied ($g(\boldsymbol{u}) \leq 0$). The first event is triggered when the trajectory leaves the set where $g_1(\boldsymbol{u}) < 2\epsilon$, causing the state s_1 to change to 1 which then starts the increase of k_1 gain. The second event happens when the trajectory returns to the set where $g_1(\boldsymbol{u}) \leq \epsilon$ and the state s_1 is reset to 0, halting the increase in gains. Events 3 and 4 happen when the trajectory leaves the sets $g_1(\boldsymbol{u}) < 2\epsilon$ and $g_2(\boldsymbol{u}) < 2\epsilon$ simultaneously. In that case, states s_1 and s_2 are set to 1 in random order. The last jumps happen when the trajectory simultaneously enters the sets $g_1(\boldsymbol{u}) \leq \epsilon$ and $g_2(\boldsymbol{u}) \leq \epsilon$. Again, the states s_1 and s_2 are reset to 0 in random order.

Lemma 5.11. *Let the Standing Assumptions hold and let $\xi(t,j)$ be a complete solution to the hybrid system (C,D,F,G) in (5.13a), (5.13b), (5.14a) and (5.14b). Then, $\xi(t,j)$ has a finite number of jumps.* □

Proof. See Appendix 5.C. ■

Apart from the gain adaptation scheme, the main difference between the dynamics in (5.13) and those in (5.10) is the fact that the flow mapping of the dual variables contains the new gain vector. Thus, one would expect similar behavior compared to that in (5.10). Furthermore, thanks to the hybrid basic assumptions, our system in (5.13) does not become unstable for arbitrarily small noise, as formalized in the following definition and robust convergence result for our hybrid adaptive algorithm.

Definition 5.12 (Structural robustness)**.** *[82] Let a compact set $\mathcal{A}$ be UGpAS (resp. SGPpAS as $\varepsilon \to 0^+$) for the hybrid system $\mathcal{H}$ with $\beta \in \mathcal{KL}$. We say that $\mathcal{H}$ is Structurally Robust if for all measurable functions $e : \mathbb{R}_{\geq 0} \to \mathbb{R}^n$ satisfying $\sup_{t\geq 0} \|e(t)\| \leq \bar{e}$, with $\bar{e} > 0$, the perturbed system*

$$x + e \in C, \quad \dot{x} = F(x+e) + e \tag{5.15a}$$

$$x + e \in D, \quad x^+ = G(x+e) + e \tag{5.15b}$$

renders the set $\mathcal{A}$ SGPpAS as $\bar{e} \to 0^+$ (resp. SGPpAS as $(\varepsilon, \bar{e}) \to 0^+$) with $\beta \in \mathcal{KL}$. □

Theorem 5.13. *Let the Standing Assumptions hold and consider the hybrid system (C, D, F, G) in (5.13a), (5.13b), (5.14a) and (5.14b). Then, for any initial condition such that $\xi(0,0) \notin \mathcal{L} \times \mathcal{K}^q \times \mathcal{S}^q$ there exists a compact set $\mathfrak{B} \supset \mathcal{A} \times \mathcal{K}^q \times \mathcal{S}^q$, such that the set $\mathcal{A} \times \mathcal{K}^q \times \mathcal{S}^q$ is UGAS for the restricted hybrid system $(C \cap \mathfrak{B}, D \cap \mathfrak{B}, F, G)$. Additionally, the restricted system is structurally robust.* □

Proof. See Appendix 5.D. ■

5.4 Zeroth-order generalized Nash equilibrium seeking

The main assumptions of Algorithms in §5.3.1 and §5.3.2 are that each agent knows their partial-gradient mapping and the actions of other agents. Such knowledge can be difficult to acquire in practical applications [93]. Our proposed zeroth-order GNE seeking algorithm requires a much weaker assumption; we assume that each agent can only measure their cost function. To estimate the pseudogradient via the measurements, we introduce additional oscillator states $\boldsymbol{\mu}$. By injecting oscillations into the inputs of the cost functions, it is possible to estimate the pseudogradient. For example of a real function of a single variable, it holds that $f(x + a\sin(t))\sin(t) \approx f(x)\sin(t) + a\nabla f(x)\sin^2(t)$ for small a. If the right-hand expression is averaged in time, only $\frac{a}{2}\nabla f(x)$ remains as the desired estimate. The principle is the same for mappings. To reduce oscillations, the estimate is then passed through a first-order filter with state $\boldsymbol{\zeta}$ and forwarded into the algorithm in §5.3.2 instead of the real pseudogradient.

Our new algorithm for the collective state $\phi := \operatorname{col}\left(\boldsymbol{u}, \boldsymbol{z}, \lambda, w, k, s, \boldsymbol{\zeta}, \boldsymbol{\mu}\right)$ is given by

$$\phi \in C_0 := C \times \mathbb{R}^m \times \mathbb{S}^m \tag{5.16a}$$

$$\begin{bmatrix} \dot{\boldsymbol{u}} \\ \dot{\boldsymbol{z}} \\ \dot{\lambda} \\ \dot{w} \\ \dot{k} \\ \dot{s} \\ \dot{\boldsymbol{\zeta}} \\ \dot{\boldsymbol{\mu}} \end{bmatrix} = F_0(\phi) := \begin{bmatrix} \boldsymbol{\nu\varepsilon}\left(-\boldsymbol{u} + \boldsymbol{z} - \Gamma(\boldsymbol{\zeta} + \nabla g(\boldsymbol{u})^\top \lambda)\right) \\ \boldsymbol{\nu\varepsilon}(-\boldsymbol{z} + \boldsymbol{u}) \\ \nu_0 \varepsilon_0 \operatorname{diag}(k) \operatorname{diag}(\lambda)(g(\boldsymbol{u}) - \lambda + w) \\ \nu_0 \varepsilon_0 (-w + \lambda) \\ \frac{1}{2} \nu_0 \varepsilon_0 c S^2 (\mathbf{1} + s) \\ \mathbf{0} \\ \boldsymbol{\nu}\left(-\boldsymbol{\zeta} + \hat{F}(\boldsymbol{u}, \boldsymbol{\mu})\right) \\ 2\pi \mathcal{R}_\kappa \boldsymbol{\mu} \end{bmatrix} \tag{5.16b}$$

where $\zeta_i \in \mathbb{R}^{m_i}$, $\mu_i \in \mathbb{S}^{m_i}$ are the oscillator states, $\varepsilon_i, \nu_i \geq 0$ for all $i \in \mathcal{I}_0 := \mathcal{I} \cup \{0\}$, $\boldsymbol{\varepsilon} := \operatorname{blkdiag}\left((\varepsilon_i I_{m_i})_{i \in \mathcal{I}}\right)$, $\boldsymbol{\gamma} := \operatorname{blkdiag}\left((\gamma_i I_{m_i})_{i \in \mathcal{I}}\right)$, $\mathcal{R}_\kappa := \operatorname{blkdiag}((\mathcal{R}_i)_{i \in \mathcal{I}})$, $\mathcal{R}_i := \operatorname{blkdiag}\left(\left(\begin{bmatrix} 0 & -\kappa_j \\ \kappa_j & 0 \end{bmatrix}\right)_{j \in \mathcal{M}_i}\right)$, $\kappa_i > 0$ for all i and $\kappa_i \neq \kappa_j$ for $i \neq j$, $\mathcal{M}_i := \{\sum_{j=1}^{i-1} m_j + 1, \ldots, \sum_{j=1}^{i-1} m_j + m_i\}$ is the set of indices corresponding to the state u_i , $\mathbb{D}^n \in \mathbb{R}^{n \times 2n}$ is a matrix that selects every odd row from the vector of size $2n$, $a_i > 0$ are small perturbation amplitude parameters, $A := \operatorname{blkdiag}\left((a_i I_{m_i})_{j \in \mathcal{I}}\right)$, $J(\boldsymbol{u}) = \operatorname{blkdiag}\left((J_i(u_i, \boldsymbol{u}_{-i}) I_{m_i})_{i \in \mathcal{I}}\right)$, and $\hat{F}(\boldsymbol{u}, \boldsymbol{\mu}) = 2A^{-1} J(\boldsymbol{u} + A\mathbb{D}^m \boldsymbol{\mu}) \mathbb{D}^m \boldsymbol{\mu}$. The flow set and map are defined as

$$D_0 := D \times \mathbb{R}^m \times \mathbb{S}^m \tag{5.17a}$$

$$\phi^+ \in G_0(\phi) := \begin{bmatrix} G(\xi) \\ \xi \\ \mu \end{bmatrix}. \tag{5.17b}$$

The existence of solutions follows directly from [94, Prop. 6.10] as the continuity of the right-hand side in (5.16), (5.17) and the definitions of flow and jump sets imply [94, Assum. 6.5]. As for most extremum seeking schemes with constant perturbation, convergence to a neighborhood of the solutions can be guaranteed. Thus, let us introduce the corresponding stability concept, the so-called semi-global practical asymptotic stability.

Definition 5.14 (SG(p)AS). [83] *For a parameterized HDS $\mathcal{H}_\varepsilon$, $\varepsilon \in \mathbb{R}^k_+$, a compact set $\mathcal{A} \subset \mathbb{R}^n$ is said to be Semi-Globally Practically pre-Asymptotically Stable (SGPpAS) as $(\varepsilon_1, \ldots, \varepsilon_k) \to 0^+$ with $\beta \in \mathcal{KL}$ if for all compact sets $K \subset \mathbb{R}^n$ and all $v > 0$, there exists $\varepsilon_0^* > 0$ such that for each $\varepsilon_0 \in \left(0, \varepsilon_0^*\right)$ there exists $\varepsilon_1^*(\varepsilon_0) > 0$ such that for each $\varepsilon_1 \in \left(0, \varepsilon_1^*(\varepsilon_0)\right)$ ... there exists $\varepsilon_j^*\left(\varepsilon_{j-1}\right) > 0$ such that for each $\varepsilon_j \in \left(0, \varepsilon_j^*\left(\varepsilon_{j-1}\right)\right) \ldots, j = \{2, \ldots, k\}$, every solution x_ε of $\mathcal{H}_\varepsilon$ with $x_\varepsilon(0,0) \in K$ satisfies*

$$\|x_\varepsilon(t, j)\|_{\mathcal{A}} \leq \beta\left(\|x_\varepsilon(0,0)\|_{\mathcal{A}}, t + j\right) + v$$

for all $(t, j) \in \operatorname{dom}(x_\varepsilon)$. If all solutions are complete, we have Semi-Globally Practically Asymptotically Stable (SGPAS). □

Our main technical result of this section is summarized in the following theorem.

Theorem 5.15. *Let the Standing Assumptions hold and consider the hybrid system* (C_0, D_0, F_0, G_0) *in (5.16) and (5.17). Then, for any initial condition such that* $\phi(0,0) \notin \mathcal{L} \times \mathcal{K}^q \times \mathcal{S}^q \times \mathbb{R}^m \times \mathbb{S}^m$ *there exists a compact set* $\mathfrak{B} \supset \mathcal{A} \times \mathcal{K}^q \times \mathcal{S}^q \times \mathbb{R}^m \times \mathbb{S}^q$, *such that the set* $\mathcal{A} \times \mathcal{K}^q \times \mathcal{S}^q \times \mathbb{R}^m \times \mathbb{S}^q$ *is SGPAS as* $(\bar{a}, \bar{\varepsilon}, \bar{v}) = (\max_{i\in\mathcal{I}} a_i, \max_{i\in\mathcal{I}_0} \varepsilon_i, \max_{i\in\mathcal{I}_0} v_i) \to 0$ *for the restricted hybrid system* $((C \cap \mathfrak{B}) \times \mathbb{R}^m \times \mathbb{S}^m), (D \cap \mathfrak{B}) \times \mathbb{R}^m \times \mathbb{S}^m, F_0, G_0)$. *Additionally, the restricted system is structurally robust.* □

Proof. See Appendix 5.E. ■

Remark 5.16. *For the sake of brevity, we made some assumptions on the structure of our proposed algorithms. Namely, we assume that the amplitudes of the perturbation signal* a_i *are constant, that the frequencies of the perturbation signals are different for every state, and that every state of the pseudogradient is estimated. Analogous results hold for slowly varying amplitudes* $a_i(t) \in [\underline{a}, \overline{a}]$ *where the upper and lower bounds are design parameters, for perturbation signals with the same frequency but sufficiently different phases, so that "learning" can occur, and for the pseudogradient with some, but not all, estimated coordinates.* □

5

5.5 Numerical simulations

5.5.1 Two-player monotone game

For illustration purposes, let us consider a two-player monotone game with the following cost functions

$$\begin{aligned} J_1(\boldsymbol{u}) &= (u_1 - 2)(u_2 - 3) \\ J_2(\boldsymbol{u}) &= -(u_1 - 2)(u_2 - 3), \end{aligned} \tag{5.18}$$

and constraints

$$u_1 \geq u_2 + 1 \text{ and } u_1 \geq 4. \tag{5.19}$$

Game in (5.18) and (5.19) has a unique GNE $(u_1^*, u_2^*) = (4, 3)$ and is known to be divergent for algorithms that require strong monotonicity of the pseudogradient. As simulation parameters we choose $c = 10$, $k_j(0,0) = 1$, $\lambda_j = 0.1$ for all $i \in \mathcal{I}$, $j \in \mathcal{Q}$, $k_{\min} = 1$, $k_{\max} = 10^5$, $(u_1(0,0), u_2(0,0)) = (10, 0)$, and all other initial parameters were set to zero. We compare the algorithm in (5.13), (5.14) with algorithm in (5.10) for different values of the gain and show the numerical simulations in Figures 5.3, 5.4, 5.5. In Figures 5.3 and 5.4, it seems that the trajectory with the highest gain does not converge to the equilibrium. However, this is not the case since the Lagrangian multipliers converge very close to zero during the initial part of the trajectory when both constraints are satisfied. Thus, as the multipliers themselves act as a "gain" in the dynamics, it takes longer for the dynamics to evolve toward the desired equilibrium. Eventually, the Lagrangian multipliers will grow large enough to let the trajectory move toward a solution. Furthermore, we note that the trajectory for the gain $k = 1$ is the second slowest with respect to convergence speed. Thus, in this scenario, choosing the gain either too small or too large is detrimental to the convergence speed. On the other hand, our adaptive gain behaves similarly to the case of gain $k = 100$, which is the "optimally tuned" gain. In Figures 5.4 and 5.5, we denote the area where the constraints are satisfied with green and red rectangles. Figure 5.6 shows how the adaptive gain turns on and off based on the constraint violation.

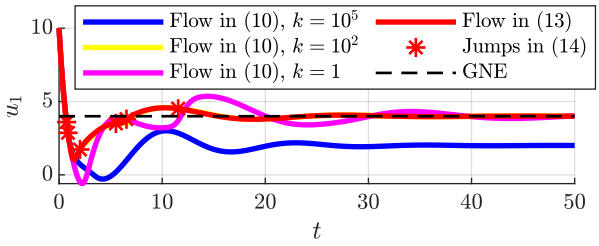

(a) Time evolution of states u_1 for the cases with and without ($k_{\min} = k_{\max}$) adaptive gain in (5.13).

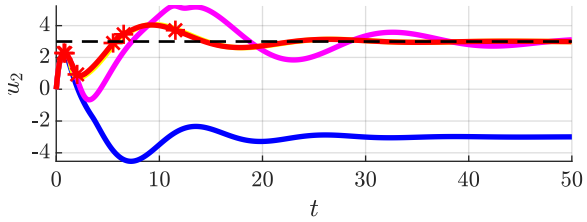

(b) Time evolution of states u_2 for the cases with and without ($k_{\min} = k_{\max}$) adaptive gain in (5.13).

Figure 5.3: The trajectory with the adaptive gain is almost identical to the trajectory with gain $k = 100$.

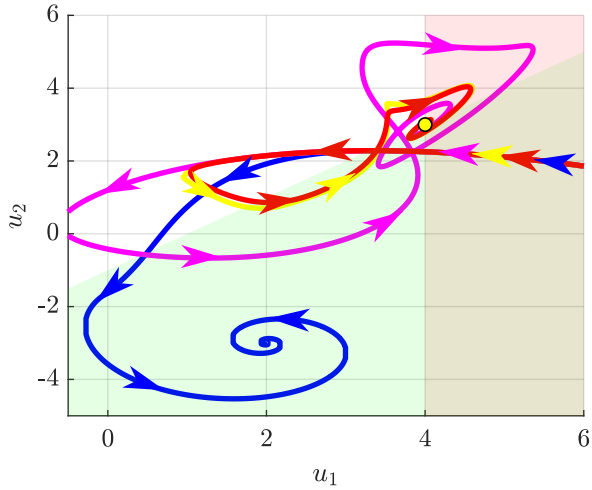

Figure 5.4: Trajectories with (red) and without (blue, magenta, yellow) adaptive gain in a phase plane. The yellow dot represents the GNE, while the other colored lines are denoted as in Figure 5.3

.

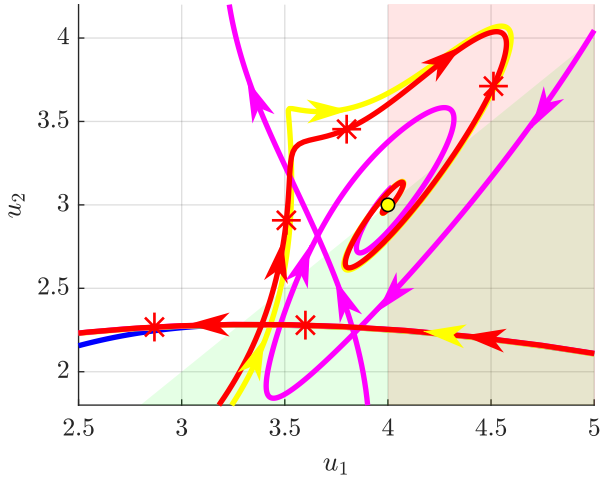

Figure 5.5: Trajectories in the neighborhood of the GNE (yellow dot). The jumps are activated when entering and leaving the half-spaces corresponding to the constraints (red and transparent green). The color code is as in Figure 5.3: blue for constant gain $k = 10^5$, yellow for constant gain $k = 10^2$, purple for constant gain $k = 1$, and red for adaptive gain.

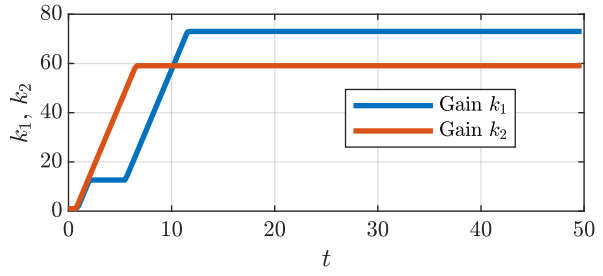

Figure 5.6: Time evolution of the gains k_1 and k_2.

5.5.2 Perturbation signal optimization in oil extraction

Oil extraction becomes financially unviable when the reservoir pressure drops under a certain threshold. To solve this problem, one can employ gas-lifting [11]. Compressed gas is injected down the well to decrease the density of the fluid and the hydrostatic pressure, causing an increase in production. The oil rate is typically a concave hard-to-model function of the gas injection rate [11] with a maximum that slowly changes over time due to changing conditions, making it an excellent candidate for extremum seeking. Extraction sites usually have multiple wells that the same processing facility operates. The goal is to maximize the oil extraction rate

$$J_1(\boldsymbol{x}) = \sum_{i=1}^{N} f_i(x_i), \tag{5.20}$$

while not exceeding a linear coupling constraint which may relate to total injection rate, power load, etc.

$$\sum_{i}^{N} b_i x_i \leq x_{\max}, \tag{5.21}$$

where $f_i : \mathbb{R} \to \mathbb{R}$ and $x_i \in \mathbb{R}$ are the oil-rate function and the injection rate, respectively, of the well i and $b_i, x_{\max} \in \mathbb{R}$. We denote the solution to this problem as x^*. Furthermore, the processing facility wants to reduce the oscillations in the total optimal extraction rate that result from the extremum seeking perturbation signals:

$$\hat{x}_i(t) = x_i(t) + d_i(t) = x_i(t) + a_i \sin(\omega t + \phi_i). \tag{5.22}$$

The oscillations of a single well's optimal extraction rate can be approximated as

$$f_i(\hat{x}_i) - f_i(x_i) \approx \nabla f_i(x_i) a_i \sin(\omega t + \phi_i).$$

The secondary goal cannot be accomplished by techniques that diminish the oscillation amplitude over time [95], [96] as the cost functions are slowly varying and the learning procedure would stop prematurely. Furthermore, we cannot use too high frequencies [97] as that would also destroy our equipment. Thus, to accomplish our goal, wells are grouped into pairs (i, j), and each pair selects perturbation signals which are in antiphase:

$$\begin{aligned} d_i(t) &= a_i \sin(\omega t + \phi_i) \\ d_j(t) &= -a_j \sin(\omega t + \phi_i). \end{aligned} \tag{5.23}$$

Without the coupling constraint and with an even number of wells, the perturbation signals in (5.23) reduce the oscillations in the neighborhood of the optimum as $\nabla f_1(x_1^*) \approx \nabla f_2(x_2^*) \approx \cdots \approx \nabla f_N(x_N^*) \approx 0$. However, if a constraint is present, the perturbation signals might not cancel out properly because for some pair (i, j), it can hold that $\nabla f_i(x_i^*) \not\approx \nabla f_j(x_j^*)$. Therefore, it is also necessary to adapt the amplitudes a_i, a_j to improve the cancellation effect. Without loss of generality, we assume that neighboring indices are paired up as in (5.23). The secondary cost function is formulated as follows:

$$\hat{J}_2(a) = \frac{l}{2} \sum_{i=1}^{\frac{N}{2}} \left(\nabla f_{2i}(x_{2i}^*) a_{2i} - \nabla f_{2i-1}(x_{2i-1}^*) a_{2i-1} \right)^2 - \sum_{i=1}^{N} \log_p ((a_i - \underline{a})(\overline{a} - a_i))$$

where $l > 0$, $\underline{a}$ and $\overline{a}$ are the minimum and maximum perturbation amplitude, respectively, and it holds $0 < \underline{a} < \overline{a}$. We denote $a^* := \operatorname{argmin} \hat{J}_2(a)$. Since x^* is not known in advance, direct computation of a^* is not possible. One can modify the previous cost function to use any value of x

$$J_2(x,a) = \frac{l}{2} \sum_{i=1}^{\frac{N}{2}} (\nabla f_{2i}(x_{2i}) a_{2i} - \nabla f_{2i-1}(x_{2i-1}) a_{2i-1})^2 - \sum_{i=1}^{N} \log_p ((a_i - \underline{a})(\overline{a} - a_i)), \tag{5.24}$$

and minimize the cost function:

$$J_p(x,a) = -\alpha J_1(x) + \beta J_2(x,a), \quad \alpha, \beta > 0, \tag{5.25}$$

with constraint (5.21). However, this approach only approximates the solution (x^*, a^*) for $\alpha \gg \beta$. With our game-theoretic formulation instead, we look for a solution (x^*, a^*) such that x^* is an optimal solution to the oil extraction problem in (5.20) and the overall pair (x^*, a^*) is variational GNE, meaning that the amplitudes are fairly and optimally chosen. To show that the game is monotone and can be solved by our algorithm, it is sufficient to show that the Jacobian matrix of the pseudogradient is positive semidefinite [98, Prop. 12.3]:

$$\mathcal{J}_F(x,a) := \begin{bmatrix} \mathcal{J}_{11} & \mathcal{J}_{12} \\ \mathcal{J}_{21} & \mathcal{J}_{22} \end{bmatrix} \succcurlyeq 0. \tag{5.26}$$

The submatrix $\mathcal{J}_{11} := \operatorname{blkdiag}\left((-\nabla^2 f_i(x_i))_{i \in \mathcal{I}}\right)$ is positive semidefinite as all of the cost functions in (5.20) are concave. Furthermore, the submatrix $\mathcal{J}_{12}$ is a zero matrix as the concave cost functions do not depend on the perturbation amplitudes. Then it holds that $\mathcal{J}_{22} := \operatorname{blkdiag}\left(\mathcal{J}_{1,2}, \mathcal{J}_{3,4}, \ldots, \mathcal{J}_{N-1,N}\right)$, where

$$\mathcal{J}_{i,j} = l \begin{bmatrix} (\nabla f_i(x_i))^2 & -\nabla f_i(x_i) \nabla f_j(x_j) \\ -\nabla f_i(x_i) \nabla f_j(x_j) & \left(\nabla f_j(x_j)\right)^2 \end{bmatrix} + \begin{bmatrix} \frac{(a_i - \overline{a})^{-2} + (a_i - \underline{a})^{-2}}{\log(p)} & 0 \\ 0 & \frac{(a_j - \overline{a})^{-2} + (a_j - \underline{a})^{-2}}{\log(p)} \end{bmatrix}. \tag{5.27}$$

As both matrices in (5.27) are positive semidefinite, and $\mathcal{J}_{22}$ is block diagonal, it follows that the matrix $\mathcal{J}_{22}$ is positive semidefinite. Finally, due to the block triangular structure of $\mathcal{J}_F$ and positive semidefinitness of $\mathcal{J}_{11}$ and $\mathcal{J}_{22}$, we conclude that $\mathcal{J}_F$ is positive semidefinite and in turn that the pseudogradient is monotone.

In our example, the amplitudes of the perturbation signals are part of the decision variable and are therefore time-varying; all perturbation signals have the same frequency but different phases (5.23); and coordinates of the pseudogradient related to cost functions in (5.24) need not be estimated, but can be computed directly. Thus, by Remark 5.16, we suitably adjust the algorithm in (5.16), (5.17) and use it for our numerical simulations. Furthermore, we use the well oil extraction rates as in [11]

$$\begin{aligned} f_1(x_1) &= -3.9 \times 10^{-7} x_1^4 + 2.1 \times 10^{-4} x_1^3 - 0.043 x_1^2 + 3.7 x_1 + 12, \\ f_2(x_2) &= -1.3 \times 10 - 7 x_2^4 + 10^{-4} x_2^3 - 2.8 \times 10^{-2} x_2^2 + 3.1 x_2 - 17, \\ f_3(x_3) &= -1.2 \times 10^{-7} x_3^4 + 10^{-4} x_3^3 - 0.028 x_3^2 + 2.5 x_3 - 16, \\ f_4(x_4) &= -4 \times 10^{-7} x_4^4 + 1.8 \times 10^{-4} x_4^3 - 0.036 x_4^2 + 3.5 x_4 + 10, \end{aligned}$$

5

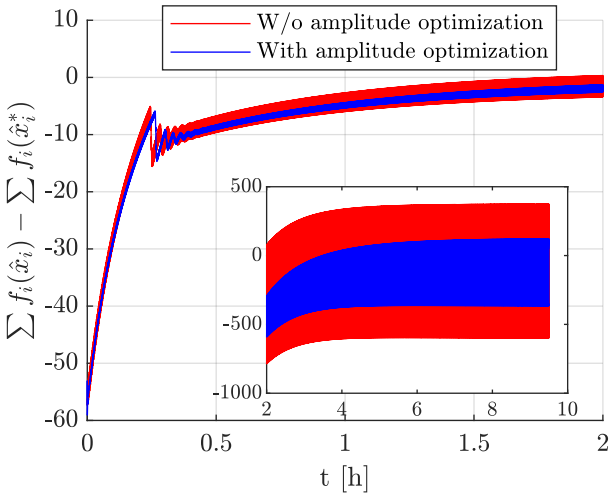

Figure 5.7: Time evolution of the total oil extraction rate for the case with and without perturbation amplitude optimization. Amplitude optimization results in a 51% steady state oscillation reduction.

and the following parameters: $l = 10$, $v_i = 0.1$, $\varepsilon_i = 0.01$ for all i, $\overline{a} = 10$, $\underline{a} = 5$, $p = 100$, $\epsilon = 10$, $\omega_i = 1$, $x_{\max} = 200, b_1 = 1, b_2 = 2, b_3 = 3, b_4 = 4$, $k_{\min} = 0.01$, $k_{\max} = 10000, c = 1000$, $\Gamma = 10$. For initial conditions: $\boldsymbol{u}(0) = \boldsymbol{z}(0) = \mathrm{col}\,(10, 10, 10, 10, 7.5, 7.5, 7.5, 7.5)$, $w(0) = 0$, $\lambda(0) = 0.1$, $\zeta(0) = \mathbf{0}$, $k(0) = 0.01$, $s(0) = 0$. Additionally, we run numerical simulations where only the total oil rate is optimized with constant perturbation amplitudes $a_i = 5$, using again the algorithm in (5.16). In Figure 5.7, we see that the amplitude optimization indeed reduces the amplitude of the oscillations in the oil rate by 51% in the steady state, even though larger amplitudes were used in the perturbation signals. In Figure 5.8, we can see how the constraints are violated over time. After half an hour, the constraints are always marginally satisfied. In Figure 5.9, we note that in each pair, one of the amplitudes converges to a neighborhood of the minimal value.

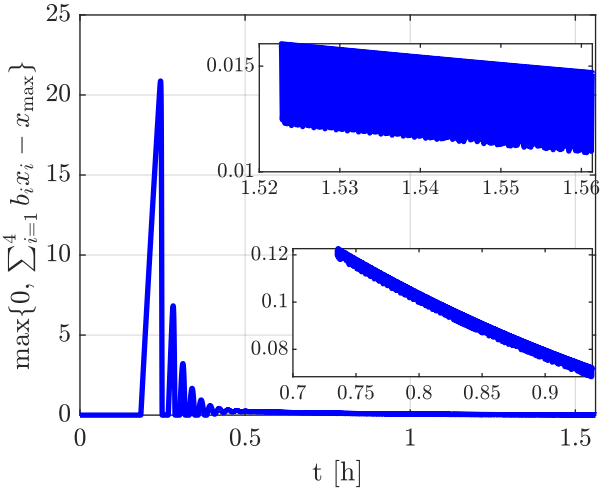

Figure 5.8: Constraint violation over time.

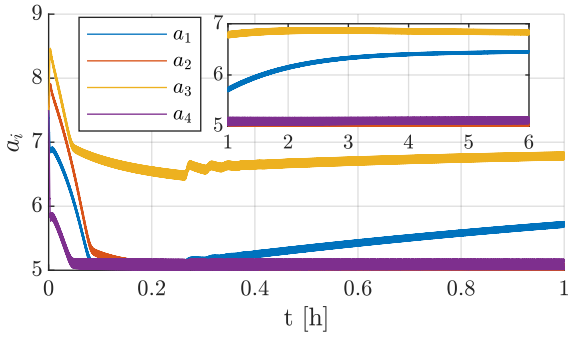

Figure 5.9: Time evolution of amplitudes a_i.

5.6 Conclusion

Monotone generalized Nash equilibrium problems with dualized constraints can be solved via the continuous-time golden ratio algorithm augmented by projection-less dual dynamics. Furthermore, the algorithm can be adapted via hybrid systems theory for use with zeroth-order information feedback.

Appendix

5.A Proof of Theorem 5.9

We choose the following Lyapunov function candidate

$$V(\omega,\omega^*) = \tfrac{1}{2}\|\boldsymbol{u}-\boldsymbol{u}^*\|^2_{\Gamma^{-1}} + \tfrac{1}{2}\|\boldsymbol{z}-\boldsymbol{z}^*\|^2_{\Gamma^{-1}} + \tfrac{1}{2}\|w-w^*\|^2 + \sum_{j\in\mathcal{Q}}\left(\lambda_j - \lambda_j^* - \lambda_j^*\log\left(\tfrac{\lambda_j}{\lambda_j^*}\right)\right), \quad (5.28)$$

5

where $\omega^* \in \mathcal{A}$ is any equilibrium point of (5.10) whose $\boldsymbol{u}^*$, λ^* states correspond to a GNE and we define $0\log 0 := 0$. The first three terms represent a weighted Euclidean distance from the solution $(\boldsymbol{u}^*, \boldsymbol{z}^*, w^*)$. As in [91], [92], the fourth addend is chosen such that its Lyapunov derivative is the same as in the case of the standard norm $\|\lambda-\lambda^*\|$ and standard dynamics $\dot\lambda = -\lambda + \mathrm{proj}_{\mathbb{R}^q_+}(g(\boldsymbol{u})-\lambda)$. By Standard assumption 5.7, equilibrium points in $\mathcal{M}\setminus\mathcal{A}$ are disconnected from $\mathcal{A}$. Furthermore, going back to the Lyapunov function, points in $\mathcal{M}\setminus\mathcal{A}$ are not in its domain, and by proving the negative semi-definiteness of the Lyapunov derivative, their potential region of attraction is reduced to set $\mathcal{L}\supset\mathcal{M}$. Thus, we do not consider points in $\mathcal{L}$ for initial conditions. The Lyapunov derivative is given by

$$\begin{aligned}
\dot V &= \left\langle \boldsymbol{u}-\boldsymbol{u}^* \,\middle|\, \Gamma^{-1}\left(-\boldsymbol{u}+\boldsymbol{z}-\Gamma(F(\boldsymbol{u})+\nabla g(\boldsymbol{u})^\top\lambda)\right)\right\rangle + \left\langle \boldsymbol{z}-\boldsymbol{u}^* \,\middle|\, \Gamma^{-1}(-\boldsymbol{z}+\boldsymbol{u})\right\rangle \\
&\quad + \langle w-\lambda^* \mid -w+\lambda\rangle + \sum_{j\in\mathcal{Q}}\left(\dot\lambda_j - \tfrac{\lambda_j^*}{\lambda_j}\dot\lambda_j\right) \\
&\le -\|\boldsymbol{u}-\boldsymbol{z}\|^2_{\Gamma^{-1}} - \left\langle \boldsymbol{u}-\boldsymbol{u}^* \,\middle|\, F(\boldsymbol{u})+\nabla g(\boldsymbol{u})^\top\lambda\right\rangle + \langle w-\lambda^* \mid -w+\lambda\rangle \\
&\quad + \sum_{j\in\mathcal{Q}}\left(\lambda_j-\lambda_j^*\right)\left(g_j(\boldsymbol{u})-\lambda_j+\omega_j\right) \\
&\le -\|\boldsymbol{u}-\boldsymbol{z}\|^2_{\Gamma^{-1}} - \left\langle \boldsymbol{u}-\boldsymbol{u}^* \,\middle|\, F(\boldsymbol{u})+\nabla g(\boldsymbol{u})^\top\lambda\right\rangle + \langle w-\lambda^* \mid -w+\lambda\rangle + \langle \lambda-\lambda^* \mid g(\boldsymbol{u})-\lambda+w\rangle \\
&\le -\|\boldsymbol{u}-\boldsymbol{z}\|^2_{\Gamma^{-1}} - \|\lambda-w\|^2 + \langle \lambda-\lambda^* \mid g(\boldsymbol{u})\rangle + \left\langle \boldsymbol{u}-\boldsymbol{u}^* \,\middle|\, F(\boldsymbol{u})+\nabla g(\boldsymbol{u})^\top\lambda\right\rangle. \qquad (5.29)
\end{aligned}$$

From the properties of v-GNE set, we conclude that

$$\begin{aligned}
\mathbf{0}_m &= F(\boldsymbol{u}^*) + \nabla g(\boldsymbol{u}^*)^\top\lambda^* \\
0 &= \left\langle \boldsymbol{u}-\boldsymbol{u}^* \,\middle|\, F(\boldsymbol{u}^*)+\nabla g(\boldsymbol{u}^*)^\top\lambda^*\right\rangle \\
0 &\le \langle g(\boldsymbol{u}^*) \mid \lambda^*-\xi\rangle \text{ for all } \xi\in\mathbb{R}^q_+ \qquad (5.30)
\end{aligned}$$

Thus, by using (5.30) within (5.29), we further derive

$$\begin{aligned}
\dot{V} &\leq -\|\boldsymbol{u}-\boldsymbol{z}\|_{\Gamma^{-1}}^2 - \|\lambda - w\|^2 - \langle \boldsymbol{u}-\boldsymbol{u}^* \mid F(\boldsymbol{u})-F(\boldsymbol{u}^*)\rangle - \left\langle \boldsymbol{u}-\boldsymbol{u}^* \,\middle|\, \nabla g(\boldsymbol{u})^\top \lambda - \nabla g(\boldsymbol{u}^*)^\top \lambda^* \right\rangle \\
&\quad + \langle \lambda - \lambda^* \mid g(\boldsymbol{u}) - g(\boldsymbol{u}^*)\rangle \\
&\leq -\|\boldsymbol{u}-\boldsymbol{z}\|_{\Gamma^{-1}}^2 - \|\lambda - w\|^2 - \underbrace{\langle \boldsymbol{u}-\boldsymbol{u}^* \mid F(\boldsymbol{u})-F(\boldsymbol{u}^*)\rangle}_{\leq 0} \\
&\quad + \sum_{j\in\mathcal{Q}} \underbrace{\lambda_j}_{\geq 0} \underbrace{\left(g_j(\boldsymbol{u}) - g_j(\boldsymbol{u}^*) + \left\langle \boldsymbol{u}^* - \boldsymbol{u} \,\middle|\, \nabla g_j(\boldsymbol{u})\right\rangle\right)}_{\leq 0} \\
&\quad - \sum_{j\in\mathcal{Q}} \underbrace{\lambda_j^*}_{\geq 0} \underbrace{\left(g_j(\boldsymbol{u}) - g_j(\boldsymbol{u}^*) - \left\langle \boldsymbol{u}-\boldsymbol{u}^* \,\middle|\, \nabla g_j(\boldsymbol{u}^*)\right\rangle\right)}_{\geq 0} \\
&\leq -\|\boldsymbol{u}-\boldsymbol{z}\|_{\Gamma^{-1}}^2 - \|\lambda - w\|^2, \qquad (5.31)
\end{aligned}$$

where the last inequality follows from the monotonicity of the pseudogradient and the convexity of the coupled constraints. Now, we prove via La Salle's theorem that the trajectories of (5.10) converge to the set $\mathcal{A}$. Let us define the following sets:

$$\begin{aligned}
\Omega_c &:= \{\omega \in \mathbb{R}^{2m} \times \mathbb{R}_+^{2q} \mid V(\omega) \leq c\} \\
\Omega_0 &:= \{\omega \in \Omega_c \mid \boldsymbol{u} = \boldsymbol{z} \text{ and } \lambda = w\} \\
\mathcal{Z} &:= \{\omega \in \Omega_c \mid \dot{V}(\omega) = 0\} \\
\mathcal{O} &:= \{\omega \in \Omega_c \mid \omega(0) \in \mathcal{Z} \Rightarrow \omega(t) \in \mathcal{Z}\ \forall t \in \mathbb{R}\}, \qquad (5.32)
\end{aligned}$$

where Ω_c is a non-empty compact sublevel set of the Lyapunov function candidate, $\mathcal{Z}$ is the set of zeros of its derivative, Ω_0 is the superset of $\mathcal{Z}$ which follows from (5.31) and $\mathcal{O}$ is the maximum invariant set as explained in [29, Chp. 4.2]. Then, for some $c > 0$ large enough, it holds that

$$\Omega_c \supseteq \Omega_0 \supseteq \mathcal{Z} \supseteq \mathcal{O} \supseteq \mathcal{A}. \qquad (5.33)$$

Firstly, for any compact set Ω_c, since the right-hand side of (5.10) is (locally) Lipschitz continuous and therefore by [29, Thm. 3.3] we conclude that solutions to (5.10) exist and are unique. Next, we show that the only ω-limit trajectories in $\mathcal{O}$ are the equilibrium points of the dynamics in (5.10), i.e. $\mathcal{O} \equiv \mathcal{A}$. It is sufficient to prove that there cannot exist any positively invariant trajectories in Ω_0, apart from stationary points in $\mathcal{A}$. For trajectories in Ω_0, it holds that

$$\mathbf{0} = \boldsymbol{u} - \boldsymbol{z} \qquad (5.34)$$
$$\mathbf{0} = \dot{\boldsymbol{u}} - \dot{\boldsymbol{z}} \qquad (5.35)$$
$$\mathbf{0} = \lambda - w \qquad (5.36)$$
$$\mathbf{0} = \dot{\lambda} - \dot{w}, \qquad (5.37)$$

and therefore

$$\mathbf{0} = F(\boldsymbol{u}) + \nabla g(\boldsymbol{u})^\top \lambda \qquad (5.38)$$
$$\mathbf{0} = \operatorname{diag}(\lambda)\, g(\boldsymbol{u}), \qquad (5.39)$$

where (5.38) follows from (5.10) and (5.35), and (5.39) follows from (5.10), (5.36) and (5.37). Equations (5.35), (5.36), (5.38) and (5.39) form the definition of set $\mathcal{M}$ in (5.11) and the fact that $\mathcal{M}\setminus\mathcal{A}$ is not in the domain, we conclude $\Omega_0 \equiv \mathcal{A}$. Since the set $\mathcal{O}$ is a subset of the set Ω_0, we conclude that $\mathcal{O} \equiv \mathcal{A}$. Therefore, by La Salle's theorem [29, Thm. 4], set $\mathcal{A}$ is attractive for the dynamics in (5.10).

Next, we prove the stability of $\mathcal{A}$. We restrict the domain of the dynamics by choosing an arbitrary ω^* and a set Λ that contains arbitrarily many initial conditions of interest not contained in the set $\mathcal{L}$, and it holds $\mathcal{A} \subset \Lambda$. Then, we compute $\bar{c} = \max_{\omega\in\Lambda} V(\omega,\omega^*)$ and define the new restricted domain to the forward invariant set $\Re$, where $\Re := \{\omega \in \mathbb{R}^{2m}\times\mathbb{R}_+^{2q} \mid V(\omega,\omega^*) \le \bar{c}\}$.

Consequently, we define the following set-valued mapping of compact sets

$$\Omega(\omega^*, c) := \{\omega \in \Re \mid V(\omega,\omega^*) \le c\}.$$

Now, we prove global stability with respect to the set $\mathcal{A}$ by showing that any Lyapunov invariant set can be upper and lower bounded by balls surrounding the solution set. Let us choose an arbitrary $\varepsilon > 0$. For a particular c and ω^*, since V does not increase, it follows that all trajectories that start in $\Omega(\omega^*,c)$ are contained in the set. Let us choose $c(\omega^*)$ such that $\Omega(\omega^*,c(\omega^*)) \subseteq (\mathcal{A}+\varepsilon\mathbb{B})\cap\Re$. By continuity of V, for every set $\Omega(\omega^*,c(\omega^*))$, it is possible to find $\delta(\omega^*) > 0$ such that $(\omega^*+\delta(\omega^*)\mathbb{B})\cap\Re \subseteq \Omega(\omega^*,c(\omega^*))$. If we take $\delta = \min_{\omega^*\in\mathcal{A}}\delta(\omega^*)$, it holds that $\cup_{\omega^*\in\mathcal{A}}(\omega^*+\delta\mathbb{B})\cap\Re = (\mathcal{A}+\delta\mathbb{B})\cap\Re$. Thus, $(\mathcal{A}+\delta\mathbb{B})\cap\Re \subseteq \cup_{\omega^*\in\mathcal{A}}\Omega(\omega^*,c(\omega^*))$ which implies that all solutions with $\omega(0) \in (\mathcal{A}+\delta\mathbb{B})$, remain in $(\mathcal{A}+\varepsilon\mathbb{B})$ for all $t \ge 0$. Therefore, set $\mathcal{A}$ is globally stable and attractive on $\Re$, hence it is UGAS.

5.B Proof of Lemma 1

We study the stability of singular equilibrium points in the set $\mathcal{M}\setminus\mathcal{A}$. The main difference between the set $\mathcal{M}\setminus\mathcal{A}$ and the set of solutions $\mathcal{A}$, is that the set $\mathcal{M}\setminus\mathcal{A}$ contains points where $\bar{\lambda}_j = 0$ and $g_i(\bar{\boldsymbol{u}}) > 0$ for some index j. Let $\hat{\omega} \in \mathcal{M}\setminus\mathcal{A}$. Without loss of generality, we assume that for $j = q$ it holds that $\hat{\lambda}_q = 0$ and $g_q(\hat{\boldsymbol{u}}) > 0$. In order to check the stability of the point $\hat{\omega}$, we study the dynamics in (5.10) linearized around $\hat{\omega}$:

$$\begin{bmatrix}\dot{\tilde{\boldsymbol{z}}}\\ \dot{\tilde{\boldsymbol{u}}}\\ \dot{\tilde{w}}\\ \dot{\tilde{\lambda}}\end{bmatrix} = \left[\begin{array}{ccc|c} -I_m & I_m & \mathbf{0} & \mathbf{0}\\ I_m & -I_m - M & \mathbf{0} & -\nabla g(\hat{\boldsymbol{u}})^\top\\ \mathbf{0} & \mathbf{0} & -I_q & I_q\\ 0 & 0 & 0 & g_1(\hat{\boldsymbol{u}})\\ \vdots & \vdots & \vdots & \vdots\\ \hline 0 & 0 & 0 & g_q(\hat{\boldsymbol{u}}) \end{array}\right]\begin{bmatrix}\tilde{\boldsymbol{z}}\\ \tilde{\boldsymbol{u}}\\ \tilde{w}\\ \tilde{\lambda}\end{bmatrix}, \tag{5.40}$$

where $M(\hat{\boldsymbol{u}},\hat{\lambda}) := \frac{\partial}{\partial \boldsymbol{u}}\left(\Gamma(F(\boldsymbol{u})+\nabla g(\boldsymbol{u})^\top\lambda)\right)\Big|_{\boldsymbol{u}=\hat{\boldsymbol{u}},\lambda=\hat{\lambda}}$, $\tilde{\boldsymbol{z}} := \boldsymbol{z}-\hat{\boldsymbol{z}}$, $\tilde{\boldsymbol{u}} := \boldsymbol{u}-\hat{\boldsymbol{u}}$, $\tilde{w} := w-\hat{w}$, and $\tilde{\lambda} := \lambda-\hat{\lambda}$. The system matrix will have at least one positive eigenvalue due to the upper triangular structure and the element $g_q(\hat{\boldsymbol{u}}) > 0$ in the last row. It follows that the equilibrium point $\hat{\omega}$ is unstable for dynamics in (5.10). As $\hat{\omega}$ was chosen arbitrarily, we conclude that any equilibrium point in $\mathcal{M}\setminus\mathcal{A}$ is unstable.

5.C Proof of Lemma 5.11

Let us assume otherwise that we have an infinite amount of jumps. By the structure of the jump set and map, we must jump between $s_i = -1$ and $s_i = 1$ an infinite amount of times for at least one of the states i. Without the loss of generality, we assume this is true for $i = j$. As we can spend only a finite amount of time in the state $s_j = 1$ ($\tau = \frac{\bar{k}-\underline{k}}{c_j}$), time between jumps from $s_j = 1$ to $s_j = -1$, t_k, has to decrease to zero, otherwise $\sum^{\infty} t_k = \infty > \tau$. Minimum time between jumps $t_{\min}$ is equal to $\frac{d_{\min}}{\max \|\dot{\boldsymbol{u}}\|}$, where $d_{\min}$ is the minimal distance between the jump sets corresponding to $s_j = -1$ and $s_j = 1$, and $\max \|\dot{\boldsymbol{u}}\|$ is finite based on the continuity of the flow map and the forward invariance of any compact set Ω_c.To show that $d_{\min} \neq 0$, let $G_j(\epsilon) := \{\boldsymbol{y} \mid g_j(\boldsymbol{y}) = \epsilon\}$ and choose ϵ such that $G_j(2\epsilon) \neq \emptyset$. By convexity property of the constraint function, for $\boldsymbol{u} \in G_j(\epsilon)$ and $\boldsymbol{v} \in G_j(2\epsilon)$, we have:

$$\begin{aligned} g_j(\boldsymbol{u}) &\geq g_j(\boldsymbol{v}) + \nabla g_j(\boldsymbol{v})(\boldsymbol{u}-\boldsymbol{v}) \\ \epsilon &\leq \nabla g_j(\boldsymbol{v})(\boldsymbol{v}-\boldsymbol{u}) \leq \left\|\nabla g_j(\boldsymbol{v})\right\| \|\boldsymbol{v}-\boldsymbol{u}\|. \\ \frac{\epsilon}{\left\|\nabla g_j(\boldsymbol{v})\right\|} &\leq \|\boldsymbol{v}-\boldsymbol{u}\| \end{aligned}$$

As the set $G_j(2\epsilon)$ is compact, and $\nabla g_j(\boldsymbol{v})$ is continuous in its coordinates, by the extreme value theorem, $\left\|\nabla g_j(\boldsymbol{v})\right\|$ reaches a maximum δ on that set. Therefore, the minimum distance is bounded bellow as $d_{\min} \geq \frac{\epsilon}{\delta}$.
As both $d_{\min}$ and $\|\dot{\boldsymbol{u}}\|$ are finite positive numbers, we conclude that $t_{\min} > 0$, which leads us to a contradiction. Therefore, we can only have a finite number of jumps. ∎

5.D Proof of Theorem 5.13

Proof of convergence is similar to that of Theorem 5.9. First, we note that the additional states are invariant to the set $\mathcal{K}^q \times \mathcal{S}^q$ regardless of the rest of the dynamics. Next, we choose the Lyapunov function candidate

$$\begin{aligned} V(\omega,\omega^*,k) &= \tfrac{1}{2}\|\boldsymbol{u}-\boldsymbol{u}^*\|^2_{\Gamma^{-1}} + \tfrac{1}{2}\|\boldsymbol{z}-\boldsymbol{u}^*\|^2_{\Gamma^{-1}} \\ &+ \tfrac{1}{2}\|w-\lambda^*\|^2 + \sum_{j\in\mathcal{Q}} \tfrac{1}{k_j}\left(\lambda_j - \lambda_j^* - \lambda_j^* \log\left(\tfrac{\lambda_j}{\lambda_j^*}\right)\right), \end{aligned} \tag{5.41}$$

which depends on the chosen equilibrium point ω^*. In a similar manner as in the proof of Theorem 5.9, it follows that

$$u_c(\xi) = \langle \nabla V(\xi) \mid F(\xi)\rangle \leq -\|\boldsymbol{u}-\boldsymbol{z}\|^2_{\Gamma^{-1}} - \|\lambda - w\|^2, \tag{5.42}$$

$$u_d(\xi) = V(\omega_+,\omega^*,k) - V(\omega,\omega^*,k) = 0. \tag{5.43}$$

We restrict the flow and jump sets by choosing an arbitrary ω^* and set Λ that contains arbitrarily many initial conditions of interest not contained in the set $\mathcal{L}$, and it holds $\mathcal{A} \subset \Lambda$. Then, we compute $\bar{c} = \max_{\omega\in\Lambda} V(\omega,\omega^*,k_{\max})$ and define the new restricted flow set as $\mathfrak{B} := \mathfrak{R} \times \mathcal{K}^q \times \mathcal{S}^q$, where $\mathfrak{R} := \{\omega \in \mathbb{R}^{2m} \times \mathbb{R}_+^{2q} \mid V(\omega,\omega^*,k_{\min}) \leq \bar{c}\}$. Consequently, we define the following set-valued mapping of compact sets

$$\Omega(\omega^*,k,c) := \{\omega \in \mathfrak{R} \mid V(\omega,\omega^*,k) \leq c\}.$$

5

Compared to the invariant sets of Theorem 5.9, the compact sets also depend on the adaptive gains. In fact, it holds that $\mathbf{0} < k' \leq k''$ implies that $\Omega(\omega^*, k', c) \subseteq \Omega(\omega^*, k'', c)$. As k is dynamic, the "invariant set", in which the trajectories of ω dynamics are contained, expands in the λ dimensions. Due to the fact that the minimal and maximal values of the gain are algorithm parameters, the "expansion" of the set is bounded.

Now, we show global stability with respect to the set $\mathcal{A} \times \mathcal{K}^q \times \mathcal{S}^q$ by showing that any invariant set can be upper and lower bounded by a ball surrounding the solution set when accounting for the "inflation" of the set due to changes of the gain. Let us choose an arbitrary $\varepsilon > 0$. For a particular c and ω^*, the trajectories are constrained to the largest Ω set for $k = k_{\max}$, and to the smallest for $k = k_{\min}$. Therefore, by the fact that V does not increase during flows or jumps and that the gains k are constrained to the set $\mathcal{K}^q$, it follows that all trajectories that start in $\Omega(\omega^*, k_{\min}, c)$ are contained in the set $\Omega(\omega^*, k_{\max}, c)$.

Let us choose $c(\omega^*)$ such that $\Omega(\omega^*, k_{\max}, c(\omega^*)) \subseteq (\mathcal{A} + \varepsilon\mathbb{B}) \cap \mathfrak{R}$. By continuity of V, for every set $\Omega(\omega^*, k_{\min}, c(\omega^*))$, it is possible to find $\delta(\omega^*) > 0$ such that $(\omega^* + \delta(\omega^*)\mathbb{B}) \cap \mathfrak{R} \subseteq \Omega(\omega^*, k_{\min}, c(\omega^*))$. If we take $\delta = \min_{\omega^* \in \mathcal{A}} \delta(\omega^*)$, it holds that $\cup_{\omega^* \in \mathcal{A}} (\omega^* + \delta\mathbb{B}) \cap \mathfrak{R} = (\mathcal{A} + \delta\mathbb{B}) \cap \mathfrak{R}$. Thus, $(\mathcal{A} + \delta\mathbb{B}) \cap \mathfrak{R} \subseteq \cup_{\omega^* \in \mathcal{A}} \Omega(\omega^*, k_{\min}, c(\omega^*))$ which implies that all maximal solutions with $\xi(0,0) \in (\mathcal{A} + \delta\mathbb{B}) \times \mathcal{K}^q \times \mathcal{S}^q$, remain in $(\mathcal{A} + \varepsilon\mathbb{B}) \times \mathcal{K}^q \times \mathcal{S}^q$ for all $(t, j) \in \operatorname{dom}\xi$.

Next, we prove global attractivity for the constrained flow and jump sets. Let ξ be a complete solution in $\mathfrak{B}$. For a fixed ω^*, we define $\hat{V}(\xi) := V(\omega, \omega^*, k)$. Via [80, Cor. 8.7] and Lemma 5.11, we conclude that for some $r \geq 0$, ξ approaches the largest weakly invariant subset in $\hat{V}^{-1}(r) \cap \mathfrak{B} \cap \overline{u_c^{-1}(0)}$, where the notation $f^{-1}(r)$ stands for the r-level set of f on $\operatorname{dom} f$, the domain of definition of f, i.e., $f^{-1}(r) := \{z \in \operatorname{dom} f \mid f(z) = r\}$. By same reasoning as in Theorem 5.9, we conclude that $\overline{u_c^{-1}(0)} = \mathcal{A} \times \mathcal{K}^q \times \mathcal{S}^q$.

Thus, the largest weakly invariant subset for ξ reads as $\hat{V}^{-1}(r) \cap (\mathcal{A} \times \mathcal{K}^q \times \mathcal{S}^q)$. Every trajectory ξ converges to a different subset. The union of invariant subsets for every trajectory is $\mathcal{A} \times \mathcal{K}^q \times \mathcal{S}^q$, as we can choose an initial condition for which it holds $\omega(0,0) = \omega^* = const.$ for all $(t, j) \in \operatorname{dom}\xi$, for any $\omega^* \in \mathcal{A}$.

Therefore, $\mathcal{A} \times \mathcal{K}^q \times \mathcal{S}^q$ is globally attractive, as all solutions are complete, which implies that the set $\mathcal{A} \times \mathcal{K}^q \times \mathcal{S}^q$ is UGAS ([80, Thm. 7.12]) on the restricted flow and jump sets. Furthermore, by [82, Prop. A.1.], the HDS $(C \cap \mathfrak{B}, D \cap \mathfrak{B}, F, G)$ is structurally robust.

5.E Proof of Theorem 5.15

We rewrite the system in (5.16b) as

$$\begin{bmatrix} \dot{\boldsymbol{u}} \\ \dot{\boldsymbol{z}} \\ \dot{\lambda} \\ \dot{\boldsymbol{w}} \\ \dot{k} \\ \dot{s} \\ \dot{\boldsymbol{\zeta}} \end{bmatrix} = \begin{bmatrix} \bar{\nu}\bar{\varepsilon}\tilde{\boldsymbol{\nu}}\tilde{\boldsymbol{\varepsilon}}\left(-\boldsymbol{u} + \boldsymbol{z} - \Gamma(\boldsymbol{\zeta} + \nabla g(\boldsymbol{u})^\top \lambda)\right) \\ \bar{\nu}\bar{\varepsilon}\tilde{\boldsymbol{\nu}}\tilde{\boldsymbol{\varepsilon}}\left(-\boldsymbol{z} + \boldsymbol{u}\right) \\ \bar{\nu}\bar{\varepsilon}\tilde{\nu}_0\tilde{\varepsilon}_0 \operatorname{diag}(k) \operatorname{diag}(\lambda)(g(\boldsymbol{u}) - \lambda + w) \\ \bar{\nu}\bar{\varepsilon}\tilde{\nu}_0\tilde{\varepsilon}_0\left(-w + \lambda\right) \\ \frac{1}{2}\bar{\nu}\bar{\varepsilon}\tilde{\nu}_0\tilde{\varepsilon}_0 c(I + S)S^2 \\ \mathbf{0} \\ \bar{\nu}\tilde{\boldsymbol{\nu}}\left(-\boldsymbol{\zeta} + \hat{F}(\boldsymbol{u}, \boldsymbol{\mu})\right) \end{bmatrix}, \tag{5.44}$$

$$\dot{\boldsymbol{\mu}} = 2\pi\mathcal{R}_\kappa \boldsymbol{\mu}, \tag{5.45}$$

where $\bar{\nu} := \max_{i \in I_0} \nu_i$, $\bar{\varepsilon} := \max_{i \in I_0} \varepsilon_i$, $\tilde{\boldsymbol{\nu}} := \boldsymbol{\nu}/\bar{\nu}$, $\tilde{\boldsymbol{\varepsilon}} := \boldsymbol{\varepsilon}/\bar{\varepsilon}$, $\tilde{\nu_0} := \nu_0/\bar{\nu}$ and $\tilde{\varepsilon_0} := \varepsilon_0/\bar{\varepsilon}$. The system in (5.44), (5.45) is in singular perturbation from where $\bar{\nu}$ is the time scale separation constant.

The goal is to average the dynamics of ξ, ζ along the solutions of $\boldsymbol{\mu}$. For sufficiently small $\bar{a} := \max_{i\in\mathcal{I}} a_i$, we can use the Taylor expansion to write down the cost functions as

$$\begin{aligned} J_i(\boldsymbol{u} + A\mathbb{D}\boldsymbol{\mu}) &= J_i(u_i, \boldsymbol{u}_{-i}) + a_i(\mathbb{D}^{m_i}\mu_i)^\top \nabla_{u_i} J_i(u_i, \boldsymbol{u}_{-i}) \\ &+ A_{-i}(\mathbb{D}^{m_{-i}}\boldsymbol{\mu}_{-i})^\top \nabla_{u_{-i}} J(u_i, \boldsymbol{u}_{-i}) + O(\bar{a}^2), \end{aligned} \tag{5.46}$$

where $A_{-i} := \text{blkdiag}\left((a_i I_{m_i})_{j\in\mathcal{I}\setminus\{i\}}\right)$. By the fact that the right-hand side of (5.44), (5.45) is continuous, by using [18, Lemma 2] and by substituting (5.46) into (5.44), we derive the well-defined average of the complete dynamics:

$$\begin{bmatrix} \dot{\boldsymbol{u}} \\ \dot{\boldsymbol{z}} \\ \dot{\lambda} \\ \dot{w} \\ \dot{k} \\ \dot{s} \\ \dot{\zeta} \end{bmatrix} = \begin{bmatrix} \bar{\varepsilon}\tilde{\boldsymbol{\nu}}\tilde{\boldsymbol{\varepsilon}}\left(-\boldsymbol{u} + \boldsymbol{z} - \Gamma(\zeta + \nabla g(\boldsymbol{u})^\top \lambda)\right) \\ \bar{\varepsilon}\tilde{\boldsymbol{\nu}}\tilde{\boldsymbol{\varepsilon}}(-\boldsymbol{z} + \boldsymbol{u}) \\ \bar{\varepsilon}\tilde{\nu}_0\tilde{\varepsilon}_0 \,\text{diag}(\lambda)(g(\boldsymbol{u}) - \lambda + w) \\ \bar{\varepsilon}\tilde{\nu}_0\tilde{\varepsilon}_0(-w + \lambda) \\ \frac{1}{2}\bar{\varepsilon}\tilde{\nu}_0\tilde{\varepsilon}_0 c(I+S)S^2 \\ \boldsymbol{0} \\ \tilde{\boldsymbol{\nu}}(-\zeta + F(\boldsymbol{u}) + \mathcal{O}(\bar{a})) \end{bmatrix}. \tag{5.47}$$

The system in (5.47) is an $\mathcal{O}(\bar{a})$ perturbed version of:

$$\begin{bmatrix} \dot{\boldsymbol{z}} \\ \dot{\boldsymbol{u}} \\ \dot{w} \\ \dot{\lambda} \\ \dot{k} \\ \dot{s} \\ \dot{\zeta} \end{bmatrix} = \begin{bmatrix} \bar{\varepsilon}\tilde{\boldsymbol{\nu}}\tilde{\boldsymbol{\varepsilon}}(-\boldsymbol{z} + \boldsymbol{u}) \\ \bar{\varepsilon}\tilde{\boldsymbol{\nu}}\tilde{\boldsymbol{\varepsilon}}\left(-\boldsymbol{u} + \boldsymbol{z} - \Gamma(\zeta + \nabla g(\boldsymbol{u})^\top \lambda)\right) \\ \bar{\varepsilon}\tilde{\nu}_0\tilde{\varepsilon}_0(-w + \lambda) \\ \bar{\varepsilon}\tilde{\nu}_0\tilde{\varepsilon}_0 \,\text{diag}(\lambda)(g(\boldsymbol{u}) - \lambda + w) \\ \frac{1}{2}\bar{\varepsilon}\tilde{\nu}_0\tilde{\varepsilon}_0 c(I+S)S^2 \\ \boldsymbol{0} \\ \tilde{\boldsymbol{\nu}}(-\zeta + F(\boldsymbol{u})) \end{bmatrix}. \tag{5.48}$$

For sufficiently small $\bar{\varepsilon}$, the system in (5.48) is in singular perturbation form with dynamics ζ acting as fast dynamics. The boundary layer dynamics are given by

$$\dot{\zeta}_{\text{bl}} = \tilde{\boldsymbol{\nu}}\left(-\zeta_{\text{bl}} + F(\boldsymbol{u}_{\text{bl}})\right) \tag{5.49}$$

For each fixed $\boldsymbol{u}_{\text{bl}}$, $\{F(\boldsymbol{u}_{\text{bl}})\}$ is a uniformly globally exponentially stable equilibrium point of the boundary layer dynamics. By [79, Exm. 1], it holds that the system in (5.48) has a well-defined average system given by

$$\begin{bmatrix} \dot{\boldsymbol{z}} \\ \dot{\boldsymbol{u}} \\ \dot{w} \\ \dot{\lambda} \\ \dot{k} \\ \dot{s} \end{bmatrix} = \begin{bmatrix} \tilde{\boldsymbol{\nu}}\tilde{\boldsymbol{\varepsilon}}(-\boldsymbol{z} + \boldsymbol{u}) \\ \tilde{\boldsymbol{\nu}}\tilde{\boldsymbol{\varepsilon}}\left(-\boldsymbol{u} + \boldsymbol{z} - \Gamma(F(\boldsymbol{u}) + \nabla g(\boldsymbol{u})^\top \lambda)\right) \\ \tilde{\nu}_0\tilde{\varepsilon}_0(-w + \lambda) \\ \tilde{\nu}_0\tilde{\varepsilon}_0 \,\text{diag}(\lambda)(g(\boldsymbol{u}) - \lambda + w) \\ \frac{1}{2}\tilde{\nu}_0\tilde{\varepsilon}_0 c(I+S)S^2 \\ \boldsymbol{0} \end{bmatrix}. \tag{5.50}$$

To prove that the system in (5.50) renders the set $\mathcal{A} \times \mathcal{K}^q \times S^q$ UGAS for restricted dynamics, we consider the following Lyapunov function candidate:

$$\begin{aligned} V(\xi, \omega^*) &= \tfrac{1}{2}\|\boldsymbol{u} - \boldsymbol{u}^*\|^2_{(\tilde{\boldsymbol{\nu}}\tilde{\boldsymbol{\varepsilon}}\Gamma)^{-1}} + \tfrac{1}{2}\|\boldsymbol{z} - \boldsymbol{u}^*\|^2_{(\tilde{\boldsymbol{\nu}}\tilde{\boldsymbol{\varepsilon}}\Gamma)^{-1}} \\ &+ \tfrac{1}{2\tilde{\nu}_0\tilde{\varepsilon}_0}\|w - \lambda^*\|^2 + \sum_{j\in\mathcal{Q}} \tfrac{1}{\tilde{\nu}_0\tilde{\varepsilon}_0 k_j}\left(\lambda_j - \lambda_j^* - \lambda_j^* \log\left(\tfrac{\lambda_j}{\lambda_j^*}\right)\right). \end{aligned} \tag{5.51}$$

The convergence proof is equivalent to the proof of Theorem 5.13 and is omitted. We restrict the flow and jump sets as $C \cap \mathfrak{B}$ and $D \cap \mathfrak{B}$, respectively.

Next, by [79, Thm. 2, Exm. 1], the dynamics in (5.48) render the set $\mathcal{A} \times \mathcal{K}^q \times \mathcal{S}^q \times \mathbb{R}^m$ SGPAS as $(\bar{\varepsilon} \to 0)$. As the right-hand side of the equations in (5.48) is continuous, the system is a well-posed hybrid dynamical system [94, Thm. 6.30] and therefore the $O(\bar{a})$ perturbed system in (5.47) renders the set $\mathcal{A} \times \mathcal{K}^q \times \mathcal{S}^q \times \mathbb{R}^m$ SGPAS as $(\bar{\varepsilon}, \bar{a}) \to 0$ [82, Prop. A.1]. By noticing that the set $\mathbb{S}^m$ is UGAS under oscillator dynamics in (5.45) that generate a well-defined average system in (5.47), and by averaging results in [18, Lemma 2], we obtain that the dynamics in (5.16b) make the set $\mathcal{A} \times \mathcal{K}^q \times \mathcal{S}^q \times \mathbb{R}^m \times \mathbb{S}^m$ SGPAS as $(\bar{\varepsilon}, \bar{a}, \bar{v}) \to 0$ for the restricted flow and jump sets. Furthermore, by [82, Prop. A.1.], HDS $((C \cap \mathfrak{B}) \times \mathbb{R}^m \times \mathbb{S}^m), (D \cap \mathfrak{B}) \times \mathbb{R}^m \times \mathbb{S}^m, F_0, G_0)$ is structurally robust.

6

Application to distortion reduction in photovoltaic current

The battle is at its height – wear my armor and beat my war drums. Do not announce my death.

Admiral Yi Sun-Shin

Everything is at stake. I hope they will succeed, and me with them, and then the people too. Victory is close, God willing, B&H will be ours. I feel like I can accomplish what we envisioned. May I have strength and luck. I've invested everything. The power went out. Good luck!

Brigadier General Izet Nanić

In this chapter, we propose a novel approach to minimize the effects of small duty cycle perturbations, due to extremum seeking control (ESC), on the output current of a photovoltaic (PV) cell array connected to the electrical grid. Specifically, we formulate a bilevel optimization problem that incorporates power maximization and current quality objectives. Next, using monotone operator theory, we show how to solve the problem via optimized ESC. Finally, we test the effectiveness of the proposed approach on a numerical simulation example.

This chapter is partly based on S. Krilašević and S. Grammatico. "Distortion reduction in photovoltaic output current via optimized extremum seeking control". In: *2023 21st European Control Conference (ECC)* (June 2023).

6.1 Introduction

Photo-voltaic (PV) cells are perhaps the most popular green energy source due to their ease of installation and low cost. In fact, future houses will all likely have solar panels on their roof so that each house will be capable of producing energy and selling it to the grid. Thus, maximal exploitation of this technology is of the outermost importance.

The typical setup is with several PV cells connected in series or in parallel; see [99], [100], [101], [102] for alternative configurations. In the simplest one-stage typology, a series of PV cells is connected via a DC to AC inverter to the grid. The inverter is controlled via a PWM signal to either regulate the output current [103], [104], the DC-link voltage [105], [106], or used for maximum power point tracking (MPPT) [107]. The low complexity of this typology makes it easy and cheap to implement. Still, on the other hand, it has a significant drawback whenever some of the cells are not irradiated as the others, since in that case, the power characteristic contains local maxima that MPPT algorithms cannot deal with [100]. This is a consequence of the fact that in the simplest setups, the cells share either the same voltage or the same current. Thus, different typologies have been proposed that solve such an issue, the most popular being the two-stage typology shown in Figure 6.1, where each module has its own DC to DC converter that decouples the module's voltage and current from the other modules.

Unsurprisingly, MPPT for PV cells has been studied extensively, and many algorithms have been proposed, such as the perturb and observe (P&O) [108], [109], incremental conductance [110], hill climbing [111] and other non-PV specific techniques like ripple correlation control [112], [113], model predictive control and extremum seeking control, [114]. In practice, it has been observed that ESC algorithms exhibit better performance than more traditional methods [115]. Since the previously mentioned algorithms are mostly zeroth-order algorithms, they necessarily introduce some noise or oscillations into the system to estimate the gradient direction and, in turn, maximize the power output. In general, the effect of these perturbations on the quality of the generated electrical power remains an open research topic. Although the source of the distortions did not originate from an ESC algorithm, authors in [116] propose an ESC algorithm to reduce harmonic distortions in naval vessels. Distortion reduction has been addressed in a limited number of cases for non-electronic systems. One example is in the field of oil extraction, where a dither signal cost function is minimized during the sampling period to obtain minimizing amplitudes for the next sampling period, as proposed in [11]. Building on this approach, the authors of [24] utilize the extremum seeking algorithm to minimize distortions and, unlike [11], demonstrate semi-global practical stability.

Based on our work in [84] and the previous Chapter, we propose a new approach to solve the maximum power point tracking problem, which not only maximizes power output but also reduces distortions in the output current caused by the control algorithm itself (§ 6.2). This is achieved through a bilevel optimization process. Firstly, we determine the input that maximizes power output. Then, we identify perturbation amplitudes that minimize current distortions with respect to the optimal inputs. We then describe the models we used for the PV cells and power electronics in our simulations (§ 6.3). Subsequently, we use a modified version of the algorithm in [84] on a simulation example without requiring any additional sensors or measurements and compare it to the standard implementation without distortion reduction (§ 6.4). For this particular example, our results demonstrate

the reduction in total harmonic distortion (THD), which can cause various undesired effects such as heating in the PV system and load, mal-operation of electronic equipment, incorrect readings on meters, and communication interference [117].

6.2 Maximum power point tracking and distortion reduction in photovoltaic systems

6.2.1 Optimization setup

We consider N PV cells, indexed by $i \in \mathcal{I} := \{1, 2, \dots, N\}$, each with their I-V characteristic represented by a function f_i, connected to the grid via power electronics as in Figure 6.1. Each PV cell has a duty cycle signal $d_i \in [0, 1]$ as input. Let there exist a vector of equilibrium voltages on the outputs of the PV cells denoted as $\boldsymbol{v} := \mathrm{col}((v_i)_{i\in\mathcal{I}})$ that corresponds to a vector of fixed input duty cycles $\boldsymbol{d} := \mathrm{col}((d_i)_{i\in\mathcal{I}})$, for any given $\boldsymbol{d} \in \mathcal{D} := [0, 1]^N$. Thus, let us define the steady-state mapping $\pi : \mathbb{R}^N \to \mathbb{R}^N$ such that $\boldsymbol{v} = \pi(\boldsymbol{d})$. In this paper, we consider two main objectives:

1. Maximize the extracted power

$$P(\boldsymbol{d}) = \frac{V_{\mathrm{grid}} I_{\mathrm{ac}}}{2} = \pi(\boldsymbol{d})^\top f(\pi(\boldsymbol{d})), \tag{6.1}$$

   where $f = \mathrm{col}((f_i)_{i\in\mathcal{I}})$;

2. Reduce the undesired harmonics in the output current, I_{ac} introduced by the maximum power point tracking procedure.

For the first objective, we propose to maximize a utility function $J_{\mathrm{d}}(\boldsymbol{d})$. For the second objective, we consider a function $J_{\mathrm{a}}(\boldsymbol{a}, \boldsymbol{d})$ to be minimized, given a solution for the first objective, where $\boldsymbol{a} := \mathrm{col}((a_i)_{i\in\mathcal{I}}) \in \mathcal{A} := [\underline{a}, \overline{a}]^N$ is the vector perturbation amplitudes. More formally, we propose to solve:

$$\begin{cases} \min\limits_{\boldsymbol{a}\in\mathcal{A}, \boldsymbol{d}^*} J_{\mathrm{a}}(\boldsymbol{a}, \boldsymbol{d}^*) \\ \quad \text{s.t. } \boldsymbol{d}^* \in \operatorname{argmax}\limits_{d\in\mathcal{D}} J_{\mathrm{d}}(\boldsymbol{d}) \end{cases} \tag{6.2}$$

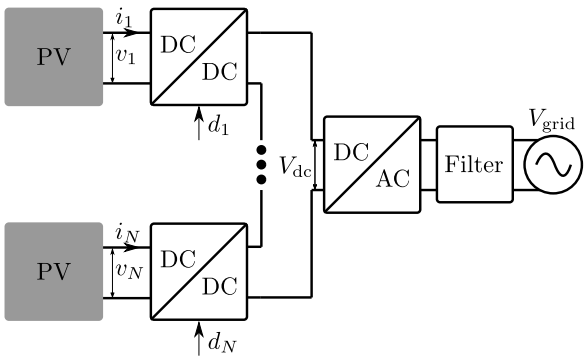

Figure 6.1: Two stage topology for PV arrays.

Let us refer to (6.2) as the bilevel optimization problem of interest here and postulate the convexity assumptions:

Standing Assumption 6.1. *The functions $-J_d(\cdot)$ and $J_a(\cdot, \boldsymbol{d})$ in (6.2) are convex for every $\boldsymbol{d}$ and differentiable in their arguments.* □

Due to Standing Assumption 6.1, a vector $(\boldsymbol{a}^*, \boldsymbol{d}^*)$ is a solution of (6.2) if and only if it satisfies the KKT optimality conditions, i.e.

$$\mathbf{0} \in \begin{bmatrix} -\nabla J_{\mathrm{d}}(\boldsymbol{d}^*) + \mathrm{N}_D(\boldsymbol{d}^*) \\ \nabla_d J_{\mathrm{a}}(\boldsymbol{a}^*, \boldsymbol{d}^*) + \mathrm{N}_{D^*}(\boldsymbol{d}^*) \\ \nabla_a J_{\mathrm{a}}(\boldsymbol{a}^*, \boldsymbol{d}^*) + \mathrm{N}_{\mathcal{A}}(\boldsymbol{a}^*) \end{bmatrix}, \tag{6.3}$$

where $D^* := \operatorname*{argmax}_{g \in D} J_{\mathrm{d}}(\boldsymbol{g})$.
The problem of finding zeros in (6.3) is monotone inclusion problem, and many solution algorithms exist. Now we move on to identifying utility and cost functions for our case study.

6.2.2 Power maximization

To maximize the power output in (6.1), it is common to use a zeroth-order algorithm, e.g. an MPPT algorithm, since the gradient of the total power is hard, if not impossible, to compute due to the complex relations and the large number of, possibly unknown, parameters. We formulate our power utility function as

$$J_{\mathrm{d}}(\boldsymbol{d}) = P(\boldsymbol{d}) + \sum_{i=1}^{N} \log_{p_1}(d_i(1-d_i)). \tag{6.4}$$

The cost function in (6.4) consists of the power output in (6.1) and a barrier function term to satisfy the constraints on the duty cycles, $d_i \in [0,1]$, at all times.

6.2.3 Reduction of the undesired harmonics

While it is known how to achieve the first objective via an MPPT algorithm [118], it is not obvious how the second one can be attained or what exactly is the effect of these algorithms on the output current. To better understand this phenomenon, we analyze the power flow of the system. If the energy losses on the electronics circuits are small, for the average power, we have as in (6.4) $P(\boldsymbol{d}) = P_{\mathrm{ac}} = \frac{V_{\mathrm{grid}} I_{\mathrm{ac}}}{2}$. The vector of duty cycle inputs $\boldsymbol{d}$ consists of a constant or slowly varying component $\overline{\boldsymbol{d}}$ and fast and small perturbations used in the MPPT learning, $\boldsymbol{\mu}$, i.e., $\boldsymbol{d} = \overline{\boldsymbol{d}} + \boldsymbol{\mu}$. It follows that

$$P(\boldsymbol{d}) = \frac{V_{\mathrm{grid}} I_{\mathrm{ac}}}{2} \simeq P(\overline{\boldsymbol{d}}) + \nabla P(\overline{\boldsymbol{d}})^\top \boldsymbol{\mu}. \tag{6.5}$$

As V_{grid} can be assumed to be constant, perturbations in the duty cycle cause perturbations in the amplitude of the output current. Thus, we conclude from (6.5) that by minimizing

the amplitude of the first order term

$$\nabla P(\overline{\boldsymbol{d}})^{\top}\boldsymbol{\mu} = \sum_{i=0}^{N} \frac{\partial P}{\partial d_i}(\overline{\boldsymbol{d}})\mu_i, \tag{6.6}$$

we contribute to the reduction of the additional harmonics caused by the MPPT algorithm. If we design the perturbations as sinusoidal, then there are many degrees of freedom and approaches we can use to minimize the amplitude of (6.6). Similarly to [23, §5.2], we group PV cells into pairs (i, j), and for each pair, select perturbation signals that are in antiphase, i.e.,

$$\begin{aligned} \mu_i(t) &= a_i \sin(\omega t) \\ \mu_j(t) &= -a_j \sin(\omega t). \end{aligned} \tag{6.7}$$

Thus, we fix frequencies and phase shifts while we leave the amplitudes as decision variables that are dynamically adapted to minimize the term in (6.6). We adopt the cost function

$$\begin{aligned} J_{\mathrm{a}}(\boldsymbol{a}, \overline{\boldsymbol{d}}) = &\frac{l}{2} \sum_{i=1}^{\frac{N}{2}} \left(\frac{\partial P}{\partial d_{2i}}(\overline{\boldsymbol{d}}) a_{2i} - \frac{\partial P}{\partial d_{2i-1}}(\overline{\boldsymbol{d}}) a_{2i-1} \right)^2, \\ &- \sum_{i=1}^{N} \log_{p_2}((a_i - \underline{a})(\overline{a} - a_i)), \end{aligned} \tag{6.8}$$

where $l > 0$, $\underline{a}$ and $\overline{a}$ are the minimum and maximum perturbation amplitude, respectively, such that $0 < \underline{a} < \overline{a}$.

6.2.4 Bilevel optimization formulation

For solving (6.2), we use a bilevel formulation. Considering that (6.4) and (6.8) satisfy certain properties, it is possible to simplify the expression in (6.3). Specifically, since (6.4) is strictly concave, $\mathcal{D}^*$ is a singleton, and we can leave out the middle row from (6.3) due to the fact that the normal cone of a single point can have any direction, thus always satisfying the inclusion. Furthermore, by noticing that (6.4) and (6.8) are not defined beyond our sets of interest, $\mathcal{D}$ and $\mathcal{A}$, we can also leave out the normal cone operators. Therefore, we obtain:

$$\mathbf{0} \in F(\boldsymbol{d}^*, \boldsymbol{a}^*) := \begin{bmatrix} -\nabla J_{\mathrm{d}}(\boldsymbol{d}^*) \\ \nabla_a J_{\mathrm{a}}(\boldsymbol{a}^*, \boldsymbol{d}^*) \end{bmatrix}. \tag{6.9}$$

We note that the last expression is equivalent to the optimality conditions associated with a two player Nash equilibrium game, where $F(\boldsymbol{d}^*, \boldsymbol{a}^*)$ is equivalent to the pseudogradient mapping of a game where player one has cost function $-J_{\mathrm{d}}$ and player two has a cost function J_{a}.

Remark 6.2. *A naïve approach for finding the solutions of (6.2) would be to define a weighted sum*

$$J_{naïve}(\overline{\boldsymbol{d}},\boldsymbol{a}) = -\alpha J_d(\overline{\boldsymbol{d}}) + \beta J_a(\overline{\boldsymbol{d}},\boldsymbol{a}),\ \textit{for some } \alpha,\beta>0, \tag{6.10}$$

and compute a solution via a zeroth-order algorithm. However, $(\boldsymbol{d}^*,\boldsymbol{a}^*)$ *is not necessarily contained in* $\operatorname{argmin} J_{naïve}(\overline{\boldsymbol{d}},\boldsymbol{a})$.

6.2.5 Proposed solution algorithm

Since the zero-finding problem in (6.9) has the same structure of a Nash game, we propose to use a modified version of the algorithm in [84] to find the maximum power point and simultaneously reduce the oscillations. Similarly, as in the "Fixed demand problem" example given in [84], we use the real values of the partial gradients in places where they can be computed exactly and do not filter them through a first-order filter. We choose this algorithm because ESC algorithms perform better than traditional MPPT methods [115], and only this ESC algorithm can handle merely monotone operators without technical restrictions.

To adopt the algorithm in [84], Standing Assumption 2 in [84] must hold as stated next.

Lemma 6.3. *The pseudogradient* $F(\boldsymbol{d},\boldsymbol{a})$ *in (6.9) is monotone.* □

Proof. By definition of monotonicity it has to hold

$$\begin{bmatrix} -\nabla J_{\mathrm{d}}(\boldsymbol{d}) + \nabla J_{\mathrm{d}}(\boldsymbol{g}) \\ \nabla_{\boldsymbol{a}} J_{\mathrm{a}}(\boldsymbol{a},\boldsymbol{d}) - \nabla_{\boldsymbol{a}} J_{\mathrm{a}}(\boldsymbol{v},\boldsymbol{g}) \end{bmatrix}^{\top} \begin{bmatrix} \boldsymbol{d}-\boldsymbol{g} \\ \boldsymbol{a}-\boldsymbol{v} \end{bmatrix} \geq \boldsymbol{0}. \tag{6.11}$$

For twice differentiable cost functions, instead of (6.11), we equivalently have that

$$\begin{bmatrix} -\nabla^2 J_{\mathrm{d}}(\boldsymbol{d}) & \boldsymbol{0} \\ \nabla^2_{\boldsymbol{ad}} J_{\mathrm{a}}(\boldsymbol{a},\boldsymbol{d}) & \nabla^2_{\boldsymbol{aa}} J_{\mathrm{a}}(\boldsymbol{a},\boldsymbol{d}) \end{bmatrix} \succcurlyeq 0.$$

Due to the triangular structure of the matrix, it is sufficient to show only

$$\nabla^2 J_{\mathrm{d}}(\boldsymbol{d}) \preccurlyeq 0 \text{ and} \tag{6.12}$$

$$\nabla^2_{\boldsymbol{aa}} J_{\mathrm{a}}(\boldsymbol{a},\boldsymbol{d}) \succcurlyeq 0. \tag{6.13}$$

Since $J_{\mathrm{d}}(\boldsymbol{d})$ is a concave function by Standing Assumption 6.1, Equation (6.12) holds. Furthermore, we have that $\nabla^2_{\boldsymbol{aa}} J_{\mathrm{a}}(\boldsymbol{d},\boldsymbol{a}) \coloneqq \operatorname{diag}\left(\mathcal{J}_{1,2},\mathcal{J}_{3,4},\dots,\mathcal{J}_{N-1,N}\right)$, where

$$\begin{aligned} \mathcal{J}_{i,j} = &\begin{bmatrix} \left(\frac{\partial P}{\partial d_i}(\boldsymbol{d})\right)^2 & -\frac{\partial P}{\partial d_i}(\boldsymbol{d})\frac{\partial P}{\partial d_j}(\boldsymbol{d}) \\ -\frac{\partial P}{\partial d_i}(\boldsymbol{d})\frac{\partial P}{\partial d_j}(\boldsymbol{d}) & \left(\frac{\partial P}{\partial d_j}(\boldsymbol{d})\right)^2 \end{bmatrix} \\ &+ \begin{bmatrix} \frac{(a_i-\overline{a})^{-2}+(a_i-\underline{a})^{-2}}{\log(p_2)} & 0 \\ 0 & \frac{(a_j-\overline{a})^{-2}+(a_j-\underline{a})^{-2}}{\log(p_2)} \end{bmatrix}. \end{aligned} \tag{6.14}$$

First addend matrix in (6.14) is positive semidefinite while the second one is positive definite. As $\nabla^2_{\boldsymbol{aa}} J_{\mathrm{a}}(\boldsymbol{d},\boldsymbol{a})$ is a block diagonal matrix composed of positive semidefinite matrices (6.14), it follows that it also is positive semidefinite. ■

Thus, our problem satisfies the necessary assumptions. In the next section, we present the details of the considered PV cell model and the power electronics.

6.3 Photo-voltaic power extraction model

6.3.1 Photo-voltaic cell

Let us use the standard PV cell model proposed in [119], which consists of an ideal current source connected in series with a resistor R_s and in parallel with a diode and a resistor R_p, as seen in Figure 6.2. The current of the source i_s is a function of irradiance S and temperature T

$$i_s = (I_s + k_i(T - T_r))\left(\frac{S}{1000}\right), \tag{6.15}$$

where I_S is the reference short-circuit current, T_r is the reference temperature and k_i is the short-circuit temperature coefficient. The diode's I-V characteristic is given by

$$i_d = i_0\left(\exp\left(\frac{v_d}{\mathrm{N}V_t}\right) - 1\right), \tag{6.16}$$

$$i_0 = I_0\left(\frac{T}{T_r}\right)^3 \exp\left[\frac{E_g}{\mathrm{N}V_t}\left(\frac{T}{T_r} - 1\right)\right], V_t = \left(\frac{kT}{q}\right), \tag{6.17}$$

where I_0 is the diode reference reverse saturation current, E_g is the semiconductor bandgap voltage, N is the emission coefficient, V_t is the thermal cell voltage, $k = 1.38 \times 10^{-23}\frac{J}{K}$ is the Boltzman constant, $q = 1.602 \times 10^{-19}C$ is the electron charge. When n_s of PV cells are connected in series, the terminal current is given by

$$i = i_s - i_0\left[\exp\left(\frac{\frac{v}{n_s} + iR_s}{\mathrm{N}V_t}\right) - 1\right] - \left[\frac{\left(\frac{v}{n_s} + iR_s\right)}{R_p}\right]. \tag{6.18}$$

Equation (6.18) relates the current i to the voltage v and is seen in Figure 6.3 for different temperature values T and constant irradiance S. For constant T, S we write the relation as

$$i = f(v). \tag{6.19}$$

It follows that the power to voltage curve is a concave function parametrized by S and T. Due to the fact that the temperature and irradiance conditions are changing over time, and

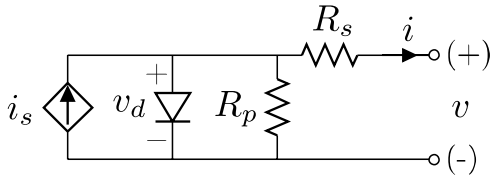

Figure 6.2: PV cell model.

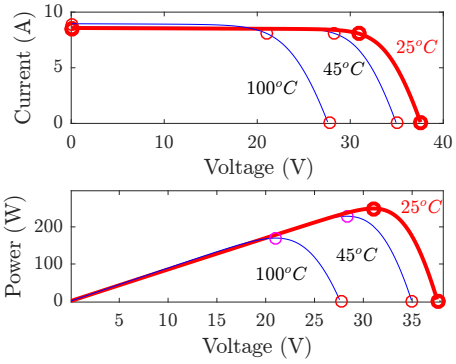

Figure 6.3: Different PV cell I-V and P-V characteristics for different temperatures and fixed irradiance.

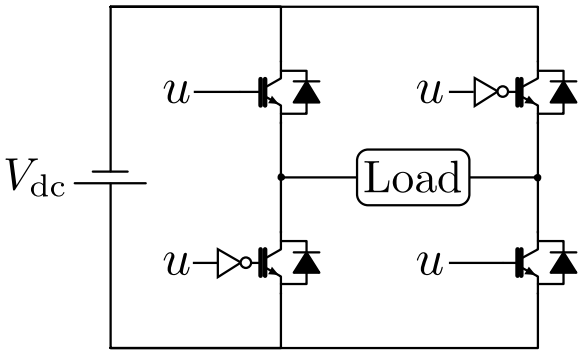

Figure 6.4: A single-phase H-bridge inverter scheme.

the panel themselves deteriorate over time, it is not possible to determine a priori a voltage for which the maximum power is achieved. This justifies using zeroth-order optimization methods to find the voltage that maximizes the power. In the simplest case where we directly connect a PV cell array to a load, we will not utilize the maximum available power as the voltage will settle in an equilibrium dictated by the circuit structure, regardless of the power maximum. Instead, connecting the array to the AC grid, the case we explore in this chapter, introduces additional complexity as we have to condition the output current to be sinusoidal and in phase with the grid voltage. Therefore, some additional electronics are required to utilize the maximum available power.

6.3.2 Power electronics

To transfer the energy from a DC source to the AC grid, it is necessary to employ an AC inverter circuit, like the one in Figure 6.4. By proper switching of the transistors, it is possible to achieve an approximation of various output signals, like the desired sinusoid. If connected to the grid, the DC voltage on the right of the circuit needs to be higher than

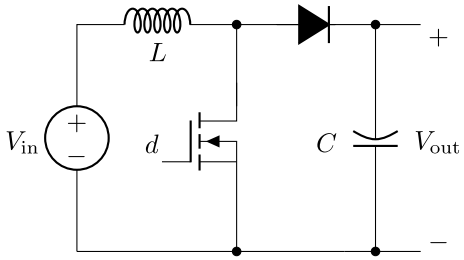

Figure 6.5: Simplified electric circuit of a boost converter.

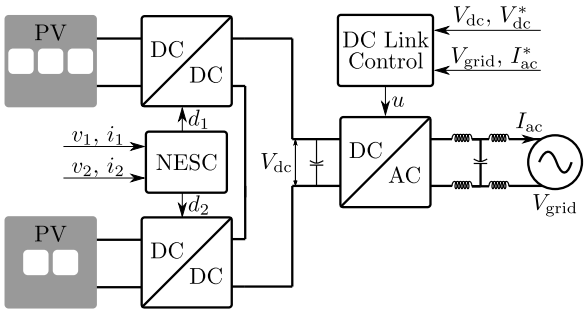

Figure 6.6: Schematic of the simulation example. For the DC/DC converter, we use a boost converter as in Figure 6.5 without the capacitor. The DC/AC converter is an H-bridge as in Figure 6.4.

the maximum amplitude of the AC voltage, or there needs to be an AC to AC transformer to raise the voltage.

Various typologies exist for connecting PV modules to the grid, each with their pros and cons. Here, we choose the two-stage typology, as in Figure 6.1, because it solves the issue of local maxima by adding DC to DC converters between the PV cells and the DC to AC inverter [100], [99]. The DC-link voltage and individual cell voltages are decoupled, hence it is possible to use MPPT techniques on each of them. It is important to mention that achieving the overall maximum power is not always possible even with this two-layer typology [120]. Similarly, as with the inverter, the DC to DC converters are controlled via PWM signals. The standard DC to DC boost converter used in PV applications can be seen in Figure 6.5. For sufficiently high switching frequencies, the output voltage and the current of the converter are given by

$$v_{\text{out}} = \frac{v_{\text{in}}}{1-d}$$
$$i_{\text{out}} = i_{\text{in}}(1-d).$$

For PV cells in series and a fixed DC-link voltage V_{DC}, we have that [121]:

$$\sum_{j=1}^{N} \frac{v_j}{1-d_j} = V_{\mathrm{dc}}, \tag{6.20}$$

$$(1-d_j) f_j(v_j) = (1-d_k) f_k(v_k), \text{for all } j,k \in \mathcal{I}. \tag{6.21}$$

The mapping π gives a vector $\boldsymbol{v}$ such that equations (6.20), (6.21) are satisfied for a given $\boldsymbol{d}$.

6.4 Numeric simulations

When applied to our problem, the algorithm in [84] reads as follows:

$$\begin{bmatrix} \dot{\boldsymbol{z}} \\ \dot{\boldsymbol{d}} \\ \dot{\boldsymbol{b}} \\ \dot{\boldsymbol{a}} \\ \dot{\boldsymbol{\xi}} \\ \dot{\boldsymbol{\mu}} \end{bmatrix} = \begin{bmatrix} \gamma\varepsilon(-\boldsymbol{z}+\boldsymbol{d}) \\ \gamma\varepsilon(-\boldsymbol{d}+\boldsymbol{z}+k\boldsymbol{\xi}+\boldsymbol{\lambda}) \\ \gamma\varepsilon(-\boldsymbol{b}+\boldsymbol{a}) \\ \gamma\varepsilon(-\boldsymbol{a}+\boldsymbol{b}-\zeta(\boldsymbol{a},\boldsymbol{\xi})) \\ \gamma\left(-\boldsymbol{\xi}+2A_{\mathrm{inv}}P(\boldsymbol{d}+A\mathbb{D}\boldsymbol{\mu})\mathbb{D}^m\boldsymbol{\mu}\right)) \\ 2\pi\mathcal{R}\boldsymbol{\mu} \end{bmatrix}, \tag{6.22}$$

where $\boldsymbol{z},\boldsymbol{b} \in \mathbb{R}^N$ are auxiliary states, $\mu_i \in \mathbb{S}^{m_i}$ are the oscillator states, $\boldsymbol{\xi} \in \mathbb{R}^N$ are the filtering states, $\varepsilon,\gamma,k \geq 0$, $\mathcal{R} := \mathrm{diag}\left(\left(\left[\begin{smallmatrix} 0 & -\kappa_i \\ \kappa_i & 0 \end{smallmatrix}\right]\right)_{i\in\mathcal{I}}\right)$, $\boldsymbol{\lambda} := \mathrm{col}\left(\left(\frac{1-2d_i}{d_i(1-d_i)\log p_i}\right)_{i\in\mathcal{I}}\right)$, $\zeta(\boldsymbol{a},\boldsymbol{\xi}) := \mathrm{col}\left(l(\xi_i a_i - \xi_j a_j)\xi_i - \left(\frac{1-2a_i}{a_i(1-a_i)\log p_i}\right)_{i\in\mathcal{I}, j=-1+2\bmod_2(i)}\right)$, $\kappa_i > 0$ for all i and $\kappa_i \neq \kappa_j$ for all i apart for the paired up ones, $\mathbb{D} \in \mathbb{R}^{N\times 2N}$ is a matrix that selects every odd row from vector of size $2N$, $A := \mathrm{diag}\left(((-1)^i a_i)_{j\in\mathcal{I}}\right)$ and $A_{\mathrm{inv}} := \mathrm{diag}\left(\left(\frac{1}{a_i}\right)_{j\in\mathcal{I}}\right)$.

Differently from [84], parts of ∇J_{d} that are known are not estimated, and the partial gradient ∇J_{a} is not estimated and filtered. We see that it holds that $\zeta(\boldsymbol{a},\nabla P(\boldsymbol{d})) = \nabla_a J_{\mathrm{a}}(\boldsymbol{a},\boldsymbol{d})$. Thus, after two time scale separations, it is possible to show that the reduced system will have the form as in [84, Equ. 18]. The rest of the proof would be the same. Since this is not the focus of this chapter, it is omitted.

In our simulation setup, we have two PV modules connected in series, each with a DC to DC converter. The first PV module consists of three PV cells, while the second module consists of two PV cells connected in a series. The PV array is connected to a DC to AC inverter, which has its controller that keeps the DC-link voltage constant and controls the output current such that it is sinusoidal and in phase with the AC grid voltage. A schematic representation is given in Figure 6.6.

We conduct two sets of simulations in Simulink. In the first set, we only have one cost function (6.4), and for the MPPT algorithm, we use the algorithm in (6.22) with constant amplitudes $\boldsymbol{a}$, i.e., without the amplitude adaptation. In the second set, we use our proposed algorithm with two cost functions. The following parameters were used: $\gamma = 0.1$, $\epsilon = 10$, $\kappa_1 = \kappa_2 = 1000$, $\underline{a} = 0.01$, $\overline{a} = 0.1$, $p_1 = 1.0101$, $p_2 = 2.2\times 10^4$, $k = 10$, $V_{\mathrm{dc}^*} = 400$, $f_c = 20\,kHz$ is the frequency of the DC/DC converter duty cycle signals, $f_i = 3780\,Hz$ is

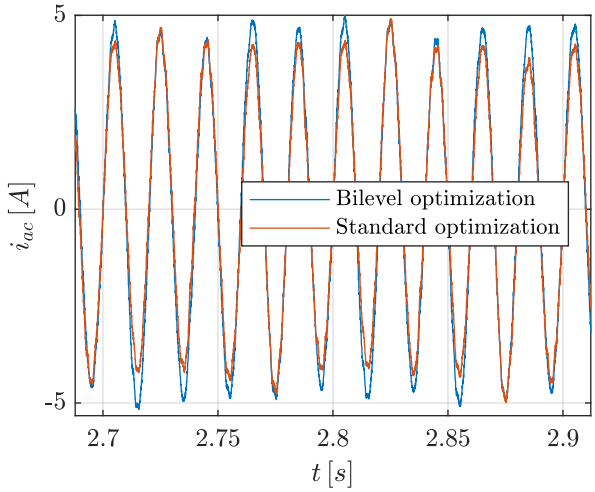

Figure 6.7: Comparison of the current outputs at a specific time interval.

the frequency of the DC/AC inverter duty cycle signal, $d_1(0) = d_2(0) = z_1(0) = z_2(0) = 0.5$, $a_1(0) = a_2(0) = b_1(0) = b_2(0) = c$, where $c = 0.01$ for the first type of simulations and $c = 0.015$ for the other.

In Figure 6.7, we can see the output current I_{ac} for both cases at a specific time interval. We note that the current in the standard optimization case appears to have a lower frequency harmonic component. The output current from our proposed approach also has lower total harmonic distortion (THD), defined as

$$THD = \frac{\sqrt{I_2^2 + I_3^2 + I_4^2 + \cdots}}{I_1}, \tag{6.23}$$

where I_j is the j-th harmonic of the output current I_{ac}, as shown in Figure 6.8. Furthermore, our proposed approach has better active power utilization, highlighted in Figure 6.9. It can be reasoned that due to the reduction of distortions in the output current, AC power output has been increased.

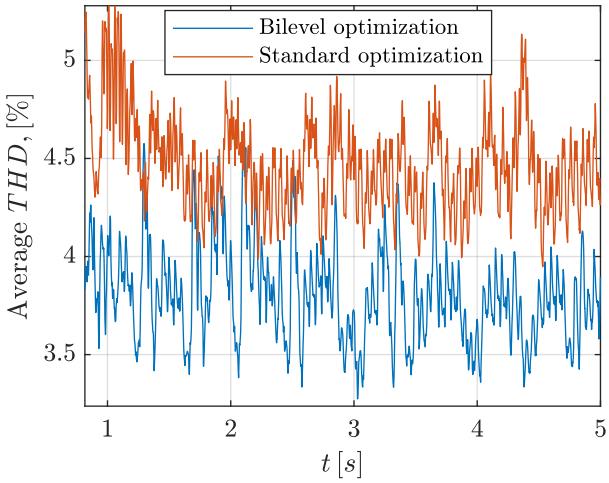

Figure 6.8: Total harmonic distortion averaged over two oscillation periods.

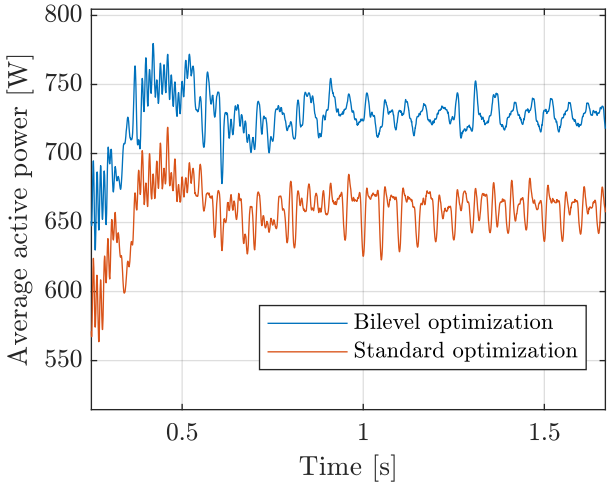

Figure 6.9: Active power transferred to the electric grid averaged over two oscillation periods.

6.5 Conclusion

The quality of the output current of a PV array can be improved via bilevel optimization and optimized extremum seeking. For future research, the robustness of the approach should be tested for different operating conditions, typologies, electrical component values, and frequencies of the duty cycle signals.

6.6 Acknowledgments

We want to thank Prof. Aleksandra Lekić for fruitful discussions on power electronics for PV systems.

III

Hybrid output feedback for equilibrium seeking

7

Averaging for discrete-time equilibrium seeking

In Bosnia, the church bell never disturbed the voice of the muezzin.

Husein kapetan Gradaščević

The greatest misfortune is that we grew fond of this dead end and do not want to abandon it. But everything has a price, and so does our love.

Meša Selimović

In this chapter, we present an averaging technique applicable to the design of zeroth-order Nash equilibrium seeking algorithms. First, we propose a multi-timescale discrete-time averaging theorem that requires only that the equilibrium is semi-globally practically stabilized by the averaged system while also allowing the averaged system to depend on "fast" states. Furthermore, sequential application of the theorem is possible, which enables its use for multi-layer algorithm design. Second, we apply the aforementioned averaging theorem to prove semi-global practical convergence of the zeroth-order information variant of the discrete-time projected pseudogradient descent algorithm in the context of strongly monotone, constrained Nash equilibrium problems. Third, we use the averaging theory to prove the semi-global practical convergence of the asynchronous pseudogradient descent algorithm to solve strongly monotone unconstrained Nash equilibrium problems. Lastly, we apply the proposed asynchronous algorithm to the connectivity control problem in multi-agent systems.

This chapter is partly based on S. Krilašević and S. Grammatico. "A discrete-time averaging theorem and its application to zeroth-order Nash equilibrium seeking". In: arXiv:2302.04854 (Feb. 2023). arXiv:2302.04854 [cs, eess, math]. DOI: 10.48550/arXiv.2302.04854.

7.1 Introduction

Given a complex dynamical system, averaging techniques are used to construct a simpler system, called the *averaged system*, that is easier to analyze than the given one. Ideally, the averaged system should satisfy certain properties so that it is possible to infer stability properties of the original system based on the averaged one. These techniques are used extensively in extremum seeking results, in continuous-time systems [12], [7], [122], discrete-time systems [13], [8], and hybrid systems [17], [82].

Literature review: Discrete-time averaging techniques have received intense attention over the years. In [123], the authors show that the original dynamics render the equilibrium exponentially stable under the assumption of exponential stability of the equilibrium for the averaged dynamics. Furthermore, they prove a similar result with similar assumptions for a mixed time-scale system where the fast dynamics converge to zero. The requirement for exponential stability is relaxed in [124] to just semi-global practical asymptotic stability, for single time-scale systems. Furthermore, the authors include noise in their analysis and provide input-to-state stability results. In [125], the authors provide upper bounds for the time-scale separation parameter in the case of linear switched averaged systems by using a time-delay approach and similar assumptions as in [123]. The previously mentioned single time-scale results assume that the jump mapping is time-varying and that this dependence gets “smoothed out" using the averaging technique. Thus, the main source of “perturbations" in the original system is this time dependence. Likewise, it is possible to assume that jump mapping is a function of some stochastic perturbations and that the goal of the averaging is to “smooth out" the dependence on these perturbations. In [126], the authors prove that under certain technical assumptions, the discrete-time stochastic algorithm can be approximated by its continuous counterpart and that equilibrium of the original dynamics is weakly exponentially stable if the equilibrium of the continuous counterpart is exponentially stable.

The usual approach to the design of extremum seeking algorithms consists of choosing a well-behaved full-information gradient-based algorithm in the case of optimization or pseudogradient-based in the case of games, integrated with a (pseudo)gradient zeroth-order information estimation scheme [12], [7], [82], [18]. The produced estimate then replaces the real value of the (pseudo)gradient in the algorithm. A typical estimation technique is that of injecting sinusoidal perturbations into the inputs of a cost function, whose output is then correlated with the same perturbations. Via averaging techniques, it can be proven that this estimation behaves as the (pseudo)gradient, on average. The theory of averaging and singular perturbations for continuous and hybrid systems [78], [79] enables the adaptation of a wide spectrum of algorithms. In [12], the authors adapt the gradient descent algorithm for the zeroth-order information case, together with the additional high-pass and low-pass filters to improve performance. An extremum seeking variant of the pseudogradient descent algorithm used for solving unconstrained games is presented in [7]. Recently, the authors in [18] propose a fixed-time zeroth-order algorithm for solving games based on a similar full-information fixed-time algorithm. An accelerated first-order algorithm has been adapted for optimization problems in [82]. Unfortunately, the same variety of extremum seeking algorithms is not available in discrete time due to the limitations of the discrete-time averaging theory. In [13], the authors prove exponential convergence to the optimum of a quadratic function under the zeroth-order variant of the

gradient descent algorithm with filtering. The authors in [127] prove ultimate boundness in a similar setup where the plant is assumed to be general dynamic nonlinear and the trajectories of the averaged system ultimately bounded. A similar approach is used in [8] to prove convergence to the Nash equilibrium in a game without constraints. In [126], the authors prove stability of its stochastic variant.

On the other hand, zeroth-order methods that use different approaches for gradient estimation appear to be more successful, and a recent overview of optimization methods can be found here [128]. The authors in [129] solve an N-coalition game without local constraints for strongly monotone games by using Gaussian smoothing to estimate the pseudogradient. In contrast, the authors in [130] propose an algorithm for solving cooperative multi-agent cost minimization problems with local constraints, also with Gaussian smoothing. Both papers assume synchronous sampling of the agents, albeit with possible information delay. A similar approach to Gaussian smoothing is the residual feedback estimator that uses a previous evaluation of the cost function for the second point of the pseudogradient approximation, thus reducing the number of cost function samples that need to be taken in one iteration. Using this approach, the authors in [131] adapt two extra-gradient algorithms and prove convergence to the Nash equilibrium in pseudo-monotone plus games for diminishing step sizes and query radiuses. Authors in [19] and [132] estimate the pseudogradient using the idea of continuous action-set learning automaton and prove convergence for strictly monotone games and merely monotone games, respectively, via diminishing step sizes, and Tikhonov regularization.

Asynchronous zeroth-order optimization algorithms have been well studied, and an overview can be found here [133]. For example, the authors in [134] use the residual feedback estimator in an asynchronous gradient decent scheme to prove convergence. In the current state of the art, zeroth-order discrete-time Nash equilibrium seeking algorithms based on averaging use pseudogradient descent without projections, while algorithms based on other methods are more general yet still assume synchronous sampling.

Contribution: Motivated by the above literature and open research problems, to the best of our knowledge, we consider an averaging technique for mixed time-scale discrete-time systems and merely semi-globally practically convergent averaged systems, with the application to the problem of learning Nash equilibria via zeroth-order discrete-time algorithms, in the cases of locally constrained agents, and asynchronous sampling. Specifically, our main technical contributions are summarized next:

- We extend the current results on averaging theory by using a mixed time-scale formulation of the original system and requiring that the averaged systems render the equilibrium set SGPAS, unlike [124, Thm. 2], where a single time-scale, time-variant system is used, and differently from [123, Thm. 2.2.4], [135, Thm. 8.2.28] where exponential stability is needed and the fast subsystem state is assumed to converge to the origin. Furthermore, we allow certain types of additive perturbation dynamics to interfere with the nominal averaging dynamics, and that the averaged jump mapping is a function of the fast states, thus enabling easier *consecutive* application of the averaging theorem and the design of more complex algorithms.

- Enabled by our extended averaging theory, we propose two novel zeroth-order algorithms for game equilibrium seeking in discrete time. The first algorithm solves

the equilibrium in games with local constraints, differently from [8], [129] where agents have no constraints. In contrast, the second one solves the problem in the case where the agents are asynchronous, i.e., the agents do not sample at the same time, nor do they coordinate in any way, differently from [8], [129] where the agents sample synchronously.

7.2 Discrete-time averaging

We consider the following discrete-time system written in hybrid system notation [80, Eq. 1.1, 1.2]

$$\begin{cases} u^+ &= u + \varepsilon G(u,\mu) \\ \mu^+ &= M(u,\mu) \end{cases}, \quad (u,\mu) \quad \in \mathcal{U}\times\Omega. \tag{7.1}$$

where u and μ are the state variables, $\mathcal{U}\subset\mathbb{R}^m$, $\Omega\subset\mathbb{R}^l$, $G:\mathcal{U}\times\Omega\to\mathbb{R}^m$ and $M:\mathcal{U}\times\Omega\to\Omega$ are the state jump functions for the states u and μ respectively, and $\varepsilon>0$ is a small parameter. Furthermore, the mapping G is parametrized by a small parameter $\gamma>0$, i.e., $G=G_\gamma$, but for notational convenience, this dependence is not written explicitly in the equations.

Next, we consider now the trajectories of the state μ oscillate indefinitely and, in turn, create oscillations in the trajectory of the state u. An equivalent system that produces trajectories $\bar{u}$ without oscillations should be easier to analyze. We refer to such systems as averaged systems [123, Eq. 2.2.12], [135, Eq. 8.33], and we focus on those of the following form:

$$\begin{cases} \tilde{u}^+ = \tilde{u} + \varepsilon G_{\text{avg}}(\tilde{u},\tilde{\mu}) \\ \tilde{\mu}^+ = M(\tilde{u},\tilde{\mu}) \end{cases}, \quad (\tilde{u},\tilde{\mu}) \quad \in \mathcal{U}\times\Omega, \tag{7.2}$$

where $G_{\text{avg}}:\mathcal{U}\times\Omega\to\mathbb{R}^m$ and is also parametrized by $\gamma>0$. Unlike [123, Thm. 2.2.4], [135, Thm. 8.2.28], we take into consideration the case where the function G_{avg} depends on the fast state $\tilde{\mu}$, not only on $\tilde{u}$.

To postulate the required relation between the function G and the mapping G_{avg}, we should introduce an auxiliary system that describes the behavior of system (7.1) when the state u is kept constant, i.e., $\varepsilon=0$, the so-called boundary layer system [79, Eq. 6]:

$$\begin{cases} u_{\text{bl}}^+ = u_{\text{bl}} \\ \mu_{\text{bl}}^+ = M(u_{\text{bl}},\mu_{\text{bl}}) \end{cases}, (u_{\text{bl}},\mu_{\text{bl}}) \in \mathcal{U}\times\Omega. \tag{7.3}$$

Thus, a function G_{avg} is called an average of the mapping G with the boundary layer dynamics in (7.2) if the following condition holds true:

Assumption 7.1. *For any compact set $K\subset U$ and any solution $(u_{\text{bl}},\mu_{\text{bl}})$ of (7.2) where u_{bl} is contained in the compact set K, it holds that:*

$$\left\| \frac{1}{N}\sum_{i=0}^{N-1}\left[G(u_{\text{bl}}(i),\mu_{\text{bl}}(i)) - G_{\text{avg}}(u_{\text{bl}}(i),\mu_{\text{bl}}(i))\right] \right\| \leq \sigma(N), \tag{7.4}$$

for some function $\sigma:\mathbb{R}_+\to\mathbb{R}_+$ of class $\mathcal{L}$. □

In plain words, in Assumption 7.1, we postulate that by using more samples over time, our approximation of the mapping G becomes better. Furthermore, let us assume local Lipschitz continuity of the mappings as in [135, Assum. 8.2.13], [124, Eq. 1, Def. 1] and compactness :

Assumption 7.2. *The functions G, M and G_{avg} in (7.1), (7.2) are continuous in their arguments and locally bounded; the mapping G_{avg} is locally Lipschitz continuous in its first argument. The set Ω is compact.* □

The averaging method can be used in unison with other algorithms via time-scale separation. In such cases, often the averaged system does not exponentially or asymptotically stabilize the equilibrium as in [123, Thm. 2.22], [135, Thm. 8.2.28], due to the introduction of perturbations from other dynamics. Here, we assume the weaker property of semi-global practical stability of the set $\mathcal{A}\times\Omega$ under v-perturbed dynamics of the averaged system, where the perturbations are given by the dynamical system

$$v^+ = U(\tilde{u},\tilde{\mu},v) \tag{7.5}$$

with $v\in\mathbb{R}^m$, $U:\mathcal{U}\times\Omega\times\mathbb{R}^m\to\mathbb{R}^m$ being a function parametrized by a some $\varepsilon>0$.

Assumption 7.3. *Consider the system in (7.2) and perturbation dynamics in (7.5), respectively. For any set $K\subset\mathcal{U}$, and all trajectories $(\tilde{u},\tilde{\mu})$ contained in $K\times\Omega$, there exists a function of class $\mathcal{K}$, $\bar{v}$, such that $\max_{k\in\text{dom}(v)}\|v(k)\|\le\bar{v}(\varepsilon)$.* □

Assumption 7.4. *The set $\mathcal{A}\times\Omega$ is SGPAS as $\gamma\to 0$ for the dynamics in (7.2), perturbations in (7.5), and the corresponding Lyapunov function V_{a} satisfies:*

$$\underline{\alpha}_{\text{a}}\left(\|z\|_{\mathcal{A}}\right)\le V_{\text{a}}(z,\mu)\le\overline{\alpha}_{\text{a}}\left(\|z\|_{\mathcal{A}}\right) \tag{7.6a}$$

$$V_{\text{a}}(z^+,\mu^+)-V_{\text{a}}(z,\mu)\le-\tilde{\alpha}_\varepsilon(\varepsilon)\alpha_{\text{a}}\left(\|z\|_{\mathcal{A}}\right)$$
$$\text{for } \|z\|_{\mathcal{A}}\ge\alpha_\gamma(\gamma), \tag{7.6b}$$

where $z=\tilde{u}+v$, $\underline{\alpha}_{\text{a}},\overline{\alpha}_{\text{a}},\tilde{\alpha}_\varepsilon,\alpha_{\text{a}},\alpha_\gamma$ are functions of class $\mathcal{K}$, and the function $\frac{\varepsilon}{\tilde{\alpha}_\varepsilon(\varepsilon)}$ is bounded for $\varepsilon\in(0,\bar{\varepsilon})$. □

Under these assumptions, we claim that the original system is semi-global practically asymptotically stable, as formalized next:

Theorem 7.5. *Let Assumptions 7.1, 7.2, 7.3 and 7.4 hold. The set $\mathcal{A}\times\Omega$ is SGPAS as $(\varepsilon,\gamma)\to 0$ for the discrete dynamics in (7.1) with perturbations in (7.5). The corresponding Lyapunov function V_{a} satisfies:*

$$\underline{\alpha}_{\text{a}}\left(\|\xi\|_{\mathcal{A}}\right)\le V_{\text{a}}(\xi,\mu)\le\overline{\alpha}_{\text{a}}\left(\|\xi\|_{\mathcal{A}}\right)$$
$$V_{\text{a}}(\xi^+,\mu^+)-V_{\text{a}}(\xi,\mu)\le-\hat{\alpha}_\varepsilon(\varepsilon)\alpha_{\text{a}}\left(\|\xi\|_{\mathcal{A}}\right)$$
$$\text{for } \|\xi\|_{\mathcal{A}}\ge\max\{\alpha_\gamma(\gamma),\alpha_\varepsilon(\varepsilon)\},$$

where $\xi:=u+v+\eta$, η is the perturbation state with dynamics

$$\eta^+=(1-\varepsilon)\eta+\varepsilon[G_{\text{avg}}(u,\mu)-G(u,\mu)],$$
$$\max_{k\in\mathbb{N}}\|\eta(k)\|\le\overline{\eta}(\varepsilon), \tag{7.7}$$

the v dynamics are given by (7.5), and $\hat{\alpha}_\varepsilon$, α_ε, $\overline{\eta}$ are functions of class $\mathcal{K}$. □

Proof. See Appendix 7.A. ∎

7.3 Applications of the averaging theorem

In this section, we apply our averaging theorem, Theorem 7.5, to derive two novel convergence results for NEPs. First, we propose a zeroth-order algorithm for solving strongly monotone NEPs with local constraints *in discrete time*. Secondly, we propose an algorithm for solving strongly monotone unconstrained NEPs where the agents sample their states *asynchronously*.

7.3.1 Zeroth-order discrete time forward-backward algorithm

Let us consider a multi-agent system with M agents indexed by $i \in \mathcal{I} := \{1, 2, \dots M\}$, each with cost function

$$J_i(x_i, \boldsymbol{x}_{-i}), \tag{7.8}$$

where $x_i \in \Omega_i \subset \mathbb{R}^{m_i}$ is the decision variable, $J_i : \mathbb{R}^{m_i} \times \mathbb{R}^{m_{-i}} \to \mathbb{R}$, $m := \sum_{j\in\mathcal{I}} m_j$, $m_{-i} := \sum_{j\neq i} m_j$, $\Omega := \Omega_i \times \cdots \times \Omega_N$. Formally, let the goal of each agent be to reach a steady state that minimizes their cost function, i.e.,

$$\forall i \in \mathcal{I} \ : \ \min_{x_i \in \Omega_i} J_i(x_i, \boldsymbol{x}_{-i}). \tag{7.9}$$

A popular solution to this problem is the so-called Nash equilibrium:

Definition 7.6 (Nash equilibrium). *A set of decision variables $\boldsymbol{x}^* := \operatorname{col}\left(\left(x_i^*\right)_{i\in\mathcal{I}}\right)$ is a Nash equilibrium if, for all $i \in \mathcal{I}$,*

$$x_i^* \in \operatorname*{argmin}_{v_i \in \Omega_i} J_i\left(v_i, \boldsymbol{x}_{-i}^*\right). \qquad \blacksquare$$

A fundamental mapping in NEPs is the pseudogradient mapping $F : \mathbb{R}^m \to \mathbb{R}^m$, which is defined as:

$$F(\boldsymbol{x}) := \operatorname{col}\left(\left(\nabla_{x_i} J_i(x_i, \boldsymbol{x}_{-i})\right)_{i\in\mathcal{I}}\right). \tag{7.10}$$

Let us also define $C_F := \overline{\text{co}}\{F(\Omega)\}$, the convex hull of the image of the pseudogradient. To ensure the existence and uniqueness of the Nash equilibrium, we assume certain regularity properties [136, Thm. 4.3]:

Assumption 7.7. *For each $i \in \mathcal{I}$, the function J_i in (7.8) is continuously differentiable in x_i and continuous in $\boldsymbol{x}_{-i}$; the function $J_i(\cdot, \boldsymbol{x}_{-i})$ is strictly convex for every fixed $\boldsymbol{x}_{-i}$.* □

Furthermore, let us assume that no agent can compute their part of the the pseudogradient F directly, but they can only measure their instantaneous cost $h_i = J_i(x_i, \boldsymbol{x}_{-i})$, a common assumption in extremum-seeking problems [23], [122], [17], [8]. The full-information problem where F is known can be solved in many ways, depending on the technical

assumptions of the problem data. Here we choose to study a simple forward-backward algorithm [42, Equ. 26.14]:

$$\boldsymbol{x}^+ = (1-\lambda)\boldsymbol{x} + \lambda \mathrm{proj}_C(\boldsymbol{x} - \gamma F(\boldsymbol{x})), \tag{7.11}$$

for which the Lyapunov function $V(\boldsymbol{x}) = \|\boldsymbol{x} - \boldsymbol{x}^*\|^2$ satisfies the inequality

$$V(\boldsymbol{x}^+) - V(\boldsymbol{x}) \leq -\lambda(1-c)(2-\lambda c)V(\boldsymbol{x}), \tag{7.12}$$

where $c := \frac{\sqrt{1+\gamma^2 L^2}}{1+\gamma\mu_F}$ and $\boldsymbol{x}^*$ is the Nash equilibrium of the game in (7.8). We note that this Lyapunov function satisfies Assumption 7.4.

A naïve approach to adapting the algorithm in (7.11) for zeroth-order implementation would be to use a gradient estimation scheme as in [13], [8] and plug in the estimate directly into (7.11). However, because of the projection, Assumption 7.1 would not be satisfied. Thus, an additional time-scale separation is hereby proposed:

$$\begin{cases} \boldsymbol{x}^+ &= (1-\alpha\beta)\boldsymbol{x} + \alpha\beta \mathrm{proj}_C(\boldsymbol{x} - \gamma\boldsymbol{\xi}) \\ \boldsymbol{\xi}^+ &= (1-\alpha)\boldsymbol{\xi} + \alpha 2A^{-1}J(\boldsymbol{x} + A\mathbb{D}\boldsymbol{\mu})\mathbb{D}\boldsymbol{\mu} \\ \boldsymbol{\mu}^+ &= \mathcal{R}\boldsymbol{\mu} \end{cases}, \tag{7.13}$$

where $\boldsymbol{\xi} \in \mathbb{R}^m$ are filter states, $\boldsymbol{\mu} \in \mathbb{S}^m$ are the oscillator states, $\alpha, \beta > 0$ are small time-scale separation parameters, $\mathcal{R} := \mathrm{blkdiag}((\mathcal{R}_i)_{i\in\mathcal{I}})$, $\mathcal{R}_i := \mathrm{blkdiag}\left(\begin{bmatrix} \cos(\omega_i^j) & -\sin(\omega_i^j) \\ \sin(\omega_i^j) & \cos(\omega_i^j) \end{bmatrix}_{j\leq m_i}\right)$, $\omega_i^j > 0$ for all i and j, $\mathbb{D} \in \mathbb{R}^{m\times 2m}$ is a matrix that selects every odd row from the vector of size $2m$, $a_i > 0$ are small perturbation amplitude parameters, $A := \mathrm{diag}((a_i)_{i\leq m})$ and $J(\boldsymbol{x}) = \mathrm{blkdiag}\left((J_i(x_i, \boldsymbol{x}_{-i})I_{m_i})_{i\in\mathcal{I}}\right)$. We claim that the dynamics in (7.13) render the set $\{\boldsymbol{x}^*\} \times C_{\mathrm{F}} \times \mathbb{S}^m$ practically stable. To the best of our knowledge, it is impossible to prove convergence of the algorithm in (7.13), using the current averaging theory for discrete-time systems, since [135, Thm. 8.2.28], [123, Thm. 2.22] require exponential stability of the origin via the averaged system, and [124, Thm. 2] does not incorporate boundary-layer dynamics. We claim that under the strong monotonicity assumption of the pseudogradient, and a proper choice of the perturbation frequencies, the algorithm in (7.13) converges to a Nash equilibrium.

Assumption 7.8. *The pseudogradient mapping F is μ_f-strongly monotone and L-Lipschitz continuous, i.e. $\langle \boldsymbol{x} - \boldsymbol{y} \mid F(\boldsymbol{x}) - F(\boldsymbol{y})\rangle \geq \mu_f\|\boldsymbol{x} - \boldsymbol{y}\|$, $\|F(\boldsymbol{x}) - F(\boldsymbol{y})\| \leq L\|\boldsymbol{x} - \boldsymbol{y}\|$, for all $(\boldsymbol{x}, \boldsymbol{y}) \in \mathbb{R}^{2m}$.* □

Assumption 7.9. *The sets $(\Omega_i)_{i\in\mathcal{I}}$ are convex, closed and bounded.* □

Assumption 7.10. *The rotational frequencies of each agent i, $\boldsymbol{\omega}_i = \mathrm{col}\left((\omega_i^j)_{j\leq m_i}\right)$, are chosen so that $\omega_i^j \pm \omega_u^v \neq 2\pi z'$, $z' \in \mathbb{Z}$, for every $u \in \mathcal{I}$, for every $j \in \{1, \ldots, m_i\}$, for every $v \in \{1, \ldots, m_u\}$, apart for the case when $i = u$ and $j = v$.* □

Theorem 7.11. *Let Assumptions 7.7, 7.8, 7.9 and 7.10 hold. The set $\{\boldsymbol{x}^*\} \times C_{\mathrm{F}} \times \mathbb{S}^m$ is SGPAS as $(\alpha, \overline{a}, \beta) \to 0$ for the dynamics in (7.13).* □

Proof. See Appendix 7.B. ■

7.3.2 Asynchronous zeroth-order discrete time forward algorithm

First-order information feedback

We now consider the same NEP as in Section 7.3.1 with $\Omega_i := \mathbb{R}^{m_i}$, but where the agent are *asynchronous*, i.e., each agent samples their states independently of others without a global clock for synchronization. For ease of exposition, we assume that the initial conditions are chosen so that simultaneous sampling never occurs. In the full-information case, such an algorithm can be represented in the following form:

$$\begin{aligned}
&\operatorname{col}\left(\dot{x}_i, \dot{\tau}_i, \dot{\kappa}_i, \dot{t}\right) = \operatorname{col}\left(\mathbf{0}, \tfrac{1}{T_i}, 0, 1\right) \\
&\text{if } \operatorname{col}(x_i, \tau_i, \kappa_i, t) \in \mathbb{R}^{m_i} \times [0,1] \times \mathbb{N} \times \mathbb{R} \qquad (7.14a) \\
&\begin{cases} x_i^+ &= x_i - \alpha \nabla_{x_i} J_i(x_i, \boldsymbol{x}_{-i}) \\ \tau_i^+ &= 0 \\ \kappa_i^+ &= \kappa_i + 1 \\ t^+ &= t \end{cases} \\
&\text{if } \operatorname{col}(x_i, \tau_i, \kappa_i, t) \in \mathbb{R}^{m_i} \times \{1\} \times \mathbb{N} \times \mathbb{R}, \qquad (7.14b)
\end{aligned}$$

which in collective form reads as

$$\begin{aligned}
&\operatorname{col}\left(\dot{\boldsymbol{x}}, \dot{\boldsymbol{\tau}}, \dot{\boldsymbol{\kappa}}, \dot{k}, \dot{t}\right) = \operatorname{col}\left(\mathbf{0}, \boldsymbol{T}^{-1}, \mathbf{0}, 0, 1\right) \\
&\text{if } \operatorname{col}(\boldsymbol{x}, \boldsymbol{\tau}, \boldsymbol{\kappa}, k, t) \in \mathbb{R}^m \times \mathcal{T} \times \mathbb{N}^{N+1} \times \mathbb{R} \qquad (7.15a) \\
&\begin{cases} \boldsymbol{x}^+ &= \boldsymbol{x} - \alpha S_x(\boldsymbol{\tau}) F(\boldsymbol{x}) \\ \boldsymbol{\tau}^+ &= (I - S_\tau(\boldsymbol{\tau}))\boldsymbol{\tau} \\ \boldsymbol{\kappa}^+ &= \boldsymbol{\kappa} + S_\tau(\boldsymbol{\tau}) \\ k^+ &= k + 1 \\ t^+ &= t \end{cases} \\
&\text{if } \operatorname{col}(\boldsymbol{x}, \boldsymbol{\tau}, \boldsymbol{\kappa}, k, t) \in \mathbb{R}^m \times \mathcal{T}_{\mathrm{R}} \times \mathbb{N}^{N+1} \times \mathbb{R}, \qquad (7.15b)
\end{aligned}$$

where τ_i are timer states, t is the "experienced" global time, $\boldsymbol{T}^{-1} := \operatorname{col}\left((\frac{1}{T_i})_{i \in \mathcal{I}}\right)$ is the vector of inverse sampling times, $\mathcal{T} \subset [0,1]^N$ is a closed invariant set in which all of the timers evolve and it excludes the initial conditions and their neighborhood for which we have concurrent sampling as seen in Figure 7.1, $\mathcal{T}_{\mathrm{R}} := \left(\cup_{i \in \mathcal{I}} [0,1]^{i-1} \times \{1\} \times [0,1]^{N-i}\right) \cap \mathcal{T}$ is the set of timer intervals where at least one agent has triggered its sampling, κ_i are private event counters, k is the global event counter, $S_x : \mathcal{T} \to \mathbb{R}^{m \times m}$ and $S_\tau : \mathcal{T} \to \mathbb{R}^{N \times N}$ are continuous functions that output diagonal matrices with ones on the positions that correspond to states and timers of agents with $\tau_i = 1$, respectively, while other elements are equal to zero, when evaluating at $\boldsymbol{\tau} \in \mathcal{T}_{\mathrm{R}}$.

Remark 7.12. *Consider a two-player system. To determine the set $\mathcal{T}$, let us introduce timer states t_1 and t_2, each corresponding to an agent. These states neither reset during jumps nor differ in initialization from the timers. Moreover, they maintain the same derivative as their respective timers. Now, for a jump to occur concurrently at time t, the following condition*

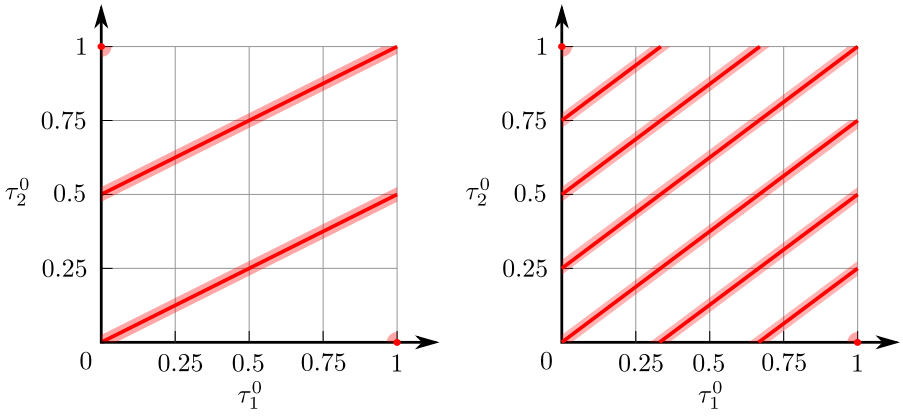

(a) $T_1 = 1, T_2 = 2$ (b) $T_1 = 3, T_2 = 4$

Figure 7.1: The figure represents the set $\mathcal{T}$ for a two-player game in two different cases. The points in red are initial conditions of the timers $\tau_i(0,0) = \tau_i^0$ for which we have concurrent sampling, while the light red is the small neighborhood around that set.

must be met:

$$t_1 = \tau_1^0 + \frac{t}{T_1} = N, \quad t_2 = \tau_2^0 + \frac{t}{T_2} = N, \quad N, M \in \mathbb{N}. \tag{7.16}$$

Thus, initial conditions of timers that have concurrent jumps are given by

$$\tau_2^0 = \tau_1^0 \frac{T_1}{T_2} + \frac{MT_2 - NT_1}{T_2}. \tag{7.17}$$

Considering that the second addend in the previous formula must be between zero and one for $T_1 > T_2$, there is only a finite number of fractions that can appear in the expressions. □

We note that the functions S_x, S_τ are introduced only to write down the algorithm in the collective form, while the agents themselves do not require them for their dynamics and just follow (7.14). Furthermore, the counter states κ_i, k and global time t are not necessary for the algorithm convergence, yet they help with understanding the setup of the algorithm. We choose to represent the algorithm in the hybrid dynamical system framework to replicate the behavior of sampled systems with different sampling periods and to see its effects on the functions S_x, S_τ. Later, we represent and model the system as a fully discrete-time system in order to study convergence.
First, we show that the solution $\boldsymbol{\tau}(t,j)$ is periodic and that implies that $S_x(\boldsymbol{\tau}(t,j))$ and $S_\tau(\boldsymbol{\tau}(t,j))$ are also periodic. We make the following assumption:

Assumption 7.13. *There exist natural numbers $(p_i)_{i\in\mathcal{I}}$, such that the proportion $T_1 : T_2 : \cdots : T_N = p_1 : p_2 \cdots : p_N$ holds, where $(T_i)_{i\in\mathcal{I}}$ are the sampling times.* □

Lemma 7.14. *Let Assumption 7.13 hold. Denote $r_i = \frac{p}{p_i}$ and $r = \sum_{i\in\mathcal{I}} r_i$, where p is the least common multiple of $(p_i)_{i\in\mathcal{I}}$. For any trajectory $S_x(\boldsymbol{\tau}(t,j))$ and $S_\tau(\boldsymbol{\tau}(t,j))$, where $\boldsymbol{\tau}(t,j)$ is a*

solution of the system in (7.15), there exists $T > 0$ such that $S_x(\boldsymbol{\tau}(t,j)) = S_x(\boldsymbol{\tau}(t+T, j+r))$ and $S_\tau(\boldsymbol{\tau}(t,j)) = S_\tau(\boldsymbol{\tau}(t+T, j+r))$ for all $(t,j) \in \mathrm{dom}(\boldsymbol{\tau})$ such that a jump occurred at time t. □

Proof. See Appendix 7.F. ■

Because the values of S_x and S_τ are used only during jumps, we define

$$\hat{S}_x(k;\boldsymbol{\tau}(0,0)) = S_x(\max_{(t\in\mathrm{dom}(\boldsymbol{\tau}(\cdot,k))} t, k) \tag{7.18}$$

$$\hat{S}_\tau(k;\boldsymbol{\tau}(0,0)) = S_\tau(\max_{(t\in\mathrm{dom}(\boldsymbol{\tau}(\cdot,k))} t, k), \tag{7.19}$$

where functions $\hat{S}_x : \mathbb{N} \to \mathbb{R}^{m\times m}$ and $\hat{S}_\tau : \mathbb{N} \to \mathbb{R}^{N\times N}$ are parametrized by the vector of initial conditions of the timers since different initial conditions can change the order in which the agents are sampling their actions (see Figure 7.2). Due to Lemma, 7.14, for every initial condition $\boldsymbol{\tau}(0,0) = \boldsymbol{\tau}^0$, it follows that $\hat{S}_x(k,\boldsymbol{\tau}^0) = \hat{S}_x(k+r,\boldsymbol{\tau}^0)$ for all $k \in \mathbb{N}$.
Now we consider the following discrete-time systems:

$$x_i(k+1) = x_i(k) - \alpha \hat{S}_x^i(k;\boldsymbol{\tau}_0)\nabla_{x_i} J_i(x_i(k), \boldsymbol{x}_{-i}(k)) \tag{7.20}$$

which in collective form read as

$$\boldsymbol{x}(k+1) = \boldsymbol{x}(k) - \alpha \hat{S}_x(k;\boldsymbol{\tau}_0) F(\boldsymbol{x}(k)), \tag{7.21}$$

where the function $\hat{S}^i : \mathbb{N} \to \mathbb{R}^{m_i\times m_i}$ returns the rows of $\hat{S}_x^i(k;\boldsymbol{\tau}_0)$ corresponding to agent i. We can show that for every solution of (7.21) there exists a corresponding solution of (7.15) and vice versa. We claim that under the strong monotonicity assumption, an additional regularity assumption due to the unboundedness of the decision set, and proper choice of the parameter α, the dynamics in (7.21) converge to the solution of the game, with the same minimal convergence rate, regardless of the initial conditions of the timers.

Assumption 7.15. *For each $i \in \mathcal{I}$, the function $J_i(\cdot, \boldsymbol{x}_{-i})$ in (7.8) is radially unbounded for every fixed $\boldsymbol{x}_{-i}$.* □

Theorem 7.16. *Let Assumptions 7.7, 7.8, 7.13 and 7.15 hold. Then, for all vectors of initial conditions $\boldsymbol{\tau}_0$, there exists α^*, such that for any $\alpha \in (0, \alpha^*)$, the NE solution $\boldsymbol{x}^*$ is UGES for the dynamics in (7.21). Furthermore, the corresponding Lyapunov function satisfies Assumption 7.4.* □

Proof. See Appendix 7.E. ■

Moreover, for the hybrid system representation in (7.15), since the trajectories of $(\boldsymbol{\tau}, \boldsymbol{\kappa}, k, t)$ are invariant to the set $\mathcal{T} \times \mathbb{N}^{N+1} \times \mathbb{R}$, and by the structure of the flow and jump sets in (7.15) that assures complete solutions with unbounded time and jump domains, it follows that the dynamics in (7.15) render the set $\{\boldsymbol{x}^*\} \times \mathcal{T} \times \mathbb{N}^{N+1} \times \mathbb{R}$ UGES, as formalized next.

Corollary 7.17. *Let the Assumptions 7.7, 7.8, 7.13 and 7.15 hold. Then, the set $\{\boldsymbol{x}^*\} \times \mathcal{T} \times \mathbb{N}^{N+1} \times \mathbb{R}$ is UGES for the dynamics in (7.15). Furthermore, the corresponding Lyapunov function satisfies Assumption 7.4.* □

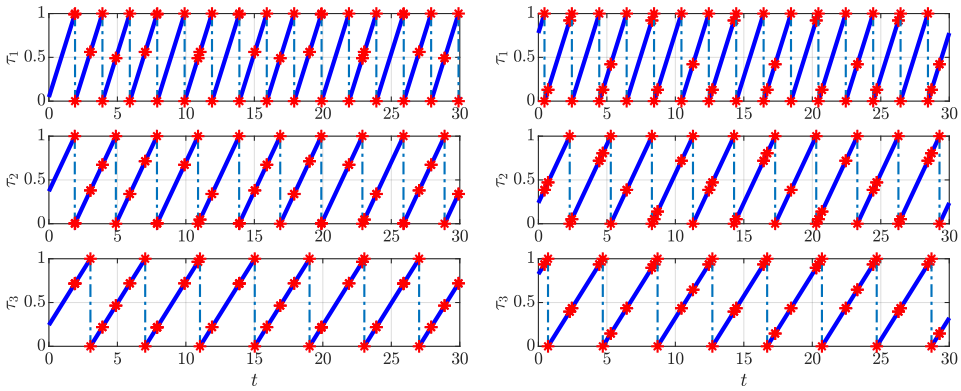

(a) Time evolution of timer states.

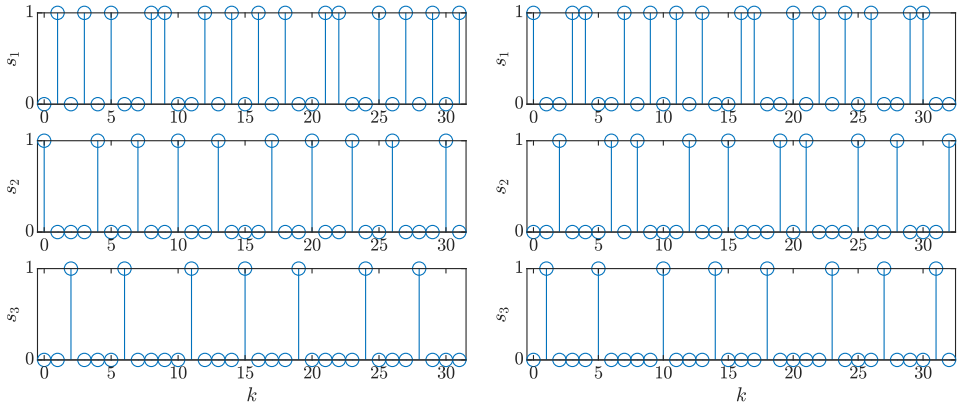

(b) Diagonal elements of $\hat{S}_\tau(k;\boldsymbol{\tau}_0)$ as a function of sample k.

Figure 7.2: Timer behaviour for the case of a 3-player game with sampling times $(T_1, T_2, T_3) = (2, 3, 4)$ and two random initializations. The sampling order is determined by the timer initialization and repeats after a certain number of samples.

Zeroth-order information feedback

Now, consider that each agent only has access to the measurements of the cost function. They can modify the algorithm in (7.14) by implementing a pseudogradient estimation scheme, similar to the one in Equation (7.13):

$$\operatorname{col}\left(\dot{x}_i,\dot{\xi}_i,\dot{\mu}_i,\dot{\tau}_i,\dot{\kappa}_i,\dot{t}\right)=\operatorname{col}\left(\mathbf{0},\mathbf{0},\mathbf{0},\tfrac{1}{T_i},0,1\right) \tag{7.22a}$$

$$\text{if } \operatorname{col}(x_i,\xi_i,\mu_i,\tau_i,\kappa_i,t)\in\mathbb{R}^{2m_i}\times\mathbb{S}^m\times[0,1]\times\mathbb{N}\times\mathbb{R},$$

$$\begin{cases} x_i^+=x_i-\alpha\beta\xi_i\\ \xi_i^+=(1-\alpha)\xi+\alpha\frac{2}{a_i}J_i(x+A\mathbb{D}\mu)\mathbb{D}_i\mu_i\\ \mu_i^+=\mathcal{R}_i\mu_i\\ \tau_i^+=0\\ \kappa_i^+=\kappa_i+1\\ t^+=t \end{cases} \tag{7.22b}$$

$$\text{if } \operatorname{col}(x_i,\xi_i,\mu_i,\tau_i,\kappa_i,t)\in\mathbb{R}^{2m_i}\times\mathbb{S}^m\times\{1\}\times\mathbb{N}\times\mathbb{R},$$

which in the collective form reads as:

$$\operatorname{col}(\dot{\boldsymbol{x}},\dot{\boldsymbol{\xi}},\dot{\boldsymbol{\mu}},\dot{\boldsymbol{\tau}},\dot{\boldsymbol{\kappa}},\dot{k},\dot{t})=\operatorname{col}\left(\mathbf{0},\mathbf{0},\mathbf{0},\boldsymbol{T}^{-1},\mathbf{0},0,1\right) \tag{7.23a}$$

$$\text{if } \operatorname{col}\left(\boldsymbol{x},\boldsymbol{\xi},\boldsymbol{\mu},\boldsymbol{\tau},\boldsymbol{\kappa},k,t\right)\in\mathbb{R}^{2m}\times\mathbb{S}^m\times\mathcal{T}\times\mathbb{N}^{N+1}\times\mathbb{R},$$

$$\begin{cases} \boldsymbol{x}^+=\boldsymbol{x}-\alpha\beta S_x(\boldsymbol{\tau})\boldsymbol{\xi}\\ \boldsymbol{\xi}^+=\boldsymbol{\xi}+\alpha S_x(\boldsymbol{\tau})\left(2A^{-1}J(\boldsymbol{x}+A\mathbb{D}\boldsymbol{\mu})\mathbb{D}\boldsymbol{\mu}-\boldsymbol{\xi}\right)\\ \boldsymbol{\mu}^+=(I-S_\mu(\boldsymbol{\tau}))\boldsymbol{\mu}+S_\mu(\boldsymbol{\tau}))\mathcal{R}\boldsymbol{\mu}\\ \boldsymbol{\tau}^+=(I-S_\tau(\boldsymbol{\tau}))\boldsymbol{\tau}\\ \boldsymbol{\kappa}^+=\boldsymbol{\kappa}+S_\tau(\boldsymbol{\tau})\\ k^+=k+1\\ t^+=t \end{cases} \tag{7.23b}$$

$$\text{if } \operatorname{col}\left(\boldsymbol{x},\boldsymbol{\xi},\boldsymbol{\mu},\boldsymbol{\tau},\boldsymbol{\kappa},k,t\right)\in\mathbb{R}^{2m}\times\mathbb{S}^m\times\mathcal{T}_{\mathrm{R}}\times\mathbb{N}^{N+1}\times\mathbb{R},$$

where $S_\mu:\mathcal{T}\to\mathbb{R}^{2m\times 2m}$ is a continuous function that outputs a diagonal matrix with ones on the positions that correspond to oscillator states of agents with $\tau_i=1$, while other elements are equal to zero when evaluating at $\boldsymbol{\tau}\in\mathcal{T}_{\mathrm{R}}$, and other notation is defined as in (7.13) and (7.15).

Under the assumption of properly chosen perturbation frequencies, we claim semi-global practical stability of the set of solutions.

Assumption 7.18. *The rotational frequencies of every agent i, $\boldsymbol{\omega}_i=\operatorname{col}\left((\omega_i^j)_{j\le m_i}\right)$, are chosen so that $\omega_i^j r_i\pm\omega_u^v r_j\neq 2\pi z'$, $z'\in\mathbb{Z}$, $r_i=\frac{p}{p_i}$, $r_j=\frac{p}{p_j}$, for every $u\in\mathcal{I}$, for every $j\in\{1,\dots,m_i\}$, for every $v\in\{1,\dots,m_u\}$, apart for the case when $i=u$ and $j=v$.* □

Theorem 7.19. *Let the Assumptions 7.7, 7.8, 7.13, 7.18 hold. The set $\{x^*\}\times\mathbb{R}^m\times\mathbb{S}^m\times\mathcal{T}\times\mathbb{N}^{N+1}\times\mathbb{R}$ is SGPAS as $(\alpha,\bar{a},\beta)\to 0$ for the dynamics in (7.23).* □

Proof. The result is proven by following the same steps as the proof of Theorem 7.11 and by using the system in (7.15) with additional filtering state $\boldsymbol{\xi}$ like in (7.60) as the second averaged system. ■

7.4 Illustrative example

The connectivity control problem has been considered in [8] as a Nash equilibrium problem. In many practical scenarios, multi-agent systems, besides their primary objective, are designed to uphold certain connectivity as their secondary objective. In what follows, we consider a similar problem in which each agent is tasked with finding a source of an unknown signal while maintaining certain connectivity. Unlike [8], we only consider the case without vehicle dynamics.Consider a system consisting of multiple agents indexed by $i \in \mathcal{I} := \{1, \dots N\}$. Each agent is tasked with locating a source of a unique unknown signal. The strength of all signals abides by the inverse-square law, i.e., proportional to $1/r^2$. Therefore, the inverse of the signal strength can be used as a cost function. Additionally, the agents must not drift apart from each other too much, as they should provide quick assistance to each other in case of critical failure. This is enforced by incorporating the signal strength of fellow agents in the cost functions. Thus, we design the cost

$$\forall i \in \mathcal{I} \; : \; J_i(\boldsymbol{x}) = \|x_i - x_i^s\|^2 + c \sum_{j \in \mathcal{I}_{-i}} \|x_i - x_j\|^2, \tag{7.24}$$

where $\mathcal{I}_{-i} := \mathcal{I} \setminus \{i\}$, $c, b > 0$ and x_i^s represents the position of the source assigned to agent i. The goal of each agent is to minimize its cost function, and the solution to this problem is a Nash equilibrium. Furthermore, agents are mutually independent, so their sampling times are not synchronized. To solve this problem, we use the asynchronous pseudogradient descent algorithm in (7.23).

For our numerical simulations, we choose the parameters: $x_1^s = (-4, -8)$, $x_2^s = (-12, -3)$, $x_3^s = (1, 7)$, $x_4^s = (16, 8)$, $c = 0.04$, $\gamma = 0.1$, $\alpha = 0.1$, $\beta = 0.003$, $a_i = 0$ for all i, $T = (0.01, 0.015, 0.02, 0.01)$, $\boldsymbol{\tau}(0,0) = (0, 0.002, 0.004, 0.006)$, the perturbation frequencies ω_i^j were chosen as different natural numbers with added random numbers of maximal amplitude of 0.5.

The numerical results are illustrated on Figures 7.3 and 7.4. We note that the trajectories converge to a small neighborhood of the Nash equilibrium. This can be partially attributed to the robustness properties of the pseudogradient descent with strongly monotone operators.

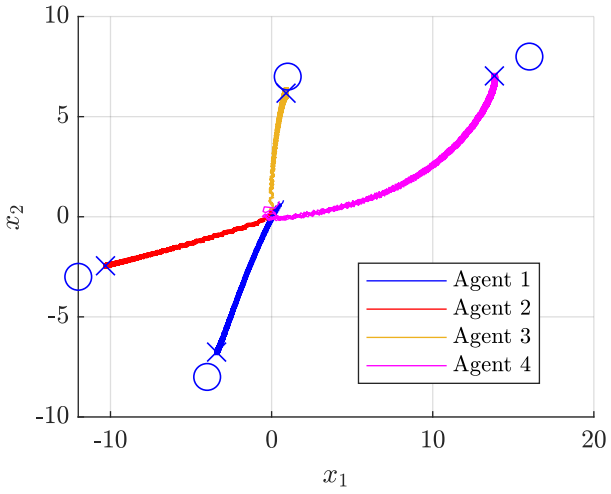

Figure 7.3: State trajectories in the $x_1 - x_2$ plane. Circle symbols represent locations of the sources, while the × symbols represent locations of the NE. Perturbation signals are added to the states.

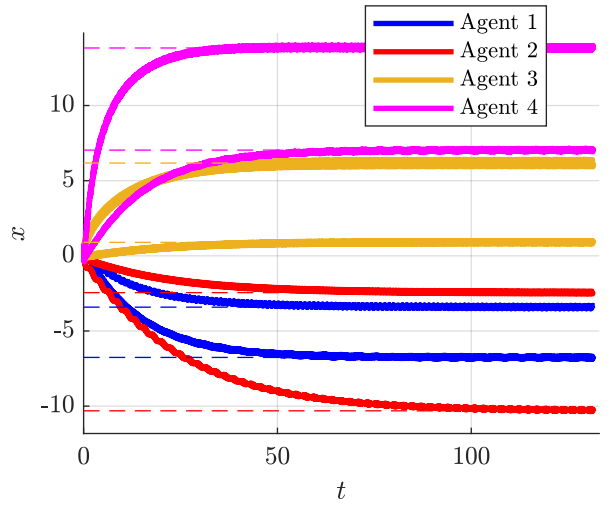

Figure 7.4: Time response of the states. The dashed lines correspond to the states of the Nash equilibrium.

7.5 Conclusion

Averaging theory can be adapted for use in discrete systems with multiple timescales. Furthermore, a strongly monotone Nash equilibrium problem with constrained action sets or asynchronous action sampling can be solved via zeroth-order discrete-time algorithms that leverage novel averaging theory results.

Appendix

7.A Proof of Theorem 7.5

Sketch of the proof: First, we show that under a change of coordinates, the system in (7.1) can be represented as an inflated version of the averaged system in (7.2). Then we show that the inflation can be arbitrarily small for small enough ε. Finally, we use the stability properties of the averaged system and the bounded inflation property to prove SGPAS.

By introducing an additional state, we construct the augmented system:

$$\begin{aligned} &\begin{cases} u^+ = u + \varepsilon G(u,\mu) \\ \mu^+ = M(u,\mu) \\ \eta^+ = (1-\varepsilon)\eta + \varepsilon \left[G_{\text{avg}}(u,\mu) - G(u,\mu)\right] \end{cases} \\ &(u,\mu,\eta) \in \mathcal{U} \times \Omega \times \mathbb{R}^m. \end{aligned} \tag{7.25}$$

With a change of coordinates $u = \tilde{u} - \eta$, $\mu = \tilde{\mu}$ the system is transformed to:

$$\begin{aligned} &\begin{cases} \tilde{u}^+ = \tilde{u} + \varepsilon G_{\text{avg}}(\tilde{u}-\eta,\tilde{\mu}) - \varepsilon\eta \\ \tilde{\mu}^+ = M(\tilde{u}-\eta,\tilde{\mu}) \\ \eta^+ = (1-\varepsilon)\eta + \varepsilon \left[G_{\text{avg}}(\tilde{u}-\eta,\tilde{\mu}) - G(\tilde{u}-\eta,\tilde{\mu})\right] \end{cases} \\ &(\tilde{u}-\eta,\tilde{\mu},\eta) \in \mathcal{U} \times \Omega \times \mathbb{R}^m \end{aligned} \tag{7.26}$$

We note that the $\tilde{u}$ dynamics in (7.26) are perturbed dynamics of the averaged system in (7.2) and $\|\eta\|$ is the upper bound on the perturbation amplitude. To prove our desired stability, we characterize the bound of this amplitude:

Lemma 7.20. *For every $a > 0$ and compact set $K \in \mathcal{U}$, there exists ε^* such that $\|\eta(t,j)\| < a$ holds for any $\varepsilon \in (0,\varepsilon^*]$ and any trajectory of system in (7.26) where $\tilde{u}$ is contained in the set K.* □

Proof. For the purposes of the proof, we construct the concatenated trajectory (u^L, μ^L), which is created by taking solutions of length L of the system in (7.2) and concatenating them together.
We derive a similar bound to (7.4) for the concatenated trajectory type using Assumption

7.1:

$$\begin{aligned}\left\|\sum_{i=1}^{N}\left[G\left(u_i^L,\mu_i^L\right)-G_{\text{avg}}\left(u_i^L,\mu_i^L\right)\right]\right\| \leq & \sum_{j=1}^{n}\left\|\sum_{i=1+L(j-1)}^{1+jL}\left[G\left(u_i^L,\mu_i^L\right)-G_{\text{avg}}\left(u_i^L,\mu_i^L\right)\right]\right\| \\ & +\left\|\sum_{i=nL+1}^{N}\left[G\left(u_i^L,\mu_i^L\right)-G_{\text{avg}}\left(u_i^L,\mu_i^L\right)\right]\right\| \\ \leq & nL\sigma(L)+(N-nL)\sigma(N-nL) \\ \leq & N\sigma(L)+L\sigma(0) \end{aligned} \tag{7.27}$$

Note that the bounds in (7.4) and (7.27) use (concatenated) boundary layer trajectories instead of the u trajectory in (7.1). In order to use the bound in (7.27), we rewrite the η dynamics in (7.25) as

$$\eta^+ = (1-\varepsilon)\eta + v_1 + v_2, \tag{7.28}$$

where

$$v_1 = \varepsilon\left[G\left(u^L,\mu^L\right)-G_{\text{avg}}\left(u^L\right)\right], \tag{7.29}$$

$$v_2 = \varepsilon\left[G(u,\mu)-G_{\text{avg}}(u)-G\left(u^L,\mu^L\right)+G_{\text{avg}}\left(u^L\right)\right]. \tag{7.30}$$

We use the superposition principle to determine the maximum value of η by analyzing the inputs v_1 and v_2 separately. Let us start with v_1. We append the subscripts to the notation of states to denote the time index. The discrete dynamics are given by:

$$\eta_{k+1} = (1-\varepsilon)\eta_k + \varepsilon\left[G\left(u_k^L,\mu_k^L\right)-G_{\text{avg}}\left(u_k^L\right)\right]. \tag{7.31}$$

We define two additional variables:

$$\phi_{k+1} = \varepsilon\sum_{i=1}^{k}\left[G\left(u_k^L,\mu_k^L\right)-G_{\text{avg}}\left(u_k^L,\mu_k^L\right)\right] \tag{7.32}$$

$$\theta_k = \eta_k - \phi_k \tag{7.33}$$

From (7.25) and (7.33) it holds

$$\begin{aligned}
\theta_{k+1} &= \eta_{k+1} - \phi_{k+1} = (1-\varepsilon)\eta_k - \phi_k \\
&= (1-\varepsilon)(\eta_k - \phi_k) - (\varepsilon - 1)\phi_k - \phi_k \\
&= (1-\varepsilon)\theta_k - \varepsilon\phi_k \\
&= (1-\varepsilon)\left[(1-\varepsilon)\theta_{k-1} - \varepsilon\phi_{k-1}\right] - \varepsilon\phi_k \\
&= (1-\varepsilon)^2\theta_{k-1} - \varepsilon\left[(1-\varepsilon)\phi_{k-1} + \phi_k\right] \\
&= \dots \\
&= -\varepsilon\left[\sum_{i=0}^{k}(1-\varepsilon)^i\phi_{k-i}\right] \\
&= \varepsilon\left[\sum_{i=0}^{k}(1-\varepsilon)^i(\phi_k - \phi_{k-i})\right] - \varepsilon\left[\sum_{i=0}^{k}(1-\varepsilon)^i\phi_k\right] \\
&= \varepsilon\left[\sum_{i=0}^{k}(1-\varepsilon)^i(\phi_k - \phi_{k-i})\right] - \phi_k\left[1-(1-\varepsilon)^{k+1}\right] \qquad (7.34)
\end{aligned}$$

From (7.31), (7.32) and (7.34) we have

$$\begin{aligned}
\eta_{k+1} &= \theta_{k+1} + \phi_{k+1} \\
&= \varepsilon\left[\sum_{i=0}^{k}(1-\varepsilon)^i(\phi_k - \phi_{k-i})\right] + (\phi_{k+1} - \phi_k) + (1-\varepsilon)^{k+1}\phi_k. \qquad (7.35)
\end{aligned}$$

We use (7.27) in (7.35) to derive:

$$\|\eta_{k+1}\| \le \underbrace{\varepsilon^2\left[\sum_{i=0}^{k}(1-\varepsilon)^i(i\sigma(L) + L\sigma(0))\right]}_{S_1} + \varepsilon\sigma(L) + \varepsilon L\sigma(0) + \underbrace{\varepsilon(1-\varepsilon)^{k+1}(k\sigma(L) + L\sigma(0))}_{S_2} \qquad (7.36)$$

To compute S_1, we start by finding the sum

$$\sum_{i=1}^{\infty} i(1-\varepsilon)^i = \sum_{k=1}^{\infty}\sum_{i=k}^{\infty}(1-\varepsilon)^i = \sum_{k=1}^{\infty}\frac{(1-\varepsilon)^k}{\varepsilon} = \frac{1-\varepsilon}{\varepsilon^2}. \qquad (7.37)$$

Thus, we bound S_1 as follows:

$$S_1 \le (1-\varepsilon)\sigma(L) + \varepsilon L\sigma(0) \le \sigma(L) + \varepsilon L\sigma(0). \qquad (7.38)$$

For S_2, we define the function $z(x) = x(1-\varepsilon)^x$. It is an easy exercise to check that the maximum of the function is given by $z\left(\frac{-1}{\log(1-\varepsilon)}\right) = \frac{-e}{\log(1-\varepsilon)}$. Therefore, for the bound of S_2 we have

$$S_2 \le \varepsilon(1-\varepsilon)\left[\frac{-e}{\log(1-\varepsilon)}\sigma(L) + L\sigma(0)\right]. \qquad (7.39)$$

As $\lim_{\varepsilon\to 0^+} \frac{\varepsilon}{\log(1-\varepsilon)} = 1$, for small enough ε, it follows:

$$\begin{aligned} &\leq e(1-\varepsilon)\sigma(L)+\varepsilon(1-\varepsilon)L\sigma(0) \\ &\leq e\sigma(L)+\varepsilon L\sigma(0). \end{aligned} \tag{7.40}$$

Finally, we have

$$\|\eta_{k+1}\| \leq (1+\varepsilon+e)\sigma(L)+3\varepsilon L\sigma(0), \tag{7.41}$$

which holds for all k. The norm can be arbitrarily small by the right choice of parameters L and ε.

Now, we move on to the input v_2. We define the inflated boundary layer system:

$$\left.\begin{aligned} u_{\mathrm{bl}}^{\delta+} &\in u_{\mathrm{bl}}^{\delta}+\delta\mathbb{B} \\ \mu_{\mathrm{bl}}^{\delta+} &= M(u_{\mathrm{bl}}^{\delta},\mu_{\mathrm{bl}}^{\delta}) \end{aligned}\right\}, (u_{\mathrm{bl}}^{\delta},\mu_{\mathrm{bl}}^{\delta}) \in \mathcal{U}\times\Omega. \tag{7.42}$$

We claim the following:

Lemma 7.21. *For any period L, positive real number a and compact set $K \in \mathcal{U}$, there exist a δ^* such that for every $\delta \in (0,\delta^*]$ and for any trajectory $(u_{\mathrm{bl}}^{\delta},\mu_{\mathrm{bl}}^{\delta})$ of the system in (7.42) that is contained in $K\times\Omega$, there exist a concatenated trajectory (u^L,μ^L) such that*

$$\|G\left(u_{\mathrm{bl}}^{\delta}(k),\mu_{\mathrm{bl}}^{\delta}(k)\right)-G_{\mathrm{avg}}\left(u_{\mathrm{bl}}^{\delta}(k)\right)-G\left(u^L(k),\mu^L(k)\right)+G_{\mathrm{avg}}\left(u^L(k)\right)\| \leq a. \tag{7.43}$$

■

Proof. L,a,K are given. Let $\xi := \mathrm{col}(u,\mu)$. Based on the continuity property of functions G, G_{avg}, there exists $\rho>0$ such that

$$\begin{aligned} \|\xi_1-\xi_2\| \leq \rho \Rightarrow \|G(\xi_1)-G(\xi_2)\| &\leq \tfrac{a}{2}, \\ \|G_{\mathrm{avg}}(\xi_1)-G_{\mathrm{avg}}(\xi_2)\| &\leq \tfrac{a}{2}. \end{aligned} \tag{7.44}$$

Next, we use [79, Lemma 2] for closeness of solutions of the inflated systems with parameters $(0,L+1,\rho)$ and set $K\times\Omega$ to determine δ^*. That means that for every trajectory of the system in (7.42) where $\xi_{\mathrm{bl}}^{\delta}(k)\in K\times\Omega$ for all $k\in\mathrm{dom}(\xi_{\mathrm{bl}}^{\delta})$, there exists a trajectory ξ_{bl} of the boundary layer system in (7.2), such that for each $k\in\mathrm{dom}(\xi_{\mathrm{bl}}^{\delta})$ with $k\leq L+1$, we have $\left\|\xi_{\mathrm{bl}}^{\delta}(k)-\xi_{\mathrm{bl}}(k)\right\|\leq\rho$. As the inflated boundary layer system is time-invariant, any sample-shifted trajectory is also a trajectory of the original system. Thus, for trajectories starting in $\xi_{\mathrm{bl}}^{\delta}(0),\xi_{\mathrm{bl}}^{\delta}(L),\ldots,\xi_{\mathrm{bl}}^{\delta}(nL)$ with $n\in\mathbb{N}, nL\in\mathrm{dom}(\xi_{\mathrm{bl}}^{\delta})$ there exist trajectories (not necessary the same one) ξ_{bl} such that the previous inequality holds for each segment of length L. We concatenate these boundary layer trajectories into ξ^L and write

$$\left\|\xi_{\mathrm{bl}}^{\delta}(k)-\xi^L(k)\right\| \leq \rho, \text{ for } k\in\mathrm{dom}(\xi_{\mathrm{bl}}^{\delta}). \tag{7.45}$$

From (7.44) and (7.45) we conclude (7.43). ■

The trajectories $\tilde{u}(k), \mu(k)$ of the transformed system in (7.26), where $\tilde{u}(k) \in K$ for all $k \in \mathrm{dom}(\tilde{u})$ and $\|\eta(0)\| \leq a$, are also trajectories of the inflated boundary layer system in (7.42) with

$$\delta = \varepsilon \max_{u \in K, \mu \in \Omega, \eta \in K_\eta} \{G_{\mathrm{avg}}(u-\eta, \mu) - \eta\}, \tag{7.46}$$

where K_η is the set in which η is contained during the trajectory of the system. Let us prove that $K_\eta \subset a\mathbb{B}$ by first showing that i.e. $\|\eta(1)\| \leq a$. First we find ε_1 and L such that $(1+\varepsilon_1+e)\sigma(L) + 3\varepsilon_1 L\sigma(0) \leq \frac{a}{2}$. Then we use the same L, positive number $\frac{a}{2}$ and set K with Lemma 7.21 to find δ^*. For $\varepsilon_2 = \frac{\delta^*}{\max_{u \in K, \eta \in a\mathbb{B}} \{G_{\mathrm{avg}}(u-\eta)-\eta\}}$, we guarantee that for one step, the solution of (7.26) is also a solution of the inflated boundary layer system in (7.42). Thus, for $\varepsilon^* = \min\{\varepsilon_1, \varepsilon_2\}$, we have that variables in (7.29) and (7.30) are bounded as $\|v_1\| \leq \frac{a}{2}$ and $\|v_2\| \leq \frac{a}{2}$, and it follows from (7.28) that

$$\|\eta(1)\| \leq \|(1-\varepsilon)\eta(0)\| + \varepsilon a \leq a.$$

The next sample will also be a solution of the δ-inflated boundary layer system and all of the previous bounds hold. Hence, the procedure can be repeated with the same δ^* for all $k \in \mathrm{dom}(\overline{u})$, and it holds $\|\varepsilon\eta(k)\| \leq a$. ∎

Now, we return to the proof of Theorem 7.5. Let the set of initial conditions K be given. From the stability of the set $\mathcal{A} \times \Omega$ in Assumption 7.4 and the dynamics in (7.26), we have:

$$\begin{aligned}
V_{\mathrm{a}}(u^+ + \eta^+ + v^+, \mu^+) - V_{\mathrm{a}}(u+\eta+v, \mu) =& V_{\mathrm{a}}(\tilde{u}^+ + v^+, \tilde{\mu}) - V_{\mathrm{a}}(\tilde{u}+v, \tilde{\mu}) \\
\leq& V_{\mathrm{a}}(\tilde{u} + \varepsilon G_{\mathrm{avg}}(\tilde{u}, \tilde{\mu}) + v^+, \tilde{\mu}^+) - V_{\mathrm{a}}(\tilde{u}+v, \mu) \\
& - V_{\mathrm{a}}(\tilde{u} + \varepsilon G_{\mathrm{avg}}(\tilde{u}, \tilde{\mu}) + v^+, \tilde{\mu}^+) \\
& + V_{\mathrm{a}}(\tilde{u} + \varepsilon G_{\mathrm{avg}}(\tilde{u}-\eta, \tilde{\mu}) - \varepsilon\eta + v^+) \\
\leq& -\tilde{\alpha}_\varepsilon(\varepsilon)\alpha_{\mathrm{a}}\left(\|\tilde{u}+v\|_{\mathcal{A}}\right) + \varepsilon L_{V_{\mathrm{a}}}(1+L_{\mathrm{G}})\|\eta\|, \\
& \text{for } \|\tilde{u}+v\|_{\mathcal{A}} \geq \alpha_\gamma(\gamma) \\
\leq& -\hat{\alpha}_\varepsilon(\varepsilon)\alpha_{\mathrm{a}}\left(\|\tilde{u}+v\|_{\mathcal{A}}\right) \\
& \text{for } \|\tilde{u}+v\|_{\mathcal{A}} \geq \max\{\alpha_\gamma(\gamma), \alpha_\varepsilon(\varepsilon)\},
\end{aligned} \tag{7.47}$$

where L_{G} and $L_{V_{\mathrm{a}}}$ are Lipschitz constants of the mapping G_{avg} and function V_{a} respectively, $\alpha_\varepsilon(\varepsilon) \geq \alpha_{\mathrm{a}}^{-1}\left[\frac{\varepsilon}{k\tilde{\alpha}_\varepsilon(\varepsilon)} L_{V_{\mathrm{a}}}(1+L_{\mathrm{G}})\|\eta\|\right]$, $\hat{\alpha}_\varepsilon(\varepsilon) := (1-k)\tilde{\alpha}_\varepsilon(\varepsilon)$ and $k \in (0,1)$. The function α_ε is a function of class $\mathcal{K}$ on interval $(0, \bar{\varepsilon})$, as due to Assumption 7.4, $\frac{\varepsilon}{\tilde{\alpha}_\varepsilon(\varepsilon)}$ is bounded on that interval and η can become arbitrarily small for proper choice of ε, per Lemma 7.20. Finally, we plug in the states of the original system to get

$$\begin{aligned}
V_{\mathrm{a}}(u^+ + \eta^+ + v^+) - V_{\mathrm{a}}(u+\eta+v) \leq -\hat{\alpha}_\varepsilon(\varepsilon)\alpha_{\mathrm{a}}\left(\|u+\eta+v\|_{\mathcal{A}}\right) \\
\text{for } \|u+\eta+v\|_{\mathcal{A}} \geq \max\{\alpha_\gamma(\gamma), \alpha_\varepsilon(\varepsilon)\}.
\end{aligned} \tag{7.48}$$

Let $\xi = u + \eta + v$. From the previous Equation, it follows

$$\begin{aligned}
V_{\mathrm{a}}(\xi(k)) \leq V_{\mathrm{a}}(\xi(0)) - \sum_{i=0}^{k-1} \hat{\alpha}_\varepsilon(\varepsilon)\alpha_{\mathrm{a}}\left(\|\xi(i)\|_{\mathcal{A}}\right) \\
\text{for } \|\xi(k)\|_{\mathcal{A}} \geq \max\{\alpha_\gamma(\gamma), \alpha_\varepsilon(\varepsilon)\}.
\end{aligned} \tag{7.49}$$

Now, we move on to proving semi-global practical stability. Let $\Delta > \delta$ be any strictly positive real numbers. We choose parameters ε and γ such that $\overline{\eta}(\varepsilon) + \overline{v}(\gamma) \leq \frac{\delta}{4}$ and $\max\{\alpha_\gamma(\gamma), \alpha_\varepsilon(\varepsilon)\} \leq \frac{\delta}{4}$. The conditional inequality in (7.49) is satisfied when $\|u(k)\|_{\mathcal{A}} \geq \frac{\delta}{2}$.

Semi-global stability

For ease of notation, we drop the explicit dependence on ε and γ in $\overline{\eta}(\varepsilon)$ and $\overline{v}(\gamma)$. We have to show that for any $R > \delta$, there exists $r > 0$, so that $\|u(0)\|_{\mathcal{A}} \leq r$ implies that $\|u(k)\|_{\mathcal{A}} \leq R$ for all $k \in \mathrm{dom}(u)$. From (7.6a) and (7.49), it follows that

$$
\begin{aligned}
&\underline{\alpha}(\|\xi(k)\|_{\mathcal{A}}) \leq V_{\mathrm{a}}(\xi(k)) \leq V_{\mathrm{a}}(\xi(0)) \leq \overline{\alpha}(\|\xi(0)\|_{\mathcal{A}}) \\
&\|\xi(k)\|_{\mathcal{A}} \leq \underline{\alpha}^{-1}\left(\overline{\alpha}(\|\xi(0)\|_{\mathcal{A}})\right) \\
&\|u(k)\|_{\mathcal{A}} - \overline{\eta} - \overline{v} \leq \underline{\alpha}^{-1}\left(\overline{\alpha}(\|u(0)\|_{\mathcal{A}} + \overline{\eta} + \overline{v})\right) \\
&\|u(k)\|_{\mathcal{A}} \leq \underline{\alpha}^{-1}\left(\overline{\alpha}(\|u(0)\|_{\mathcal{A}} + \overline{\eta} + \overline{v})\right) + \overline{\eta} + \overline{v} \\
&\qquad \text{for } \|u\|_{\mathcal{A}} \geq \max\{\alpha_\gamma(\gamma), \alpha_\varepsilon(\varepsilon)\} + \overline{\eta} + \overline{v}
\end{aligned}
$$

From last equation it follows that $R = \underline{\alpha}^{-1}(\overline{\alpha}(r + \overline{\eta} + \overline{v})) + \overline{\eta} + \overline{v}$. Thus, it holds $r = \overline{\alpha}^{-1}(\underline{\alpha}(R - \overline{\eta} - \overline{v})) - \overline{\eta} - \overline{v}$. Considering that the infimum value of R is δ and that $\overline{\eta} + \overline{v} \leq \frac{\delta}{4}$, to ensure r is positive, we assume ε and γ are chosen so that $\overline{\eta} + \overline{v} \leq \frac{1}{2}\overline{\alpha}^{-1}\left(\underline{\alpha}\left(\frac{3}{4}\delta\right)\right)$ which implies that $r \leq \frac{1}{2}\overline{\alpha}^{-1}\left(\underline{\alpha}\left(\frac{3}{4}\delta\right)\right)$. Furthermore, do assure that the Lyapunov difference is defined for those radiuses, we impose an additional inequality on the tuning parameters: $\max\{\alpha_\gamma(\gamma), \alpha_\varepsilon(\varepsilon)\} + \overline{\eta} + \overline{v} < \frac{1}{2}\overline{\alpha}^{-1}\left(\underline{\alpha}\left(\frac{3}{4}\delta\right)\right)$.

7

Practical attractivity

We have to show that for any R, r that satisfy $\Delta > R > r > \delta > 0$, there exists T, such that $\|u(0)\|_{\mathcal{A}} \leq R$ implies that $\|u(k)\|_{\mathcal{A}} \leq r$ for all $k \in \mathrm{dom}(u)$ and $k \geq T$. First, we use the bound we derived in the proof of stability to define $r' := \overline{\alpha}^{-1}(\underline{\alpha}(r - \overline{\eta} - \overline{v})) - \overline{\eta} - \overline{v}$, from which we can conclude that $\|u(0)\|_{\mathcal{A}} \leq r'$ implies that $\|u(k)\|_{\mathcal{A}} \leq r$ for all $k \in \mathrm{dom}(u)$. Let us define

$$
T := \left\lceil \frac{\overline{\alpha}(R + \overline{\eta} + \overline{v}) - \underline{\alpha}\left(r' - \overline{\eta} - \overline{v}\right)}{\hat{\alpha}_\varepsilon(\varepsilon)\alpha(r - \overline{\eta} - \overline{v})} \right\rceil + 1. \tag{7.50}
$$

To prove via contradiction, we assume that $\|u(k)\| > r'$ for all $k \leq T$. Now, by using the upper and lower bound of the Lyapunov function on Equation in (7.49), it follows

$$
\begin{aligned}
&\underline{\alpha}\left(\|u(k)\|_{\mathcal{A}} - \overline{\eta} - \overline{v}\right) \leq \overline{\alpha}(R + \overline{\eta} + \overline{v}) - k\hat{\alpha}_\varepsilon(\varepsilon)\alpha(r' - \overline{\eta} - \overline{v}) \\
&\|u(k)\|_{\mathcal{A}} \leq \underline{\alpha}^{-1}\left(\overline{\alpha}(R + \overline{\eta} + \overline{v}) - k\hat{\alpha}_\varepsilon(\varepsilon)\alpha(r' - \overline{\eta} - \overline{v})\right) + \overline{\eta} + \overline{v}
\end{aligned} \tag{7.51}
$$

Let us choose $k = T - 1$. When we plug in the chosen value of k into inequality (7.51), it follows that:

$$
\|u(k)\|_{\mathcal{A}} \leq r', \tag{7.52}
$$

which leads us to a contradiction. Thus, in the first T steps, $u(k)$ trajectory will enter at least once the set $A + r'\mathbb{B}$. From the stability properties, we know that once the trajectory enters

the aforementioned set, it will never leave the set $\mathcal{A}+r\mathbb{B}$, which proves practical attractivity.

Hence, to have semi-global practical asymptotic stability we have to choose our parameters ε,γ so that they satisfy inequalities

$$\overline{\eta}(\varepsilon)+\overline{v}(\gamma)\leq\tfrac{\delta}{4} \tag{7.53}$$

$$\max\{\alpha_\gamma(\gamma),\alpha_\varepsilon(\varepsilon)\}\leq\tfrac{\delta}{4} \tag{7.54}$$

$$\max\{\alpha_\gamma(\gamma),\alpha_\varepsilon(\varepsilon)\}+\overline{\eta}+\overline{v}<\tfrac{1}{2}\overline{\alpha}^{-1}\left(\underline{\alpha}\left(\tfrac{3}{4}\delta\right)\right) \tag{7.55}$$

That concludes the proof of semi-global practical asymptotic stability. ∎

7.B Proof of Theorem 7.11

First, we show how to derive the boundary layer and averaged systems. Then we show that we can apply Theorem 7.5 to prove stability.
The parameter α can be used as a time-scale separation parameter of the first layer in algorithm (7.13). We derive the first boundary layer system ($\alpha=0$):

$$\begin{cases} x_{\mathrm{bl}}^{1\,+} &= x_{\mathrm{bl}}^1 \\ \xi_{\mathrm{bl}}^{1\,+} &= \xi_{\mathrm{bl}}^1 \\ \mu_{\mathrm{bl}}^{1\,+} &= \mathcal{R}\mu_{\mathrm{bl}}^1 \end{cases}, \tag{7.56}$$

and the first averaged system

$$\begin{cases} \hat{x}^+ &= (1-\alpha\beta)\hat{x}+\alpha\beta\mathrm{proj}_C(\hat{x}-\gamma\xi) \\ \hat{\xi}^+ &= (1-\alpha)\hat{\xi}+\alpha(F(\hat{x})+\mathcal{O}(\overline{a})) \\ \hat{\mu}^+ &= \mathcal{R}\hat{\mu} \end{cases}, \tag{7.57}$$

which is an $\mathcal{O}(\overline{a})$ inflation of the nominal averaged system

$$\begin{cases} \hat{x}^+ &= (1-\alpha\beta)\hat{x}+\alpha\beta\mathrm{proj}_C\left(\hat{x}-\gamma\hat{\xi}\right) \\ \hat{\xi}^+ &= (1-\alpha)\hat{\xi}+\alpha F(\hat{x}) \\ \hat{\mu}^+ &= \mathcal{R}\hat{\mu} \end{cases}. \tag{7.58}$$

Furthermore, we use $\alpha\beta$ for the parameter of the second-time layer separation to determine the second boundary layer system

$$\begin{cases} x_{\mathrm{bl}}^{2\,+} &= x_{\mathrm{bl}}^2 \\ \xi_{\mathrm{bl}}^{2\,+} &= (1-\alpha)\xi_{\mathrm{bl}}^2+\alpha F(x_{\mathrm{bl}}^2) \\ \mu_{\mathrm{bl}}^{2\,+} &= \mathcal{R}\mu_{\mathrm{bl}}^2 \end{cases}, \tag{7.59}$$

and the second averaged system

$$\begin{cases} \tilde{x}^+ &= (1-\alpha\beta)\tilde{x}+\alpha\beta\mathrm{proj}_C(\tilde{x}-\gamma F(\tilde{x})) \\ \tilde{\xi}^+ &= (1-\alpha)\tilde{\xi}+\alpha F(\tilde{x}) \\ \tilde{\mu}^+ &= \mathcal{R}\tilde{\mu} \end{cases}, \tag{7.60}$$

which is the algorithm in (7.11) with additional bounded dynamics that renders the set $\{x^*\}\times C_{\mathrm{F}}\times \mathbb{S}^m$ UGAS.
In order to satisfy Assumption 7.1 for both averaged systems, we establish the following result:

Lemma 7.22. *For any solution of the first boundary layer system $(x^1_{\mathrm{bl}},\xi^1_{\mathrm{bl}},\mu^1_{\mathrm{bl}})$ and compact set C such that $x^1_{\mathrm{bl}}\in C$ for all $k\in \mathrm{dom}\,(x^1_{\mathrm{bl}})$, it holds that:*

$$\left\|\frac{1}{N}\sum_{i=1}^{N}\left[2A^{-1}J\left(x^1_{\mathrm{bl}}(i)+A\mathbb{D}\mu^1_{\mathrm{bl}}(i)\right)\mathbb{D}\mu^1_{\mathrm{bl}}(i)-F(x^1_{\mathrm{bl}}(i))-\mathcal{O}(\bar{a})\right]\right\|\leq\sigma_1(N), \tag{7.61}$$

where $\sigma_1:\mathbb{R}^+\to\mathbb{R}^+$ is a function of class $\mathcal{L}$. □

Proof. See Appendix 7.C. ■

Lemma 7.23. *For any solution of the second boundary layer system $(x^2_{\mathrm{bl}},\xi^2_{\mathrm{bl}})$ and compact set C such that $\mathrm{col}\,(x^1_{\mathrm{bl}},\xi^1_{\mathrm{bl}})\in C$ for all $k\in\mathrm{dom}\,(x^1_{\mathrm{bl}})$, it holds that:*

$$\left\|\frac{\gamma}{N}\sum_{i=1}^{N}\left[\xi^2_{\mathrm{bl}}(i)-F(x^2_{\mathrm{bl}}(i))\right]\right\|\leq\sigma_2(N), \tag{7.62}$$

where $\sigma_2:\mathbb{R}^+\to\mathbb{R}^+$ is a function of class $\mathcal{L}$. □

Proof. See Appendix 7.D. ■

7

To prove stability, we start from the second layer and "move" upwards. As the second averaged system satisfies Assumptions 7.1 due to Lemma 7.22, Assumption 7.2 due to the nonexpansivnes of the projection mapping [42, Prop. 12.28, 29.1], Assumption 7.3 due to Lemma 7.20 and Assumption 7.4 due to (7.12), we have that due to Theorem 7.5, the nominal averaged system in (7.58) renders the set $\{x^*\}\times C_{\mathrm{F}}\times\mathbb{S}^m$ SGPAS as $\alpha\beta\to 0$, with the Lyapunov difference given by

$$\begin{aligned}&V(\tilde{x}^+ +\eta_1^+)-V(\tilde{x}+\eta_1)\leq-\tfrac{1}{2}\alpha\beta(1-c)(2-\alpha\beta c)\|\tilde{x}+\eta_1-x^*\|_{\mathcal{A}}\\&\text{for }\|\tilde{x}+\eta_1\|_{\mathcal{A}}\geq\alpha_\varepsilon(\alpha\beta)\geq\sqrt{\tfrac{\alpha\beta L\|\eta_1\|}{2\alpha\beta(1-c)(2-\alpha\beta c)}}\end{aligned} \tag{7.63}$$

and the perturbation dynamics

$$\eta_1^+=(1-\alpha\beta)\eta_1+\alpha\beta(\mathrm{proj}_C(\tilde{x}-\gamma F(\tilde{x}))-\tilde{\xi}). \tag{7.64}$$

We note that we had to take $\alpha\beta$ as the time-scale separation parameter. If we had chosen only β, as might be the intuition, the function α_ε of class $\mathcal{K}$ that appears in the inequality in (7.63), would have an implicit dependence on the parameter α. In fact, decreasing α would increase the value of the function α_ε, as it would hold

$$\alpha_\varepsilon(\beta)\geq\sqrt{\tfrac{\beta L\|\eta_1\|}{2\alpha\beta(1-c)(2-\alpha\beta c)}}, \tag{7.65}$$

which would invalidate all of the following stability analysis. Thus, it is important to capture all parameters affecting convergence speed. Nevertheless, if we assume that the parameter α is contained in the set $(0,\overline{\alpha})$, it is possible to construct a function of class $\mathcal{K}$, such that it holds $\|\tilde{x}+\eta_1\|_{\mathcal{A}} \geq \alpha_\beta(\beta) \geq \alpha_\varepsilon(\alpha\beta)$. Hence, the averaged system in (7.58) renders the set $\{x^*\}\times C_{\mathrm{F}}\times \mathbb{S}^m$ SGPAS as $\beta \to 0$.
The first averaged system is an $\mathcal{O}(\bar{a})$ inflation of the nominal averaged system, and it can be shown that the inflation introduces a small perturbation in the Lyapunov difference inequality, which can be made arbitrarily small by choosing $\bar{a}$ small enough. For the sake of the proof, we set $\bar{a} = \alpha_a(\beta)$, where α_a is a function of class $\mathcal{K}$. Thus, it also satisfies Assumption 7.4, Assumption 7.1 due to (7.64), Assumption 7.2 because of [42, Prop. 12.28, 29.1], and Assumption 7.3 as a result of (7.64). Hence, the system in (7.13) renders the set $\{x^*\}\times C_{\mathrm{F}}\times \mathbb{S}^m$ SGPAS as $(\alpha,\bar{a},\beta)\to 0$. ∎

7.C Proof of Lemma 7.22

Without the loss of generality, let a solution of the first boundary layer system is given by $\mu_{\mathrm{bl}}^{1,i}(k) = \mathrm{col}\left((\sin(\omega_i^j k),\cos(\omega_i^j k))_{j\leq m_i}\right)$, $\mu_{\mathrm{bl}}^1(k) = \mathrm{col}\left((\mu_{\mathrm{bl}}^{1,i}(k))_{i\in\mathcal{I}}\right)$, $x_{\mathrm{bl}}^1(k) = x_{\mathrm{bl}}^1 = const.$, $\xi_{\mathrm{bl}}^1 = const$. First, with the following Lemma, we characterize the properties of average discrete-time sinusoidal signals:

Lemma 7.24. *For any $\phi,\phi_i,\phi_l \in \mathbb{R}$ such that $\phi \neq 2\pi t$, $\phi_i \pm \phi_l \neq 2\pi p, t, p \in \mathbb{Z}$, it holds that:*

$$\frac{1}{N}\left\|\sum_{k=0}^{N-1}\sin(\phi k)\right\| \leq \frac{c_1}{N}, \tag{7.66}$$

$$\frac{1}{N}\left\|\sum_{k=0}^{N-1}\cos(\phi k)\right\| \leq \frac{c_2}{N}, \tag{7.67}$$

$$\frac{1}{N}\left\|\sum_{k=0}^{N-1}\sin(\phi_i k)\sin(\phi_l k)\right\| \leq \frac{c_3}{N}, \tag{7.68}$$

$$\frac{1}{N}\left\|\sum_{k=0}^{N-1}(\sin^2(\phi k)-\tfrac{1}{2})\right\| \leq \frac{c_4}{N}, \tag{7.69}$$

for some $c_1,c_2,c_3,c_4 > 0$. □

Proof. We note that for $\phi \neq 2\pi p, p \in \mathbb{Z}$, it follows:

$$\left\|\sum_{k=0}^{N-1}e^{j\phi k}\right\|^2 = \left\|\sum_{k=0}^{N-1}\cos(\phi k)\right\|^2 + \left\|\sum_{k=0}^{N-1}\sin(\phi k)\right\|^2 = \left\|\frac{e^{j\phi N}-1}{e^{j\phi}-1}\right\|^2 \leq \frac{4}{\left\|e^{j\phi}-1\right\|^2}. \tag{7.70}$$

Therefore, we have

$$\left\|\sum_{k=0}^{N-1}\cos(\phi k)\right\| \leq \frac{2}{\left\|e^{j\phi}-1\right\|} := c_1, \tag{7.71}$$

$$\left\|\sum_{k=0}^{N-1}\sin(\phi k)\right\| \leq \frac{2}{\left\|e^{j\phi}-1\right\|} := c_2. \tag{7.72}$$

Equations (7.66), (7.67) follow from the previous equations.
Let $\phi = \phi_i \pm \phi_l$. From (7.71), we have

$$\left\| \sum_{k=0}^{N-1} (\sin(\phi_i k)\sin(\phi_l k) \mp \cos(\phi_i k)\cos(\phi_l k)) \right\| \leq \frac{2}{\min_{\phi \in \phi_i \pm \phi_l} \left\| e^{j\phi} - 1 \right\|} := c_3 \tag{7.73}$$

For any scalars $a, b \in \mathbb{R}, c \in \mathbb{R}_+$, that satisfy equation $\|a \pm b\| \leq c$, it holds

$$-c \leq a + b \leq c, \text{ and } -c \leq a - b \leq c. \tag{7.74}$$

By summing the last two inequalities, we have

$$\|a\| \leq c. \tag{7.75}$$

Thus from (7.73), (7.74) and (7.75), we conclude

$$\left\| \sum_{k=0}^{N-1} \sin(\phi_i k)\sin(\phi_l k) \right\| \leq c_3. \tag{7.76}$$

Again, (7.68) follows trivially. Finally, using the identity $\sin^2(x) = \frac{1-\cos(2x)}{2}$, we rewrite Equation (7.69) as

$$\frac{1}{2N} \left\| \sum_{k=0}^{N-1} \cos(2\phi k) \right\| \leq \frac{c_4}{N}. \tag{7.77}$$

By switching 2ϕ instead of ϕ in (7.71), analogously, it is possible to prove (7.69). ∎

Via the Taylor expansion of the an addend in (7.61), we have

$$\begin{aligned} 2A^{-1}J\left(x_{\text{bl}}^1 + A\mathbb{D}\mu_{\text{bl}}^1(i)\right)\mathbb{D}\mu_{\text{bl}}^1(i) - F(x_{\text{bl}}^1) - \mathcal{O}(\bar{a}) =& 2A^{-1}J(x_{\text{bl}}^1)\mathbb{D}\mu_{\text{bl}}^1(i) \\ &+ F(x_{\text{bl}}^1)^\top \mathbb{D}\mu_{\text{bl}}^1(i)\mathbb{D}\mu_{\text{bl}}^1(i) - F(x_{\text{bl}}^1) \end{aligned} \tag{7.78}$$

Due to the inequality $\sqrt{\sum_{i=0}^m x_i^2} \leq \sum_{i=0}^m |x_i|$, we can bound the expression in (7.61) via the bounds for each row:

$$\begin{aligned} &\left\| \frac{1}{N} \sum_{i=1}^{N} \left[2A^{-1}J\left(x_{\text{bl}}^1 + A\mathbb{D}\mu_{\text{bl}}^1(i)\right)\mathbb{D}\mu_{\text{bl}}^1(i) - F(x_{\text{bl}}^1) - \mathcal{O}(\bar{a}) \right] \right\| \leq \\ &\sum_{j=1}^{m} \left\| \sum_{k=0}^{N-1} \left[\tfrac{2}{a_j} J_j(x_{\text{bl}}^1)\sin(\phi_j k) + \nabla_{x_j} J_j(x_{\text{bl}}^1)(2\sin^2(\phi_j k) - 1) + 2\sum_{l \neq j}^{n} \nabla_{x_l} J_j(x_{\text{bl}}^1)\sin(\phi_l k)\sin(\phi_j k) \right] \right\| \\ &\leq \frac{2m}{\underline{a}} \left\| J(x_{\text{bl}}^1) \right\| \frac{c_1}{N} + \left\| \nabla J(x_{\text{bl}}^1) \right\|_\infty \frac{2\bar{c}m^2}{N}, \end{aligned} \tag{7.79}$$

where $\underline{a} := \min_i a_i$ and $\bar{c} := \max\{c_3, c_4\}$. Thus for the compact set C, we define $\sigma_1(N) := \frac{2m}{\underline{a}} \max_{x \in C} \|J(x)\| \frac{c_1}{N} + \max_{x \in C} \|\nabla J(x)\|_\infty \frac{2\bar{c}m^2}{N}$ which belongs to the class of $\mathcal{L}$ functions. ∎

7.D Proof of Lemma 7.23

Solutions of the second boundary layer system are given by $\boldsymbol{x}^2_{\text{bl}}(k) = \boldsymbol{x}^2_{\text{bl}} = const.$, and $\boldsymbol{\xi}^2_{\text{bl}}(k) = (1-\alpha)^k \left(\boldsymbol{\xi}^2_{\text{bl}}(0) - F(\boldsymbol{x}^2_{\text{bl}})\right) + F(\boldsymbol{x}^2_{\text{bl}})$. Thus, the norm in (7.62) can be rewritten as

$$\begin{aligned}\left\| \frac{\gamma}{N} \sum_{i=0}^{N-1} \left[\boldsymbol{\xi}^2_{\text{bl}}(i) - F(\boldsymbol{x}^2_{\text{bl}}(i))\right] \right\| &\leq \frac{\gamma}{N} \left\| \sum_{i=0}^{N-1} \left[(1-\alpha)^i \left(\boldsymbol{\xi}^2_{\text{bl}}(0) - F(\boldsymbol{x}^2_{\text{bl}})\right)\right] \right\| \\ &\leq \frac{\gamma}{N\alpha} \left\| \boldsymbol{\xi}^2_{\text{bl}}(0) - F(\boldsymbol{x}^2_{\text{bl}}) \right\|. \end{aligned} \tag{7.80}$$

Thus, for the compact set C, we define $\sigma_2(N) := \frac{\gamma}{N\alpha} \max_{\text{col}(\boldsymbol{\xi},\boldsymbol{x})\in C} \|\boldsymbol{\xi} - F(\boldsymbol{x})\|$, which belongs to the class of $\mathcal{L}$ functions. ∎

7.E Proof of Theorem 7.16

For notational simplicity, we denote $S(k) := \hat{S}_x(k; \boldsymbol{\tau}_0)$. Thus, the algorithm reads as

$$\begin{cases} \boldsymbol{x}^+ &= \boldsymbol{x} - \alpha S(k) F(\boldsymbol{x}) \\ k^+ &= k+1. \end{cases} \tag{7.81}$$

One epoch is defined as r iterations of the algorithm in (7.81), where r is the period of the function S from Lemma 7.14. From the proof of the Lemma, it follows that every agent *individually* jumps r_i times in one epoch. Let $F_j : \mathbb{R}^m \to \mathbb{R}^m$ be the mapping that returns the rows of the pseudogradient that correspond to the agents that sample at $k = j + rn$, $n \in \mathbb{N}$, $0 \leq j \leq r-1$, i.e. $F_j(\boldsymbol{x}) := S(j)F(\boldsymbol{x})$. We define the full update operator, the asynchronous update operator, and the error operator respectively, as

$$T := I - \alpha \Gamma F, \tag{7.82}$$

$$E := (I - \alpha F_1) \ldots (I - \alpha F_r), \tag{7.83}$$

$$R := \tfrac{1}{\alpha}(T - E). \tag{7.84}$$

where $\Gamma := \text{diag}\left((r_i I_{m_i})_{i\in\mathcal{I}}\right)$. We note that the E operator represents one epoch of the algorithm in (7.81), i.e. $\boldsymbol{x}(k+r) = E(x(k))$. The proof of convergence is analogous to the proof in [137], and here we just provide the outlines. The error operator can be bounded as

$$\|R(x)\|^2 \leq \frac{\alpha^2 L^2 r^2 \bar{r}^2}{2} (1+\alpha L)^{2m} \|S(x)\|^2, \tag{7.85}$$

where $\bar{r} = \max_{i\in\mathcal{I}} r_i$. For the Lyapunov function candidate, we propose

$$V(\boldsymbol{x}) = \|\boldsymbol{x} - \boldsymbol{x}^*\|^2_{\Gamma^{-1}}. \tag{7.86}$$

It can be proven that

$$\|E(\boldsymbol{x}) - \boldsymbol{x}^*\|^2_{\Gamma^{-1}} \leq \left(1 - \frac{\alpha \mu^2_{\Gamma} \underline{r}^2}{2}\right) \|\boldsymbol{x} - \boldsymbol{x}^*\|^2_{\Gamma^{-1}}, \tag{7.87}$$

where $\underline{r} = \min_{i\in\mathcal{I}} r_i$, if α is chosen such that

$$\tfrac{1}{2} + \tfrac{\bar{r}\eta}{\mu_F^2} - (1-\alpha\eta)\left(1-\alpha - \tfrac{(\alpha L \bar{r}(1+\alpha L)^r)^2}{2\eta}\right) \leq 0.$$

The inequality is satisfied for η and α small enough, and $\alpha \ll \eta$. We note that the inequality does not depend on the initial conditions of the timers $\boldsymbol{\tau}_0$. Equation (7.87) holds for *epochs*, not necessarily the individual samples. Due to the Lipschitz continuity of the pseudogradient, it follows that

$$\left\|\boldsymbol{x}^+ - \boldsymbol{x}^*\right\|_{\Gamma^{-1}} \leq (1+\alpha L \tfrac{\bar{r}}{\underline{r}}) \left\|\boldsymbol{x}-\boldsymbol{x}^*\right\|_{\Gamma^{-1}}.$$

Thus, for some $k = ir + j$, where $i, j \in \mathbb{N}$ we have

$$\left\|\boldsymbol{x}(k)-\boldsymbol{x}^*\right\|^2_{\Gamma^{-1}} \leq \left(1+\alpha L \tfrac{\bar{r}}{\underline{r}}\right)^{2r} \left(1 - \frac{\alpha \mu_F^2 \underline{r}^2}{2}\right)^i \left\|\boldsymbol{x}(0)-\boldsymbol{x}^*\right\|^2_{\Gamma^{-1}}. \tag{7.88}$$

It holds $i = \lfloor \frac{k}{r} \rfloor \geq \frac{k}{r} - 1$. Hence, the previous inequality becomes

$$\left\|\boldsymbol{x}(k)-\boldsymbol{x}^*\right\|^2_{\Gamma^{-1}} \leq \left(1+\alpha L \tfrac{\bar{r}}{\underline{r}}\right)^{2r} \left(1 - \frac{\alpha \mu_F^2 \underline{r}^2}{2}\right)^{\frac{k}{r}-1} \left\|\boldsymbol{x}(0)-\boldsymbol{x}^*\right\|^2_{\Gamma^{-1}}.$$

The last inequality is the $\mathcal{KL}$ exponential stability bound for all initial timer state conditions $\boldsymbol{\tau}_0$. Thus, the dynamics in (7.81) render $\boldsymbol{x}^*$ UGES.

7

Additionally, we need to establish the Lyapunov difference convergence speed. To do this, we construct a Lyapunov function using a similar procedure as in the proof of [29, Thm. 4.14]. Let

$$a := \frac{\left(1+\alpha L \tfrac{\bar{r}}{\underline{r}}\right)^{2r}}{1 - \frac{\alpha \mu_F^2 \underline{r}^2}{2}}, \quad b := \left(1 - \frac{\alpha \mu_F^2 \underline{r}^2}{2}\right)^{\frac{1}{r}}. \tag{7.89}$$

Then, the Lyapunov function satisfies the following properties

$$\frac{1-\left(1-\alpha L \tfrac{\bar{r}}{\underline{r}}\right)^{2\delta r}}{2\alpha L \tfrac{\bar{r}}{\underline{r}}(1-\alpha L \tfrac{\bar{r}}{\underline{r}})} \left\|\boldsymbol{x}-\boldsymbol{x}^*\right\|^2_{\Gamma^{-1}} \leq V(\boldsymbol{x}) \leq \frac{a(b^\delta r - 1)}{b-1} \left\|\boldsymbol{x}-\boldsymbol{x}^*\right\|^2_{\Gamma^{-1}}$$
$$V(\boldsymbol{x}^+) - V(\boldsymbol{x}) \leq -(1-ab^{\delta r}) \left\|\boldsymbol{x}-\boldsymbol{x}^*\right\|^2_{\Gamma^{-1}},$$

where δ is large integer. Using the Taylor expansion, for small values of α, it holds

$$(1-ab^{\delta r}) \approx \alpha \left(\frac{\mu^2 \underline{r}^2(\delta-1)}{2} - 2rL\tfrac{\bar{r}}{\underline{r}}\right). \tag{7.90}$$

Thus, for δ large enough, we can guarantee that the Lyapunov difference is negative. Furthermore, we have that $\frac{\alpha}{(1-ab^{\delta r})}$ is bounded on some interval $(0, \alpha^*)$ and the Lyapunov function satisfies the conditions from Assumption (7.4). ∎

7.F Proof of Lemma 7.14

First, let us denote the least common sampling time as $T = T_i \frac{p}{p_i}$.

Claim 1. The number of jumps in any time interval $[\hat{t}, \hat{t}+T)$ is constant. □

Let us denote as the number of jumps in this interval as q. We "slide" the interval by some ΔT, i.e. $[\hat{t}+\Delta T, \hat{t}+T+\Delta T)$, so that we exclude one event in $[\hat{t}, \hat{t}+\Delta T)$. As $T = T_i r_i$ for all $i \in \mathcal{I}$, it follows that there must be an event in the interval $[\hat{t}+T, \hat{t}+T+\Delta T)$, thus the total number of jumps in the interval $[\hat{t}+\Delta T, \hat{t}+T+\Delta T)$ remains the same. We can repeat this procedure for any $\Delta\hat{T}$ by sliding the interval for every jump by ΔT_j until $\Delta\hat{T} = \sum_j \Delta T_j$. The number of jumps in the interval is equal to q.

Claim 2. For every $(\hat{t}, \hat{j}) \in \mathrm{dom}(\boldsymbol{\tau})$ where a jump occurred, it holds $\boldsymbol{\tau}(\hat{t}, \hat{j}) = \boldsymbol{\tau}(\hat{t}+T, \hat{j}+r)$. □

We observe that if an agent initiates a jump at $t = \hat{t}$, these same agents will also initiate a jump at $t = \hat{t}+T$. Furthermore, if an agent did not jump at $\hat{t}$, it will also not jump at $\hat{t}+T$. Thus, in the moment $t = \hat{t}+T$, the same agent will jump, i.e. $\tau_i = T_i$ and it follows that $\boldsymbol{\tau}(\hat{t}, \hat{j}) = \boldsymbol{\tau}(\hat{t}+T, \hat{j}+r)$.
As the functions S_x and S_τ are single-valued, the claim of the Lemma holds. ■

7.G Proof of Theorem 7.19

As the proof is analogous to the proof of Theorem 7.11, we provide just the required system definitions and averaging Lemmas. The equivalent discrete-time system of (7.23) is given by

$$\begin{cases} \boldsymbol{x}^+ &= \boldsymbol{x} - \alpha\beta S(k)\xi \\ \xi^+ &= \xi + \alpha S(k)\left(2A^{-1}J(\boldsymbol{x}+A\mathbb{D}\boldsymbol{\mu})\mathbb{D}\boldsymbol{\mu} - \xi\right) \\ \boldsymbol{\mu}^+ &= (I - S_\mu(k))\boldsymbol{\mu} + S_\mu(k)\mathcal{R}\boldsymbol{\mu} \\ \boldsymbol{\kappa}^+ &= \boldsymbol{\kappa} + S_\tau(\boldsymbol{\tau}) \\ k^+ &= k+1. \end{cases} \tag{7.91}$$

The first boundary-layer system is defined as

$$\begin{cases} {\boldsymbol{x}_{\mathrm{bl}}^1}^+ &= \boldsymbol{x}_{\mathrm{bl}}^1 \\ {\xi_{\mathrm{bl}}^1}^+ &= \xi_{\mathrm{bl}}^1 \\ {\boldsymbol{\mu}_{\mathrm{bl}}^1}^+ &= (I - S_\mu(k))\boldsymbol{\mu}_{\mathrm{bl}}^1 + S_\mu(k))\mathcal{R}\boldsymbol{\mu}_{\mathrm{bl}}^1 \\ \boldsymbol{\kappa}^+ &= \boldsymbol{\kappa} + S_\tau(k) \\ k^+ &= k+1, \end{cases} \tag{7.92}$$

while the first averaged system is given as

$$\begin{cases} \tilde{\boldsymbol{x}}^+ &= \tilde{\boldsymbol{x}} - \alpha\beta S(k)\tilde{\xi} \\ \tilde{\xi}^+ &= \tilde{\xi} + \alpha S(k)\left(F(\tilde{\boldsymbol{x}}) - \tilde{\xi}\right) \\ \tilde{\boldsymbol{\mu}}^+ &= (I - S_\mu(k))\tilde{\boldsymbol{\mu}} + S_\mu(k))\mathcal{R}\tilde{\boldsymbol{\mu}} \\ \boldsymbol{\kappa}^+ &= \boldsymbol{\kappa} + S_\tau(k) \\ k^+ &= k+1. \end{cases} \tag{7.93}$$

The second boundary-layer system follows the dynamics

$$\begin{cases} \boldsymbol{x}_{\mathrm{bl}}^{2\,+} & = \boldsymbol{x}_{\mathrm{bl}}^{2} \\ \boldsymbol{\xi}_{\mathrm{bl}}^{2\,+} & = \boldsymbol{\xi}_{\mathrm{bl}}^{2} - \alpha S(k)(F(\boldsymbol{x}_{\mathrm{bl}}^{2}) - \boldsymbol{\xi}_{\mathrm{bl}}^{2}) \\ \boldsymbol{\mu}_{\mathrm{bl}}^{2\,+} & = (I - S_{\mu}(k))\boldsymbol{\mu}_{\mathrm{bl}}^{2} + S_{\mu}(k))\mathcal{R}\boldsymbol{\mu}_{\mathrm{bl}}^{2} \\ \boldsymbol{\kappa}^{+} & = \boldsymbol{\kappa} + S_{\tau}(k) \\ k^{+} & = k+1, \end{cases} \tag{7.94}$$

whereas the second averaged system is defined as

$$\begin{cases} \tilde{\boldsymbol{x}}^{+} & = \tilde{\boldsymbol{x}} - \alpha\beta S(k)F(\tilde{\boldsymbol{x}}) \\ \tilde{\boldsymbol{\xi}}^{+} & = \tilde{\boldsymbol{\xi}} + \alpha S(k)\left(F(\tilde{\boldsymbol{x}}) - \tilde{\boldsymbol{\xi}}\right) \\ \tilde{\boldsymbol{\mu}}^{+} & = (I - S_{\mu}(k))\tilde{\boldsymbol{\mu}} + S_{\mu}(k))\mathcal{R}\tilde{\boldsymbol{\mu}} \\ \boldsymbol{\kappa}^{+} & = \boldsymbol{\kappa} + S_{\tau}(k) \\ k^{+} & = k+1. \end{cases} \tag{7.95}$$

To prove Assumption 7.1, the following two Lemmas are needed:

Lemma 7.25. *For any solution of the first boundary layer system* $(\boldsymbol{x}_{\mathrm{bl}}^{1}, \boldsymbol{\xi}_{\mathrm{bl}}^{1}, \boldsymbol{\mu}_{\mathrm{bl}}^{1})$ *and compact set* C*, such that* $\boldsymbol{x}_{\mathrm{bl}}^{1} \in C$ *for all* $k \in \operatorname{dom}\left(\boldsymbol{x}_{\mathrm{bl}}^{1}\right)$*, it holds that:*

$$\left\| \frac{1}{N} \sum_{i=1}^{N} \left[2A^{-1} J\left(\boldsymbol{x}_{\mathrm{bl}}^{1}(i) + A\mathbb{D}\boldsymbol{\mu}_{\mathrm{bl}}^{1}(i)\right) \mathbb{D}\boldsymbol{\mu}_{\mathrm{bl}}^{1}(i) - F(\boldsymbol{x}_{\mathrm{bl}}^{1}(i)) - \mathcal{O}(\bar{a}) \right] S(i) \right\| \leq \sigma_1(N), \tag{7.96}$$

where $\sigma_1 : \mathbb{R}^+ \to \mathbb{R}^+$ *is a function of class* $\mathcal{L}$. □

Proof. First, we note that the difference in the previous inequality for rows corresponding to agent i equals zero whenever the agent is not jumping. This motivates us to study the "isolated" system of agent i instead of the group dynamics in (7.92). Consider the dynamics

$$\mu^{i}(\kappa_i + 1) = \mathcal{R}_i \mu^{i}(\kappa_i). \tag{7.97}$$

Without the loss of generality, let a solution of the previous system be given by $\mu^{i}(\kappa_i) = \operatorname{col}((\cos(\omega_i^j \kappa_i), \sin(\omega_i^j \kappa_i))_{j \leq m_i})$. The solution of $\mu_{\mathrm{bl}}^{1,i}$ is similar to the solution of μ^{i}, as it also has the same samples, but they "persist" for more iterations, i.e., until the agent i jumps again. If we define the set-valued mapping $k(v,i) := \{u \mid \kappa_i(u) = v\}$ that relates the global jump counter to the internal counter of agent i, it holds that $\mu_{\mathrm{bl}}^{1,i}(k(v,i)) = \mu^{i}(v)$. Furthermore, at the sample v given by the internal counter for agent i, or given by $\bar{k}(v,i) = \max k(v,i)$ by the global counter, the internal counter of some other agent j is given by

$$\kappa_j(v,i) := \left\lfloor \Delta_j^i + \tfrac{T_i}{T_j} v \right\rfloor. \tag{7.98}$$

where $\Delta_j^i := \kappa_j^0 + \frac{\tau_i - \kappa_i^0 T_i}{T_j}$. Hence it holds $\mu_{\mathrm{bl}}^{1,j}(\bar{k}(v,i)) = \mu^{j}(\kappa_j(v,i))$. Lastly, we see that diagonal elements of $S(k)$ corresponding to agent i are different from zero for $k \in \{u \mid u = \bar{k}(v,i), v \in \mathbb{N}\}$. Let us denote the norm in (7.96) as Φ and write $N = rl + o, l \in \mathbb{N}, 0 \leq o < r$. The previous

7

iterator relations and properties of $S(k)$ allow us to bound the inequality as

$$
\begin{aligned}
N\Phi &\leq \sum_{i=1}^{M} \left\| \sum_{v=\kappa_i(0)}^{\kappa_i(0)+r_i l-1} \left[-F(\boldsymbol{x}_{\mathrm{bl}}) - \mathcal{O}(\bar{a}) + \tfrac{2}{a_i} J_i\left(\boldsymbol{x}^1_{\mathrm{bl}} + A\mathbb{D}\boldsymbol{\mu}^1_{\mathrm{bl}}(\bar{k}(v,i))\right) \mathbb{D}_i \mu^{1,i}_{\mathrm{bl}}(\bar{k}(v,i)) \right] \right\| + \Phi_{\mathrm{r}} \\
&\leq \sum_{i=1}^{M} \left\| \sum_{v=\kappa_i(0)}^{\kappa_i(0)+r_i l-1} \left[\tfrac{2}{a_i} J_i\left(\boldsymbol{x}^1_{\mathrm{bl}}\right) \mathbb{D}_i \mu_i(v) + 2\nabla_{x_i} J_i(\boldsymbol{x}^1_{\mathrm{bl}})^\top \mathbb{D}_i \mu_i(v) \mathbb{D}_i \mu_i(v) - \nabla_{x_i} J_i(\boldsymbol{x}^1_{\mathrm{bl}}) \right.\right. \\
&\quad \left.\left. + 2\sum_{j\neq i}^{M} \nabla_{x_j} J_i(\boldsymbol{x}^1_{\mathrm{bl}})^\top \mathbb{D}_j \mu_i(\kappa_j(v,i)) \mathbb{D}_i \mu_i(v) \right] \right\| + \Phi_{\mathrm{r}} \\
&\leq \sum_{i=1}^{M} \sum_{u=1}^{m_i} \left\| \sum_{v=\kappa_i(0)}^{\kappa_i(0)+r_i l-1} \left[\tfrac{2}{a_i} J_i\left(\boldsymbol{x}^1_{\mathrm{bl}}\right) \sin\left(\omega_i^u v\right) + \nabla_{x_i^u} J_i(\boldsymbol{x}^1_{\mathrm{bl}}) \left[2\sin\left(\omega_i^u v\right) \sum_{j=1}^{m_i} \sin(\omega_i^j v) - 1 \right] \right.\right. \\
&\quad \left.\left. + 2\sum_{j\neq i}^{M} \sum_{s=1}^{m_j} \nabla_{x_j^s} J_i(\boldsymbol{x}^1_{\mathrm{bl}}) \sin(\omega_j^s \kappa_j(v,i)) \sum_{j=1}^{m_i} \sin(\omega_i^j v) \right] \right\| + \Phi_{\mathrm{r}}, \qquad (7.99)
\end{aligned}
$$

where

$$
\Phi_{\mathrm{r}} := \sum_{i=1}^{M} r_i m M \max_{\boldsymbol{x}\in C} \left\| \tfrac{1}{a_i} J\left(\boldsymbol{x} + A\mathbb{B}\right) \right\| + \left\| F(\boldsymbol{x}) + \mathcal{O}(\bar{a}) \right\|. \qquad (7.100)
$$

Using Lemma (7.23) and Assumption 7.18, we can derive the upper bounds of all of the sums in the norm, apart from the last one, which contains addends of form $\sin(\omega_i^j v)\sin(\omega_j^s \kappa_j(v,i))$. Using the same procedure as in the proof of Lemma 7.22 and Equation (7.98), we find the equivalent exponential representation. For some ω_1, ω_2, consider the sum

$$
\begin{aligned}
\sum_{v=\kappa_i(0)}^{\kappa_i(0)+r_i l-1} e^{j\left(\omega_1 v + \omega_2 \left\lfloor \Delta_j^i + \frac{p_i}{p_j} v \right\rfloor\right)} &= \sum_{v=\kappa_i(0)}^{\kappa_i(0)+r_i-1} e^{j\left(\omega_1 v + \omega_2 \left\lfloor \Delta_j^i + \frac{p_i}{p_j} v \right\rfloor\right)} \times \sum_{u=0}^{l-1} e^{j(\omega_1 r_i + \omega_2 r_j)u} \\
&= \frac{1 - e^{j(\omega_1 r_i + \omega_2 r_j)l}}{1 - e^{j(\omega_1 r_i + \omega_2 r_j)}} \sum_{v=\kappa_i(0)}^{\kappa_i(0)+r_i-1} e^{j\left(\omega_1 v + \omega_2 \left\lfloor \Delta_j^i + \frac{p_i}{p_j} v \right\rfloor\right)},
\end{aligned}
$$

where the second equality follows from Assumption 7.13, the properties of the least common multiple $p = p_i r_i = p_j r_j$, and last equality holds for $\omega_1 r_i + \omega_2 r_j \neq 2\pi z, z \in \mathbb{Z}$. Thus, we have

$$
\left\| \sum_{v=\kappa_i(0)}^{\kappa_i(0)+r_i l-1} e^{j\left(\omega_1 v + \omega_2 \left\lfloor \Delta_j^i + \frac{p_i}{p_j} v \right\rfloor\right)} \right\|^2 \leq \left\| \frac{r_i}{1 - e^{j(\omega_1 r_i + \omega_2 r_j)}} \right\|^2 \leq C_e,
$$

where C_e is the supremum with respect to all possible combinations of r_i and ω_i^j. The rest of the procedure follows the same steps as after Equation (7.73) in the proof of Lemma 7.23. The bound that holds regardless of the initial conditions of the timers $\boldsymbol{\tau}(0)$. Thus, the Lemma holds. ∎

Lemma 7.26. *For any solution of the second boundary layer system* $(\boldsymbol{x}^2_{\mathrm{bl}}, \boldsymbol{\xi}^2_{\mathrm{bl}})$*, it holds that:*

$$\left\| \frac{\gamma}{N} \sum_{i=1}^{N} S(i) \left[\boldsymbol{\xi}^2_{\mathrm{bl}}(i) - F(\boldsymbol{x}^2_{\mathrm{bl}}(i)) \right] \right\| \leq \sigma_2(N), \tag{7.101}$$

where $\sigma_2 : \mathbb{R}^+ \to \mathbb{R}^+$ *is a function of class* $\mathcal{L}$. □

Proof. The proof is analogous to the proof of Lemmas 7.23 and 7.25. ■

8

Singular perturbations for boundary layer flows and jumps

There are two ways to do great mathematics. The first is to be smarter than everybody else. The second way is to be stupider than everybody else - but persistent.

Raoul Bott

I have discovered a truly remarkable proof of this theorem which this margin is too small to contain.

Pierre de Fermat

We present a singular perturbation theory applicable to systems with hybrid boundary layer systems and hybrid reduced systems with jumps from the boundary layer manifold. First, we prove practical attractivity of an adequate attractor set for small enough tuning parameters and a sufficiently long time between almost all jumps. Second, under mild conditions on the jump mapping, we prove semi-global practical asymptotic stability of a restricted attractor set. Finally, for certain classes of dynamics, we prove semi-global practical asymptotic stability of the restricted attractor set for small enough tuning parameters and sufficiently long periods between almost all jumps of the slow states only.

This chapter is partly based on S. Krilašević and S. Grammatico. "Stability of singularly perturbed hybrid systems with restricted systems evolving on boundary layer manifolds". In: arXiv:2303.18238 (Mar. 2023). arXiv:2303.18238 [cs, eess, math]. DOI: 10.48550/arXiv.2303.18238.

8.1 Introduction

Realistic modeling of many control systems requires high-order nonlinear differential equations that might be difficult to analyze fully. To alleviate this problem, we often design control systems with various parameters that, with proper tuning, can effectively reduce the order of the model and thus simplify the stability analysis. The main theoretical framework for such analysis is singular perturbation theory [138], [29]. The associated model reduction is accomplished by splitting the states into fast and slow states; for each constant value of the slow states, the fast states should converge to an equilibrium point defined by the slow states, and the union of these equilibrium points for all possible slow states defines the so-called boundary layer manifold. Then, the reduced system contains just the slow states and their dynamics, assuming they are evolving along that manifold.

Singular perturbation theory has been successfully applied to equilibrium seeking in optimization and game theory. One common method of applying zeroth-order algorithms to dynamical systems with cost measurements as output is through a time-time scale separation of the controller and the plant, as demonstrated in [12] and [17]. Timescale separation can be useful for algorithms where consensus on specific states must be reached before initiating the equilibrium seeking process [139], [140], [141], [142]. Furthermore, in some works [17], [143], [122], via singular perturbation analysis, the (pseudo)gradient estimate is filtered before being incorporated into the algorithm. Singular perturbation theory is also used to demonstrate algorithm convergence in problems with slowly varying parameters [144].

Several extensions of singular perturbation theory are known for hybrid systems. In [78], the authors examine a singularly perturbed system in which the boundary layer system is continuous and the reduced system is hybrid, and both render the corresponding sets globally asymptotically stable. While the work in [79] proposes averaging theory results, it can also be used to prove stability in singularly perturbed systems. Similarly to [78], the authors assume that the boundary layer system is continuous and that the averaged system, which plays the role of the reduced system, is hybrid. In [145], the same authors extend the results for the case when the boundary layer system itself is hybrid. In the aforementioned works, the reduced system is derived by assuming that the slow states "flow" along the boundary layer manifold, while the slow states *do not* jump from that manifold. Therefore, the reduced system jumps cannot use the properties of the boundary layer manifold to support stabilization; essentially, only the continuous dynamics are used to prove stability, "despite" the jumps.

For the discrete-time dynamics to support the stabilization of singularly perturbed systems, we can design the dynamics so that we jump when we are in the proximity of the manifold. This scenario, in principle, is similar to that in [146], [147] where the authors prove that there exists a sampling period such that a discrete-time optimization-based controller (the reduced system) can find a neighborhood of the optimum of a steady-state output map of a continuous system with an input (boundary layer system). In [81], the authors take a step further and design an event-triggered framework to accomplish the same task by measuring the changes in the output and, in turn, determine when the system has approached the boundary layer manifold. Although these methods better incorporate discrete-time reduced system dynamics, the boundary layer system is still only continuous. In this paper, we instead deal with a hybrid boundary layer system and thus extend the current state of the

art.

Contribution: In view of the above literature, our theoretical contributions are summarized next:

- We propose a singular perturbation theory for hybrid systems, where the reduced system takes into account the jumps from the boundary layer manifold, differently from [78], [79] where jumps are assumed not to interfere with stability. Furthermore, we allow for the set of fast variables not to be bounded a priori, thus enabling the use of reference trajectories and counter variables in the boundary layer system.

- We prove semi-global practical asymptotic stability of the restricted attractor set under certain mild assumptions on the jump mapping. This attractor set includes only the steady-state values of the fast states that correspond to the slow attractor states rather than the complete range of possible fast variables.

- We show that in a system resembling the one described in [145], where a distinction is made between jumps in the slow and fast states, the aforementioned results remain valid if there are sufficiently long intervals between nearly all jumps in the *slow states*.

Our theory enables the analysis of multiple timescale control systems where both the controller and the plant are hybrid. Furthermore, as the jumps occur at the boundary layer, it would also be possible to incorporate state/output feedback into the controller jump mappings.
We define semi-global practical asymptotic stability (SGPAS) similarly as in [148].

Definition 8.1 (SGPAS). *The set $\mathcal{A}$ is SGPAS as $(\varepsilon_1,\dots,\varepsilon_k)\to 0$ for the parametrized hybrid system $\mathcal{H}_\varepsilon$, if for each given $\Delta>\delta>0$, there exists a parameter ε_1^* such that for each $\varepsilon_1\in\left(0,\varepsilon_1^*\right)$ there exists $\varepsilon_2^*(\varepsilon_1)>0$ such that for each $\varepsilon_2\in(0,\varepsilon_2^*(\varepsilon_1))$ ... there exists $\varepsilon_k^*(\varepsilon_{k-1})>0$ such that for each $\varepsilon_k\in\left(0,\varepsilon_k^*(\varepsilon_{k-1})\right)$ it holds:*

1. *(Semi-global stability) for each $R\geq\delta$, there exists $r>0$, such that $\|\phi(l,i)\|_{\mathcal{A}}\leq r \implies \|\phi(t,j)\|_{\mathcal{A}}\leq R$ for $l+i\leq t+j$ and each solution ϕ.*

2. *(Practical attractivity) for each R,r that satisfy $\Delta\geq R\geq r\geq\delta$, there exists a period $T(r,R)\geq 0$, such that $\|\phi(l,i)\|_{\mathcal{A}}\leq R \implies \|\phi(t,j)\|_{\mathcal{A}}\leq r$ for all $t+j\geq T(r,R)+l+i$ and each solution ϕ.* □

8.2 Singular perturbation theory for hybrid systems

We consider two different system setups, with the first case featuring a hybrid reduced system and a continuous boundary layer system. In the second, both the reduced and boundary layer system are hybrid. Despite the different scenarios, we require similar assumptions in all configurations. Notably, we provide the most comprehensive coverage of the first case.

8.2.1 Continuous boundary layer dynamics

We consider the following hybrid dynamical system, denoted by $\mathcal{H}_1$:

$$\dot{x} \in \begin{bmatrix} I_{n_1} & 0 \\ 0 & \frac{1}{\varepsilon} I_{n_2} \end{bmatrix} F(x), \qquad \text{if } x \in \mathcal{X}_1 \times \mathcal{X}_2, \tag{8.1a}$$

$$x^+ \in G(x), \qquad \text{if } x \in D_1 \times D_2, \tag{8.1b}$$

where $x := \mathrm{col}(x_1, x_2) \in \mathcal{X}_1 \times \mathcal{X}_2 \subset \mathbb{R}^{n_1} \times \mathbb{R}^{n_2}$ are the system states, $\varepsilon > 0$ is small parameter used to speed up the x_2 dynamics, $\mathcal{X}_1, D_1 \subset \mathcal{X}_1$, $\mathcal{X}_2, D_2 \subset \mathcal{X}_2$ are flow and jump sets for the slow states x_1 and the fast states x_2, respectively. Other than ε, the system is implicitly parametrized by parameters β, γ and τ i.e. $F = F_{\beta,\gamma,\tau}$ and $G = G_{\beta,\gamma,\tau}$. As it is common for hybrid dynamical systems, we postulate certain regularity assumptions that provide useful properties.

Assumption 8.2. *The hybrid dynamical system in (8.1) satisfies the basic regularity assumptions for hybrid systems [80, Assum. 6.5] for all parameters $\beta \in (0, \overline{\beta}], \gamma \in (0, \overline{\gamma}]$, $\tau \in (0, \overline{\tau}]$. The mapping G satisfies item [80, Assum. 6.5, A3] also for $\beta = 0, \gamma = 0, \tau = 0$. Furthermore, all of the systems' solutions are complete.* □

Furthermore, we define two auxiliary systems in view of that in (8.1), the boundary layer system and the reduced system. The former, $\mathcal{H}_1^\rho$, for any given constant $\rho > 0$, is defined as

$$\dot{x} \in \begin{bmatrix} 0 & 0 \\ 0 & I_{n_2} \end{bmatrix} F(x) \qquad x \in ((\mathcal{A} + \rho\mathbb{B}) \cap \mathcal{X}_1) \times \mathcal{X}_2, \tag{8.2}$$

where $\mathcal{A} \subset \mathbb{R}^n$ is the equilibrium set of a reduced system to be introduced later. Furthermore, the system dynamics are parametrized by a small parameter β, which is used for tuning the desired convergence radius. In (8.2), the dynamics of x_1 are frozen, i.e., $\dot{x}_1 = 0$. Thus they approximate the behavior of those in (8.1) when $\varepsilon > 0$ is chosen very small. Since the first state is constant, it is natural to assume that the equilibrium set, if it exists, contains all possible x_1, i.e., the ones contained in the set $(\mathcal{A} + \rho\mathbb{B}) \cap \mathcal{X}_1$, and that for every x_1, there exists a specific set of equilibrium points x_2. We characterize this dependence with the "steady-state" mapping H and assume that it satisfies certain regularity properties [78, Assum. 2], [17, Assum. 2].

Assumption 8.3. *The set-valued mapping $H : \mathcal{X}_1 \rightrightarrows \mathcal{X}_2$,*

$$H(\overline{x}_1) := \{\overline{x}_2 \mid F(\overline{x}_1, \overline{x}_2) = 0\} \tag{8.3}$$

is outer semicontinuous and locally bounded; for each $\overline{x}_1 \in \mathcal{X}_1, H(\overline{x}_1)$ is a non-empty subset of $\mathcal{X}_2$. □

Now, we can define the complete equilibrium set of the system in (8.2), the boundary layer manifold, as

$$\mathcal{M}_\rho := \{(x_1, x_2) \mid x_1 \in (\mathcal{A} + \rho\mathbb{B}) \cap \mathcal{X}_1, x_2 \in H(x_1)\}. \tag{8.4}$$

The set $\mathcal{M}_\rho$ may contain some unbounded states corresponding to the logic states or reference trajectories of the boundary layer system. We denote the bounded states with

$x_2' \in \mathcal{X}_2'$ and the unbounded states with $x_2'' \in \mathcal{X}_2''$, $\mathcal{X}_2' \times \mathcal{X}_2'' = \mathcal{X}_2$. Furthermore, we assume that these unbounded states only affect each other during jumps and that the bounded states are a priori contained in a compact set.

Assumption 8.4. *The jump mapping G in (8.1b), and the steady-state mapping H in 8.3 are decomposed as follows:*

$$G(x) = \begin{bmatrix} G_1(x_1, x_2') \\ G_2'(x) \end{bmatrix}, \tag{8.5}$$

$$H(x_1) = H_1(x_1) \times \mathcal{X}_2'', \tag{8.6}$$

where $G_1 : \mathcal{X}_1 \times \mathcal{X}_2' \rightrightarrows \mathcal{X}_1 \times \mathcal{X}_2'$, $G_2' : \mathcal{X} \rightrightarrows \mathcal{X}_2''$, and $H_1 : \mathcal{X}_1 \rightrightarrows \mathcal{X}_2'$. □

Assumption 8.5. *The set $\mathcal{X}_2'$ in Assumption 8.4 is compact.* □

Furthermore, we assume that the set $\mathcal{M}_\rho$ is SGPAS for boundary layer dynamics in Equation (8.2).

Assumption 8.6. *The set $\mathcal{M}_\rho$ in (8.4) is SGPAS as $\beta \to 0$ for the dynamics in (8.2). Let $\Delta > \delta > 0$ be given by the definition of SGPAS. For every $\Delta > 0$, the corresponding Lyapunov function is given by*

$$\underline{\alpha_{2,\rho}}\left(\|x\|_{\mathcal{M}_\rho}\right) \leq V_{2,\rho}(x) \leq \overline{\alpha_{2,\rho}}\left(\|x\|_{\mathcal{M}_\rho}\right) \tag{8.7a}$$

$$\sup_{\begin{bmatrix} f_1 \\ f_2 \end{bmatrix} \in F(x)} \left\langle \nabla V_{2,\rho}(x) \,\middle|\, \begin{bmatrix} 0 \\ f_2 \end{bmatrix} \right\rangle \leq -\alpha_{2,\rho}(\|x\|_{\mathcal{M}_\rho})$$

$$\text{for all } x \text{ such that } \|x\|_{\mathcal{M}_\rho} \geq \alpha_\beta(\beta), \tag{8.7b}$$

$$\sup_{\begin{bmatrix} f_1 \\ f_2 \end{bmatrix} \in F(x)} \left\langle \nabla V_{2,\rho}(x) \,\middle|\, \begin{bmatrix} 0 \\ f_2 \end{bmatrix} \right\rangle \leq \hat{\alpha}_\beta(\beta)$$

$$\text{for all } x \text{ such that } \|x\|_{\mathcal{M}_\rho} \leq \alpha_\beta(\beta) \tag{8.7c}$$

$$\nabla V_{2,\rho}(x) = 0 \text{ for all } x \in \mathcal{M}_\rho, \tag{8.7d}$$

where $\alpha_{2,\rho}, \overline{\alpha_{2,\rho}}, \alpha_{2,\rho}, \alpha_\beta, \hat{\alpha}_\beta$ are functions of class $\mathcal{K}$, where $\alpha_{2,\rho}, \alpha_\beta$ are possibly parametrized by Δ. Furthermore, for each compact set $K \in \mathcal{X}_1$, there exists $M > 0$, such that

$$\sup_{x \in K \times \mathcal{X}_2} \left\|V_{2,\rho}(x)\right\| + \left\|\nabla_{x_1} V_{2,\rho}(x)\right\| \leq M. \tag{8.8}$$

Remark 8.7. *In Assumption 8.6, we allow the set $\mathcal{X}_2$ to be unbounded. Nevertheless, the Lyapunov function is assumed to take bounded values, as in (8.8). For example, this can be achieved if the Lyapunov function does not depend on the states from the unbounded set.* □

On the other hand, since the x_2 dynamics are much faster than those of x_1 in (8.1), from the time scale of the latter, it seems that the x_2 dynamics are evolving on the manifold defined by the mapping H. To characterize this behavior, we can define the reduced system $\mathcal{H}_1^{\mathrm{r}}$ as:

$$\dot{x}_1 \in F_{\mathrm{r}}(x_1) \qquad \text{if } x_1 \in \mathcal{X}_1 \tag{8.9a}$$

$$x_1^+ \in G_{\mathrm{r}}(x_1) \qquad \text{if } x_1 \in D_1, \tag{8.9b}$$

where $F_r(x_1) := \overline{\text{co}}\{v_1 \mid (v_1, v_2) \in F(x_1, x_2), x_2 \in H(x_1)\}$, $G_r(x_1) := \{v_1 \mid (v_1, v_2) \in G(x_1, x_2), x_2 \in H(x_1)\}$. Furthermore, the system dynamics are parametrized by the parameter γ, which is used for the tuning of the convergence radius to the attractor set, and the parameter τ adjusts the minimum time interval between consecutive jumps, for *almost all* jumps of the systems in (8.1) (consequently also the reduced system in (8.9)), as formalized next:

Definition 8.8 (τ-regular jump)**.** *A jump j in a solution trajectory ϕ is a τ-*regular jump *if it occurs after an interval of flowing greater or equal than τ, i.e., $\tau_j := \sup\{|t - t'| : (t, j-1), (t', j-1) \in \operatorname{dom}\phi\} \geq \tau$. Otherwise, the jump j is called τ-irregular.* □

Assumption 8.9. *Let ϕ be any solution of the system in (8.1) with $\|\phi(0,0)\|_{\mathcal{A}\times\mathcal{X}_2} \leq \Delta$. Then, there exists a finite number of jumps N^* and finite time interval T^*, such that ϕ has at most N^* $\underline{\sigma}(\tau)$-irregular jumps, and they all occur before $t \leq T^*$, where $\underline{\sigma}$ is a function of class $\mathcal{L}$, and τ is the parameter of the system.* □

Differently from [78], where the reduced mapping is defined as $G_r(x_1) := \{v_1 \mid (v_1, v_2) \in G(x_1, x_2), x_2 \in \mathcal{X}_2\}$, the mapping in (8.9b) only includes the jumps from the stead-state "pairs" $(x_1, H(x_1))$ that belong to the manifold. Thus, our next assumption is weaker than [78, Assum. 4], as it requires that the jumps stabilize the set $\mathcal{A}$ via a much more restricted set of dynamics. This is due to the fact that the reduced mapping G_r does not contain all possible jumps from the set D_1, but only those from the boundary layer manifold $\mathcal{M}_\rho$.

Assumption 8.10. *The set $\mathcal{A}$ is SGPAS as $\gamma \to 0$ for the reduced system in (8.9). Let $\Delta > \delta > 0$ be given by the definition of SGPAS. For all $\Delta > 0$, there exists a Lyapunov function V. Its properties are given by*

$$\underline{\alpha_1}\left(\|x_1\|_{\mathcal{A}}\right) \leq V_1(x_1) \leq \overline{\alpha_1}\left(\|x_1\|_{\mathcal{A}}\right) \tag{8.10a}$$

$$\sup_{f_{1r}\in F_r(x_1)} \langle \nabla V_1(x_1) \mid f_{1r}\rangle \leq -\hat{\sigma}_\tau(\tau)\hat{\alpha}_\gamma(\gamma)\alpha_1\left(\|x_1\|_{\mathcal{A}}\right) \tag{8.10b}$$

$$\sup_{g_{1r}\in G_r(x_1)} V_1(g_{r1}) - V_1(x_1) \leq -\hat{\alpha}_\gamma(\gamma)\alpha_1\left(\|x_1\|_{\mathcal{A}}\right) \tag{8.10c}$$

$$\text{for } \|x_1\|_{\mathcal{A}} \geq \alpha_\gamma(\gamma), \tag{8.10d}$$

where $\underline{\alpha_1}, \overline{\alpha_1}, \alpha_1, \alpha_\gamma, \hat{\alpha}_\gamma$ are functions of class $\mathcal{K}$, where α_1, α_γ are possibly parametrized by Δ, and $\hat{\sigma}_\tau$ is a function of class $\mathcal{L}$. □

We claim that our original system in (8.1) renders the set $\mathcal{A}\times\mathcal{X}_2$ practically attractive if, for almost all intervals of flow, we allow the state of the system to converge to the neighborhood of the $\mathcal{M}_\rho$ manifold. The intuition is that in the neighborhood of the manifold, "the jumps of the *reduced system*" also contribute to the stabilization.

Theorem 8.11. *Let Assumptions 8.2—8.10 hold. Then the set $\mathcal{A}\times\mathcal{X}_2$ is practically attractive as $(\gamma, \frac{1}{\tau}, \varepsilon, \beta) \to 0$ for the hybrid system in (8.1).* □

Proof. See Appendix 8.A. ■

Example 1. *Consider the hybrid dynamical system*

$$\begin{cases} \dot{u} &= \gamma \max\{0, 1 - \frac{\|u\|}{R}\} \\ \dot{v} &= \frac{1}{\tau} \\ \dot{x} &= -\frac{1}{\varepsilon}(x-u) \end{cases}$$
$$if\, (u,v,x) \in [0,R]\times[0,1]\times[0,R]; \tag{8.11a}$$
$$\begin{cases} u^+ &= \frac{x}{2} \\ v^+ &= 0 \\ x^+ &= R \end{cases}$$
$$if\, (u,v,x) \in [0,R]\times\{1\}\times[0,R], \tag{8.11b}$$

where $\gamma, \tau, \varepsilon$ are tuning parameters, and $R > 0$ is the maximal trajectory radius. We show that the set $\{0\}\times[0,1]\times[0,R]$ is practically attractive. First, we see that the boundary layer system reads as

$$\begin{cases} \dot{u} &= 0 \\ \dot{v} &= 0 \\ \dot{x} &= -(x-u) \end{cases}$$
$$if\, (u,v,x) \in [0,R]\times[0,1]\times[0,R], \tag{8.12}$$

while the reduced system is given by

$$\begin{cases} \dot{u} &= \gamma \max\{0, 1 - \frac{\|u\|}{R}\} \\ \dot{v} &= \frac{1}{\tau} \end{cases}$$
$$if\, (u,v) \in [0,R]\times[0,1]; \tag{8.13a}$$
$$\begin{cases} u^+ &= \frac{u}{2} \\ v^+ &= 0 \end{cases}$$
$$if\, (u,v) \in [0,R]\times\{1\}. \tag{8.13b}$$

Assumptions 8.2—8.9 are satisfied. Regarding Assumption 8.10, let the Lyapunov function of the reduced system be $V_1(u,v) = (2-v)u^2$. It follows that

$$\begin{aligned} \dot{V}_1(u,v) &\leq -\tfrac{1}{\tau}u^2 + 4\gamma a R, \\ V_1(u^+,v^+) - V_1(u,v) &\leq -\tfrac{1}{2}u^2. \end{aligned} \tag{8.14}$$

Since the reduced system satisfies Assumption 8.10, in view of Theorem 8.11, practical attractivity is ensured. Unlike previous works [145], [78], and [79], our reduced jump mapping includes jumps only from the boundary layer, which allows us to establish attractivity results using jumps, as seen in Figure 8.1. In the aforementioned works, the reduced system jump mapping includes all possible jumps [78, Equ. 13], [79, Equ. 17], [145, Equ. 13], and and for our example, it is given by $u^+ \in [-\frac{R}{2}, \frac{R}{2}]$. Thus, the assumption on the stability for reduced system dynamics [78, Assum. 4], [79, Thm. 2], [145, Thm. 2] does not hold. □

We note that Theorem 8.11 gives us no guarantee on the attractivity of the state x_2 due to the fact that jumps can move the state arbitrarily far away from any set in $\mathcal{X}_2$ (also seen in

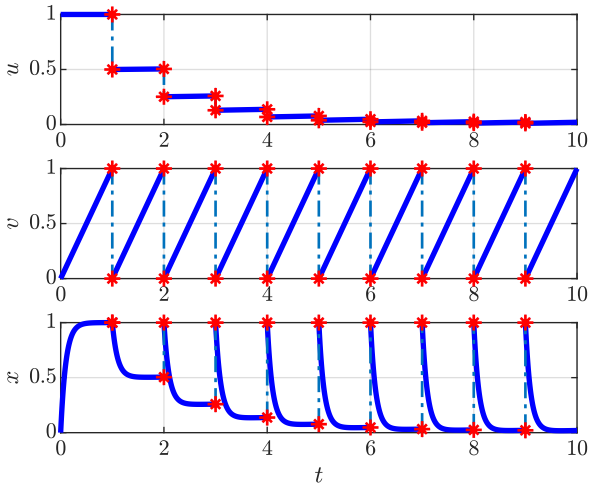

Figure 8.1: Consider the system in Example 1 with parameters $\gamma = 0.01$, $R = 1$, $\tau = 1$, $\varepsilon = 0.1$. The state trajectories are represented in the Figure. Even though the flows tend to steer the state away, the convergence of u is still achieved within the neighborhood of 0.

Figure 8.1 for jumps of state x). Under an additional assumption, it is possible to bound both the states x_1 and x_2 to a neighborhood of the set $\mathcal{M}_{\mathcal{A}} := \{(x_1, x_2) \mid x_1 \in \mathcal{A}, x_2 \in H(x_1)\}$, and prove stability.

Assumption 8.12. *The jump mapping G in (8.1b) is such that $G(\mathcal{M}_{\mathcal{A}}) \subset \mathcal{M}_{\mathcal{A}}$.* □

Assumption 8.12 is sufficient to guarantee that for any neighborhood of the equilibrium set $\mathcal{M}_{\mathcal{A}} + \bar{r}\mathbb{B}$, there exists a neighborhood $\mathcal{M}_{\mathcal{A}} + \underline{r}\mathbb{B}$, such that jumps from the latter do not exit the former, i.e. $G(\mathcal{M}_{\mathcal{A}} + \underline{r}\mathbb{B}) \subset \mathcal{M}_{\mathcal{A}} + \bar{r}\mathbb{B}$. Lastly, we do not need to assume the compactness of the set $\mathcal{X}_2'$, as the distance from the set $\mathcal{M}_{\mathcal{A}}$ also bounds the values of the x_2' state.

Theorem 8.13. *Let Assumptions 8.2—8.4, 8.6—8.12 hold. Then the set $\mathcal{M}_{\mathcal{A}}$ is SGPAS as $(\gamma, \frac{1}{\tau}, \varepsilon, \beta) \to 0$ for the hybrid system in (8.1).* □

Proof. See Appendix 8.B. ■

Example 2. *We consider a hybrid dynamical system similar to one in (8.11):*

$$\begin{cases} \dot{u} &= \gamma \\ \dot{v} &= \frac{1}{\tau} \\ \dot{x} &= -\frac{1}{\varepsilon}(x - u) \end{cases}$$

$$\text{if } (u, v, x) \in \mathbb{R} \times [0, 1] \times \mathbb{R}; \tag{8.15a}$$

$$\begin{cases} u^+ &= \frac{x}{2} \\ v^+ &= 0 \\ x^+ &= 2x \end{cases}$$

$$\text{if } (u, v, x) \in \mathbb{R} \times \{1\} \times \mathbb{R}, \tag{8.15b}$$

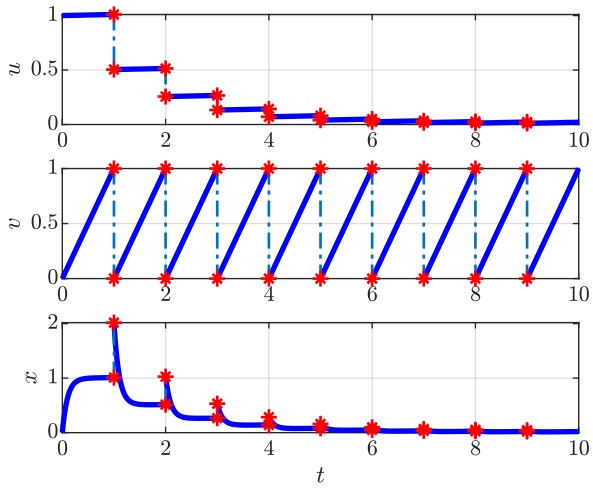

Figure 8.2: Consider the system in Example 2 with parameters $\gamma = 0.01$, $R = 1$, $\tau = 1$, $\varepsilon = 0.1$. The state trajectories are represented in the Figure. Due to the new jump mapping of x, the convergence of x is also achieved within the neighborhood of 0.

where $\gamma, \tau, \varepsilon$ are tuning parameters. Differently from (8.11), the jump mapping is such that Assumption 8.12 is satisfied. Furthermore, as Theorem 8.13 does not require compactness of the set $\mathcal{X}_2'$ in Assumption 8.5, the flow and jump sets are both unbounded. The boundary layer system has the same dynamics as the system in (8.12), apart from the flow set, which now reads as $\mathbb{R} \times [0,1] \times \mathbb{R}$. The reduced system is given by

$$\begin{cases} \dot{u} &= \gamma \\ \dot{v} &= \frac{1}{\tau} \end{cases} \quad \text{if } (u,v) \in \mathbb{R} \times [0,1]; \tag{8.16a}$$

$$\begin{cases} u^+ &= \frac{u}{2} \\ v^+ &= 0 \end{cases} \quad \text{if } (u,v) \in \mathbb{R} \times \{1\}. \tag{8.16b}$$

Similarly to the previous example, all the Assumptions hold, thus due to Theorem 8.13, the set $\{0\} \times [0,1] \times \{0\}$ is SGPAS as $(\gamma, \frac{1}{\tau}, \varepsilon, \beta) \to 0$ for the dynamics in (8.16a). Differently from [145, Thm. 2], [78, Thm. 1], and [79, Thm. 2, Cor. 2] where the fast states *are only a priori bounded to a compact set, here we can prove their convergence to the equilibrium set, as seen in Figure 8.2.* □

8.2.2 Hybrid boundary layer dynamics

Theorems 8.11 and 8.13 assume a lower limit on the time between *all consecutive jumps* that occur in the system in (8.1). However, under certain conditions, it is possible to make a distinction between consecutive jumps of x_1 and the consecutive jumps of x_2. This is useful when the convergence of the boundary layer system is, in fact, driven by jumps in x_2, and imposing a high lower limit on the period between consecutive jumps slows down

convergence. Consider the following hybrid dynamical system, denoted with $\mathcal{H}_2$:

$$\dot{x} \in \begin{bmatrix} I_{n_1} & 0 \\ 0 & \frac{1}{\varepsilon} I_{n_2} \end{bmatrix} F(x), \text{ if } x \in \mathcal{X}_1 \times \mathcal{X}_2 \tag{8.17a}$$

$$x^+ \in \begin{cases} \begin{bmatrix} x_1 \\ G_2(x) \end{bmatrix}, \text{ if } x \in \mathcal{X}_1 \times D_2 \\ \begin{bmatrix} G_1(x) \\ x_2 \end{bmatrix}, \text{ if } x \in D_1 \times \mathcal{X}_2 \\ \begin{bmatrix} x_1 \\ G_2(x) \end{bmatrix} \cup \begin{bmatrix} G_1(x) \\ x_2 \end{bmatrix}, \text{ if } x \in D_1 \times D_2. \end{cases} \tag{8.17b}$$

In this formulation, the distinction between the jumps of states x_1 and x_2 is highlighted because during the jumps of x_1, x_2 stays constant, and vice versa. Furthermore, we define the boundary layer system, $\mathcal{H}_2^\rho$, as

$$\dot{x} \in \begin{bmatrix} 0 & 0 \\ 0 & I_{n_2} \end{bmatrix} F(x) \qquad \text{if } x \in \mathcal{X}_1 \times \mathcal{X}_2, \tag{8.18a}$$

$$x^+ \in \begin{bmatrix} x_1 \\ G_2(x) \end{bmatrix} \qquad \text{if } x \in \mathcal{X}_1 \times D_2, \tag{8.18b}$$

and the reduced system, $\mathcal{H}_2^r$, as

$$\dot{x}_1 \in F_r(x_1) \qquad \text{if } x_1 \in \mathcal{X}_1, \tag{8.19a}$$

$$x_1^+ \in G_r(x_1) \qquad \text{if } x_1 \in D_1, \tag{8.19b}$$

where $F_r(x_1) := \overline{\text{co}}\{v_1 \mid (v_1, v_2) \in F(x_1, x_2), x_2 \in H(x_1)\}$, $G_r(x_1) := \{v_1 \mid v_1 \in G_1(x_1, x_2), x_2 \in H(x_1)\}$. Differently from the boundary layer system in (8.2), jumps are also included in this formulation, while the formulation of the reduced system is the same. Next, we pose analogous technical assumptions as for the system in (8.1) and, in turn, provide results analogous to Theorem 8.13.

Assumption 8.14. *The hybrid dynamical system in (8.17) satisfies the same conditions as in Assumption 8.2.* □

Assumption 8.15. *The jump mapping G in (8.17b), and the steady-state mapping H in 8.3 are decomposed as in Equations (8.5) and (8.6).* □

Assumption 8.16. *The set $\mathcal{M}_\rho$ is SGPAS as $\beta \to 0$ for the dynamics in (8.18). Let $\Delta > \delta > 0$ be given by the definition of SGPAS. The corresponding Lyapunov function is given by (8.7), with the additional equation*

$$\sup_{g_1 = x_1, g_2 \in G_2(x)} V_{2,\rho}(g) - V_{2,\rho}(x) \leq 0,$$

and for each compact set $K \in \mathcal{X}_1 \times \mathcal{X}_2'$, there exists $M > 0$, such that

$$\sup_{x \in K \times \mathcal{X}_2''} \left\| V_{2,\rho}(x) \right\| + \left\| \nabla_{x_1} V_{2,\rho}(x) \right\| \leq M. \tag{8.20}$$

Assumption 8.17. *The set $\mathcal{A}$ is SGPAS as $\gamma \to 0$ for the reduced system in (8.19). Let $\Delta > \delta > 0$ be given by the definition of SGPAS. For every $\Delta > 0$, the corresponding Lyapunov function is given by Equation (8.10) with the redefined mappings in (8.19).* □

Definition 8.18 (τ-regular jump in x_1)**.** *A jump j in a solution trajectory ϕ of the system in (8.17) is a τ-*regular in x_1 jump *if it occurs after an interval of flowing in the x_1 state greater or equal than τ, i.e. $\tau_j^1 := \min\{|t-t'| : \phi_1(t,j+1) \in G_1(\phi(t,j)); \phi_2(t,j+1) = \phi_2(t,j); (t,j),(t,j+1) \in \operatorname{dom}\phi; \phi_1(t',j'+1) \in G_1(\phi(t',j')); \phi_2(t',j'+1) = \phi_2(t',j'); (t',j'),(t',j'+1) \in \operatorname{dom}\phi; j' > j\} \geq \tau$. Otherwise, if τ_j^1 exists and $\tau_j^1 < \tau$, jump j is called τ-irregular in x_1.* □

Assumption 8.19. *Let ϕ be any solution of the system in (8.17) with $\|\phi(0,0)\|_{\mathcal{A}\times\mathcal{X}_2} \leq \Delta$. Then, there exists a finite number of jumps N^* and finite time interval T^*, such that ϕ has at most N^* $\underline{\sigma}(\tau)$-irregular jumps in x_1, and they all occur before $t \leq T^*$, where $\underline{\sigma}$ is a function of class $\mathcal{L}$.* □

Corollary 8.20. *Let Assumptions 8.3, 8.12—8.19 hold. Then the set $\mathcal{M}_{\mathcal{A}}$ is SGPAS as $(\gamma, \frac{1}{\tau}, \varepsilon, \beta) \to 0$ for the hybrid system in (8.17).* □

Proof. The proof is analogous to the proofs of Theorems 8.11 and 8.13. An equivalent for Lemma 8.23 can be constructed with jumps of the x_2 state. The rest of the proof is essentially the same. ■

8.3 Illustrative example

In [8], the issue of connectivity control was approached as a Nash equilibrium problem. In numerous practical situations, multi-agent systems are constructed with the goal of maintaining specific connectivity as a secondary objective in addition to their primary objective. In the subsequent discussion, we consider a comparable problem in which each agent is responsible for detecting an unknown signal source while preserving a certain level of connectivity. Unlike [8], both the robots and the controllers have hybrid dynamics in our example.

Consider a multi-agent system consisting of unicycle vehicles, indexed by $i \in \mathcal{I} := \{1, \dots N\}$. Each agent is tasked with locating a source of a unique unknown signal. The strength of all signals abides by the inverse-square law, i.e., proportional to $1/r^2$. Therefore, the inverse of the signal strength can be used as a cost function. Additionally, the agents must not drift apart from each other too much, as they should provide quick assistance to each other in case of critical failure. This is enforced by incorporating the signal strength of fellow agents in the cost functions. Thus, we design the cost functions as follows:

$$\forall i \in \mathcal{I} : h_i(u) = \|u_i - u_i^s\|^2 + c \sum_{j \in \mathcal{I}_{-i}} \|u_i - u_j\|^2. \tag{8.21}$$

where $\mathcal{I}_{-i} := \mathcal{I} \setminus \{i\}$, $c, b > 0$ and u_i^s represents the position of the source assigned to agent i. The goal of each agent is to minimize its cost function, and the solution to this problem is a Nash equilibrium.

8.3.1 Unicycle dynamics

As the unicycles are dynamical systems, a reference tracking controller is necessary in order to move them to the desired positions. In our example, let each agent implement a hybrid feedback controller similar to one in [149] for trajectory tracking:

$$\begin{aligned}
&\chi_i^{\mathrm{u}} = \mathrm{col}\left(x_i, y_i, \theta_i^e, \tau_i, \theta_i, \hat{v}_i, \hat{\omega}_i\right),\\
&\dot{\chi}_i^{\mathrm{u}} = F_i^{\mathrm{u}}(\chi_i^{\mathrm{u}}) := \mathrm{col}\left(\hat{v}_i\cos(\theta_i), \hat{v}_i\sin(\theta_i), \omega_{\mathrm{r}} - \hat{\omega}_i, \tfrac{1}{\sigma_i}, \hat{\omega}_i, 0, 0\right)\\
&\text{if } \chi_i^{\mathrm{u}} \in C_i^{\mathrm{u}} := \mathbb{R}^3 \times [0,1] \times \mathbb{R}^3, \qquad (8.22a)\\
&\chi_i^{\mathrm{u}+} = G_i^{\mathrm{u}}(\chi_i^{\mathrm{u}}) := \mathrm{col}\left(x_i, y_i, \theta_i^e, 0, \theta_i, v_i, \omega_i\right)\\
&\text{if } \chi_i^{\mathrm{u}} \in D_i^{\mathrm{u}} := \mathbb{R}^3 \times \{1\} \times \mathbb{R}^3, \qquad (8.22b)
\end{aligned}$$

where $v_i = c_1(x_i^e - c_3\omega_i y_i^e) - c_3 c_{2,i}(\omega_{\mathrm{r}} - \omega_i)y_i^e + c_3\omega_i^2 x_i^e$, $x_i^e := \cos(\theta_i)(u_i^1 - x_i) + \sin(\theta_i)(u_i^2 - y_i)$, $y_i^e := -\sin(\theta_i)(u_i^1 - x_i) + \cos(\theta_i)(u_i^2 - y_i)$, $\theta_i^e = \theta_{\mathrm{r}} - \theta_i$, $\omega_i := \omega_{\mathrm{r}} + c_{2,i}\theta_i^e$, $\dot{\theta}_{\mathrm{r}} = \omega_{\mathrm{r}} = const.$, $c_1, c_{2,i}, c_3 > 0$ are tuning parameters, σ_i is the sampling period parameter, u_i^1 and u_i^2 are the reference positions. Differently from [149], the jumps are triggered by a timer, and the reference trajectory is that of a unicycle with a fixed position (u_i^1, u_i^2) and constant rotational velocity ω_{r}. Similarly to [149, Lemma 4., Thm. 5], it is possible to prove that the dynamics in (8.22) render the set $\{\mathrm{col}\left(u_i^1, u_i^2, 0\right)\} \times \tilde{\mathcal{T}}_i \times \mathbb{R}^3$ SGPAS as $\sigma_i \to 0$.

Theorem 8.21. *For $c_{2,i} = \sigma_i$, $c_3 = \frac{1}{3\omega_{\mathrm{r}}}$, $c_1 = \frac{1}{2c_3}$, the dynamics in (8.22) render the set $\{\mathrm{col}\left(u_i^1, u_i^2, 0\right)\} \times \tilde{\mathcal{T}}_i \times \mathbb{R}^3$ SGPAS as $\sigma_i \to 0$.* □

Proof. See Appendix 8.C. ■

From the proof of Theorem 8.21, it follows that system in (8.22), for all $i \in \mathcal{I}$, satisfies Assumptions 8.16.

8

8.3.2 Nash equilibrium seeking reference controller

To steer the reference positions toward the Nash equilibrium, we implement the following asynchronous zeroth-order controller:

$$\begin{aligned}
&\chi^{\mathrm{c}} = \mathrm{col}\left(\boldsymbol{u}, \boldsymbol{\xi}, \boldsymbol{\mu}, \boldsymbol{t}\right),\\
&\dot{\chi}^{\mathrm{c}} = F^{\mathrm{c}}(\chi^{\mathrm{c}}) := \mathrm{col}\left(\mathbf{0}, \mathbf{0}, \mathbf{0}, \boldsymbol{\tau}^{-1}\right)\\
&\text{if } \chi^{\mathrm{c}} \in C^{\mathrm{c}} := \mathbb{R}^m \times \mathcal{N} \times \mathbb{S}^m \times [0,1]^N, \qquad (8.23a)\\
&\chi^{\mathrm{c}+} = G^{\mathrm{c}}(\chi^{\mathrm{c}}), \text{i.e.}\\
&\begin{cases}
\boldsymbol{u}^+ = \boldsymbol{u} - \alpha\beta S_x(\boldsymbol{\tau})\boldsymbol{\xi}\\
\boldsymbol{\xi}^+ = \boldsymbol{\xi} + \alpha S_x(\boldsymbol{t})\left(2A^{-1}J(\boldsymbol{x} + A\mathbb{D}\boldsymbol{\mu})\mathbb{D}\boldsymbol{\mu} - \boldsymbol{\xi}\right)\\
\boldsymbol{\mu}^+ = (I - S_\mu(\boldsymbol{t}))\boldsymbol{\mu} + S_\mu(\boldsymbol{t}))\mathcal{R}\boldsymbol{\mu}\\
\boldsymbol{t}^+ = (I - S_\tau(\boldsymbol{t}))\boldsymbol{t}
\end{cases}\\
&\text{if } \chi^{\mathrm{c}} \in D^{\mathrm{c}} := \mathbb{R}^m \times \mathcal{N} \times \mathbb{S}^m \times \mathcal{T}_{\mathbb{R}}, \qquad (8.23b)
\end{aligned}$$

where $\boldsymbol{u} = \operatorname{col}\left(\left(u_i^1, u_i^2\right)_{i\in\mathcal{I}}\right)$ is used as the reference position for the systems in (8.22), $\boldsymbol{\xi}$ is the collective filter state bound in a compact set $\mathcal{N} \subset \mathbb{R}^N$ chosen large enough to encompass all possible values of the state for all practical applications, $\boldsymbol{\mu} \in \mathbb{S}^{2N}$ are oscillator states, $\boldsymbol{t}$ are the timer states that control the sampling of each individual robot, $\boldsymbol{\tau}^{-1} = \tau_0 \operatorname{col}\left(\left(\tau_i^{-1}\right)_{i\in\mathcal{I}}\right)$ are the sampling periods that satisfy [26, Assum. 9], $\boldsymbol{x}$ are the positions of the unicycles, $\alpha, \beta > 0$ are small time-scale separation parameters, $\mathcal{R} \coloneqq \operatorname{blkdiag}((\mathcal{R}_i)_{i\in\mathcal{I}})$, $\mathcal{R}_i \coloneqq \operatorname{blkdiag}\left(\begin{bmatrix} \cos(\omega_i^j) & -\sin(\omega_i^j) \\ \sin(\omega_i^j) & \cos(\omega_i^j) \end{bmatrix}_{j\le m_i}\right)$, $\omega_i^j > 0$ for all i and j are rotational frequencies and they satisfy [26, Assum. 8], $\mathbb{D} \in \mathbb{R}^{2N\times 4N}$ is a matrix that selects every odd row from the vector of size $2N$, $a_i > 0$ are small perturbation amplitude parameters, $A \coloneqq \operatorname{diag}((a_i)_{i\le m})$, $J(\boldsymbol{x}) = \operatorname{blkdiag}\left(\left(J_i(x_i, \boldsymbol{x}_{-i})I_{m_i}\right)_{i\in\mathcal{I}}\right)$, $\mathcal{T} \subset [0,1]^N$ is a closed invariant set in which all of the timers evolve and it excludes the initial conditions and their neighborhood for which we have concurrent sampling, $\mathcal{T}_{\mathrm{R}} \coloneqq \left(\cup_{i\in\mathcal{I}}[0,1]^{i-1}\times\{1\}\times[0,1]^{N-i}\right)\cap\mathcal{T}$ is the set of timer intervals where one agent has triggered its sampling, $S_x : \mathcal{T} \to \mathbb{R}^{m\times m}$ and $S_\tau : \mathcal{T} \to \mathbb{R}^{N\times N}$ are continuous functions that output diagonal matrices with ones on the positions that correspond to states and timers of agents with $t_i = 1$, respectively, while other elements are equal to zero, when evaluating at $\boldsymbol{t} \in \mathcal{T}_{\mathrm{R}}$.

8.3.3 The full system

We define the collective state $\chi \coloneqq \operatorname{col}\left(\chi^{\mathrm{c}}, (\chi_i^{\mathrm{u}})_{i\in\mathcal{I}}\right)$, collective flow map $F(\chi) \coloneqq \operatorname{col}(F^{\mathrm{c}}(\chi^{\mathrm{c}}), \frac{1}{\varepsilon}(F_i^{\mathrm{u}}(\chi_i^{\mathrm{u}}))_{i\in\mathcal{I}})$, collective flow set $C \coloneqq C^{\mathrm{c}} \times (C_i^{\mathrm{u}})_{i\in\mathcal{I}}$, collective jump map $G(\chi) \coloneqq \operatorname{col}(G^{\mathrm{c}}(\chi^{\mathrm{c}}), (G_i^{\mathrm{u}}(\chi_i^{\mathrm{u}}))_{i\in\mathcal{I}})$, collective flow set $D \coloneqq (D^{\mathrm{c}} \times (C_i^{\mathrm{u}})_{i\in\mathcal{I}}) \cup (C^{\mathrm{c}} \times (D_i^{\mathrm{u}})_{i\in\mathcal{I}})$, and the equilibrium set $\mathcal{A}_\chi \coloneqq \{\boldsymbol{u}^*\} \times \mathcal{N} \times \mathbb{S}^N \times \mathcal{T} \times \{\operatorname{col}(\boldsymbol{u}^*, \boldsymbol{0})\} \times [0,1]^N \times \mathbb{R}^{3N}$.
We see that the steady state mapping is given by $H(\chi^{\mathrm{c}}) = \operatorname{col}(\boldsymbol{u}, \boldsymbol{0}) \times [0,1]^N \times \mathbb{R}^{3N}$. Hence, the restricted system is equivalent to the one in [26, Equ. 22]. To show that Assumption 8.17 is satisfied, we note that [26, Thm. 1] and [26, Equ. E.10] assure that the fully discrete-time zeroth-order variant of the algorithm in [26, Equ. 22], has a Lyapunov function of the form

$$\begin{aligned} &\underline{\alpha}_{\mathrm{a}}(\|\boldsymbol{z} - \boldsymbol{u}^*\|) \le V_{\mathrm{a}}(\boldsymbol{z}) \le \overline{\alpha}_{\mathrm{a}}(\|\boldsymbol{z} - \boldsymbol{u}^*\|) \\ &V_{\mathrm{a}}(\boldsymbol{z}^+) - V_{\mathrm{a}}(\boldsymbol{z}) \le -\hat{\alpha}_\alpha(\alpha)\alpha_{\mathrm{a}}(\|\boldsymbol{z} - \boldsymbol{u}^*\|) \\ &\text{for } \|\boldsymbol{z} - \boldsymbol{u}^*\| \ge \max\{\alpha_\beta(\beta), \alpha_\alpha(\alpha)\}, \end{aligned}$$

where $\boldsymbol{z} \coloneqq \boldsymbol{u} + \boldsymbol{\eta}$, and $\boldsymbol{\eta}$ is a state of a bounded discrete system [26, Equ. 7]. For the sampled variant we have as our restricted system, we propose the following Lyapunov function

$$V_1(\boldsymbol{z}) \coloneqq \tfrac{1}{2}\langle \boldsymbol{1} - \boldsymbol{t} \mid \boldsymbol{1}\rangle\, \hat{\alpha}_\alpha(\alpha)\alpha_{\mathrm{a}}\left(\overline{\alpha}_{\mathrm{a}}^{-1}\left(\underline{\alpha}_{\mathrm{a}}(\|\boldsymbol{z} - \boldsymbol{u}^*\|)\right)\right) + V_{\mathrm{a}}(\boldsymbol{z}). \tag{8.24}$$

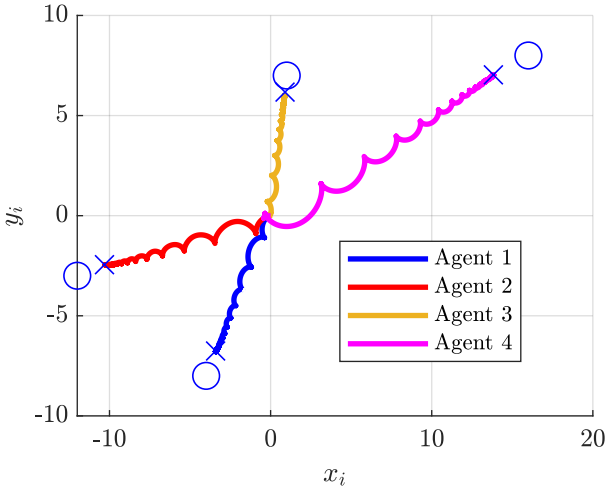

Figure 8.3: State trajectories in the $x-y$ plane. Circle symbols represent locations of the sources, while the × symbols represent locations of the NE.

Hence, it holds

$$\begin{aligned}
&\underline{\alpha}_{\mathrm{a}}(\|z-u^*\|) \leq V_1(z) \leq (\overline{\alpha}_{\mathrm{a}} + \alpha_{\mathrm{a}} \circ \overline{\alpha}_{\mathrm{a}}^{-1} \circ \underline{\alpha}_{\mathrm{a}})(\|z-u^*\|) \\
&\dot{V}_1(z) \leq -\tfrac{1}{2\tau_0} \sum_{i \in \mathcal{I}} \tau_i^{-1} \hat{\alpha}_\alpha(\alpha) \alpha_{\mathrm{a}}\left(\overline{\alpha}_{\mathrm{a}}^{-1}\left(\underline{\alpha}_{\mathrm{a}}(\|z-u^*\|)\right)\right) \\
&V_1(z^+) - V_1(z) \leq -\tfrac{1}{2}\hat{\alpha}_\alpha(\alpha)\alpha_{\mathrm{a}}(\|z-u^*\|) \\
&\text{for } \|z-u^*\| \geq \max\{\alpha_\beta(\beta), \alpha_\alpha(\alpha)\},
\end{aligned}$$

8

which satisfies Assumption 8.17. Furthermore, it is easy to show that Assumptions 8.3, 8.12, 8.14, 8.15 hold as well. Since τ_0 can be considered a tuning parameter for jump periods in the timers states t in (8.23), we can guarantee satisfaction of Assumption 8.19. Hence, we satisfy all the Assumptions of the Corollary 8.20, and for small enough parameters, the combined dynamics render the set $\mathcal{A}_\chi$ SGPAS as $(\alpha, \beta, \max \tau_i^{-1}, \varepsilon, \max \sigma_i) \to 0$.
For our numerical simulations, we choose the parameters: $u_1^s = (-4,-8)$, $u_2^s = (-12,-3)$, $u_3^s = (1,7)$, $u_4^s = (16,8)$, $(\sigma_1, \sigma_2, \sigma_3, \sigma_4) = \mathrm{col}(2,3,4,2) \times 10^{-3}$, $c_1 = \frac{1}{3}$, $c_3 = 1.5$, $\alpha = 0.05$, $\beta = 0.003$, $c_{2,i} = \sigma_i$, $a_i = 0.1$ for all i, $t(0,0) = (0, 0.002, 0.004, 0.006)$, the perturbation frequencies ω_i^j were chosen as different natural numbers with added random numbers of maximal amplitude of 0.5, and the sampling of the Nash equilibrium seeking controller in (8.23) is five time slower than the sampling of the unicycle controller in (8.22a), i.e. $\tau = \mathrm{col}(1, 1.5, 2, 1) \times 10^{-2}$. The numerical results are illustrated in Figures 8.3 and 8.4. We note that the trajectories converge to the neighborhood of the Nash equilibrium.

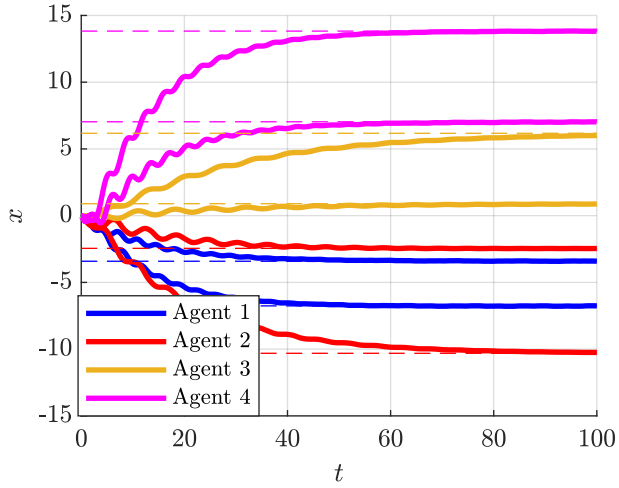

Figure 8.4: Time response of the unicycle position coordinates. The dashed lines correspond to the corresponding state of the Nash equilibrium.

8.4 Conclusion

The application of singular perturbation theory can be extended to systems where the restricted system evolves on the boundary layer manifold through both flows and jumps. Moreover, by introducing some mild technical assumptions, one can show convergence of the fast state components towards a restricted attractor set that does not encompass the complete space of fast variables. With this theoretical extension, we can examine control systems that employ hybrid plants, along with controllers that are "jump-driven", such as sampled controllers.

8

Appendix

8.A Proof of Theorem 8.11

Let $\Delta > \delta > 0$ be given. We denote with ρ the maximum distance to the equilibrium set $\mathcal{A}\times\mathcal{X}_2$ for trajectories starting in $(\mathcal{A}+\Delta\mathbb{B})\times\mathcal{X}_2$, which we characterize later on. Next, due to the fact that both $\mathcal{A}\times\mathcal{X}_2$ and $\mathcal{M}_\rho$ are unbounded in the dimensions corresponding to the same states, it follows that for any $\rho > 0$, there exists a $P > 0$ such that $\|x\|_{\mathcal{A}\times\mathcal{X}_2} \leq \rho$ implies that $\|x\|_{\mathcal{M}_\rho} \leq P$. We consider the system in (8.1) with restricted flow and jump sets:

$$C := ((\mathcal{A}+\rho\mathbb{B})\cap\mathcal{X}_1)\times\mathcal{X}_2 \tag{8.25a}$$

$$D := ((\mathcal{A}+\rho\mathbb{B})\cap D_1)\times D_2. \tag{8.25b}$$

By plugging in $\Delta = P$ in Assumption 8.6, and $\Delta = \rho$ in Assumptions 8.10, we construct the following Lyapunov function candidate:

$$V(x) = V_1(x_1) + \sqrt{\varepsilon}V_{2,\rho}(x). \tag{8.26}$$

8.A.1 Analysis of the jumps

The Lyapunov function after jumps equals to

$$V(g) = V_1(g_1) + \sqrt{\varepsilon} V_{2,\rho}(g), \tag{8.27}$$

where $\left[\begin{smallmatrix} g_1 \\ g_2 \end{smallmatrix}\right] = g \in G(x)$. We prove the following Lemma:

Lemma 8.22. *Consider the hybrid system in (8.1) with restricted flow and jump sets in (8.25), and let Assumptions 8.2—8.10 hold. For every $e > 0$ and $\Delta > 0$, there exists $v > 0$, such that $\|x\|_{\mathcal{M}_\rho} \leq v$ implies that*

$$\sup_{\left[\begin{smallmatrix} g_1 \\ g_2 \end{smallmatrix}\right] \in G(x)} V_1(g_1) - V_1(x_1) \leq \sup_{g_1^{\mathrm{r}} \in G_{\mathrm{r}}(x_1)} V_1(g_1^{\mathrm{r}}) - V_1(x_1) + \tfrac{e}{2}.$$

Proof. For the sake of contradiction, we assume that there exists $e > 0$ such it holds

$$\begin{aligned} &\sup_{\left[\begin{smallmatrix} g_1 \\ g_2 \end{smallmatrix}\right] \in G(x)} V_1(g_1) - V_1(x_1) > \sup_{g_1^{\mathrm{r}} \in G_{\mathrm{r}}(x_1)} V_1(g_1^{\mathrm{r}}) - V_1(x_1) + \tfrac{e}{2}, \\ &\forall x \in ((\mathcal{A} + \rho \mathbb{B}) \cap \mathcal{X}_1) \times \mathcal{X}_2. \end{aligned} \tag{8.28}$$

We define a sequence $\left(x^i\right)_{i \in \mathbb{N}} \in \mathcal{X}_1 \times \mathcal{X}_2$ such that $\left\|x^i\right\|_{\mathcal{M}_\rho} \leq \frac{1}{i}$ and that it satisfies the inequality in Equation (8.28). Let $x' := \mathrm{col}\left(x_1, x_2'\right)$, and ${\mathcal{M}_\rho}'$ be a projection of $\mathcal{M}_\rho$ onto the subspace of bounded states, $\mathcal{X}_1 \times \mathcal{X}_2'$. It holds that $\left\|x^i\right\|_{\mathcal{M}_\rho} \leq \frac{1}{i}$ implies $\left\|x'^i\right\|_{{\mathcal{M}_\rho}'} \leq \frac{1}{i}$. Furthermore, it follows that the sequence x'^i is bounded. Due to Assumption 8.2, we conclude that the sequence $\left(g'^i\right)_{i \in \mathbb{N}}$, where $g'^i \in G_1(x'^i)$, is also bounded. Thus, due to the Weierstrass theorem, there exists a convergent subsequence that converges to the point (x'^*, g'^*), where $x'^* \in {\mathcal{M}_\rho}'$. Next, due to the outer semi-continuity of the mappings G and H, it holds that $x_2'^* \in H_1(x_1^*)$, $g'^* \in G_1(x'^*)$ and $g_1^* \in G_{\mathrm{r}}(x_1^*)$. Therefore, it follows that

$$\sup_{\left[\begin{smallmatrix} g_1^* \\ g_2'^* \end{smallmatrix}\right] \in G_1(x_1^*, x_2'^*)} V_1(g_1^*) - V_1(x_1^*) > \sup_{g_1^{\mathrm{r}} \in G_{\mathrm{r}}(x_1^*)} V_1(g_1^{\mathrm{r}}) - V_1(x_1^*) + \tfrac{e}{2} \implies 0 > \tfrac{e}{2}$$

which leads us to a contradiction and, in turn, proves the Lemma. ∎

If ε is chosen such that $\sqrt{\varepsilon} \leq \frac{e}{2\overline{V}}$, where $\overline{V} := \sup_{x \in \mathcal{X}_1 \cap (\mathcal{A} + \rho \mathbb{B}) \times \mathcal{X}_2, g \in G(x)} \left\|V_{2,\rho}(g)\right\|$, then due to Lemma 8.22, it holds that for any $e > 0$ and $\Delta > 0$, there exist $v > 0$ and ε^* such that for every $\varepsilon \in (0, \varepsilon^*)$, inequality $\|x\|_{\mathcal{M}_\rho} \leq v$ implies that

$$\begin{aligned} &\sup_{g \in G(x)} V(g) - V(x) \leq -\hat{\alpha}_\gamma(\gamma) \alpha_1(\|x_1\|_{\mathcal{A}}) + e \\ &\text{for } \|x_1\|_{\mathcal{A}} \geq \alpha_\gamma(\gamma) \end{aligned} \tag{8.29}$$

The previous condition is always satisfied during jumps if $\|x\|_{\mathcal{M}_\rho} \leq v$ holds true before jumps. Thus, we have the following result:

Lemma 8.23. *Consider the hybrid system in (8.1) with restricted flow and jump sets in (8.25), and let Assumptions 8.2, 8.3, 8.6 hold. Then, for every $v > 0$, and $\rho > 0$ there exists $\tau^* > 0$, ε^* and β^*, such that for every $\varepsilon \in (0, \varepsilon^*)$, $\beta \in (0, \beta^*)$, it holds that if trajectory x satisfies $\|x(t,j)\|_{\mathcal{A}\times\mathcal{X}_2} \leq \rho$ for all $t \in \operatorname{dom}(x(\cdot, j))$, then $\|x(t,j)\|_{\mathcal{M}_\rho} \leq v$ for all $t \in \operatorname{dom}(x(\cdot, j))$ such that $t \geq \tau^*$.* □

Proof. From Assumption 8.6, the derivative of the Lyapunov function candidate, for $\Delta = P$, reads as

$$\left\langle \nabla V_{2,\rho}(x) \,\middle|\, \begin{bmatrix} f_1 \\ \frac{1}{\varepsilon} f_2 \end{bmatrix} \right\rangle \leq -\tfrac{1}{\varepsilon}\alpha_{2,\rho}\left(\|x\|_{\mathcal{M}_\rho}\right) + \left\langle \nabla V_{2,\rho}(x) \,\middle|\, \begin{bmatrix} f_1 \\ 0 \end{bmatrix} \right\rangle$$
$$\text{for } \|x\|_{\mathcal{M}_\rho} \geq \alpha_\beta(\beta).$$

We define the constant

$$\mu := \sup_{x \in \mathcal{X}_1 \cap (\mathcal{A}+\rho\mathbb{B})\times\mathcal{X}_2} \left\langle \nabla V_{2,\rho}(x) \,\middle|\, \begin{bmatrix} f_1 \\ 0 \end{bmatrix} \right\rangle.$$

Then, the Lyapunov derivative is given by

$$\left\langle \nabla V_{2,\rho}(x) \,\middle|\, \begin{bmatrix} f_1 \\ \frac{1}{\varepsilon} f_2 \end{bmatrix} \right\rangle \leq -\tfrac{1}{\varepsilon}\alpha_{2,\rho}\left(\|x\|_{\mathcal{M}_\rho}\right) + \mu$$
$$\text{for } \|x\|_{\mathcal{M}_\rho} \geq \alpha_\beta(\beta).$$

Let $\beta^* = \alpha_\beta^{-1}\left(\overline{\alpha_{2,\rho}}^{-1}\left(\underline{\alpha_{2,\rho}}(v)\right)\right)$, $m = \frac{1}{2}\alpha_{2,\rho}\left(\overline{\alpha_{2,\rho}}^{-1}\left(\underline{\alpha_{2,\rho}}(v)\right)\right)$ and $\varepsilon^* = \frac{m}{\mu}$. It follows that for any time interval $(t, t+\tau)$ where only flowing occurred, for any $\varepsilon \in (0, \varepsilon^*)$, $\beta \in (0, \beta^*)$ it holds

$$\begin{aligned}
&\dot{V}^P_{2,\rho}(x(t,j)) \leq -\mu \\
&\text{for } \|x\|_{\mathcal{M}_\rho} \geq \overline{\alpha_{2,\rho}}^{-1}\left(\underline{\alpha_{2,\rho}}(v)\right) \\
&\int_t^{t+\tau} dV_{2,\rho}(x(t,j)) \leq -\mu \int_t^{t+\tau} dt \\
&V_{2,\rho}(x(t+\tau,j)) \leq V_{2,\rho}(x(t,j)) - \mu\tau \\
&\text{for } \|x\|_{\mathcal{M}_\rho} \geq \overline{\alpha_{2,\rho}}^{-1}\left(\underline{\alpha_{2,\rho}}(v)\right).
\end{aligned} \tag{8.30}$$

As we assume $\|x(t,j)\|_{\mathcal{M}_\rho} \leq P$, from the bounds of the Lyapunov function in 8.6, we have

$$\begin{aligned}
\|x(t+\delta t, j)\|_{\mathcal{M}_\rho} &\leq \underline{\alpha_{2,\rho}}^{-1}\left(\overline{\alpha_{2,\rho}}(\|x(t,j)\|) - \mu\delta t\right) \\
&\leq \underline{\alpha_{2,\rho}}^{-1}\left(\overline{\alpha_{2,\rho}}(P) - \mu\delta t\right) \leq v.
\end{aligned} \tag{8.31}$$

From the last inequality, it follows that $\tau \geq \tau^* := \underline{\sigma}^{-1}\left(\frac{\overline{\alpha_{2,\rho}}(P) - \underline{\alpha_{2,\rho}}(v)}{\mu}\right)$, which proves the Lemma. ■

It follows from (8.29) and Lemmas 8.22 and 8.23 that for any $e > 0$, $\Delta > 0$, there exist parameters ε_1^*, β_1^*, and τ^* such that for any $\varepsilon \in (0, \varepsilon_1^*)$, $\beta \in (0, \beta_1^*)$, if the time between consecutive jumps is larger than τ^*, it holds that

$$\sup_{g \in G(x)} V(g) - V(x) \leq -\hat{\alpha}_\gamma(\gamma)\alpha_1\left(\|x_1\|_{\mathcal{A}}\right) + e \quad \text{for } \|x_1\|_{\mathcal{A}} \geq \alpha_\gamma(\gamma). \tag{8.32}$$

8.A.2 Analysis of the flows

The Lyapunov derivative is given by

$$\begin{aligned}
&\sup_{\begin{bmatrix} f_1 \\ f_2 \end{bmatrix} \in F(x)} \left\langle \nabla V(x) \,\middle|\, \begin{bmatrix} f_1 \\ \frac{1}{\varepsilon} f_2 \end{bmatrix} \right\rangle = \sup_{\begin{bmatrix} f_1 \\ f_2 \end{bmatrix} \in F(x)} \left(\langle \nabla V_1(x) \mid f_1 \rangle + \sqrt{\varepsilon} \left\langle \nabla V_{2,\rho}(x) \,\middle|\, \begin{bmatrix} f_1 \\ \frac{1}{\varepsilon} f_2 \end{bmatrix} \right\rangle \right) \\
&\leq \sup_{\begin{bmatrix} f_1 \\ f_2 \end{bmatrix} \in F(x)} \left(\langle \nabla V_1(x) \mid f_1 \rangle + \left| \left\langle \nabla V_{2,\rho}(x) \,\middle|\, \begin{bmatrix} f_1 \\ 0 \end{bmatrix} \right\rangle \right| + \tfrac{1}{\sqrt{\varepsilon}} \left\langle \nabla V_{2,\rho}(x) \,\middle|\, \begin{bmatrix} 0 \\ f_2 \end{bmatrix} \right\rangle \right) \\
&\leq -\hat{\sigma}_\tau(\tau)\hat{\alpha}_\gamma(\gamma)\alpha_1\left(\|x_1\|_{\mathcal{A}}\right) + \mu(x) + \sup_{\begin{bmatrix} f_1 \\ f_2 \end{bmatrix} \in F(x)} \tfrac{1}{\sqrt{\varepsilon}} \left\langle \nabla V_{2,\rho}(x) \,\middle|\, \begin{bmatrix} 0 \\ f_2 \end{bmatrix} \right\rangle, \\
&\text{for } \|x_1\|_{\mathcal{A}} \geq \alpha_\gamma(\gamma), \|x\|_{\mathcal{M}_\rho} \geq \alpha_\beta(\beta),
\end{aligned} \tag{8.33}$$

$$\text{where } \mu(x) = -\sup_{f_1^{\mathrm{r}} \in F_{\mathrm{r}}(x_1)} \left(-\langle \nabla V_1(x) \mid f_1^{\mathrm{r}} \rangle \right) + \sup_{\begin{bmatrix} f_1 \\ f_2 \end{bmatrix} \in F(x),} \left(\langle \nabla V_1(x) \mid f_1 \rangle + \left| \left\langle \nabla V_{2,\rho}(x) \,\middle|\, \begin{bmatrix} f_1 \\ 0 \end{bmatrix} \right\rangle \right| \right).$$

Let $v > \alpha_\beta(\beta)$ be chosen arbitrarily and let

$$\varepsilon^* = \frac{{\alpha_2}_\rho^2(v)}{\sup_{x \in \mathcal{X}_1 \cap (\mathcal{A} + \rho \mathrm{B}) \times \mathcal{X}_2} \|\mu(x)\|^2}. \tag{8.34}$$

Then it holds that

$$\begin{aligned}
&\sup_{\begin{bmatrix} f_1 \\ f_2 \end{bmatrix} \in F(x)} \left\langle \nabla V(x) \,\middle|\, \begin{bmatrix} f_1 \\ \frac{1}{\varepsilon} f_2 \end{bmatrix} \right\rangle \leq -\hat{\sigma}_\tau(\tau)\hat{\alpha}_\gamma(\gamma)\alpha_1\left(\|x_1\|_{\mathcal{A}}\right), \\
&\text{for } \|x\|_{\mathcal{M}_\rho} \geq v, \|x_1\|_{\mathcal{A}} \geq \alpha_\gamma(\gamma),
\end{aligned} \tag{8.35}$$

$$\begin{aligned}
&\sup_{\begin{bmatrix} f_1 \\ f_2 \end{bmatrix} \in F(x)} \left\langle \nabla V(x) \,\middle|\, \begin{bmatrix} f_1 \\ \frac{1}{\varepsilon} f_2 \end{bmatrix} \right\rangle \leq -\hat{\sigma}_\tau(\tau)\hat{\alpha}_\gamma(\gamma)\alpha_1\left(\|x_1\|_{\mathcal{A}}\right) + \mu(x) + \tfrac{1}{\sqrt{\varepsilon}}\hat{\alpha}_\beta(\beta), \\
&\text{for } \|x\|_{\mathcal{M}_\rho} < v, \|x_1\|_{\mathcal{A}} \geq \alpha_\gamma(\gamma),
\end{aligned} \tag{8.36}$$

which is combined into

$$\begin{aligned}
&\sup_{\begin{bmatrix} f_1 \\ f_2 \end{bmatrix} \in F(x)} \left\langle \nabla V(x) \,\middle|\, \begin{bmatrix} f_1 \\ \frac{1}{\varepsilon} f_2 \end{bmatrix} \right\rangle \leq -\hat{\sigma}_\tau(\tau)\hat{\alpha}_\gamma(\gamma)\alpha_1\left(\|x_1\|_{\mathcal{A}}\right) + \sup_{\|x\|_{\mathcal{M}_\rho} \leq v} \mu(x) + \tfrac{1}{\sqrt{\varepsilon}}\hat{\alpha}_\beta(\beta), \\
&\text{for } \|x_1\|_{\mathcal{A}} \geq \alpha_\gamma(\gamma).
\end{aligned} \tag{8.37}$$

The next Lemma shows that the positive terms in the Lyapunov derivative, with the proper choice of tuning parameters ε and β, can be made arbitrarily small.

Lemma 8.24. *Consider the hybrid system in (8.1) with restricted flow and jump sets in (8.25), and let Assumptions 8.2—8.10 hold. For every $e > 0$, $\Delta > 0$, there exists $\varepsilon^* > 0$, $\beta^*(\varepsilon) > 0$, such that for any $\varepsilon \in (0, \varepsilon^*)$, $\beta \in (0, \beta^*(\varepsilon))$, it holds that $\sup_{\|x\|_{\mathcal{M}_\rho} \le \upsilon} \mu(x) + \frac{1}{\sqrt{\varepsilon}} \hat{\alpha}_\beta(\beta) \le e$.* □

Proof. We consider the following inequalities:

$$\sup_{\|x\|_{\mathcal{M}_\rho} \le \upsilon} \mu(x) \le \tfrac{e}{2} \tag{8.38}$$

$$\tfrac{1}{\sqrt{\varepsilon}} \hat{\alpha}_\beta(\beta) \le \tfrac{e}{2}. \tag{8.39}$$

If they hold, so does the inequality in the Lemma. The proof that inequality in (8.38) can be made arbitrarily small by choice of small υ, and hence smaller ε^* due to (8.34), is analogous to the proof of Lemma 8.22, and thus it is omitted. Then, to satisfy inequality (8.39), it is sufficient to have $\beta^* := \min\left(\hat{\alpha}_\beta^{-1}(e\sqrt{\varepsilon}), \alpha_\beta^{-1}(\upsilon)\right)$ and $\beta \in (0, \beta^*)$. ∎

From Equations (8.37) and Lemma 8.24, it follows that for any $e > 0$, $\Delta > 0$, there exists ε_2^*, $\beta_2^*(\varepsilon_2)$ such that for any $\varepsilon \in (0, \varepsilon_2^*)$ and $\beta_2 \in (0, \beta_2^*(\varepsilon_2))$, we have

$$\sup_{\begin{bmatrix} f_1 \\ f_2 \end{bmatrix} \in F(x)} \left\langle \nabla V(x) \,\middle|\, \begin{bmatrix} f_1 \\ \frac{1}{\varepsilon} f_2 \end{bmatrix} \right\rangle \le -\hat{\sigma}_\tau(\tau)\hat{\alpha}_\gamma(\gamma)\alpha_1\left(\|x_1\|_{\mathcal{A}}\right) + e,$$
$$\text{for } \|x_1\|_{\mathcal{A}} \ge \alpha_\gamma(\gamma). \tag{8.40}$$

8.A.3 Complete Lyapunov analysis

We denote by $\phi(t, j)$ a solution of the system that contains only $\underline{\sigma}(\tau)$ regular jumps. Let γ be chosen so that $\gamma \in (0, \gamma^*)$, where $\gamma^* := \min(\alpha_\gamma^{-1}(\overline{\alpha_1}^{-1}(\frac{1}{2}\underline{\alpha_1}(\delta))), \overline{\gamma})$. Next, η is defined as $\eta := \frac{1}{2}\min\{\underline{\alpha_1}(\delta), \alpha_1(\alpha_\gamma(\gamma^*)), 2\}$. Via Equation (8.29) and Lemmas 8.22 and 8.23, for $e = \hat{\alpha}_\gamma(\gamma)\eta$, we have τ^*, ε_1^*, β_1^*. Next, we choose $\tau \in (0, \min(\tau^*, \overline{\tau}))$. From Equation (8.37) and Lemma 8.24 for $e = \hat{\sigma}(\tau)\hat{\alpha}_\gamma(\gamma)\eta$, we have ε_2^*, $\beta_2^*(\varepsilon)$. Finally, let

$$\varepsilon_3^* = \frac{\eta^2}{\sup_{x \in \mathcal{X}_1 \cap (\mathcal{A} + \rho \mathbb{B}) \times \mathcal{X}_2} \overline{\alpha_{2,\rho}}\left(\|x\|_{\mathcal{M}_\rho}\right)^2}. \tag{8.41}$$

We define $\varepsilon^* := \min\{\varepsilon_1^*, \varepsilon_2^* \varepsilon_3^*, \overline{\varepsilon}\}$, $\beta^*(\varepsilon) := \min\{\beta_1^*, \beta_2^*(\varepsilon), \overline{\beta}\}$, and set the parameters as follows: $\varepsilon \in (0, \varepsilon^*)$, $\beta \in (0, \beta^*(\varepsilon))$. From Equations (8.32) and (8.40), it follows that

$$\begin{aligned}
&V(\phi(t,j)) - V(\phi(0,0)) \\
&\le -\sum_{i=0}^{j} \int_{t_i}^{t_{i+1}} \hat{\sigma}_\tau(\tau)\hat{\alpha}_\gamma(\gamma)\alpha_1\left(\|\phi_1(s,i)\|_{\mathcal{A}}\right) ds - \sum_{i=1}^{j} \hat{\alpha}_\gamma(\gamma)\alpha_1\left(\|\phi_1(t_i, i-1)\|_{\mathcal{A}}\right) \\
&\le -(\hat{\sigma}_\tau(\tau)t + j)\hat{\alpha}_\gamma(\gamma)\left(\alpha_1\left(\|x_1\|_{\mathcal{A}}\right) - \eta\right), \\
&\text{for } \|\phi_1(t,j)\|_{\mathcal{A}} \ge \alpha_\gamma(\gamma).
\end{aligned} \tag{8.42}$$

As $\eta \leq \frac{1}{2}\alpha_1(\alpha_\gamma(\gamma))$ and $\alpha_\gamma(\gamma^*) < \alpha_\gamma(\gamma^*)$, we rewrite the last inequality as

$$V(\phi(t,j)) \leq V(\phi(0,0)) - \tfrac{1}{2}(\hat{\sigma}_\tau(\tau)t + j)\alpha_1\left(\alpha_\gamma(\gamma^*)\right), \quad \text{for } \|\phi_1(t,j)\|_{\mathcal{A}} \geq \alpha_\gamma(\gamma^*), \tag{8.43}$$

We can guarantee the decrease of the Lyapunov function up to the smallest Lyapunov level set that contains the set $(\mathcal{A} + \alpha_\gamma(\gamma^*))\mathbb{B}) \times \mathcal{X}_2$. Via equation 8.43, we move on to proving semi-global boudness and practical attractivity of the equilibrium set.

Semi-global boundness

By definition, $\varepsilon \leq \varepsilon_3^*$. Thus, the upper and lower bound of the Lyapunov function candidate are given by

$$\begin{aligned} \underline{\alpha_1}\left(\|x_1\|_{\mathcal{A}}\right) \leq V(x) &\leq \overline{\alpha_1}\left(\|x_1\|_{\mathcal{A}}\right) + \sqrt{\varepsilon\overline{\alpha}_{2,\rho}}\left(\|x\|_{\mathcal{M}_\rho}\right) \\ &\leqq \overline{\alpha_1}\left(\|x_1\|_{\mathcal{A}}\right) + \eta \end{aligned} \tag{8.44}$$

From (8.43) and (8.44), for $\underline{\sigma}(\tau)$-reggular trajectories ϕ, it holds that

$$\underline{\alpha_1}\left(\|\phi_1(t,j)\|_{\mathcal{A}}\right) \leq \overline{\alpha_1}\left(\|\phi_1(0,0)\|_{\mathcal{A}}\right) + \eta, \quad \text{for } \|\phi_1(t,j)\|_{\mathcal{A}} \geq \alpha_\gamma(\gamma^*). \tag{8.45}$$

The maximal distance to the equilibrium of a $\underline{\sigma}(\tau)$-regular trajectory $\phi(t,j)$ starting at $(t,j) = (0,0)$ is given in (8.45) by $\|\phi_1(t,j)\|_{\mathcal{A}} \leq \rho_{\mathrm{C}}\left(\overline{\alpha_1}\left(\|\phi_1(0,0)\|_{\mathcal{A}}\right)\right)$, where $\rho_{\mathrm{C}} : \mathbb{R}_+ \to \mathbb{R}_+, \rho_{\mathrm{C}}(a) := \underline{\alpha_1}^{-1}(\overline{\alpha_1}(a) + 1)$. By the outer semi-continuity and local boundness of the mapping G in (8.5) for all allowed sets of parameters, for each $\underline{r} > 0$, there exists a $\bar{r}, r > 0$, such that $G_1\left((\mathcal{A} + \underline{r}\mathbb{B}) \times \mathcal{X}_2'\right) \subset G_1(\mathcal{A} \times \mathcal{X}_2') + \bar{r}\mathbb{B} \subset (\mathcal{A} + r\mathbb{B}) \times \mathcal{X}_2'$. Via this property, we define the mapping $\rho_{\mathrm{D}} : \mathbb{R}_+ \to \mathbb{R}_+, \rho_{\mathrm{C}}(\underline{r}) := r$. Thus, for any initial condition such that $\|\phi(0,0)\|_{\mathcal{A}\times\mathcal{X}_2} \leq \Delta$, the maximal distance from the equilibrium set after N irregular jumps, not necessarily consecutive jumps, is given by $\rho = \rho_{\mathrm{C}} \circ \rho_{\mathrm{D}} \circ \cdots \circ \rho_{\mathrm{C}}(\Delta)$, where ρ_{D} repeats N times, and ρ_{C} repeats $N+1$ times.

Semi-global stability for $\underline{\sigma}(\tau)$ trajectories

Let us consider trajectories after the N irregular jumps. We show that for any $R \geq \delta$, there exists $r > 0$, such that $\|\phi(l,i)\|_{\mathcal{A}\times\mathcal{X}_2} \leq r \implies \|\phi(t,j)\|_{\mathcal{A}\times\mathcal{X}_2} \leq R$ for $l + i \leq t + j$. From (8.45) and $\eta \leq \frac{1}{2}\underline{\alpha_1}(\delta)$, it follows that

$$\|\phi_1(l,i)\|_{\mathcal{A}} \leq \overline{\alpha_1}^{-1}\left(\underline{\alpha_1}(R) - \tfrac{1}{2}\underline{\alpha_1}(\delta)\right), \quad \text{for } \|\phi_1(t,j)\|_{\mathcal{A}} \geq \alpha_\gamma(\gamma^*). \tag{8.46}$$

We note that the previous inequality holds up to the smallest radius of interest $r = \overline{\alpha_1}^{-1}\left(\frac{1}{2}\underline{\alpha_1}(\delta)\right)$, because $\gamma^* \leq \alpha_\gamma^{-1}(\overline{\alpha_1}^{-1}\left(\frac{1}{2}\underline{\alpha_1}(\delta)\right))$. Then, for any $R \geq \delta$, and all $\gamma \in (0, \gamma^*)$, we have $r(R) := \min\left\{\overline{\alpha_1}^{-1}\left(\underline{\alpha_1}(R) - \eta\right), \Delta\right\}$.

Practical attractivity

Without of loss of generality, we assume R, r are given so that $\Delta \geq R \geq r \geq \delta$. We have to show that there exists a period $T \geq 0$, such that $\|\phi(0,0)\|_{\mathcal{A}\times\mathcal{X}_2} \leq R \implies \|\phi(t,j)\|_{\mathcal{A}\times\mathcal{X}_2} \leq r$ for all (t,j) such that $t+j \geq T$.

Let (l,i) be the hybrid time instant after the N irregular jumps. By Assumption 8.9, it holds $l+i \leq T^*$. Then, from (8.43), for $\phi(0,0)$ replaced with $\phi(l,i)$, it follows

$$\underline{\alpha_1}(r) \leq \overline{\alpha_1}(\rho) - \tfrac{1}{2}\alpha_1\left(\alpha_\gamma(\gamma^*)\right)\left[(\hat{\sigma}_\tau(\tau)(t-l)+j-i)\right], \tag{8.47}$$

Then, when we have

$$t+j \leq \frac{2(\overline{\alpha_1}(\rho)-\underline{\alpha_1}(r))}{\min\{\hat{\sigma}_\tau,1\}\alpha_1\left(\alpha_\gamma(\gamma^*)\right)} + T^* = T(R,r). \tag{8.48}$$

Conclusion

Our restricted system renders the set $\mathcal{A}\times\mathcal{X}_2$ practically attractive. Finally, to show the equivalence between the solutions of the original and restricted system, it is possible to use the same procedure as in [78] after Equation (29). ∎

8.B Proof of Theorem 8.13

Let $\Delta > \delta > 0$ be the parameters of semi-global practical stability. We denote with ρ the maximum distance $\|\phi(t,j)\|_{\mathcal{A}\times\mathcal{X}}$ for trajectories starting in $\mathcal{M}_\mathcal{A} + \Delta\mathbb{B}$. On the other hand, as it is possible to a priori bound the distance $\|\phi(t,j)\|_{\mathcal{M}_\mathcal{A}}$ with $P > 0$, see Remark 8.29, we "redefine" the set $\mathcal{X}_2'$ as a compact set $\left(\{x_2' \mid x_1 \in \mathcal{A}, x_2' \in H_1(x_1)\} + P\mathbb{B}\right) \cap \mathcal{X}_2'$. The same procedure as in the proof of Theorem 8.11 can be repeated. From Equations (8.31) and (8.48), we have

$$\begin{aligned} &\|\phi(t,j)\|_{\mathcal{M}_\rho} \leq v \text{ for all } t \in \operatorname{dom}(\phi(\cdot,j)) \\ &\text{s.t. } t \geq \underline{\sigma}(\tau^*(P,v)), \end{aligned} \tag{8.49}$$

$$\begin{aligned} &\|\phi(t,j)\|_{\mathcal{A}\times\mathcal{X}_2} \leq r \text{ for all } (t,j) \in \operatorname{dom}(\phi) \\ &\text{s.t. } t+j \geq T(\Delta,r), \end{aligned} \tag{8.50}$$

A key observation is that the intersection of sets $\mathcal{A}\times\mathcal{X}_2$ and $\mathcal{M}_\rho$ gives us the set $\mathcal{M}_\mathcal{A}$, for which we want to prove stability. Distance to the set $\mathcal{A}\times\mathcal{X}_2$ is given by (8.50), and the distance to the set $\mathcal{M}_\rho$ is given by (8.49). Thus, it is possible to quantify the distance to the equilibrium set using the distances of the latter two sets using the following results:

Lemma 8.25. *Let $\mathcal{A}, \mathcal{B}$ be nonempty sets defined on a metric space, where at least one is bounded. Let their intersection $\mathcal{S}$ be nonempty. Then, for every $d > 0$, there exists $\underline{d} > 0$, such that $\|x\|_\mathcal{A} \leq \underline{d}$ and $\|x\|_\mathcal{B} \leq \underline{d}$ implies that $\|x\|_\mathcal{S} \leq d$.* □

Proof. Let us assume otherwise, i.e., there exists some $d > 0$ such that for any $\underline{d} > 0$, there exists x such that it holds $\|x\|_\mathcal{S} > d$. Let us create a sequence of these points, $(x_i)_{i\in\mathbb{N}}$, such that $\|x_i\|_\mathcal{A} \leq \frac{1}{i}$ and $\|x_i\|_\mathcal{B} \leq \frac{1}{i}$. Because the sequence is bounded, there must exist a convergent subsequence. Let one such subsequence converge to x^*. Because of the continuity of the metric, it holds that $\|x^*\|_\mathcal{A} = 0$ and $\|x^*\|_\mathcal{B} = 0$. Thus, $x^* \in \operatorname{cl}(\mathcal{A})$ and $x^* \in \operatorname{cl}(\mathcal{B})$, or in other words $x^* \in \operatorname{cl}(\mathcal{A}) \cap \operatorname{cl}(\mathcal{B}) \equiv \operatorname{cl}(\mathcal{S})$. Then it holds $\|x^*\|_\mathcal{S} = 0$, which is opposite of our assumption. ∎

Lemma 8.26. *Let $\mathcal{A},\mathcal{B}$ be nonempty sets defined on a metric space. Let their intersection $\mathcal{S}$ be nonempty and bounded. Then, for every $\overline{d}>0$, there exists $d>0$, such that $\|x\|_{\mathcal{S}}\leq d$ implies $\|x\|_{\mathcal{A}}\leq\overline{d}$ and $\|x\|_{\mathcal{B}}\leq\overline{d}$.* □

Proof. Let us assume otherwise, i.e there exists some $\overline{d}>0$ such that for any $d>0$, there exists x such that $\|x\|_{\mathcal{A}}>\overline{d}$ and $\|x\|_{\mathcal{B}}>\overline{d}$. Let us create a sequence of these points, $(x_i)_{i\in\mathbb{N}}$, such that $\|x\|_{\mathcal{A}}\leq\frac{1}{i}$. Because the sequence is bounded, there must exist a convergent subsequence. Let one such subsequence converge to x^*. Because of the continuity of the metric, it holds that $\|x^*\|_{\mathcal{S}}=0$. Thus, $x^*\in\mathrm{cl}(\mathcal{S})$ or in other words $x^*\in\mathrm{cl}(\mathcal{S})\equiv\mathrm{cl}(\mathcal{A})\cap\mathrm{cl}(\mathcal{B})$. Then it holds $\|x^*\|_{\mathcal{A}}=0$ and $\|x^*\|_{\mathcal{B}}=0$, which is opposite of our assumption. ■

Remark 8.27. *Although we assume boundedness of some of the sets in Lemmas 8.25 and 8.26, it is possible to prove the same results for the cases when $\mathcal{A}$ and $\mathcal{B}$ are unbounded in the same dimensions, which is the case in our setup.*

Semi-global stability

To prove practical stability, we show that for any $R\geq\delta$, there exists a neighborhood of the equilibrium, $\mathcal{M}_{\mathcal{A}}+r\mathbb{B}$, such that any trajectory initiated in the neighborhood will stay inside the set $\mathcal{M}_{\mathcal{A}}+R\mathbb{B}$, for properly chosen parameters. But first, we prove a similar result for regular trajectories of the restricted system.

Lemma 8.28 (Semi-global stability-like property)**.** *Consider the hybrid system in (8.1) with restricted flow and jump sets in (8.25), and let Assumptions 8.2, 8.3, 8.4, 8.6, 8.10 hold. Then, for every $\overline{v}\geq\delta$, there exists a $\underline{v}>0$, and a set of tuning parameters $\varepsilon^*,\tau^*,\beta^*(\varepsilon),\gamma^*$, such that for all regular trajectories ϕ with $\|\phi(0,0)\|_{\mathcal{M}_{\mathcal{A}}}\leq\underline{v}$ and $\varepsilon\in(0,\varepsilon^*),\tau\geq\tau^*,\beta\in(0,\beta^*(\varepsilon)),\gamma\in(0,\gamma^*)$, it holds that $\|\phi(t,j)\|_{\mathcal{M}_{\mathcal{A}}}\leq\overline{v}$ for all $(t,j)\in\mathrm{dom}(\phi)$.* □

Proof. Sketch of the proof

First, we find $\hat{v}>0$ such that any trajectory initiated in $\mathcal{M}_{\mathcal{A}}+\hat{v}\mathbb{B}$, stays in $\mathcal{M}_{\mathcal{A}}+\overline{v}\mathbb{B}$ during flows. Then we find $\tilde{v}>0$ such that jumps from $\mathcal{M}_{\mathcal{A}}+\tilde{v}\mathbb{B}$ will end in $\mathcal{M}_{\mathcal{A}}+\hat{v}\mathbb{B}$. Next, we find $\underline{v}$ such that any trajectory initiated in $\mathcal{M}_{\mathcal{A}}+\underline{v}\mathbb{B}$, stays in $\mathcal{M}_{\mathcal{A}}+\tilde{v}\mathbb{B}$ during flows. Finally, we choose $\varepsilon,\frac{1}{\tau},\beta,\gamma$ small enough such that all trajectories end up in $\mathcal{M}_{\mathcal{A}}+\underline{v}\mathbb{B}$ before jumps.

Consider the following system of implications:

$$\|\phi(0,0)\|_{\mathcal{M}_{\mathcal{A}}}\leq\underline{v}\overset{(1)}{\Rightarrow}\begin{matrix}\|\phi(0,0)\|_{\mathcal{A}\times\mathcal{X}_2}\leq\underline{u}\\ \|\phi(0,0)\|_{\mathcal{M}_\rho}\leq\underline{u}\end{matrix}\overset{(2)}{\Rightarrow}\begin{matrix}\|\phi(t,0)\|_{\mathcal{A}\times\mathcal{X}_2}\leq\tilde{u}\\ \|\phi(t,0)\|_{\mathcal{M}_\rho}\leq\tilde{u}\end{matrix}\overset{(3)}{\Rightarrow}\|\phi(t,0)\|_{\mathcal{M}_{\mathcal{A}}}\leq\tilde{v}$$
$$\overset{(4)}{\Rightarrow}\|\phi(t,1)\|_{\mathcal{M}_{\mathcal{A}}}\leq\hat{v}\overset{(5)}{\Rightarrow}\begin{matrix}\|\phi(t,1)\|_{\mathcal{A}\times\mathcal{X}_2}\leq\hat{u}\\ \|\phi(t,1)\|_{\mathcal{M}_\rho}\leq\hat{u}\end{matrix}\overset{(6)}{\Rightarrow}\begin{matrix}\|\phi(l,1)\|_{\mathcal{A}\times\mathcal{X}_2}\leq\overline{u}\\ \|\phi(l,1)\|_{\mathcal{M}_\rho}\leq\overline{u}\end{matrix}\overset{(7)}{\Rightarrow}\|\phi(l,1)\|_{\mathcal{M}_{\mathcal{A}}}\leq\overline{v}.$$

Implication (7) follows from Lemma 8.25, while implication (6) follows from Equations (8.46) with $\hat{u}^1\leq\overline{\alpha_1}^{-1}\left(\underline{\alpha_1}\left(\frac{1}{2}\overline{u}\right)\right)$, Equation (8.30) and $\hat{u}^1=\overline{\alpha_{2,\rho}}^{-1}\left(\underline{\alpha_{2,\rho}}(\overline{u})\right)$, and $\hat{u}=\min\{\hat{u}^1,\hat{u}^2\}$; Implication (5) follows from Lemma 8.26; Implication (4) proceeds from [80, Lemma 5.15], outer semicontinuity, local boundedness of the mapping G, Assumption 8.12, thus for every $\hat{v}>0$, there exists a $\tilde{v}\leq\hat{v}$ such that $G(\mathcal{M}_{\mathcal{A}}+\tilde{v}\mathbb{B})\subset\mathcal{M}_{\mathcal{A}}+\hat{v}\mathbb{B}$; Implication

(3) follows from Lemma 8.25, while implication (2) follows from Equations (8.46) with $\underline{u}^1 = \overline{\alpha_1}^{-1}\left(\underline{\alpha_1}\left(\frac{1}{2}\tilde{u}\right)\right)$, Equation (8.30) and $\underline{u}^2 = \overline{\alpha_{2,\rho}}^{-1}\left(\underline{\alpha_{2,\rho}}(\tilde{u})\right)$ and $\underline{u} = \min\{\underline{u}^1, \underline{u}^2\}$; Implication (1) follows from Lemma 8.26. To satisfy the inequalities in Equations (8.46), (8.30), let $\eta = \frac{1}{2}\min\{\underline{\alpha_1}(\underline{u}), \alpha_1\left(\overline{\alpha_1}^{-1}\left(\frac{1}{2}\underline{\alpha_1}(\underline{u})\right)\right), 2\}$, $\gamma^* := \alpha_\gamma^{-1}\left(\overline{\alpha_1}^{-1}\left(\frac{1}{2}\underline{\alpha_1}(\underline{u})\right)\right)$, $\gamma \in (0, \gamma^*)$; Via Equation (8.29) and Lemmas 8.22 and 8.23, for $e = \hat{\alpha}_\gamma(\gamma)\eta$, we have τ^*, ε_1^*, β_1^*. Next, we choose $\tau \in (0, \min(\tau^*, \overline{\tau}))$. From Equation (8.37) and Lemma 8.24 for $e = \hat{\sigma}(\tau)\hat{\alpha}_\gamma(\gamma)\eta$, we have ε_2^*, $\beta_2^*(\varepsilon)$. Finally, let ε_3^* be defined as in (8.41). We define $\varepsilon^* := \min\{\varepsilon_1^*, \varepsilon_2^*\varepsilon_3^*, \overline{\varepsilon}\}$, $\beta^*(\varepsilon) := \min\{\beta_1^*, \beta_2^*(\varepsilon), \overline{\beta}\}$, and set the parameters as follows: $\varepsilon \in (0, \varepsilon^*)$, $\beta \in (0, \beta^*(\varepsilon))$. Furthermore, as Equation (8.46) holds for jumps and flows, it follows that $\|\phi(l,1)\|_{\mathcal{A}\times\mathcal{X}_2} \leq \tilde{u}$, and due to Lemma 8.23, it holds that $\|\phi(l,1)\|_{\mathcal{M}_\rho} \leq \tilde{u}$ for $l \geq \min_t \operatorname{dom}(\phi(\cdot,1)) + \underline{\sigma}(\tau^*)$. Thus, it is possible to follow the same reasoning with implications (3) to (7) for the next and all the following regular jumps, which proves our Lemma. ∎

Remark 8.29. *We can "reverse" Lemma 8.28 so that we claim that for every $\underline{v} > 0$, there exists a $\overline{v} > 0$ that satisfies the same inequality. Then, by doing an inverse procedure of the proof of stability, we can derive $P > 0$ such that $\|\phi(0,0)\|_{\mathcal{M}_\mathcal{A}} \leq \Delta$ implies that $\|\phi(t,j)\|_{\mathcal{M}_\mathcal{A}} \leq P$. These bounds depend on the proprieties of mapping G and the lower and upper bounds of the Lyapunov functions, thus, can be computed a priori.* □

Let N be the number of irregular jumps for the given Δ. Via Lemma 8.28, for $\overline{v} = R$, we find $\overline{r}_N = \underline{v}$ and parameters $\varepsilon_N^*, \tau_N^*, \beta_N^*(\varepsilon), \gamma_N^*$. Then, from [80, Lemma 5.15], outer semicontinuity, local boundedness of the mapping G, Assumption 8.12, we can find $\underline{r}_N$ such that $G(\mathcal{M}_\mathcal{A} + \underline{r}_N\mathbb{B}) \subset \mathcal{M}_\mathcal{A} + \overline{r}_N\mathbb{B}$. Then again we use Lemma 8.28, with $\overline{v} = \underline{r}_N$, to find $\underline{v} = \overline{r}_{N-1}$ and parameters $\varepsilon_{N-1}^*, \tau_{N-1}^*, \beta_{N-1}^*(\varepsilon), \gamma_{N-1}^*$. These steps are repeated until we reach the first jump. Then, we use Lemma 8.28, for $\overline{v} = \underline{r}_1$ to find $r = \underline{v}$ and parameters $\varepsilon_0^*, \tau_0^*, \beta_0^*(\varepsilon), \gamma_0^*$. We note that for $\varepsilon^* := \min\{\varepsilon_0^*, \ldots, \varepsilon_N^*\}$, $\tau^* := \max\{\tau_0^*, \ldots, \tau_N^*\}$, $\beta^*(\varepsilon) := \min\{\beta_0^*(\varepsilon), \ldots, \beta_N^*(\varepsilon)\}$ and $\gamma^* := \min\{\gamma_0^*, \ldots, \gamma_N^*\}$, all the inequalities hold.

Practical attractivity

Without the loss of generality, we assume R, r are given so that $\Delta \geq R \geq r \geq \delta$. Let (l,i) be a hybrid time instant after the N irregular jumps. By Assumption 8.9, it holds $l + i \leq T^*$. Furthermore, Lemma 8.28 gives us $\underline{r} = \underline{v}$ for $\overline{v} = \delta$, and the corresponding tuning parameters $\varepsilon^*, \tau^*, \beta^*(\varepsilon), \gamma^*$. From the definition of parameters in Lemma 8.28, it follows that the Lyapunov derivatives and differences for functions in Equation (8.26) and Assumption 8.6, are defined for $\|\phi(t,j)\|_{\mathcal{A}\times\mathcal{X}_2} \geq \underline{u}, \|\phi(t,j)\|_{\mathcal{M}_\rho} \geq \underline{u}$, where $\underline{u}$ is given in the the system of implications in (8.51). Thus Equations (8.49) and (8.50) guarantee that the trajectories eventually enter and stay in $\tilde{u}$ neighborhoods before jumps, for $v = r = \underline{u}$. And from our practical-stability result, it follows that the trajectory stays in the $\overline{r}$ neighborhood ∎

8.C Proof of Theorem 8.21

Similarly to [149, Equ. 13], let the Lyapunov function candidate be given by

$$V_i(q_i) := \frac{1}{2}\left(x_i^e - c_3\omega_i y_i^e\right)^2 + \frac{1}{2}y_i^{e2} + \frac{1}{2}\theta_i^{e2}, \tag{8.51}$$

where $q_i = \operatorname{col}\left(x_i, y_i, \theta_i^e, \tau_i, \theta_i, \hat{v}_i, \hat{\omega}_i\right)$. First, we characterize the upper and lower bounds of the Lyapunov function candidate. It holds

$$\begin{aligned}
V_i(q_i) &= \tfrac{1}{2}x_i^{e2} - c_3\omega_i x_i^e y_i^e + \tfrac{1}{2}c_3^2\omega_i^2 y_i^{e2} + \tfrac{1}{2}y_i^{e2} + \tfrac{1}{2}\theta_i^{e2} \\
&\geq \tfrac{1}{2}x_i^{e2}(1-\gamma) + \tfrac{1}{2}c_3^2\omega_i^2 y_i^{e2}\left(1-\tfrac{1}{\gamma}\right) + \tfrac{1}{2}y_i^{e2} + \tfrac{1}{2}\theta_i^{e2} \\
&\geq \tfrac{1}{4}x_i^{e2} + \tfrac{1}{2}\left(1 - c_3^2\omega_i^2\right)y_i^{e2} + \tfrac{1}{2}\theta_i^{e2} \\
&\geq \tfrac{1}{4}\left(x_i - u_i^1\right)^2 + \tfrac{1}{4}\left(y_i - u_i^2\right)^2 + \tfrac{1}{4}\theta_i^{e2} = \tfrac{1}{4}\left\|r_i\right\|^2,
\end{aligned}$$

where the second line follows from $ab \leq \frac{\gamma}{2}a^2 + \frac{1}{2\gamma}b^2$, third line follows from $\gamma = \frac{1}{2}$, in the forth line we assume that $c_3 \leq \frac{\sqrt{2}}{2\omega_i}$, and $r_i \coloneqq \operatorname{col}\left(x_i - u_i^1, y_i - u_i^2, \theta_i - \theta_{\mathrm{r}}\right)$. Furthermore, for the upper bound, we have

$$\begin{aligned}
V_i(q_i) &\leq x_i^{e2} + c_3^2\omega^2 y_i^{e2} + \tfrac{1}{2}y_i^{e2} + \tfrac{1}{2}\theta_i^{e2} \\
&\leq x_i^{e2} + y_i^{e2} + \theta_i^{e2} = \left\|r_i\right\|^2,
\end{aligned}$$

where the second line follows from the former assumption on constant c_3. Thus, the bound on the Lyapunov function is given by.

$$\tfrac{1}{4}\left\|r_i\right\|^2 \leq V_i(q_i) \leq \left\|r_i\right\|^2.$$

The Lyapunov derivative is bounded similarly to [149, Equ. 14]:

$$\langle \nabla V_i(q_i) \mid f_i(q_i)\rangle = -\Sigma_i(q_i) + \Lambda_i(q_i),$$

where $\Sigma_i(q_i) \coloneqq c_1\left(x_i^e - c_3\omega_i y_i^e\right)^2 + c_2\theta_i^{e2} + c_3\omega_i^2 y_i^{e2}$ and $\Lambda_i(q_i) \coloneqq \left(x_i^e - c_3\omega_i y_i^e\right)\left(e_i^w y_i^e - e_i^v - c_3 y_i^e e_i^w c_2 + c_3 w e_i^\omega x_i^e\right) - y_i^e e_i^w x_i^e - \theta_i^e e_i^w$, with $e_i^w \coloneqq \hat{\omega}_i - \omega_i$, $e_i^v = \hat{v}_i - v_i$, and $v_i \coloneqq c_1(x_i^e - c_3\omega_i y_i^e) - c_3c_2(\omega_{\mathrm{r}} - \omega_i)y_i^e + c_3\omega_i^2 x_i^e$. To characterize the convergence rate, we upper bound $\Sigma(q_i)_i$ as follows:

$$\begin{aligned}
\Sigma_i(q_i) &= c_1\left(x_i^e - c_3\omega_i y_i^e\right)^2 + c_2\theta_i^{e2} + c_3\omega_i^2 y_i^{e2} \\
&\geq c_1 x_i^{e2}(1-\gamma) + c_1c_3^2\omega_i^2 y_i^{e2}\left(1-\tfrac{1}{\gamma}\right) + c_3\omega_i^2 y_i^{e2} + c_2\theta_i^{e2} \\
&\geq \tfrac{1}{2}c_1 x_i^{e2} + \left(c_3\omega_i^2 - c_1c_3^2\omega_i^2\right)y_i^{e2} + c_2\theta_i^{e2} \\
&\geq \tfrac{1}{2}c_1 x_i^{e2} + \tfrac{1}{2}c_3\omega_i^2 y_i^{e2} + c_2\theta_i^{e2} \\
&\geq \underline{c}\left\|r_i\right\|^2,
\end{aligned}$$

where the third line follows for $\gamma = \frac{1}{2}$, in fourth line we assume $c_1 \leq \frac{1}{2c_3}$, $\underline{c} \coloneqq \min\{\frac{1}{2}c_1, c_2, \frac{1}{2}c_3\omega_i^2\}$ Now, we write the Lyapunov derivative as

$$\langle \nabla V_i(q_i) \mid f_i(q_i)\rangle \leq -\underline{c}V_i(q_i) + \Lambda_i(q_i).$$

As the jumps restart $\Lambda_i(q_i)$ to 0, the jumps of the Lyapunov given by

$$V(q_i^+) - V(q_i) \leq 0.$$

Let $\Delta > \delta > 0$ be the parameters of the semi-global practical stability. If our Lyapunov derivative is negative on the desired domain, it follows that

$$\tfrac{1}{4}\left\|r_i(t,j)\right\|^2 \leq V_i(q_i(t,j)) \leq V_i(q_i(0,0)) \leq \left\|r_i(0,0)\right\|^2,$$

Thus for any initial condition with $\|r_i(0,0)\| \leq \Delta$, it holds that $\|r_i(t,j)\| \leq 2\Delta$. Using the previous bound, we can estimate the minimal and maximal value of ω_i as

$$\underline{\omega}_i \coloneqq \min \omega_i = \omega_{\mathrm{r}} - 2c_2\Delta \tag{8.52}$$

$$\overline{\omega}_i \coloneqq \max \omega_i = \omega_{\mathrm{r}} + 2c_2\Delta. \tag{8.53}$$

Hence, we choose $c_2 = \frac{\omega_{\mathrm{r}}}{4\Delta}$ to ensure $\underline{\omega}_i$ is positive, $c_3 = \frac{1}{3\omega_{\mathrm{r}}} \leq \frac{\sqrt{2}}{3\omega_{\mathrm{r}}}$, and $c_1 = \frac{1}{2c_3}$.
As $\Lambda_i(q_i)$ is differentiable and all of its variables and their derivatives are bounded, we can approximate it with a constant M and write the derivative as

$$\begin{aligned}\langle \nabla V_i(q_i) \mid f_i(q_i) \rangle &\leq -\underline{c} V_i(q_i) + M\tilde{\tau}_i \\ &\leq -\underline{c} V_i(q_i) + M\sigma_i\end{aligned}$$

Parameter σ_i can be made arbitrarily small, thus enabling arbitrarily close convergence to the equilibrium point. As there is a constant time between jumps, semi-global practical stability follows for $c_1 = \sigma_i \to 0$ [78, Cor. 8.7].

IV

Conclusion

9

Concluding remarks

Pride is not the opposite of shame, but its source. True humility is the only antidote to shame.

Uncle Iroh

If someone tried to take control of your body and make you a slave, you would fight for freedom. Yet how easily you hand over your mind to anyone who insults you. When you dwell on their words and let them dominate your thoughts, you make them your master.

Epictetus

In this thesis, we have studied zeroth-order Nash equilibrium seeking algorithms for both static and dynamical agents. We summarize our main contributions to the field of zeroth-order game-theoretic control, argue to which extent we have answered the research questions, and propose possible directions for future research.

9.1 Contributions

We have advanced the field of zeroth-order game-theoretic control by developing continuous-time, discrete-time, and hybrid dynamical algorithms for zeroth-order NE and GNE seeking in this thesis. The main contributions are summarized next:

- **Zeroth-order GNE seeking via output derivative estimators**
  In the first part of this thesis, we identify limitations with an state-of-the-art extremum seeking method that relies on output derivative estimates (Chapter 2). We develop a zeroth-order method for seeking Nash Equilibria in a restricted class of linear systems based on our findings (Chapter 3). To expand our results to general nonlinear systems, we adopt a multi-timescale strategy and incorporate dual dynamics and existing projections in the dynamics to tackle Generalized Nash Equilibrium Problems (GNEPs) (Chapter 4).

- **Generalized equilibrium seeking without projections**
  In the second part of the thesis, we develop a continuous time algorithm without projections that can handle merely monotone generalized Nash equilibrium problems and adapt it for zeroth-order equilibrium seeking (Chapter 5). To improve the convergence speed, we develop a hybrid gain adaptation scheme. Moreover, because strong monotonicity of the monotone operator is no longer necessary for convergence, we propose a method to reduce distortions caused by the standard extremum seeking algorithm. We then demonstrate the effectiveness of this approach in two practical applications: oil extraction and photo-voltaic cells (Chapters 5, 6).

- **Discrete-time zeroth-order NE seeking**
  We formulate an algorithm for finding Nash equilibria in a discrete-time setting, where agents are subject to local constraints. Our approach utilizes novel averaging theory results, allowing us to incorporate three timescales into the algorithm: one for perturbations, another for pseudogradient filtering, and a third for equilibrium seeking. Furthermore, we show that an asynchronous variant of the aforementioned algorithm where agents sample at different frequencies and are not subject to local constraints, also converges to the NE, as long as the sampling order eventually repeats itself and some other mild constraints (Chapter 7).

- **Averaging and singular perturbations theory**
  Our investigation of zeroth-order equilibrium seeking methods in discrete-time and their application to hybrid plant control has resulted in contributions to the theory of averaging for discrete-time systems (Chapter 7) and singular perturbation theory for hybrid systems (Chapter 8). We have developed an averaging theory that accounts for dynamics with multiple timescales and semi-global practical asymptotic stability of the averaged system. Moreover, our formulation allows for sequential application, which eases proving convergence in more complex systems. Additionally, we have developed a theory for singular perturbations where both reduced, and boundary layer systems are hybrid systems. Notably, in our theory, the reduced systems jump from the boundary layer manifold, which allows for "jump-driven" convergence of the restricted system. This enables the use of sampled controllers with output feedback on hybrid system plants.

Answering the research questions

Next, we assess the extent to which we have addressed the original research questions posed in Section 1.3 of this thesis.

(Q_1) **How to design derivative-free equilibrium seeking for GNEPs?**
In order to modify a full-information GNE-seeking algorithm for zeroth-order information, several conditions must be satisfied. First, the algorithm should not incorporate more than one pseudogradient flow or computation in its formulation, as the pseudogradient estimation scheme generates only one pseudogradient value. This limitation arises from the fact that the pseudogradient value is estimated through output measurements based on the current system state, making it challenging to estimate a pseudogradient evaluated at a state not currently held by the system without introducing an auxiliary clone system. In strongly monotone games, as demonstrated in Chapter 4 of this thesis, simple preconditioned pseudogradient descent is sufficient. For merely monotone games, Chapter 5 illustrates that this can be achieved using a modified golden-ratio-like algorithm.

Second, since the problem definition includes constraints shared among agents, the algorithm must be able to handle at least dual Lagrangian variables by ensuring their non-negativity. This can be accomplished through projections onto convex sets (Parts I and III) or by employing novel Lagrangian product dynamics that remain invariant within the positive orthant (Part II).

(Q_2) **Is time-scale separation necessary for equilibrium seeking in systems with dynamical agents?**
In some instances, single time-scale equilibrium seeking with dynamic agents can be achieved by leveraging the specific structure of the equilibrium seeking algorithms and/or the agent dynamics. In Chapter 3, we construct a scenario where the steady-state mapping is equal to one of the parameters in the output time derivative estimation scheme, allowing for equilibrium seeking without time-scale separation. However, this method does not generalize to a broader context (Chapter 2), and it seems that time-scale separation between the algorithm and dynamical system is the only viable approach.

Conversely, output derivative-based equilibrium seeking methods (Part I) applied to static systems do not explicitly use singular perturbation or averaging theory for convergence proof. In contrast, more common sinusoidal perturbation methods (Parts II and III) employ both averaging for pseudogradient estimation and singular perturbation theory to filter the estimate through a first-order filter before integrating it into the equilibrium seeking algorithm. This stems from the fact that averaging theory fails to demonstrate the convergence of the estimate in the presence of projections. While these methods utilize two time scales, they can achieve relatively fast convergence in practice, as the filtered, well-behaved pseudogradient estimate allows for smaller time-scale separation between the filter and the equilibrium seeking algorithm.

(Q_3) **Is monotonicity of the pseudogradient sufficient to ensure convergence of derivative-free continuous-time equilibrium seeking?**

Yes. By appending dual Lagrangian dynamics onto the continuous-time projectionless golden-ratio algorithm, it is possible to construct a continuous-time algorithm that requires only monotonicity of the pseudogradient for convergence and that can be adapted for the zeroth-order information scenario (Chapter 5). Such a complex algorithm is necessary because other algorithms that only require monotonicity of the pseudogradient involve more than one pseudogradient computation, and the continuous-time version of the golden ratio algorithm with projections onto convex sets lacks an analytic proof of convergence. Therefore, a projectionless dual Lagrangian dynamic that converges without relying on the strict monotonicity assumption of the KKT operator has to be constructed.

(Q_4) **Is discrete-time equilibrium seeking applicable to systems with hybrid dynamical agents?**

The discrete-time equilibrium seeking algorithms can be implemented as sampled controllers, with the dynamical agents acting as the controlled plants. Since the controller needs the steady-state output value for the pseudogradient estimation scheme, a time-scale separation using singular perturbation theory should be employed to study stability. In contrast to existing theory, it is also crucial to consider jumps from the boundary layer system (Chapter 8). This can be achieved by requiring a minimum time between the slow state jumps, which correspond to the jumps of the equilibrium seeking algorithm. It is worth mentioning that the controller remains a hybrid system, even though it implements a discrete-time algorithm. By leveraging discrete-time averaging theory that encompasses both multi-timescale dynamics and SGPAS of the averaged system (Chapter 7), it can be shown that this approach can effectively solve strongly monotone NEPs with local constraints and strongly monotone NEPs without local constraints but with asynchronous uncoordinated sampling, just like its continuous-time counterparts.

9.2 Future research and recommendations

Although there are many open problems left in this field of study, we propose some possible future research directions based on the work presented in this thesis.

- **Projection-based zeroth-order equilibrium seeking**
  In Chapter 5, we devised a projectionless equilibrium seeking algorithm to take advantage of the robustness characteristics of outer semicontinuous systems and demonstrate stability. The latest work in hybrid systems theory [150] facilitates the employment of discontinuous projections while maintaining both robustness and stability. By leveraging these findings, it should be possible to establish the stability of the zeroth-order adaptation of conventional equilibrium seeking algorithms when applied to games with local and coupled constraints.

- **Stochastic equilibrium seeking methods for dynamical systems**
  In Chapter 7, we established a deterministic averaging result that enables a deterministic pseudogradient estimation approach. Conversely, the literature is abundant with probabilistic (pseudo)gradient estimation techniques and, consequently, probabilistic

zeroth-order equilibrium seeking methods. By modifying the singular perturbation theory from Chapter 8 to accommodate cases where the restricted system is a stochastic hybrid dynamical system [151], [152], it should be possible to expand the range of equilibrium seeking algorithms that can be utilized as controllers for hybrid dynamical plants.

- **Averaged algorithms for merely monotone operators**
  The averaging theory in Chapter 7, unlike in our proposed discrete-time zeroth-order algorithms, does not require exponential stability of the averaged system (Assumption 7.4). As a result, it might be feasible to employ algorithms that require merely the monotonicity of the (pseudo)gradient. The primary challenge lies in the fact that providing Lyapunov-like convergence rate bounds for these algorithms is generally quite difficult. Moreover, the tuning parameter should decelerate the dynamics and, for its minimal value, reduce the jump mapping to the identity mapping. Consequently, if the algorithms do not conform to this form, they may need to be adapted in a manner similar to the Krasnosel'skiĭ–Mann iteration. Whether this is possible is a question for future research.

- **Fixed-time GNE seeking**
  In other works [18], [153], a special class of continuous-time dynamics is adapted for fixed-time NE seeking, meaning that the convergence time to the solution is predetermined. Moreover, these algorithms can be adjusted for cases with zeroth-order information. The primary reason for not adapting these algorithms to the generalized case is strong monotonicity requirement to ensure convergence, while the KKT operator exhibits mere monotonicity. It might be feasible to exploit the structure of the KKT operator to overcome this issue, akin to how preconditioning was employed in [44] for the forward-backward operator splitting. The exact approach remains an open question. Furthermore, numerical simulations indicate that the discretized version of the fixed-time algorithm shares similar characteristics. Consequently, developing the corresponding discrete-time theory and establishing analytical guarantees would be worthwhile.

9.3 Research beyond the scope of this thesis

Finally, we acknowledge some weaknesses of our work that could emerge in practical applications, which have not been substantially addressed.

- **Measurement noise**
  The primary feature of zeroth-order algorithms is the measurement of the cost function, making it vulnerable to noise corruption in practical applications. In Section 4.5.1, we tackle this issue through comprehensive numerical simulations. In Chapter 5, we assert robustness to minor disturbances due to the outer semi-continuity of flow and jump mappings. Nevertheless, this robustness is not quantified theoretically or numerically in this or other chapters. As a result, additional research is warranted.

- **Parameter tuning**
  Singular perturbation and averaging theory are undoubtedly powerful tools for

proving various stability results, yet they come with certain drawbacks. While these theories suggest the existence of numerous small tuning parameters, they do not offer their maximum values. Consequently, in practical applications, tuning is achieved by initially setting the parameters to arbitrarily small values and then adjusting them to observe stability. This approach can potentially result in conservative convergence rates or, worse, instability if the chosen parameters do not guarantee stability for some unexamined initial conditions. Since our research relies heavily on singular perturbation and averaging theory in deriving results, we do not present any findings related to tuning the various small parameters that emerge in our results. It may be feasible to establish these bounds on a problem-specific basis rather than in general terms, but such analysis was beyond the scope of our work.

- **Implementability**
  The equilibrium-seeking algorithms proposed in Parts I and II of this thesis are presented in continuous time. As a result, implementing them in real-life scenarios would require the use of an analog computer capable of performing operations such as addition, constant and variable gains, sinusoidal generation, complex calculations involved in the derivative estimation scheme, and signal multiplication. However, such computers may be expensive or hard to come by. An alternative, more straightforward approach would be to discretize the control algorithm. Unfortunately, this procedure might introduce approximations that fail to maintain the stability properties of the original algorithm. Consequently, further analysis is required to determine suitable discretization techniques and sampling times.

- **Nonconforming strategies**
  In this thesis, we assume that all agents adopt the same strategy, specifically, our proposed algorithms. We do not investigate the impact on equilibrium stability if an agent opts for a different strategy or algorithm. In general, this subject attracts minimal research attention. Fundamentally, the selection of an algorithm represents a game in itself, a meta-game, with the situation where all agents adhere to the same strategy constituting a Nash equilibrium. No agent has a motive to deviate from the common strategy, as there is no theoretical assurance that pursuing an alternative strategy would yield better outcomes. In fact, adhering to the same strategy as others ensures their minimum guaranteed payoff, providing an incentive to conform. On the other hand, that would not explain how and why the strategies would evolve into the Nash equilibrium. Such analysis was not conducted in our research.

Bibliography

[1] F. Facchinei and C. Kanzow. "Generalized Nash equilibrium problems". In: *Annals of Operations Research* 175.1 (Mar. 2010), pp. 177–211. ISSN: 0254-5330. DOI: 10.1007/s10479-009-0653-x.

[2] M. Nisen. *Billionaire Eddie Lampert Is Running Sears Like The Coliseum, And It's A Disaster*. https://web.archive.org/web/20230424110613/https://www.businessinsider.com/eddie-lamperts-sears-strategy-disaster-2013-7?international=true&r=US&IR=T. [Accessed 24-Apr-2023].

[3] M. Kimes. *At Sears, Eddie Lampert's Warring Divisions Model Adds to the Troubles*. https://web.archive.org/web/20160313065855/https://www.bloomberg.com/news/articles/2013-07-11/at-sears-eddie-lamperts-warring-divisions-model-adds-to-the-troubles. [Accessed 24-Apr-2023].

[4] D. Kotz and F. Weir. *Russia's Path from Gorbachev to Putin*. en. 0th ed. Routledge, May 2007. ISBN: 978-1-135-99206-4. DOI: 10.4324/9780203799369. URL: https://www.taylorfrancis.com/books/9781135992064.

[5] Y. Qi, N. Stern, T. Wu, J. Lu, and F. Green. "China's post-coal growth". en. In: *Nature Geoscience* 9.88 (Sept. 2016), pp. 564–566. ISSN: 1752-0908. DOI: 10.1038/ngeo2777.

[6] P. A. Samuelson and W. D. Nordhaus. *Economics*. en. 19th ed. The McGraw-Hill series economics. Boston: McGraw-Hill Irwin, 2010. ISBN: 978-0-07-351129-0.

[7] P. Frihauf, M. Krstic, and T. Basar. "Nash equilibrium seeking in noncooperative games". In: *IEEE Transactions on Automatic Control* 57.5 (May 2011), pp. 1192–1207. ISSN: 0018-9286. DOI: 10.1109/tac.2011.2173412.

[8] M. S. Stankovic, K. H. Johansson, and D. M. Stipanovic. "Distributed seeking of Nash equilibria with applications to mobile sensor networks". In: *IEEE Transactions on Automatic Control* 57.4 (Apr. 2011), pp. 904–919. ISSN: 0018-9286. DOI: 10.1109/tac.2011.2174678.

[9] J. Barreiro-Gomez, C. Ocampo-Martinez, F. Bianchi, and N. Quijano. "Model-free control for wind farms using a gradient estimation-based algorithm". In: *2015 IEEE European Control Conference (ECC)*. IEEE, July 2015, pp. 1516–1521. DOI: 10.1109/ecc.2015.7330753. URL: http://www.iri.upc.edu/files/scidoc/1626-Model-free-Control-for-Wind-Farms-using-a-Gradient-Estimation-based-Algorithm.pdf.

[10] J. R. Marden, G. Arslan, and J. S. Shamma. "Cooperative control and potential games". In: *IEEE Transactions on Systems, Man, and Cybernetics, Part B (Cybernetics)* 39.6 (Dec. 2009), pp. 1393–1407. ISSN: 1083-4419. DOI: 10.1109/tsmcb.2009.2017273. URL: https://authors.library.caltech.edu/16311/1/Marden2009p6043Ieee_T_Syst_Man_Cy_B.pdf.

[11] T. L. Silva and A. Pavlov. "Dither signal optimization for multi-agent extremum seeking control". In: *2020 European Control Conference (ECC)*. IEEE. IEEE, May 2020, pp. 1230–1237. DOI: 10.23919/ecc51009.2020.9143610.

[12] M. Krstić and H.-H. Wang. "Stability of extremum seeking feedback for general nonlinear dynamic systems". In: *Automatica* 36.4 (Apr. 2000), pp. 595–601. ISSN: 0005-1098. DOI: 10.1016/s0005-1098(99)00183-1.

[13] J.-Y. Choi, M. Krstic, K. B. Ariyur, and J. S. Lee. "Extremum seeking control for discrete-time systems". In: *IEEE Transactions on automatic control* 47.2 (2002), pp. 318–323. ISSN: 0018-9286. DOI: 10.1109/9.983370.

[14] Y. Nesterov and V. Spokoiny. "Random Gradient-Free Minimization of Convex Functions". en. In: *Foundations of Computational Mathematics* 17.2 (Apr. 2017), pp. 527–566. ISSN: 1615-3375, 1615-3383. DOI: 10.1007/s10208-015-9296-2.

[15] P. Hansen and B. Jaumard. "Lipschitz Optimization". en. In: *Handbook of Global Optimization*. Ed. by R. Horst and P. M. Pardalos. Nonconvex Optimization and Its Applications. Boston, MA: Springer US, 1995, pp. 407–493. ISBN: 978-1-4615-2025-2. DOI: 10.1007/978-1-4615-2025-2_9. URL: https://doi.org/10.1007/978-1-4615-2025-2_9.

[16] M. Avriel. *Nonlinear programming: analysis and methods*. Courier Corporation, 2003. ISBN: 978-0-486-43227-4.

[17] J. I. Poveda and A. R. Teel. "A framework for a class of hybrid extremum seeking controllers with dynamic inclusions". In: *Automatica* 76 (Feb. 2017), pp. 113–126. ISSN: 0005-1098. DOI: 10.1016/j.automatica.2016.10.029.

[18] J. I. Poveda and M. Krstić. "Nonsmooth extremum seeking control with user-prescribed fixed-time convergence". In: *IEEE Transactions on Automatic Control* 66.12 (Dec. 2021), pp. 6156–6163. ISSN: 0018-9286. DOI: 10.1109/tac.2021.3063700.

[19] T. Tatarenko and M. Kamgarpour. "Learning generalized Nash equilibria in a class of convex games". In: *IEEE Transactions on Automatic Control* 64.4 (Apr. 2018), pp. 1426–1439. ISSN: 0018-9286. DOI: 10.1109/tac.2018.2841319.

[20] M. Guay and D. Dochain. "A proportional-integral extremum-seeking controller design technique". In: *Automatica* 77 (Mar. 2017), pp. 61–67. ISSN: 0005-1098. DOI: 10.1016/j.automatica.2016.11.018.

[21] S. Krilašević and S. Grammatico. "Comments on "A proportional-integral extremum-seeking controller design technique"[Automatica 77 (2017) 61–67]". In: *Automatica* 135 (Jan. 2022), p. 109932. ISSN: 0005-1098. DOI: 10.1016/j.automatica.2021.109932.

[22] S. Krilašević and S. Grammatico. "An integral Nash equilibrium control scheme for a class of multi-agent linear systems". In: *IFAC WC* 53 (2020), pp. 5375–5380. ISSN: 2405-8963. DOI: 10.1016/j.ifacol.2020.12.1521.

[23] S. Krilašević and S. Grammatico. "Learning generalized Nash equilibria in multi-agent dynamical systems via extremum seeking control". In: *Automatica* 133 (Nov. 2021), p. 109846. ISSN: 0005-1098. DOI: 10.1016/j.automatica.2021.109846.

[24] S. Krilašević and S. Grammatico. "Learning generalized Nash equilibria in monotone games: A hybrid adaptive extremum seeking control approach". en. In: *Automatica* 151 (May 2023), p. 110931. ISSN: 0005-1098. DOI: 10.1016/j.automatica.2023.110931.

[25] S. Krilašević and S. Grammatico. "Distortion reduction in photovoltaic output current via optimized extremum seeking control". In: *2023 21st European Control Conference (ECC)* (June 2023).

[26] S. Krilašević and S. Grammatico. "A discrete-time averaging theorem and its application to zeroth-order Nash equilibrium seeking". In: arXiv:2302.04854 (Feb. 2023). arXiv:2302.04854 [cs, eess, math]. DOI: 10.48550/arXiv.2302.04854.

[27] S. Krilašević and S. Grammatico. "Stability of singularly perturbed hybrid systems with restricted systems evolving on boundary layer manifolds". In: arXiv:2303.18238 (Mar. 2023). arXiv:2303.18238 [cs, eess, math]. DOI: 10.48550/arXiv.2303.18238.

[28] M. Guay and D. Dochain. "Author's Reply to 'Comment on "A proportional-integral extremum seeking controller design technique"[Automatica 77 (2017) 61–67]'". In: *Automatica* 135 (Jan. 2022), p. 109944. ISSN: 0005-1098. DOI: 10.1016/j.automatica.2021.109944.

[29] H. K. Khalil. *Nonlinear systems*. Prentice Hall, Jan. 2002, pp. 119–138.

[30] Y. Tan, D. Nešić, and I. Mareels. "On non-local stability properties of extremum seeking control". In: *Automatica* 42.6 (June 2006), pp. 889–903. ISSN: 1474-6670. DOI: 10.3182/20050703-6-cz-1902.00747. URL: http://people.eng.unimelb.edu.au/dnesic/IFAC05-extremum.pdf.

[31] A. Ghaffari, M. Krstić, and D. Nešić. "Multivariable Newton-based extremum seeking". en. In: *Automatica* 48.8 (Aug. 2012), pp. 1759–1767. ISSN: 0005-1098. DOI: 10.1016/j.automatica.2012.05.059.

[32] H.-B. Dürr, M. S. Stanković, C. Ebenbauer, and K. H. Johansson. "Lie bracket approximation of extremum seeking systems". In: *Automatica* 49.6 (June 2013), pp. 1538–1552. ISSN: 0005-1098. DOI: 10.1016/j.automatica.2013.02.016. URL: http://arxiv.org/pdf/1109.6129.

[33] W. Saad, Z. Han, H. V. Poor, and T. Basar. "Game-theoretic methods for the smart grid: Game-theoretic methods for the smart grid: An overview of microgrid systems, demand-side management, and smart grid communications". In: *IEEE Signal Processing Magazine* 29 (2012), pp. 86–105.

[34] G. Belgioioso and S. Grammatico. "Semi-decentralized Nash equilibrium seeking in aggregative games with separable coupling constraints and non-differentiable cost functions". In: *IEEE control systems letters* 1.2 (Oct. 2017), pp. 400–405. ISSN: 2475-1456. DOI: 10.1109/lcsys.2017.2718842.

[35] W. Lin, Z. Qu, and M. A. Simaan. "Distributed game strategy design with application to multi-agent formation control". In: *53rd IEEE Conference on Decision and Control*. IEEE, Dec. 2014, pp. 433–438. DOI: 10.1109/cdc.2014.7039419.

[36] D. Gadjov and L. Pavel. "A passivity-based approach to Nash equilibrium seeking over networks". In: *IEEE Transactions on Automatic Control* 64.3 (Mar. 2018), pp. 1077–1092. ISSN: 0018-9286. DOI: 10.1109/tac.2018.2833140. URL: http://arxiv.org/pdf/1705.02424.

[37] A. R. Romano and L. Pavel. "Dynamic NE seeking for multi-integrator networked agents with disturbance rejection". In: *IEEE Transactions on Control of Network Systems* 7.1 (Mar. 2019), pp. 129–139. ISSN: 2325-5870. DOI: 10.1109/tcns.2019.2920590. URL: http://arxiv.org/pdf/1903.02587.

[38] C. De Persis and S. Grammatico. "Distributed averaging integral Nash equilibrium seeking on networks". In: *Automatica* 110 (Dec. 2019), p. 108548. ISSN: 0005-1098. DOI: 10.1016/j.automatica.2019.108548. URL: https://pure.rug.nl/ws/files/109236667/1_s2.0_S0005109819304091_main.pdf.

[39] M. Bianchi and S. Grammatico. "A continuous-time distributed generalized Nash equilibrium seeking algorithm over networks for double-integrator agents". In: *arXiv preprint arXiv:1910.11608* (May 2019), pp. 1474–1479. DOI: 10.23919/ecc51009.2020.9143714. URL: https://repository.tudelft.nl/islandora/object/uuid%3A3c9c5fb6-0229-4fc1-afcc-febb89bfbad3/datastream/OBJ/download.

[40] S.-J. Liu and M. Krstić. "Stochastic Nash equilibrium seeking for games with general nonlinear payoffs". In: *SIAM Journal on Control and Optimization* 49.4 (Jan. 2011), pp. 1659–1679. ISSN: 0363-0129. DOI: 10.1007/978-1-4471-4087-0_9.

[41] M. Guay, I. Vandermeulen, S. Dougherty, and P. J. McLellan. "Distributed extremum-seeking control over networks of dynamically coupled unstable dynamic agents". In: *Automatica* 93 (July 2018), pp. 498–509. ISSN: 0005-1098. DOI: 10.1016/j.automatica.2018.03.081.

[42] H. H. Bauschke, P. L. Combettes, et al. *Convex analysis and monotone operator theory in Hilbert spaces*. 2nd ed. Vol. 408. Springer, 2011, pp. 1–468. ISBN: 9781441994660. DOI: 10.1007/978-1-4419-9467-7. URL: https://link.springer.com/content/pdf/bfm%3A978-1-4419-9467-7%2F1.

[43] C.-K. Yu, M. Van Der Schaar, and A. H. Sayed. "Distributed learning for stochastic generalized Nash equilibrium problems". In: *IEEE Transactions on Signal Processing* 65.15 (Aug. 2017), pp. 3893–3908. ISSN: 1053-587X.

[44] P. Yi and L. Pavel. "An operator splitting approach for distributed generalized Nash equilibria computation". In: *Automatica* 102 (Apr. 2019), pp. 111–121. ISSN: 0005-1098. DOI: 10.1016/j.automatica.2019.01.008. URL: http://arxiv.org/pdf/1703.05388.

[45] V. Adetola and M. Guay. "Finite-time parameter estimation in adaptive control of nonlinear systems". In: *IEEE Transactions on Automatic Control* 53.3 (Apr. 2008), pp. 807–811. ISSN: 0018-9286. DOI: 10.1109/tac.2008.919568.

[46] A. Nagurney and D. Zhang. *Projected dynamical systems and variational inequalities with applications*. Vol. 2. Springer Science & Business Media, 2012. ISBN: 9781461359722. DOI: 10.1007/978-1-4615-2301-7. URL: https://link.springer.com/content/pdf/bfm:978-1-4615-2301-7/1?pdf=chapter%20toc.

[47] A.-H. Mohsenian-Rad, V. W. Wong, J. Jatskevich, R. Schober, and A. Leon-Garcia. "Autonomous demand-side management based on game-theoretic energy consumption scheduling for the future smart grid". In: *IEEE transactions on Smart Grid* 1.3 (Dec. 2010), pp. 320–331. ISSN: 1949-3053. DOI: 10.1109/tsg.2010.2089069. URL: http://www.ee.ucr.edu/%7Ehamed/MRWJSLGjTSG2010_Correction.pdf.

[48] Z. Ma, D. S. Callaway, and I. A. Hiskens. "Decentralized charging control of large populations of plug-in electric vehicles". In: *IEEE Transactions on control systems technology* 21.1 (Jan. 2011), pp. 67–78. ISSN: 1063-6536. DOI: 10.1109/tcst.2011.2174059.

[49] S. Li, W. Zhang, J. Lian, and K. Kalsi. "Market-based coordination of thermostatically controlled loads—Part I: A mechanism design formulation". In: *IEEE Transactions on Power Systems* 31.2 (Mar. 2015), pp. 1170–1178. ISSN: 0885-8950. DOI: 10.1109/tpwrs.2015.2432057.

[50] S. Li, W. Zhang, J. Lian, and K. Kalsi. "Market-based coordination of thermostatically controlled loads—Part II: Unknown parameters and case studies". In: *IEEE Transactions on Power Systems* 31.2 (Mar. 2015), pp. 1179–1187. ISSN: 0885-8950. DOI: 10.1109/tpwrs.2015.2432060.

[51] E. K. Ryu and S. Boyd. "A primer on monotone operator methods". In: *Appl. Comput. Math* 15.1 (2016), pp. 3–43.

[52] D. Gadjov and L. Pavel. "Distributed GNE seeking over networks in aggregative games with coupled constraints via forward-backward operator splitting". In: *2019 IEEE 58th Conference on Decision and Control (CDC)*. IEEE, Dec. 2019, pp. 5020–5025. DOI: 10.1109/cdc40024.2019.9029369.

[53] G. Belgioioso, A. Nedich, and S. Grammatico. "Distributed generalized Nash equilibrium seeking in aggregative games on time-varying networks". In: *IEEE Transactions on Automatic Control* 66 (May 2020), pp. 2061–2075. ISSN: 0018-9286. DOI: 10.1109/tac.2020.3005922. URL: http://arxiv.org/pdf/1907.00191.

[54] B. Franci, M. Staudigl, and S. Grammatico. "Distributed forward-backward (half) forward algorithms for generalized Nash equilibrium seeking". In: *2020 IEEE European Control Conference (ECC)*. IEEE, May 2020, pp. 1274–1279. DOI: 10.23919/ecc51009.2020.9143676.

[55] M. Bianchi and S. Grammatico. "Continuous-time fully distributed generalized Nash equilibrium seeking for multi-integrator agents". In: *Automatica* 129 (July 2021), p. 109660. ISSN: 0005-1098. DOI: 10.1016/j.automatica.2021.109660. URL: http://arxiv.org/pdf/1911.12266.

[56] T. Goto, T. Hatanaka, and M. Fujita. "Payoff-based inhomogeneous partially irrational play for potential game theoretic cooperative control: Convergence analysis". In: *2012 IEEE American Control Conference (ACC)*. IEEE, June 2012, pp. 2380–2387. DOI: 10.1109/acc.2012.6314613.

[57] J. R. Marden and J. S. Shamma. "Revisiting log-linear learning: Asynchrony, completeness and payoff-based implementation". In: *Games and Economic Behavior* 75.2 (Sept. 2012), pp. 788–808. ISSN: 0899-8256. DOI: 10.1109/allerton.2010.5707044.

[58] M. Guay and D. Dochain. "A time-varying extremum-seeking control approach". In: *Automatica* 51 (Jan. 2015), pp. 356–363. ISSN: 0005-1098. DOI: 10.1016/j.automatica.2014.10.078.

[59] M. Ye, G. Hu, and S. Xu. "An extremum seeking-based approach for Nash equilibrium seeking in N-cluster noncooperative games". In: *Automatica* 114 (2020), p. 108815. DOI: 10.1016/j.automatica.2020.108815.

[60] J. I. Poveda and N. Quijano. "Shahshahani gradient-like extremum seeking". In: *Automatica* 58 (Aug. 2015), pp. 51–59. ISSN: 0005-1098. DOI: 10.1016/j.automatica.2015.05.002.

[61] C. De Persis and S. Grammatico. "Continuous-time integral dynamics for a class of aggregative games with coupling constraints". In: *IEEE Transactions on Automatic Control* 65 (May 2019), pp. 2171–2176. ISSN: 0018-9286. DOI: 10.1109/tac.2019.2939639. URL: https://pure.rug.nl/ws/files/159652677/08825548.pdf.

[62] R. I. Boţ and E. R. Csetnek. "A dynamical system associated with the fixed points set of a nonexpansive operator". In: *Journal of dynamics and differential equations* 29.1 (Mar. 2017), pp. 155–168. ISSN: 1040-7294. DOI: 10.1007/s10884-015-9438-x. URL: http://arxiv.org/pdf/1411.4442.

[63] S. Oh and H. K. Khalil. "Nonlinear output-feedback tracking using high-gain observer and variable structure control". In: *Automatica* 33.10 (1997), pp. 1845–1856. DOI: 10.1016/s0005-1098(97)00111-8.

[64] S.-O. Lee, Y.-J. Cho, M. Hwang-Bo, B.-J. You, and S.-R. Oh. "A stable target-tracking control for unicycle mobile robots". In: *2000 IEEE/RSJ International Conference on Intelligent Robots and Systems (IROS 2000)(Cat. No. 00CH37113)*. Vol. 3. IEEE, Nov. 2002, pp. 1822–1827. DOI: 10.1109/iros.2000.895236.

[65] E. Koutroulis and K. Kalaitzakis. "Design of a maximum power tracking system for wind-energy-conversion applications". In: *IEEE transactions on industrial electronics* 53.2 (Apr. 2006), pp. 486–494. ISSN: 0278-0046. DOI: 10.1109/tie.2006.870658.

[66] B. Boukhezzar, H. Siguerdidjane, and M. M. Hand. "Nonlinear control of variable-speed wind turbines for generator torque limiting and power optimization". In: *J. Sol. Energy Eng.* 128 (Nov. 2006), pp. 516–530. ISSN: 0199-6231. DOI: 10.1115/1.2356496.

[67] A. Ghaffari, M. Krstic, and S. Seshagiri. "Extremum seeking for wind and solar energy applications". In: *Mechanical Engineering* 136.03 (June 2014), S13–S21. DOI: 10.1109/wcica.2014.7053780.

[68] M. Soltani, R. Wisniewski, P. Brath, and S. Boyd. "Load reduction of wind turbines using receding horizon control". In: *2011 IEEE international conference on control applications (CCA)*. IEEE, Sept. 2011, pp. 852–857. DOI: 10.1109/cca.2011.6044407. URL: http://stanford.edu/~boyd/papers/pdf/wind_turbine_rhc.pdf.

[69] M. Soliman, O. Malik, and D. T. Westwick. "Multiple model predictive control for wind turbines with doubly fed induction generators". In: *IEEE Transactions on Sustainable Energy* 2.3 (July 2011), pp. 215–225. ISSN: 1949-3029. DOI: 10.1109/tste.2011.2153217.

[70] J. R. Marden, S. D. Ruben, and L. Y. Pao. "A model-free approach to wind farm control using game theoretic methods". In: *IEEE Transactions on Control Systems Technology* 21.4 (July 2013), pp. 1207–1214. ISSN: 1063-6536. DOI: 10.1109/tcst.2013.2257780.

[71] J. Ebegbulem and M. Guay. "Distributed extremum seeking control for wind farm power maximization". In: *IFAC-PapersOnLine* 50.1 (July 2017), pp. 147–152. ISSN: 2405-8963. DOI: 10.1016/j.ifacol.2017.08.025.

[72] F. Blanchini and S. Miani. *Set-theoretic methods in control*. Springer, 2008. ISBN: 9780817632557. DOI: 10.1007/978-0-8176-4606-6. URL: https://link.springer.com/content/pdf/bfm%3A978-0-8176-4606-6%2F1.

[73] S. Grammatico. "Dynamic control of agents playing aggregative games with coupling constraints". In: *IEEE Transactions on Automatic Control* 62.9 (Sept. 2017), pp. 4537–4548. ISSN: 0018-9286. DOI: 10.1109/tac.2017.2672902. URL: http://arxiv.org/pdf/1609.08962.

[74] V. Grushkovskaya, A. Zuyev, and C. Ebenbauer. "On a class of generating vector fields for the extremum seeking problem: Lie bracket approximation and stability properties". In: *Automatica* 94 (Aug. 2018), pp. 151–160. ISSN: 0005-1098. DOI: 10.1016/j.automatica.2018.04.024. URL: http://arxiv.org/pdf/1703.02348.

[75] C.-K. Liao, C. Manzie, A. Chapman, and T. Alpcan. "Constrained extremum seeking of a MIMO dynamic system". In: *Automatica* 108 (Oct. 2019), p. 108496. ISSN: 0005-1098. DOI: 10.1016/j.automatica.2019.108496.

[76] G. Shao, A. R. Teel, Y. Tan, K.-Z. Liu, and R. Wang. "Extremum seeking control with input dead-zone". In: *IEEE Transactions on Automatic Control* 65.7 (July 2019), pp. 3184–3190. ISSN: 0018-9286. DOI: 10.1109/tac.2019.2946427.

[77] C. Labar, E. Garone, M. Kinnaert, and C. Ebenbauer. "Newton-based extremum seeking: A second-order Lie bracket approximation approach". In: *Automatica* 105 (July 2019), pp. 356–367. ISSN: 0005-1098. DOI: 10.1016/j.automatica.2019.04.010.

[78] R. G. Sanfelice and A. R. Teel. "On singular perturbations due to fast actuators in hybrid control systems". In: *Automatica* 47.4 (Apr. 2011), pp. 692–701. ISSN: 0005-1098. DOI: 10.1016/j.automatica.2011.01.055.

[79] W. Wang, A. R. Teel, and D. Nešić. "Analysis for a class of singularly perturbed hybrid systems via averaging". In: *Automatica* 48.6 (June 2012), pp. 1057–1068. ISSN: 0005-1098. DOI: 10.1016/j.automatica.2012.03.013.

[80] R. Goebel, R. G. Sanfelice, and A. R. Teel. *Hybrid dynamical systems*. Princeton University Press, Mar. 2012. ISBN: 9781400842636. DOI: 10.1515/9781400842636.

[81] J. I. Poveda and A. R. Teel. "A robust event-triggered approach for fast sampled-data extremization and learning". In: *IEEE Transactions on Automatic Control* 62.10 (Oct. 2017), pp. 4949–4964. ISSN: 0018-9286. DOI: 10.1109/tac.2017.2674519.

[82] J. I. Poveda and N. Li. "Robust hybrid zero-order optimization algorithms with acceleration via averaging in time". In: *Automatica* 123 (Jan. 2021), p. 109361. ISSN: 0005-1098. DOI: 10.1016/j.automatica.2020.109361.

[83] J. I. Poveda, R. Kutadinata, C. Manzie, D. Nešić, A. R. Teel, and C.-K. Liao. "Hybrid extremum seeking for black-box optimization in hybrid plants: An analytical framework". In: *2018 IEEE Conference on Decision and Control (CDC)*. IEEE. IEEE, Dec. 2018, pp. 2235–2240. DOI: 10.1109/cdc.2018.8618907.

[84] S. Krilašević and S. Grammatico. "An extremum seeking algorithm for monotone Nash equilibrium problems". In: *2021 IEEE Conference on Decision and Control (CDC)* (Dec. 2021), pp. 1232–1237. DOI: 10.1109/cdc45484.2021.9683700. URL: http://arxiv.org/pdf/2109.07975.

[85] F. Facchinei and J.-S. Pang. *Finite-dimensional variational inequalities and complementarity problems*. Springer Science & Business Media, 2007. ISBN: 9780387955810. DOI: 10.1007/b97544. URL: https://link.springer.com/content/pdf/bfm:978-0-387-21814-4/1?pdf=chapter%20toc.

[86] G. M. Korpelevich. "The extragradient method for finding saddle points and other problems". In: *Matecon* 12 (1976), pp. 747–756.

[87] Y. Censor, A. Gibali, and S. Reich. "The subgradient extragradient method for solving variational inequalities in Hilbert space". In: *Journal of Optimization Theory and Applications* 148.2 (Feb. 2011), pp. 318–335. ISSN: 0022-3239. DOI: 10.1007/s10957-010-9757-3. URL: https://europepmc.org/articles/pmc3073511?pdf=render.

[88] Y. Malitsky. "Golden ratio algorithms for variational inequalities". In: *Mathematical Programming* 184 (Nov. 2019), pp. 1–28. ISSN: 0025-5610. DOI: 10.1007/s10107-019-01416-w. URL: http://arxiv.org/pdf/1803.08832.

[89] R. I. Bot, E. R. Csetnek, and P. T. Vuong. "The forward-backward-forward method from continuous and discrete perspective for pseudo-monotone variational inequalities in Hilbert spaces". In: *European Journal of Operational Research* 287 (Nov. 2020), pp. 49–60. ISSN: 0377-2217. DOI: 10.1016/j.ejor.2020.04.035. URL: https://eprints.soton.ac.uk/439623/1/1_s2.0_S037722172030388X_main.pdf.

[90] D. Gadjov and L. Pavel. "On the exact convergence to Nash equilibrium in monotone regimes under partial-information". In: *2020 59th IEEE Conference on Decision and Control (CDC)*. IEEE, Dec. 2020, pp. 2297–2302. DOI: 10.1109/cdc42340.2020.9303904.

[91] H.-B. Dürr and C. Ebenbauer. "A smooth vector field for saddle point problems". In: *2011 50th IEEE Conference on Decision and Control and European Control Conference*. IEEE, Dec. 2011, pp. 4654–4660. DOI: 10.1109/cdc.2011.6161102.

[92] H.-B. Dürr, C. Zeng, and C. Ebenbauer. "Saddle point seeking for convex optimization problems". In: *IFAC Proceedings Volumes* 46.23 (2013). Ed. by S. Tarbouriech and M. Krstic, pp. 540–545. ISSN: 1474-6670. DOI: 10.3182/20130904-3-fr-2041.00023.

[93] K. B. Ariyur and M. Krstic. *Real-time optimization by extremum-seeking control*. John Wiley & Sons, Sept. 2003. ISBN: 9780471669784.

[94] R. Goebel, R. G. Sanfelice, and A. R. Teel. "Hybrid dynamical systems". In: *IEEE control systems magazine* 29.2 (Mar. 2009), pp. 28–93. DOI: 10.1515/9781400842636.

[95] M. Abdelgalil and H. Taha. "Lie bracket approximation-based extremum seeking with vanishing input oscillations". In: *Automatica* 133 (Nov. 2021), p. 109735. ISSN: 0005-1098. DOI: 10.1016/j.automatica.2021.109735. URL: http://arxiv.org/pdf/2002.09101.

[96] D. Bhattacharjee and K. Subbarao. "Extremum seeking control with attenuated steady-state oscillations". In: *Automatica* 125 (Mar. 2021), p. 109432. ISSN: 0005-1098. DOI: 10.1016/j.automatica.2020.109432.

[97] R. Suttner. "Extremum seeking control with an adaptive dither signal". In: *Automatica* 101 (Mar. 2019), pp. 214–222. ISSN: 0005-1098. DOI: 10.1016/j.automatica.2018.11.055.

[98] R. T. Rockafellar and R. J.-B. Wets. *Variational analysis*. Vol. 317. Springer Science & Business Media, 2009. ISBN: 9783540627722. DOI: 10.1007/978-3-642-02431-3.

[99] G. R. Walker and P. C. Sernia. "Cascaded DC-DC converter connection of photovoltaic modules". In: *IEEE transactions on power electronics* 19.4 (June 2004), pp. 1130–1139. DOI: 10.1109/psec.2002.1023842.

[100] Y. S. Kumar and R. Gupta. "Maximum power point tracking of multiple photovoltaic arrays". In: *2012 Students Conference on Engineering and Systems*. IEEE. IEEE, Mar. 2012, pp. 1–6. DOI: 10.1109/sces.2012.6199027.

[101] F. El Aamri, H. Maker, D. Sera, S. V. Spataru, J. M. Guerrero, and A. Mouhsen. "A direct maximum power point tracking method for single-phase grid-connected PV inverters". In: *IEEE Transactions on Power Electronics* 33.10 (Oct. 2017), pp. 8961–8971. ISSN: 0885-8993. DOI: 10.1109/tpel.2017.2780858. URL: https://vbn.aau.dk/ws/files/280261817/A_Direct_Maximum_Power_Point_Tracking_Method_for_Single_Phase_Grid_Connected_PV_Inverters.pdf.

[102] M. T. Azary, M. Sabahi, E. Babaei, and F. A. A. Meinagh. "Modified single-phase single-stage grid-tied flying inductor inverter with MPPT and suppressed leakage current". In: *IEEE Transactions on Industrial Electronics* 65.1 (Jan. 2017), pp. 221–231. ISSN: 0278-0046. DOI: 10.1109/tie.2017.2719610.

[103] D. N. Zmood and D. G. Holmes. "Stationary frame current regulation of PWM inverters with zero steady-state error". In: *IEEE Transactions on power electronics* 18.3 (May 2003), pp. 814–822. ISSN: 0885-8993. DOI: 10.1109/tpel.2003.810852.

[104] H. Cha, T.-K. Vu, and J.-E. Kim. "Design and control of Proportional-Resonant controller based Photovoltaic power conditioning system". In: *2009 IEEE Energy Conversion Congress and Exposition*. IEEE. IEEE, Sept. 2009, pp. 2198–2205. DOI: 10.1109/ecce.2009.5316374.

[105] F. He, Z. Zhao, L. Yuan, and S. Lu. "A DC-link voltage control scheme for single-phase grid-connected PV inverters". In: *2011 IEEE Energy Conversion Congress and Exposition*. IEEE. IEEE, Sept. 2011, pp. 3941–3945. DOI: 10.1109/ecce.2011.6064305.

[106] M. Merai, M. W. Naouar, I. Slama-Belkhodja, and E. Monmasson. "An adaptive PI controller design for DC-link voltage control of single-phase grid-connected converters". In: *IEEE Transactions on Industrial Electronics* 66.8 (Aug. 2018), pp. 6241–6249. ISSN: 0278-0046. DOI: 10.1109/tie.2018.2871796.

[107] S. Ozdemir, N. Altin, and I. Sefa. "Single stage three level grid interactive MPPT inverter for PV systems". In: *Energy Conversion and Management* 80 (Apr. 2014), pp. 561–572. ISSN: 0196-8904. DOI: 10.1016/j.enconman.2014.01.048.

[108] M. A. Elgendy, B. Zahawi, and D. J. Atkinson. "Assessment of perturb and observe MPPT algorithm implementation techniques for PV pumping applications". In: *IEEE transactions on sustainable energy* 3.1 (Jan. 2011), pp. 21–33. ISSN: 1949-3029. DOI: 10.1109/tste.2011.2168245.

[109] M. Tajuddin, M. Arif, S. Ayob, and Z. Salam. "Perturbative methods for maximum power point tracking (MPPT) of photovoltaic (PV) systems: a review". In: *International Journal of Energy Research* 39.9 (July 2015), pp. 1153–1178. ISSN: 0363-907X.

[110] K. Ishaque, Z. Salam, and G. Lauss. "The performance of perturb and observe and incremental conductance maximum power point tracking method under dynamic weather conditions". In: *Applied Energy* 119 (Apr. 2014), pp. 228–236. ISSN: 0306-2619. DOI: 10.1016/j.apenergy.2013.12.054.

[111] S. Molaei, S. Jalilzadeh, and M. Mokhtarifard. "A new controlling method for maximum power point tracking in photovoltaic systems". In: *IJTPE* 7.1 (2015), pp. 1–7.

[112] A. M. Bazzi and P. T. Krein. "Ripple correlation control: An extremum seeking control perspective for real-time optimization". In: *IEEE Transactions on Power Electronics* 29.2 (Feb. 2013), pp. 988–995. ISSN: 0885-8993. DOI: 10.1109/tpel.2013.2256467.

[113] S. L. Brunton, C. W. Rowley, S. R. Kulkarni, and C. Clarkson. "Maximum power point tracking for photovoltaic optimization using ripple-based extremum seeking control". In: *IEEE transactions on power electronics* 25.10 (Oct. 2010), pp. 2531–2540. ISSN: 0885-8993. DOI: 10.1109/tpel.2010.2049747.

[114] W. Nwesaty, A. I. Bratcu, and A. Hably. "Extremum seeking control techniques applied to photovoltaic systems with multimodal power curves". In: *2013 International Conference on Renewable Energy Research and Applications (ICRERA)*. IEEE. IEEE, Oct. 2013, pp. 85–90. DOI: 10.1109/icrera.2013.6749731.

[115] N. Bizon. "Global Maximum Power Point Tracking (GMPPT) of Photovoltaic array using the Extremum Seeking Control (ESC): A review and a new GMPPT ESC scheme". In: *Renewable and Sustainable Energy Reviews* 57 (May 2016), pp. 524–539. ISSN: 1364-0321. DOI: 10.1016/j.rser.2015.12.221.

[116] M. Haring, E. Skjong, T. A. Johansen, and M. Molinas. "Extremum-seeking control for harmonic mitigation in electrical grids of marine vessels". In: *IEEE Transactions on Industrial Electronics* 66.1 (Jan. 2018), pp. 500–508. ISSN: 0278-0046. DOI: 10.1109/tie.2018.2826472.

[117] L. Alhafadhi and J. Teh. "Advances in reduction of total harmonic distortion in solar photovoltaic systems: A literature review". In: *International Journal of Energy Research* 44.4 (2020), pp. 2455–2470.

[118] A. Ghaffari, S. Seshagiri, and M. Krstić. "Multivariable maximum power point tracking for photovoltaic micro-converters using extremum seeking". In: *Control Engineering Practice* 35 (2015), pp. 83–91. DOI: 10.1016/j.conengprac.2014.11.007.

[119] G. Vachtsevanos and K. Kalaitzakis. "A hybrid photovoltaic simulator for utility interactive studies". In: *IEEE Transactions on Energy Conversion* PER-7.2 (June 1987), pp. 227–231. ISSN: 0272-1724. DOI: 10.1109/mper.1987.5527123.

[120] N. Femia, G. Lisi, G. Petrone, G. Spagnuolo, and M. Vitelli. "Distributed maximum power point tracking of photovoltaic arrays: Novel approach and system analysis". In: *IEEE Transactions on Industrial Electronics* 55.7 (July 2008), pp. 2610–2621. ISSN: 0278-0046. DOI: 10.1109/tie.2008.924035.

[121] A. Ghaffari, M. Krstić, and S. Seshagiri. "Power optimization and control in wind energy conversion systems using extremum seeking". In: *IEEE transactions on control systems technology* 22.5 (June 2014), pp. 1684–1695. DOI: 10.1109/acc.2013.6580168.

[122] J. I. Poveda and M. Krstić. "Fixed-time gradient-based extremum seeking". In: *2020 IEEE American Control Conference (ACC)*. IEEE, July 2020, pp. 2838–2843. DOI: 10.23919/acc45564.2020.9148026.

[123] E.-W. Bai, L.-C. Fu, and S. S. Sastry. "Averaging analysis for discrete time and sampled data adaptive systems". In: *IEEE Transactions on Circuits and Systems* 35.2 (1988), pp. 137–148. ISSN: 0098-4094. DOI: 10.1109/31.1715.

[124] W. Wang and D. Nešić. "Input-to-state stability analysis via averaging for parameterized discrete-time systems". In: *Proceedings of the 48h IEEE Conference on Decision and Control (CDC) held jointly with 2009 28th Chinese Control Conference*. IEEE. IEEE, Dec. 2009, pp. 1399–1404. DOI: 10.1109/cdc.2009.5399993.

[125] X. Yang, J. Zhang, and E. Fridman. "Periodic Averaging of Discrete-Time Systems: A Time-Delay Approach". In: *IEEE Transactions on Automatic Control* (2022), pp. 1–8. ISSN: 0018-9286. DOI: 10.1109/tac.2022.3209496.

[126] S.-J. Liu and M. Krstic. "Stochastic averaging in discrete time and its applications to extremum seeking". In: *IEEE Transactions on Automatic control* 61.1 (Jan. 2015), pp. 90–102. ISSN: 0018-9286. DOI: 10.1109/tac.2015.2427672. URL: http://arxiv.org/pdf/1502.04940.

[127] H. Zargarzadeh, S. Jagannathan, and J. A. Drallmeier. "Extremum-seeking for nonlinear discrete-time systems with application to HCCI engines". In: *2014 American Control Conference*. IEEE. IEEE, June 2014, pp. 861–866. DOI: 10.1109/acc.2014.6858872.

[128] S. Liu, P.-Y. Chen, B. Kailkhura, G. Zhang, A. O. Hero III, and P. K. Varshney. "A primer on zeroth-order optimization in signal processing and machine learning: Principals, recent advances, and applications". In: *IEEE Signal Processing Magazine* 37.5 (Sept. 2020), pp. 43–54. ISSN: 1053-5888. DOI: 10.1109/msp.2020.3003837.

[129] Y. Pang and G. Hu. "Nash equilibrium seeking in n-coalition games via a gradient-free method". In: *Automatica* 136 (2022), p. 110013. DOI: 10.1016/j.automatica.2021.110013.

[130] Y. Tang, Z. Ren, and N. Li. "Zeroth-order feedback optimization for cooperative multi-agent systems". In: *Automatica* 148 (Feb. 2023), p. 110741. ISSN: 0005-1098. DOI: 10.1016/j.automatica.2022.110741. URL: http://arxiv.org/pdf/2011.09728.

[131] Y. Huang and J. Hu. *Zeroth-Order Learning in Continuous Games via Residual Pseudogradient Estimates*. 2023. DOI: 10.48550/ARXIV.2301.02279. URL: https://arxiv.org/abs/2301.02279.

[132] T. Tatarenko and M. Kamgarpour. "Bandit online learning of nash equilibria in monotone games". In: *arXiv preprint arXiv:2009.04258* (2020).

[133] X. Lian, H. Zhang, C.-J. Hsieh, Y. Huang, and J. Liu. "A comprehensive linear speedup analysis for asynchronous stochastic parallel optimization from zeroth-order to first-order". In: *Advances in Neural Information Processing Systems* 29 (2016). Ed. by D. D. Lee, M. Sugiyama, U. V. Luxburg, I. Guyon, and R. Garnett.

[134] Y. Shen, Y. Zhang, S. Nivison, Z. I. Bell, and M. M. Zavlanos. "Asynchronous zeroth-order distributed optimization with residual feedback". In: *2021 60th IEEE Conference on Decision and Control (CDC)*. IEEE. IEEE, Dec. 2021, pp. 3349–3354. DOI: 10.1109/cdc45484.2021.9683470. URL: http://arxiv.org/pdf/2109.13866.

[135] I. Mareels and J. W. Polderman. "Adaptive systems". In: *Adaptive Systems*. Springer, 1996, pp. 1–26. ISBN: 9781461264149. DOI: 10.1007/978-0-8176-8142-5_1.

[136] T. Başar and G. J. Olsder. *Dynamic noncooperative game theory*. Vol. 85. SIAM, Sept. 1998, pp. 687–688. DOI: 10.1016/0377-2217(95)90173-6.

[137] Y. T. Chow, T. Wu, and W. Yin. "Cyclic coordinate-update algorithms for fixed-point problems: Analysis and applications". In: *SIAM Journal on Scientific Computing* 39.4 (Jan. 2017), A1280–A1300. ISSN: 1064-8275. URL: http://arxiv.org/pdf/1611.02456.

[138] D. S. Naidu. *Singular perturbation methodology in control systems*. IET, Jan. 1988. ISBN: 9780863411076.

[139] G. Carnevale and G. Notarstefano. "Nonconvex Distributed Optimization via Lasalle and Singular Perturbations". In: *IEEE Control Systems Letters* 7 (2023), pp. 301–306. ISSN: 2475-1456. DOI: 10.1109/LCSYS.2022.3187918.

[140] D. E. Ochoa and J. I. Poveda. "Momentum-Based Nash Set Seeking over Networks via Multi-Time Scale Hybrid Dynamic Inclusions". en. In: *arXiv preprint arXiv:2110.07269* (Dec. 2022). URL: http://arxiv.org/abs/2110.07269.

[141] X.-F. Wang, A. R. Teel, X.-M. Sun, K.-Z. Liu, and G. Shao. "A Distributed Robust Two-Time-Scale Switched Algorithm for Constrained Aggregative Games". In: *IEEE Transactions on Automatic Control* (2023), pp. 1–16. ISSN: 1558-2523. DOI: 10.1109/TAC.2023.3240981.

[142] C. Sun and G. Hu. "Continuous-Time Penalty Methods for Nash Equilibrium Seeking of a Nonsmooth Generalized Noncooperative Game". In: *IEEE Transactions on Automatic Control* 66.10 (Oct. 2021), pp. 4895–4902. ISSN: 1558-2523. DOI: 10.1109/TAC.2020.3040377.

[143] J. I. Poveda and N. Li. "Robust Hybrid Zero-Order Optimization Algorithms with Acceleration via Averaging in Continuous Time". In: *arXiv preprint arXiv:1909.00265* (2019).

[144] F. Galarza-Jimenez, J. Poveda, and E. Dall'Anese. "Sliding-Seeking Control: Model-Free Optimization with Safety Constraints". In: *Learning for Dynamics and Control Conference*. PMLR. 2022, pp. 1100–1111.

[145] W. Wang, A. R. Teel, and D. Nešić. "Averaging in singularly perturbed hybrid systems with hybrid boundary layer systems". In: *2012 IEEE 51st IEEE Conference on Decision and Control (CDC)*. IEEE. IEEE, Dec. 2012, pp. 6855–6860. DOI: 10.1109/cdc.2012.6425965.

[146] A. R. Teel and D. Popovic. "Solving smooth and nonsmooth multivariable extremum seeking problems by the methods of nonlinear programming". In: *Proceedings of the 2001 American Control Conference.(Cat. No. 01CH37148)*. Vol. 3. IEEE. IEEE, 2001, pp. 2394–2399. DOI: 10.1109/acc.2001.946111.

[147] S. Z. Khong, D. Nešić, Y. Tan, and C. Manzie. "Unified frameworks for sampled-data extremum seeking control: global optimisation and multi-unit systems". In: *Automatica* 49.9 (Sept. 2013), pp. 2720–2733. ISSN: 0005-1098. DOI: 10.1016/j.automatica.2013.06.020.

[148] A. R. Teel, J. Peuteman, and D. Aeyels. "Semi-global practical asymptotic stability and averaging". In: *Systems & control letters* 37.5 (Aug. 1999), pp. 329–334. ISSN: 0167-6911. DOI: 10.1016/s0167-6911(99)00039-0.

[149] R. Postoyan, M. C. Bragagnolo, E. Galbrun, J. Daafouz, D. Nešić, and E. B. Castelan. "Event-triggered tracking control of unicycle mobile robots". In: *Automatica* 52 (Feb. 2015), pp. 302–308. ISSN: 0005-1098. DOI: 10.1016/j.automatica.2014.12.009.

[150] A. Hauswirth, S. Bolognani, and F. Dörfler. "Projected Dynamical Systems on Irregular, Non-Euclidean Domains for Nonlinear Optimization". en. In: *SIAM Journal on Control and Optimization* 59.1 (Jan. 2021), pp. 635–668. ISSN: 0363-0129, 1095-7138. DOI: 10.1137/18M1229225.

[151] A. R. Teel. "Lyapunov conditions certifying stability and recurrence for a class of stochastic hybrid systems". en. In: *Annual Reviews in Control* 37.1 (Apr. 2013), pp. 1–24. ISSN: 1367-5788. DOI: 10.1016/j.arcontrol.2013.02.001.

[152] A. R. Teel, A. Subbaraman, and A. Sferlazza. "Stability analysis for stochastic hybrid systems: A survey". en. In: *Automatica* 50.10 (Oct. 2014), pp. 2435–2456. ISSN: 0005-1098. DOI: 10.1016/j.automatica.2014.08.006.

[153] K. Garg, M. Baranwal, R. Gupta, and M. Benosman. "Fixed-Time Stable Proximal Dynamical System for Solving MVIPs". In: *IEEE Transactions on Automatic Control* (2022), pp. 1–8. ISSN: 1558-2523. DOI: 10.1109/TAC.2022.3214795.

[154] B. Ciuffo, M. Makridis, V. Padovan, E. Benenati, K. Boriboonsomsin, M. T. Chembakasseril, P. Daras, V. Das, A. Dimou, S. Grammatico, R. Hartanto, M. Hoelscher, Y. Jiang, S. Krilasevic, S. Liu, Q. N. Nguyen Le, C. Rosier, P. Ruan, Z. Wei, G. Wu, X. Zhao, and Z. Zhao. "Robotic Competitions to Design Future Transport Systems: The Case of JRC AUTOTRAC 2020". en. In: (Aug. 2022), p. 03611981221110566. ISSN: 0361-1981. DOI: 10.1177/03611981221110566.

[155] M. J. van der Linden, S. Krilašević, and S. Grammatico. "A Hybrid Source Seeking Algorithm in Unknown Environments". In: *2021 29th Mediterranean Conference on Control and Automation (MED)*. June 2021, pp. 1040–1045. DOI: 10.1109/MED51440.2021.9480267.

Acronyms

AC	alternating current
AIL	axial induction factor
DC	direct current
ESC	extremum seeking control
FB	forward-backward
GNE	generalized Nash equilibrium
GNEP	generalized Nash equilibrium problem
I-NESC	integral Nash equilibrium seeking control
KKT	Karush-Kuhn-Tucker
MMPT	Maximum power point tracking
NE	Nash equilibrium
NEP	Nash equilibrium problem
P&O	perturb and observe
PI	proportional integral
PV	photo-voltaic
PWM	pulse width modulation
SGPAS	semi-global practical asymptotic stability
SGPpAS	semi-global practical pre-asymptotic stability
THD	total harmonic distortion
UGAS	uniform global asymptotic stability
UGES	uniform global exponential stability
UGpAS	uniform global pre-asymptotic stability
ULAS	uniform local asymptotic stability
ULpAS	uniform local pre-asymptotic stability

vGNE	variational generalized Nash equilibrium
VI	variational inequality

Curriculum Vitæ

Suad Krilašević

1995/02/12 Born in Sarajevo, Republic of Bosnia and Herzegovina

Education

2019-2023 **PhD in Systems & Control**
Delft University of Technology
Thesis: Derivative-free Equilibrium Seeking in Multi-Agent Systems
Promotor: Prof. dr. Sergio Grammatico
Copromotor: Prof. dr. ir. Bart De Schutter

2016-2018 **Masters of Electrical Engineering, Programme Automatic control and electronics**
University of Sarajevo, Faculty of Electrical Engineering
Thesis: Suboptimal control of nonlinear systems via LQR-RRT path planing
Supervisor: Dr. Adnan Tahirović

2013-2016 **Bachelor of Electrical Engineering, Programme Automatic control and electronics**
University of Sarajevo, Faculty of Electrical Engineering
Thesis: Conductance in thin foil isolators
Supervisor: Dr. Adnan Mehonić

Awards and honors

2023 Winner of the 36hours@DCSC Pub quiz

2021 1st place at the AUTOTRAC2020 competition organized by JRC

2018 Best student of the Master Programme at the Faculty of Electrical Engineering, University of Sarajevo

2018 1st place in the Mathematics Arena at the STEM Games - International competition for students in STEM fields of study

2016 Best student of the Bachelor Programme at the Faculty of Electrical Engineering, University of Sarajevo

2015	1st place in Physics at the International Electrical Engineering Students' Gathering - Elektrijada
2013	Honorable mention at the International Physics Olympiad

List of Publications

Journal articles and preprints

1. S. Krilašević and S. Grammatico. "Comments on "A proportional-integral extremum-seeking controller design technique"[Automatica 77 (2017) 61–67]". In: *Automatica* 135 (Jan. 2022), p. 109932. ISSN: 0005-1098. DOI: 10.1016/j.automatica.2021.109932

2. S. Krilašević and S. Grammatico. "Learning generalized Nash equilibria in multi-agent dynamical systems via extremum seeking control". In: *Automatica* 133 (Nov. 2021), p. 109846. ISSN: 0005-1098. DOI: 10.1016/j.automatica.2021.109846

3. S. Krilašević and S. Grammatico. "Learning generalized Nash equilibria in monotone games: A hybrid adaptive extremum seeking control approach". en. In: *Automatica* 151 (May 2023), p. 110931. ISSN: 0005-1098. DOI: 10.1016/j.automatica.2023.110931

4. S. Krilašević and S. Grammatico. "A discrete-time averaging theorem and its application to zeroth-order Nash equilibrium seeking". In: arXiv:2302.04854 (Feb. 2023). arXiv:2302.04854 [cs, eess, math]. DOI: 10.48550/arXiv.2302.04854

5. S. Krilašević and S. Grammatico. "Stability of singularly perturbed hybrid systems with restricted systems evolving on boundary layer manifolds". In: arXiv:2303.18238 (Mar. 2023). arXiv:2303.18238 [cs, eess, math]. DOI: 10.48550/arXiv.2303.18238

Conference papers

1. S. Krilašević and S. Grammatico. "An integral Nash equilibrium control scheme for a class of multi-agent linear systems". In: *IFAC WC* 53 (2020), pp. 5375–5380. ISSN: 2405-8963. DOI: 10.1016/j.ifacol.2020.12.1521

2. S. Krilašević and S. Grammatico. "An extremum seeking algorithm for monotone Nash equilibrium problems". In: *2021 IEEE Conference on Decision and Control (CDC)* (Dec. 2021), pp. 1232–1237. DOI: 10.1109/cdc45484.2021.9683700. URL: http://arxiv.org/pdf/2109.07975

3. B. Ciuffo, M. Makridis, V. Padovan, E. Benenati, K. Boriboonsomsin, M. T. Chembakasseril, P. Daras, V. Das, A. Dimou, S. Grammatico, R. Hartanto, M. Hoelscher, Y. Jiang, S. Krilasevic, S. Liu, Q. N. Nguyen Le, C. Rosier, P. Ruan, Z. Wei, G. Wu, X. Zhao, and Z. Zhao. "Robotic Competitions to Design Future Transport Systems: The Case of JRC AUTOTRAC 2020". en. In: (Aug. 2022), p. 03611981221110566. ISSN: 0361-1981. DOI: 10.1177/03611981221110566

4. M. J. van der Linden, S. Krilašević, and S. Grammatico. "A Hybrid Source Seeking Algorithm in Unknown Environments". In: *2021 29th Mediterranean Conference on Control and Automation (MED)*. June 2021, pp. 1040–1045. DOI: 10.1109/MED51440.2021.9480267

5. S. Krilašević and S. Grammatico. “Distortion reduction in photovoltaic output current via optimized extremum seeking control”. In: *2023 21st European Control Conference (ECC)* (June 2023)

Included in this thesis.

Acknowledgments

Well, here at last, dear friends, on the shores of the Sea comes the end of our fellowship... Go in peace! I will not say: do not weep; for not all tears are an evil.

J.R.R. Tolkien, The Return of the King

Formulating a novel idea often requires strong foundational knowledge and the right environment, both in and outside work. In their acknowledgments, authors vary in the extent to which they analyze these influences. Some keep it short, acknowledging only those directly connected to their work, while others opt for a more comprehensive approach, tracing back to the very roots. My approach leans towards the latter, and there are a few reasons for this. Some studies suggest that practicing gratitude can enhance one's happiness. Therefore, this acknowledgment section will also acts as an exercise in gratitude. Additionally, given my occasionally forgetful nature, which my friends and family can attest to, this section also serves as a brief memoir of my PhD journey. I apologize in advance for any omissions. The events and names mentioned are in no particular order. What follows is an extensive but not exhaustive list of my acknowledgments.

Firstly, I would like to thank my supervisor, dr. Sergio Grammatico, for taking the risk with me and giving me the opportunity to do the PhD in his group despite my academic background not being from exactly "Ivy League" institutions. Collaborating with him has been a rich learning experience, and I hope I did not disappoint. I extend my gratitude to my PhD committee members, Prof. Bart De Schutter, Dr. Jorge Poveda, Prof. Dragan Nešić, Prof. Tamás Keviczky, and Prof. Martijn Wisse, for their valuable feedback and the time invested in judging this dissertation.

The people in our group, Giuseppe, Carlo, Barbara, Filippo, Raja, Mattia, Emilio, Wicak, Luyao, Reza, and Giorgios, have always been helpful and very kind to me, which I appreciate, and I hope we keep in touch even after we all leave Delft. With a great effort of Cas, Jelle, Max, Xander, Jurriaan, Anand (the first iteration of the team), and the finishing touches of Cas, Emilio, and Viswanath, we managed to win the AUTOTRAC 2020 competition, showing once and for all the superiority of PID control over deep neural networks. I will always remember how unexpected this victory was.

During my research visit to Australia, Professor Dragan Nešić was a great host. Our discussions spanned not only work but also other topics, like politics and Australian culture. Unfortunately, our research was left unfinished, and I hope I will find the time soon to complete it. Members of his group, Mathieu, Elena, Alejandro, Gabriel, and Seth were also very helpful, and I hope to see them in some future conferences. Besides work, I've had the pleasure of meeting many great people. I am grateful to Johannes, Yannick, Jugal, Luka, Ghazal, Wan Chee, Paula, Loyd, Daan and Naiya for their companionship and the adventures we shared exploring Australia.

I owe immense gratitude to my country for providing me with a nearly free, good-quality education and to my teachers, who were a critical part of this process. Furthermore, I believe that the system of mathematics and physics competitions from primary school to high school created a love for interesting problems and made me better at handling stress. Being born in challenging times, I extend profound gratitude to those who valiantly fought for my freedom in every possible way, with a special remembrance for those who lost their lives. Thanks to my big group of friends - Adna, Ahmed, Amina, Belmin, Dženan, Eldar, Emela, Emir, Poplata, Hadžem, Sumejja, Zubejda, for the sense of community they've created, to Bilal for the time spent and the fun we had on our various semi-successful projects, and to Harun for always pushing me to be better. Additionally, I'm grateful to Amina, Ena, Džemil, Fuad, Ena, and Nandin for the online quizzes we organized during the early days of the pandemic. These sessions were a highlight of my week. While our startup, Expert Experiments, hasn't quite taken off yet (soon™), conversations and planning sessions with Bahrudin, Selver, and Nudžeim were always a delight. Thanks to Aleksandar, Imran, and Semad for carrying me in all the video games we played over the years, I just couldn't git gud. I'm also grateful for my involvement with the "Association for the Advancement of Science and Technology" through which I had the chance to regularly meet with some of Bosnia and Herzegovina's brightest minds and gain insights into various subjects.

The people of the Netherlands have been very welcoming towards me, even as I made, regrettably, little effort to learn their language. I admire their ingenuity and how they managed to "tame" the sea in order to make their country livable. I want to thank Soran and Erdan from Polat shop for always reminding me to buy Runder Polat. Enel, Amina, Armin, Zlatan, and Edna, along with the broader community of ICC Selam, ensured that I felt at home through various gatherings and that I was in touch with Bosnian culture.

I could write a lot about the people of TU Delft, but in an effort to not make this section too long, I am doing a speed round. I want to thank: my officemates Yvo, Barbara, Emilio, Steven, Mohammad for making the working atmosphere pleasant; The first cake group (Tomas, Manyu, Maulong, Carlos, Carlos-Jesus, Barbara, Mattia, Momo, Sunny) for, as the name implies, the cakes ; Raja and Mattia, who began their PhDs slightly ahead of mine, for provided invaluable guidance and insights; Leonor and Athina for helping me with the second-floor renovation meetings; Pedro, Leila and Athina for tolerating my occasional intrusions in their office when I was bored; all the Italians and Rayyan for sharing their love of good food and coffee with me; Marten and Clara for organizing the best DCSC pub quiz with me; Carlos, Emilio, Mattia, Manyu and Coen for making me laugh the most; Roger for taking over my PhD representative duties and doing a better job than I did; Claudia for good anime and movie recommendations; Steven, Eva, Pedro and Athina for listening to my ramblings about Bosnian history; Emilio, Wicak, Frederik, Maarten, Luyao, Eva, Alex, Rudi, the members of the second cake group, for the cakes again; Coen and Roger for being members of the party planning committee; Tian for alawys beeing cheerful; Mattia for the BBQs, Barbara for the pizzas, Claudia and Emilio for the cookies; Frederik for the cool house parties; Clara and Athina for organizing the 3mE video competition with me; Steven for helping me with all things related to the Netherlands and translating the summary of this thesis; Obaadah, Arish, Rehan, Musab, for the enlightening khutbhas, and members of Ibn Firmas for organizing many wonderful events; Dingshan, Maulong, Jianing,

Jingwei, Alessandro, Pedro, Sander, Sam, Amins, Carlos, Caio, Filippo, Max, Mohammads, Hassan, Theodoulos, Rodrigo, Twan, Reza, Estban, Pablo, Obaadah, Shabnam, Alex, Hamed, Kanghui, Xiaoyu, Maarten, Rayyan, Roger, Rudi for the various weekly sports we played together; Erica, Marieke, Heleen, Francy for sorting out any problems I had quickly and efficiently. Special thanks to Emilio for doing me many favors over the years, especially for providing lodging whenever I needed it. He often reminded me 'things can get hard, but you have to keep pushing', advice that has seen me through many challenges. Furthermore, special thanks to Carlos and Claudia for making me take a break most often, as I easily get lost in my work and responsibilities.

My family has also been of great importance in this journey. My late mother, Vildana, and my father, Muradif, worked tirelessly to provide for their family. My sisters, Elmedina and Melina, have been additional maternal figures to my brother and me, taking great care of us both when we were young and as we got older. Melina jokes that the only way to repay the debt is by babysitting her children, while I hope that expressing my gratitude in a publicly available book might be enough. I'd like to extend my gratitude to my brothers-in-law, David and Emin, who have added richness to our family with their diverse interests and keen sense of humor. My nephew Benjamin never fails to bring immense joy to our lives, and my cat, Mrljica, lightens up our days with her antics. Additionally, a heartfelt thanks to my twin brother, Senad, for always being wonderful company.

Finally, all my highest praise is for God, Who gave me the strength and knowledge needed to finish this PhD successfully.

Suad Krilašević
Sarajevo, September 2023